



THE UNIVERSITY
of ADELAIDE

SCHOOL OF MECHANICAL
ENGINEERING

Flame Stabilisation in the Transition to MILD Combustion

Michael J. Evans

*A thesis submitted in fulfilment of
the requirement for the degree of
Doctor of Philosophy*

March 2017

*Dedicated, in loving memory, to Elizabeth “Betty” Evans
“Grandma”
(1933–2015)*

For all the love, and all the Lego

Abstract

Emissions reduction and energy management are current and future concerns for governments and industries alike. The primary source of energy worldwide for electricity, air transport and industrial processes is combustion. Moderate or intense low oxygen dilution (MILD) combustion offers improved thermal efficiency and a significant reduction of CO and NO_x pollutants, soot and thermo-acoustic instabilities compared to conventional combustion. Whilst combustion in the MILD regime offers considerable advantages over conventional combustion, neither the structure of reacting jets under MILD conditions, nor the boundaries of the MILD regime are currently well understood. This work, therefore, serves to fill this gap in the understanding of flame structure near the boundaries of the MILD regime.

The MILD combustion regime has been previously investigated experimentally and numerically in premixed reactors and non-premixed flames. In this study, definitions of MILD combustion are compared and contrasted, with the phenomenological premixed description of MILD combustion extended to describe non-premixed flames. A simple criterion is derived analytically which offers excellent agreement with observations of previously studied cases and new, non-premixed MILD and autoignitive flames presented in this work. This criterion facilitates a simple, predictive approach to distinguish MILD combustion, autoignitive flames, and the transition between the two regimes.

The adequacy of simplified reactors as a tool for predicting non-premixed ignition behaviour in the transition between MILD combustion and autoignition has not previously been resolved, and is addressed in this work. The visual lift-off behaviour seen in the transition between MILD combustion and conventional autoignitive flames seen experimentally is successfully replicated using simplified reactors. The location of the visible flame base in a jet-in-hot-coflow burner is shown to be highly sensitive to the relative location of the most reactive mixture fraction and the high strain-rate shear layer due to the strong coupling of between ignition chemistry and the underlying flow-field.

Previous studies have demonstrated a strong dependence of ignition delay times

to significant concentrations of minor species. Simulations presented in this work demonstrate that small concentrations of the hydroxyl radical (OH), similar to those expected in practical environments, significantly affect ignition delay and intensity of non-premixed MILD combustion, however have little effect on autoignitive flames. Importantly, such concentrations of OH do not result in a change in flame structure for the cases investigated. Whilst these results stress the importance of minor species in modelling the transient ignition of non-premixed MILD combustion, steady-state simulations do not demonstrate the same sensitivity to concentrations of minor species expected in hot combustion products. These results suggest that the temperature and oxygen concentration in the oxidant stream are the most important factors governing the boundaries of the MILD combustion regime.

Investigations of reaction zone structure and ignition in, and near the boundaries of, the MILD combustion regime have demonstrated the relative importance of different aspects of ambient conditions and differences in structure between non-premixed MILD and autoignitive flames. These findings build upon the understanding of this regime and provide critical insight for future studies towards both fundamental research, and the practical implementation, of MILD combustion.

Contents

Abstract	iii
Contents	v
List of Figures	ix
List of Tables	xi
Declaration	xiii
Acknowledgements	xv
Papers Included in this Thesis-by-Publication	xvii
Additional Published Works Related to this Thesis	xix
Nomenclature	xxi
1 Introduction	1
1.1 Aims	2
1.2 Details of the Publications	3
1.2.1 Synopsis of Paper 1	3
1.2.2 Synopsis of Paper 2	4
1.2.3 Synopsis of Paper 3	4
1.2.4 Synopsis of Paper 4	5
1.2.5 Synopsis of Paper 5	5
References	6
2 Background	13
2.1 Benefits of MILD Combustion	13
2.2 Fluid Mechanics and Combustion	15
2.2.1 Fluid Mechanics, Turbulent Flow and The Reynolds Number . .	15

2.2.2	Combustion and the Damköhler Number	17
2.3	Numerical and Analytical Tools for Combustion Research	19
2.3.1	Computational Fluid Dynamics	19
2.3.2	Chemical Kinetics	20
2.3.3	Laminar Flames and Flamelet Theory	22
2.3.4	Modelling Turbulence-Chemistry Interactions	25
	References	28
3	Literature Review	39
3.1	Studies of MILD Combustion	40
3.1.1	Premixed Studies of MILD Combustion	40
3.1.2	Non-Premixed Studies of MILD Combustion	42
3.2	Studies of Autoignition	45
3.2.1	Autoignitive Flame Stabilisation	45
3.2.2	Assessment of Ignition Delay in Autoignitive Flames	47
3.3	Flame Stabilisation in the Transition to MILD Combustion	47
3.3.1	Transitional Flame Structure	47
3.3.2	Species Transport in Non-Premixed Flames in Hot Coflows	49
3.3.3	Effects of Gaseous Fuel Composition on Flames in Hot Coflows	50
3.3.4	Heat Release and Temperature Peaks in Non-Premixed Flames	50
3.3.5	Response of Lift-off Height to Changes in Coflow	51
3.4	Jet Flame Modelling in MILD Combustion	54
3.4.1	Modelling Jet Flames with the Eddy Dissipation Concept	55
	References	56
4	Classification and Lift-Off Height Prediction of Non-Premixed MILD and Autoignitive Flames	69
5	Effects of Oxidant Stream Composition on Non-Premixed, Laminar Flames with Heated and Diluted Coflows	81
6	Ignition Characteristics in Spatially Zero-, One- and Two-Dimensional Laminar Ethylene Flames	111
7	Modelling Lifted Jet Flames in a Heated Coflow using an Optimised Eddy Dissipation Concept Model	125
8	Ignition Features of Methane and Ethylene Fuel-Blends in Hot and Diluted Coflows	147

9 Summary and Conclusions	175
9.1 Identifying and Understanding MILD Combustion	175
9.2 Factors Influencing Ignition with Hot and Diluted Oxidants	177
9.3 Prediction of Non-Premixed Ignition Delay	179
9.4 Future Work	180
9.5 Conclusions	181
References	183
A Supplementary Data for Chapter 5	189
B Supplementary Data for Chapter 8	201

List of Figures

2.1	NO _x emissions from the Alstom GT24/26	14
2.2	Borghi diagram	18
2.3	Annotated illustration of an S-shaped curve	24
3.1	S-shaped curves for three stoichiometric flamelets.	44

List of Tables

3.1	Combustion regimes in a well-stirred reactor configuration.	41
-----	---	----

Declaration

I certify that this work contains no material which has been accepted for the award of any other degree or diploma in any university or other tertiary institution and, to the best of my knowledge and belief, contains no material previously published or written by another person, except where due reference has been made in the text. In addition, I certify that no part of this work will, in the future, be used in a submission for any other degree or diploma in any university or other tertiary institution without the prior approval of the University of Adelaide and where applicable, any partner institution responsible for the joint-award of this degree.

I give consent to this copy of my thesis when deposited in the University Library, being made available for loan and photocopying, subject to the provisions of the Copyright Act 1968.

The author acknowledges that copyright of published works contained within this thesis resides with the copyright holder(s) of those works.

I also give permission for the digital version of my thesis to be made available on the web, via the University's digital research repository, the Library Search and also through web search engines, unless permission has been granted by the University to restrict access for a period of time.

Michael J. Evans

3 March 2017

Acknowledgements

I am gratefully indebted to the knowledge, guidance, enthusiasm and time-commitment of A/Prof. Paul Medwell and Dr Zhao Tian, without their expertise and direction, this project would simply not have been possible. I feel incredibly privileged to have had Paul's advice and mentoring – his passion for this field of research is contagious, even when nothing seems to be working! I am also grateful to A/Profs. Alessio Frassoldati and Alberto Cuoci (along with the rest of the CRECK group) from the Politecnico di Milano (POLIMI), and Asst. Prof. Matthias Ihme (and his group) at Stanford University for hosting and advising me at different stages.

This body of work has consumed hundreds of thousands (if not millions) of hours of CPU-time, and hundreds of hours of lab-time. I would like to acknowledge support of all the staff at eResearchSA, Stanford University, POLIMI but especially Mr Billy Constantine for his technical assistance and music recommendations. I would also like to thank the mechanical and electrical workshops in Schools of Mechanical and Chemical Engineering. I'd particularly like to thank Mr Marc Simpson at the Thebarton Laboratory for his help and practical advice.

I have made many friends from a host of places throughout my candidature, and have had a wealth of memorable times, but unfortunately cannot list them all here (that would make for a book in itself). However the friendships of Drs John Codrington, Lloyd Fletcher and Alfonso Chinnici, Miss Jingjing Ye and Messrs Sarwo Edhy Sofyan and Hywel Bennet have been invaluable, but a special mention must go to Dr Alessandro Stagni – my office-and-caffè-mate from Milan to Palo Alto. I'd like to separately thank my friends outside my academic circles for accepting my absence from events, because I've been home working, or 'inconveniently' overseas.

I must thank my family – in particular Mum, Dad, Grandpa and (late) Grandma – for their investment of time, love, unwavering support, limitless encouragement and patience in helping me to get to this point; and last, but certainly not least, my fiancée Alyce, for her constant love, support, patience and understanding during the great times, and the difficult times. Words cannot express my gratitude.

I could not have done this without them.

Papers Included in this Thesis-by-Publication

Published

1. **Evans, M. J.**, Medwell, P. R., Wu, H., Stagni, A. & Ihme, M. (In Press). “Classification and Lift-Off Height Prediction of Non-Premixed MILD and Autoignitive Flames.” *Proceedings of the Combustion Institute*. DOI: 10.1016/j.proci.2016.06.013
2. **Evans, M. J.**, Medwell, P. R., Tian, Z. F., Frassoldati, A., Cuoci, A. & Stagni, A. (2016). “Ignition Characteristics in Spatially Zero-, One- and Two-Dimensional Laminar Ethylene Flames.” *AIAA Journal*, vol. 54, no. 10, pp. 3255-3264. DOI: 10.2514/1.J054958
3. **Evans, M. J.**, Medwell, P. R. & Tian, Z. F. (2015). “Modelling Lifted Jet Flames in a Heated Coflow using an Optimised Eddy Dissipation Concept Model.” *Combustion Science and Technology*, vol. 187, no. 7, pp. 1093-1109. DOI: 10.1080/00102202.2014.1002836

Submitted

4. **Evans, M. J.**, Medwell, P. R., Tian, Z. F., Ye, J., Frassoldati A. & Cuoci, A. “Effects of Oxidant Stream Composition on Non-Premixed Laminar Flames with Heated and Diluted Coflows.” Submitted to: *Combustion and Flame*.
5. **Evans, M. J.**, Chinnici, A., Medwell, P. R. & Ye, J. “Ignition Features of Methane and Ethylene Fuel-Blends in Hot and Diluted Coflows.” Submitted to: *Fuel*.

Additional Published Works Related to this Thesis

Published Journal Papers

1. Ye, J., Medwell, P. R., Dally, B. B. & **Evans, M. J.** (2016). “The Transition of Ethanol Flames from Conventional to MILD Combustion.” *Combustion and Flame*, vol. 171, Sept. 2016, pp. 173-184. DOI: 10.1016/j.combustflame.2016.05.020
2. Medwell, P. R., **Evans, M. J.**, Chan, Q. N. & Katta, V. R. (2016). “Laminar Flame Calculations for Analysing Trends in Autoignitive Jet Flames in a Hot and Vitiated Coflow.” *Energy and Fuels*, vol. 30, no. 10, pp. 8680-8690. DOI: 10.1021/acs.energyfuels.6b01264

Conference Papers

1. **Evans, M. J.**, Medwell, P. R. & Ye, J. (2015). *Laser-Induced Fluorescence of Hydroxyl in Ethylene Jet Flames in Hot and Diluted Coflows*. In Proceedings of the 7th Australian Conference on Laser Diagnostics in Fluid Mechanics and Combustion, The University of Melbourne, Melbourne, Australia. 9-11 December 2015, pp. 75-80. ISBN: 978-0-646-94892-8.
2. Ye, J., Medwell, P. R., **Evans, M. J.** & Dally, B. B. (2015). *Quantitative Rayleigh temperature imaging in turbulent flames of prevaporised n-heptane*. In Proceedings of the 7th Australian Conference on Laser Diagnostics in Fluid Mechanics and Combustion, The University of Melbourne, Melbourne, Australia. 9-11 December 2015, pp. 85-89. ISBN: 978-0-646-94892-8.
3. **Evans, M. J.**, Medwell, P. R., Wu, H., Stagni, A. & Ihme, M. (2015). *Classification of Non-Premixed MILD and Autoignitive Flames*. In Proceedings of the Australian Combustion Symposium, The University of Melbourne, Melbourne,

- Australia. 7-9 December 2015, pp. 80-83. ISSN: 1839-8170 (Print), 1839-8162 (Online).
4. Medwell, P. R., **Evans, M. J.**, Chan, Q. N. & Katta, V. R. (2015). *The adequacy of laminar flame calculations for identifying MILD combustion*. In Proceedings of the Australian Combustion Symposium, The University of Melbourne, Melbourne, Australia. 7-9 December 2015, pp. 88-91. ISSN: 1839-8170 (Print), 1839-8162 (Online).
 5. Ye, J., Medwell, P. R., **Evans, M. J.** & Dally, B. B. (2015). *The impact of carrier gas on ethanol flame behaviour in a jet in hot coflow (JHC) burner*. In Proceedings of the Australian Combustion Symposium, The University of Melbourne, Melbourne, Australia. 7-9 December 2015, pp. 84-87. ISSN: 1839-8170 (Print), 1839-8162 (Online).
 6. Wu, H., **Evans, M.** & Ihme, M. (2015). *LES of Mild Combustion using Pareto-efficient Combustion Adaptation*. In 68th Annual Meeting of the American Physical Society (APS) Division of Fluid Dynamics, vol. 60, no. 21, Boston, Massachusetts. 22-24 November 2015.
 7. **Evans, M. J.**, Medwell, P. R., Tian, Z. F., Frassoldati, A., Cuoci, A. & Stagni, A. (2015). *Ignition Characteristics in Spatially Zero-, One- and Two-Dimensional Laminar Ethylene Flames*. In 22nd AIAA Computational Fluid Dynamics Conference, Dallas, Texas, United States of America. 22-26 June 2015, paper no. AIAA 2015-3210. Full paper: ISBN: 978-1-62410-366-7 (Online).
 8. **Evans, M. J.**, Medwell, P. R. & Tian, Z. F. (2013) *Parametric study of EDC model constants for modelling lifted jet flames in a heated coflow*. In Proceedings of the Australian Combustion Symposium, University of Western Australia, Perth, Australia. 6-8 November 2013, pp. 348-351. ISSN: 1839-8170 (Print), 1839-8162 (Online).
 9. **Evans, M. J.**, Tian, Z. F., & Medwell, P. R. (2013) *Modelling Ethylene-Hydrogen Jet Flames in the MILD Combustion Regime*. In MODSIM2013, 20th International Congress on Modelling and Simulation, Adelaide, Australia. 1-6 December 2013, pp. 1554-1560. ISBN: 978-0-9872143-3-1.

Nomenclature

Latin

- C_T A constant in the EDC combustion model, default = 0.4082
- C_ξ A constant in the EDC combustion mode, default = 2.1377
- c_r Reaction rate constant – maximum chemical reaction rate normalised by fluid density
- D Characteristic length (such as a pipe diameter)
- D_Z Diffusion coefficient of Z
- Da Damköhler number $\equiv \tau_{fluid}/\tau_{chem}$
- Da_f First Damköhler number $\equiv c_r/\text{Local strain rate}$
- Da_T Turbulence Damköhler number $\equiv ((\nu c_r^2)/\epsilon)^{1/2}$
- k Turbulent kinetic energy
- Ka Karlovitz number = $Re_t^{1/2} Da^{-1}$
- L Characteristic length scale of turbulent flow = $(u'_{rms})^3/\epsilon$
- l_η Kolmogorov length scale = $(\nu^3/\epsilon)^{1/4}$
- Le The Lewis number (of a particular quantity or chemical species) – the ratio of heat to mass diffusivities
- m Mass
- n_i Number density of species i
- R_i Reaction rate of species i (a mean value in the EDC combustion model)
- Re Reynolds number $\equiv \rho u D/\mu$

Re_t	Turbulent Reynolds number = $\frac{4}{9}k^2/(v\varepsilon)$
s_L^0	Flame Speed
T	Temperature
u	Fluid velocity
\bar{u}	Mean component of turbulent fluid velocity
u'	Fluctuating component of turbulent fluid velocity
Y	Mass fraction
Y_i^*	Mass fraction of species i within a fine structure in the EDC combustion model
Z	Mixture fraction $\equiv m_F/(m_F + m_O)$

Greek

χ	Scalar dissipation rate $\equiv 2D_Z \nabla Z ^2$
δ	Flame Thickness
ε	Turbulent dissipation rate
μ	Fluid dynamic viscosity
ν	Fluid kinematic viscosity
ρ	Fluid density
τ^*	Mean residence time of fluid spent within fine structures in the EDC combustion model
τ_η	Kolmogorov time scale = $(\nu/\varepsilon)^{1/2}$
τ_{ign}	Ignition delay
τ_{res}	Residence time $\approx \chi^{-1} \approx \tau_{fluid}$
τ_{chem}	Chemical time scale \approx the ratio of laminar flame width to laminar flame speed
τ_{fluid}	Turbulent time scale $\approx L/u'$

ξ^* Fine structure length in the EDC combustion model

Abbreviations

CFD Computational fluid dynamics

DME Dimethyl-ether

DNG Dutch natural gas

DNS Direct numerical simulation

EDC Eddy dissipation concept – a combustion model for detailed, finite-rate chemistry

EDM Eddy dissipation model – a combustion model for global, instantaneous chemistry

EGR Exhaust gas recirculation

EMST Euclidean minimum spanning tree – a composition PDF transport mixing model

HRR Heat release rate]

JHC Jet in hot cross-/co-flow [burner configuration]

LES Large eddy simulation

LIF Laser-induced fluorescence

LPG Liquefied petroleum gas

MILD Moderate or intense low oxygen dilution [combustion]

NG Natural gas – primarily composed of CH₄

PDF [Composition] Probability density function – a combustion model for detailed, finite-rate chemistry

RANS Reynolds-averaged Navier-Stokes

VCB Vitiated coflow burner

WSR Well-stirred reactor

Subscripts

0	Initial condition
ad	Adiabatic flame condition
ai	Autoignition condition
b	Burning condition
F	Denotes fuel stream
i	Pertaining to species i
mr	Most reactive mixture condition
O	Denotes oxidant stream
u	Unburnt (mixing) condition
rms	Denotes root-mean-square value of a quantity
st	Stoichiometric mixture fraction

Chapter 1

Introduction

The contemporary world is dependent on combustion. From electricity generation, to the jet engines powering international and domestic air travel, combustion has shaped the technology of the modern era. Combustion supplies 98% of Australia's energy usage [22], with gas production expected to triple from its current level [22] to over 8000 PJ per annum by 2034-35 [23] and combustion of oil, gas and black coal still predicted to provide 86% of Australia's energy in 2050 [6]. Our continuing reliance on combustion requires further development of cleaner, more efficient combustion systems and research to further the fundamental understanding for such systems.

Moderate or intense low oxygen dilution (MILD) combustion (alternatively, "flameless oxidation" or FLOX[®]) occurs in hot, low oxygen conditions, resulting in a distributed, homogeneous reaction zone in contrast to the well-defined flame-fronts typical of conventional combustion [10]. Operation in the MILD combustion regime is advantageous over conventional combustion, offering improved thermal efficiency in addition to a significant reduction of CO and NO_x pollutants, soot and the rapid pressure and temperature fluctuations responsible for thermo-acoustic noise emissions [10]. These pollutant emissions are harmful to the environment [24, 58], and pressure fluctuations may damage turbomachinery contained within gas turbine systems, thus their reduction have been sought within industrial applications through technologies similar to MILD combustion [9, 25, 30, 34, 37, 51, 59].

Current gas turbine technologies attempting to incorporate MILD combustion have either encountered deficiencies in power output in laboratory-scale systems [37] or operate outside of the MILD regime [25]. The shortcomings in these current implementations can be attributed to attempts to operate the entire combustor stage in the MILD regime, resulting in a lower power output [34, 37], or design of a sequential combustion system [25], with the hazard of flame extinction in the tran-

sition towards MILD combustion. The implementation of sequential MILD burners to combine current approaches and maintain the environmental and stability benefits of MILD combustion may therefore be pivotal for next generation combustion systems. The success of these systems hinges on the understanding of the fundamental mechanics and stability of the transition to the MILD combustion regime and more research is required to understand the optimal set of conditions for MILD combustion in gas turbine environments.

1.1 Aims

The overarching aim of this project is to understand the stability of flames in the transition between the MILD and lifted combustion regimes. This has not been investigated by previous experimental [2, 3, 7, 8, 16, 29, 41, 42, 44, 47–49, 55] or numerical [1, 4, 15, 17, 28, 31–33, 38, 39, 54, 60, 61] studies into MILD or autoignited, lifted jet flames and the changes in structure and underlying stabilisation mechanisms have not been identified. This project specifically aims to:

1. *Understand and classify the differences in flame ignition mechanisms and structure between MILD and autoignitive, lifted jet flames in heated coflows.*

The majority of previous experimental and numerical studies into MILD [1, 15, 16, 28, 31, 32, 38, 43, 44, 54, 55] and lifted [2–4, 7, 8, 17, 29, 33, 39, 47–49, 60, 61] jet flames have focussed on single cases, or a very limited range of conditions in either the MILD or lifted flame regime without the capacity to compare differences between the two regimes. These studies have been complemented by an experimental study of visual lift-off of flames in this transition, indicating the significant change between the regimes, however the structural differences in the flames were not investigated [42]. This body of work will bridge this gap by establishing criteria for distinguishing MILD and autoignitive, lifted jet flames in heated coflows.

2. *Investigate the effects of the oxidiser and jet conditions on the structure of flames in the MILD and autoignitive combustion regimes.*

MILD and lifted jet flames operate near the boundaries of extinction and blow-off, with chemical analysis of MILD flames demonstrating less sensitivity to ambient conditions than under lifted conditions [41, 45]. Despite the hazard of blow-off in lifted flames and in the transition to MILD combustion, the effects of temperature, major and minor species concentrations and the jet flow-field on the structure and stability of jet flames has not been investigated from a fundamental perspective. The impact of these parameters will,

therefore, be assessed on flames in both the MILD and autoignitive combustion regimes.

3. *Identify the validity of simplified zero-, one- and two-dimensional models in predicting the ignition delay and structure of experimental jet flames in MILD, transitional and autoignitive conditions.*

Studies of complex, turbulent jet flames have been complemented using zero- or one-dimensional chemical kinetics simulations which cannot account for the turbulence-chemistry interactions in practical combustion systems [19, 21, 35, 36, 40, 52, 53, 56]. Whilst comparisons have been drawn between jet flame ignition and such analyses [7, 56, 60, 61], their relationship to jet flames in the MILD regime and transition to lifted flames has not been established and their value for assessment of realistic combustion systems operating in, or in the transition to, the MILD regime is subsequently uncertain. The validity of these simplified models will, hence, be evaluated and discussed in this thesis.

1.2 Details of the Publications

The body of this thesis is comprised of five publications in leading, international peer-reviewed journals. Each stand-alone publication is presented as a chapter which details the relevant literature specific to that study, describes the methodology of the contained work, presents and discuss the results and offers conclusions. Each chapter also contains an individual reference list and nomenclature, where appropriate. The titles of these works, and their publication statuses, are listed below. These are accompanied by a short description of how they relate to the individual aims.

1.2.1 Synopsis of Paper 1

Chapter 4, containing paper entitled: *Classification and Lift-Off Height Prediction of Non-Premixed MILD and Autoignitive Flames*

The differences in flame structure between non-premixed MILD combustion and autoignitive, lifted jet flames in hot and diluted coflows may be described in the context of one-dimensional ‘flamelets’ and ‘S-shaped curves’ [46, 50]. These descriptions have previously been used to phenomenologically define the MILD combustion regime, but have inherently required the assumption of a quenching temperature in non-premixed configurations [5]. This is addressed by deriving a simple criterion for non-premixed MILD combustion with respect to initial and final tem-

peratures and the effective activation energy of an equivalent one-step chemical reaction. This new criterion is then compared with previous definitions of premixed MILD combustion [10, 46] to provide insight into combustion in the MILD regime and previous attempts to reconcile premixed and non-premixed classifications of MILD combustion, addressing Aim 1. Following this, the new classification of MILD combustion is compared with turbulent flames studied in the literature, and new experimental observations. The characteristics of this simplified zero- and one-dimensional analysis shows good agreement with experimental observations, and transient analyses (again, in one spatial dimension) are successfully used to explain the non-monotonic trends in lift-off height which are observed experimentally. This demonstrates the value of reduced dimension analyses in predicting the structure of experimental jet flames in the MILD and autoignitive combustion regimes, addressing Aim 3.

1.2.2 Synopsis of Paper 2

Chapter 5, containing paper entitled: *Effects of Oxidant Stream Composition on Non-Premixed, Laminar Flames with Heated and Diluted Coflows*

Chapter 5 continues the theme from Chapter 4, drawing distinctions between non-premixed combustion in the MILD and autoignitive regimes. This chapter addresses the two-dimensional flame structures in these two combustion regimes, drawing parallels between features of new experimental cases and those identified in previous experiments [11–13] and numerical studies [14, 18–21, 45, 57]. Following the classification of each flame, addressing Aim 1, the effects of ambient conditions on CH_4 and C_2H_4 flames are investigated through changing the laminar oxidant composition. This component of the work addresses Aim 2, by identifying the impact of oxidant temperature, oxygen content and $\text{H}_2\text{O}/\text{CO}_2$ ratio have on the structure of CH_4 and C_2H_4 flames. Crucially, this work demonstrates the importance of the OH minor species in flame stabilisation in concentrations similar to those found in hot coflows of combustion products. The different impacts of small concentrations of OH on MILD and autoignitive flame stabilisation are assessed, and the impact of OH on non-premixed MILD flames is explained chemically. Finally, the results are briefly compared against two-dimensional, steady-state results, complementing the previous work towards Aim 3.

1.2.3 Synopsis of Paper 3

Chapter 6, containing paper entitled: *Ignition Characteristics in Spatially Zero-, One- and Two-Dimensional Laminar Ethylene Flames*

Ignition delay may be defined using a variety of different metrics. Chapter 6 predominantly addresses Aim 3 by assessing the applicability of several metrics in zero-dimensional batch reactors, one-dimensional opposed-flow flame models and two-dimensional laminar flame simulations against previous studies of turbulent C_2H_4 flames in hot coflows [42, 60]. This work draws correlations between thermal runaway [27, 40] in batch reactor simulations, small temperature increases in non-premixed flames and the lift-off heights of the turbulent flames [42, 60]. Differences in the effectiveness of the different metrics used to define ignition are compared for different flames across the MILD and autoignitive combustion regimes, and some conclusions are drawn about the differences between the regimes. This analysis further adds to Aim 1.

1.2.4 Synopsis of Paper 4

Chapter 7, containing paper entitled: *Modelling Lifted Jet Flames in a Heated Coflow using an Optimised Eddy Dissipation Concept Model*

Modelling visually-lifted, turbulent flames in jet-in-hot-coflow (JHC) burners in the transition to the MILD combustion has previously met with limited success [54]. Therefore, the eddy dissipation concept (EDC) combustion model is optimised to model a series of ‘transitional’ [26, 42, 44] flames, resulting in excellent agreement between the numerical and experimental [16, 44] results. Results using this model are compared to measured data and assessed with a chemiluminescence mechanism and shows very good agreement with experimental observations of visual lift-off heights, and the transitional flame structure. This verifies the use of this EDC model in understanding flame structure and stabilisation near the boundaries of the MILD combustion regime, and offers insights into the reaction zone structure of transitional flames, contributing to both Aim 1 and Aim 3. Finally, this work expands on the response of autoignitive flames to the inclusion of small amounts of minor species in the oxidant, inline with the discussion in Chapter 5, and adding to the work towards Aim 2.

1.2.5 Synopsis of Paper 5

Chapter 8, containing paper entitled: *Ignition Features of Methane and Ethylene Fuel-Blends in Hot and Diluted Coflows*

Chapter 8 addresses Aims 1-Aim 3 in the context of laminar and turbulent flames in the MILD and autoignitive combustion regimes. This chapter presents a comparison between new experimental observations of turbulent jet flames in different hot and diluted coflows, complemented by zero- and one-dimensional kinetics simula-

tions and two-dimensional turbulent modelling (based on Chapter 7). This chapter explores the effects of coflow temperatures between 1100 and 1500 K, O₂ concentrations between 3 and 9% by volume, the effects of detailed descriptions of the minor species pool, and changing the fuel jet composition. The combined analysis are linked in the discussion, and turbulent modelling results in physical- and mixture-fraction-space are used to explain the stabilisation mechanism of these flames. This culminates in the final results and new understanding required to address the aims of the thesis-by-publication.

References

- [1] Aminian, J., Galletti, C., Shahhosseini, S., & Tognotti, L. (2012). Numerical Investigation of a MILD Combustion Burner: Analysis of Mixing Field, Chemical Kinetics and Turbulence-Chemistry Interaction. *Flow Turbul. Combust.*, 88(4), 597–623.
- [2] Arndt, C., Gounder, J., Meier, W., & Aigner, M. (2012). Auto-ignition and flame stabilization of pulsed methane jets in a hot vitiated coflow studied with high-speed laser and imaging techniques. *Appl. Phys. B*, 108(2), 407–417.
- [3] Arndt, C. M., Schießl, R., Gounder, J. D., Meier, W., & Aigner, M. (2013). Flame stabilization and auto-ignition of pulsed methane jets in a hot coflow: Influence of temperature. *Proc. Combust. Inst.*, 34, 1483–1490.
- [4] Bhaya, R., De, A., & Yadav, R. (2014). Large Eddy Simulation of MILD combustion using PDF based turbulence-chemistry interaction models. *Combust. Sci. Technol.*, 186(9), 1138–1165.
- [5] Bray, K., Champion, M., & Libby, P. A. (1996). Extinction of premixed flames in turbulent counterflowing streams with unequal enthalpies. *Combust. Flame*, 107(1-2), 53–64.
- [6] Bureau of Resources and Energy Economics (BREE) (2013). Energy in Australia 2013. *BREE, Canberra*.
- [7] Cabra, R., Chen, J.-Y., Dibble, R., Karpetis, A., & Barlow, R. (2005). Lifted methane-air jet flames in a vitiated coflow. *Combust. Flame*, 143(4), 491–506.
- [8] Cabra, R., Myhrvold, T., Chen, J., Dibble, R., Karpetis, A., & Barlow, R. (2002). Simultaneous laser raman-rayleigh-lif measurements and numerical modeling results of a lifted turbulent H₂/N₂ jet flame in a vitiated coflow. *Proc. Combust. Inst.*, 29, 1881–1888.

-
- [9] Can Gülen, S. (2015). Étude on Gas Turbine Combined Cycle Power Plant–Next 20 Years. *J. Eng. Gas Turb. Power*, 138(5), 051701.
- [10] Cavaliere, A., & de Joannon, M. (2004). Mild Combustion. *Prog. Energ. Combust.*, 30(4), 329–366.
- [11] Choi, B., & Chung, S. (2010). Autoignited laminar lifted flames of methane, ethylene, ethane, and n-butane jets in coflow air with elevated temperature. *Combust. Flame*, 157(12), 2348–2356.
- [12] Choi, B., Kim, K., & Chung, S. (2009). Autoignited laminar lifted flames of propane in coflow jets with tribrachial edge and mild combustion. *Combust. Flame*, 156(2), 396–404.
- [13] Choi, B. C., & Chung, S. H. (2012). Autoignited laminar lifted flames of methane/hydrogen mixtures in heated coflow air. *Combust. Flame*, 159(4), 1481–1488.
- [14] Choi, S. K., Kim, J., Chung, S. H., & Kim, J. S. (2009). Structure of the edge flame in a methane-oxygen mixing layer. *Combust. Theor. Model.*, 13(1), 39–56.
- [15] Christo, F. C., & Dally, B. B. (2005). Modeling turbulent reacting jets issuing into a hot and diluted coflow. *Combust. Flame*, 142(1-2), 117–129.
- [16] Dally, B., Karpetis, A., & Barlow, R. (2002). Structure of turbulent non-premixed jet flames in a diluted hot coflow. *Proc. Combust. Inst.*, 29, 1147–1154.
- [17] De, A., Oldenhof, E., Sathiah, P., & Roekaerts, D. (2011). Numerical Simulation of Delft-Jet-in-Hot-Coflow (DJHC) Flames Using the Eddy Dissipation Concept Model for Turbulence-Chemistry Interaction. *Flow Turbul. Combust.*, 87(4), 537–567.
- [18] de Joannon, M., Matarazzo, A., Sabia, P., & Cavaliere, A. (2007). Mild Combustion in Homogeneous Charge Diffusion Ignition (HCDI) regime. *Proc. Combust. Inst.*, 31(2), 3409–3416.
- [19] de Joannon, M., Sabia, P., Cozzolino, G., Sorrentino, G., & Cavaliere, A. (2012). Pyrolytic and Oxidative Structures in Hot Oxidant Diluted Oxidant (HODO) MILD Combustion. *Combust. Sci. Technol.*, 184(7-8), 1207–1218.
- [20] de Joannon, M., Sabia, P., Sorrentino, G., & Cavaliere, A. (2009). Numerical study of mild combustion in hot diluted diffusion ignition (HDDI) regime. *Proc. Combust. Inst.*, 32(2), 3147–3154.

- [21] de Joannon, M., Sorrentino, G., & Cavaliere, A. (2012). MILD combustion in diffusion-controlled regimes of Hot Diluted Fuel. *Combust. Flame*, 159, 1832–1839.
- [22] Department of Industry, Innovation and Science (DIIS) (2015). Energy in Australia 2015. *DIIS, Canberra*.
- [23] Department of Resources, Energy and Tourism (RET) (2012). Energy White Paper 2012. *RET, Canberra*.
- [24] Dimitriades, B. (1972). Effects of hydrocarbon and nitrogen oxides on photochemical smog formation. *Environ. Sci. Technol.*, 6(3), 253–260.
- [25] Döbbeling, K., Hellat, J., & Koch, H. (2007). 25 Years of BBC/ABB/Alstom Lean Premix Combustion Technologies. *J. Eng. Gas Turb. Power*, 1, 2–12.
- [26] Duwig, C., & Dunn, M. J. (2013). Large Eddy Simulation of a premixed jet flame stabilized by a vitiated co-flow: Evaluation of auto-ignition tabulated chemistry. *Combust. Flame*, 160(12), 2879–2895.
- [27] Echehki, T., & Chen, J. H. (2003). Direct numerical simulation of autoignition in non-homogeneous hydrogen-air mixtures. *Combust. Flame*, 134(3), 169–191.
- [28] Frassoldati, A., Sharma, P., Cuoci, A., Faravelli, T., & Ranzi, E. (2010). Kinetic and fluid dynamics modeling of methane/hydrogen jet flames in diluted coflow. *Appl. Therm. Eng.*, 30(4), 376–383.
- [29] Gordon, R. L., Masri, A. R., & Mastorakos, E. (2008). Simultaneous Rayleigh temperature, OH- and CH₂O-LIF imaging of methane jets in a vitiated coflow. *Combust. Flame*, 155(1-2), 181–195.
- [30] Guyot, D., Tea, G., & Appel, C. (2015). Low NO_x Lean Premix Reheat Combustion in Alstom GT24 Gas Turbines. *J. Eng. Gas Turb. Power*, 138(5), 051503.
- [31] Ihme, M., & See, Y. C. (2011). LES flamelet modeling of a three-stream MILD combustor: Analysis of flame sensitivity to scalar inflow conditions. *Proc. Combust. Inst.*, 33, 1309–1217.
- [32] Ihme, M., Zhang, J., He, G., & Dally, B. B. (2012). Large-Eddy Simulation of a Jet-in-Hot-Coflow Burner Operating in the Oxygen-Diluted Combustion Regime. *Flow, Turbul. Combust.*, 89, 449–464.

- [33] Kulkarni, R. M., & Polifke, W. (2013). LES of Delft-Jet-In-Hot-Coflow (DJHC) with tabulated chemistry and stochastic fields combustion model. *Fuel Process. Technol.*, *107*, 138–146.
- [34] Lammel, O., Schütz, H., Schmitz, G., Lückcrath, R., Stöhr, M., Noll, B., Aigner, M., Hase, M., & Krebs, W. (2010). FLOX[®] combustion at high power density and high flame temperatures. *J. Eng. Gas Turb. Power*, *132*(12), 121503.
- [35] Li, X., Jia, L., Onishi, T., Grajetzki, P., Nakamura, H., Tezuka, T., Hasegawa, S., & Maruta, K. (2014). Study on stretch extinction limits of CH₄/CO₂ versus high temperature O₂/CO₂ counterflow non-premixed flames. *Combust. Flame*, *161*(6), 1526–1536.
- [36] Liu, W., Kelley, A., & Law, C. (2010). Flame propagation and counterflow non-premixed ignition of mixtures of methane and ethylene. *Combust. Flame*, *157*(5), 1027–1036.
- [37] Lückcrath, R., Meier, W., & Aigner, M. (2008). FLOX[®] combustion at high pressure with different fuel compositions. *J. Eng. Gas Turb. Power*, *130*(1), 011505.
- [38] Mardani, A., Tabejamaat, S., & Mohammadi, M. B. (2011). Numerical study of the effect of turbulence on rate of reactions in the MILD combustion regime. *Combust. Theor. Model.*, *15*(6), 753–772.
- [39] Masri, A. R., Cao, R., Pope, S. B., & Goldin, G. M. (2003). PDF calculations of turbulent lifted flames of H₂/N₂ fuel issuing into a vitiated co-flow. *Combust. Theor. Model.*, *8*(1), 1–22.
- [40] Medwell, P. R., Blunck, D. L., & Dally, B. B. (2014). The role of precursors on the stabilisation of jet flames issuing into a hot environment. *Combust. Flame*, *161*(2), 465–474.
- [41] Medwell, P. R., & Dally, B. B. (2012). Effect of fuel composition on jet flames in a heated and diluted oxidant stream. *Combust. Flame*, *159*(10), 3138–3145.
- [42] Medwell, P. R., & Dally, B. B. (2012). Experimental Observation of Lifted Flames in a Heated and Diluted Coflow. *Energy Fuels*, *26*(9), 5519–5527.
- [43] Medwell, P. R., Kalt, P. A. M., & Dally, B. B. (2007). Simultaneous imaging of OH, formaldehyde, and temperature of turbulent nonpremixed jet flames in a heated and diluted coflow. *Combust. Flame*, *148*(1-2), 48–61.

- [44] Medwell, P. R., Kalt, P. A. M., & Dally, B. B. (2008). Imaging of diluted turbulent ethylene flames stabilized on a Jet in Hot Coflow (JHC) burner. *Combust. Flame*, 152, 100–113.
- [45] Medwell, P. R., Kalt, P. A. M., & Dally, B. B. (2009). Reaction Zone Weakening Effects under Hot and Diluted Oxidant Stream Conditions. *Combust. Sci. Technol.*, 181(7), 937–953.
- [46] Oberlack, M., Arlitt, R., & Peters, N. (2000). On stochastic Damköhler number variations in a homogeneous flow reactor. *Combust. Theor. Model.*, 4(4), 495–510.
- [47] Oldenhof, E., Tummers, M. J., van Veen, E. H., & Roekaerts, D. J. E. M. (2010). Ignition kernel formation and lift-off behaviour of jet-in-hot-coflow flames. *Combust. Flame*, 157(6), 1167–1178.
- [48] Oldenhof, E., Tummers, M. J., van Veen, E. H., & Roekaerts, D. J. E. M. (2011). Role of entrainment in the stabilisation of jet-in-hot-coflow flames. *Combust. Flame*, 158(8), 1553–1563.
- [49] Oldenhof, E., Tummers, M. J., van Veen, E. H., & Roekaerts, D. J. E. M. (2012). Transient response of the Delft jet-in-hot coflow flames. *Combust. Flame*, 159(2), 697–706.
- [50] Plessing, T., Peters, N., & Wüning, J. G. (1998). Laseroptical investigation of highly preheated combustion with strong exhaust gas recirculation. *Proc. Combust. Inst.*, 27(2), 3197–3204.
- [51] Prathap, C., Galeazzo, F. C. C., Kasabov, P., Habisreuther, P., Zarzalis, N., Beck, C., Krebs, W., & Wegner, B. (2012). Analysis of NOX Formation in an Axially Staged Combustion System at Elevated Pressure Conditions. *J. Eng. Gas Turb. Power*, 134(3), 031507.
- [52] Sabia, P., de Joannon, M., Picarelli, A., Chinnici, A., & Ragucci, R. (2012). Modeling Negative Temperature Coefficient region in methane oxidation. *Fuel*, 91(1), 238–245.
- [53] Sabia, P., de Joannon, M., Picarelli, A., & Ragucci, R. (2013). Methane auto-ignition delay times and oxidation regimes in MILD combustion at atmospheric pressure. *Combust. Flame*, 160(1), 47–55.

-
- [54] Shabanian, S. R., Medwell, P. R., Rahimi, M., Frassoldati, A., & Cuoci, A. (2013). Kinetic and fluid dynamic modeling of ethylene jet flames in diluted and heated oxidant stream combustion conditions. *Appl. Therm. Eng.*, 52, 538–554.
- [55] Sidey, J., & Mastorakos, E. (2015). Visualization of MILD combustion from jets in cross-flow. *Proc. Combust. Inst.*, 35(3), 3537–3545.
- [56] Sidey, J., Mastorakos, E., & Gordon, R. L. (2014). Simulations of Autoignition and Laminar Premixed Flames in Methane/Air Mixtures Diluted with Hot Products. *Combust. Sci. Technol.*, 186(4-5), 453–465.
- [57] Sidey, J. A., & Mastorakos, E. (2016). Simulations of laminar non-premixed flames of methane with hot combustion products as oxidiser. *Combust. Flame*, 163, 1–11.
- [58] Solomon, S. (1999). Stratospheric ozone depletion: A review of concepts and history. *Rev. Geophys.*, 37(3), 275–316.
- [59] Sturgess, G., Zelina, J., Shouse, D. T., & Roquemore, W. (2005). Emissions reduction technologies for military gas turbine engines. *J. Propul. Power*, 21(2), 193–217.
- [60] Yoo, C. S., Richardson, E. S., Sankaran, R., & Chen, J. H. (2011). A DNS study on the stabilization mechanism of a turbulent lifted ethylene jet flame in highly-heated coflow. *Proc. Combust. Inst.*, 33, 1619–1627.
- [61] Yoo, C. S., Sankaran, R., & Chen, J. H. (2009). Three-dimensional direct numerical simulation of a turbulent lifted hydrogen jet flame in heated coflow: flame stabilization and structure. *J. Fluid Mech*, 640, 453–481.

Chapter 2

Background

The study of gaseous flames in the moderate or intense low oxygen dilution (MILD) combustion regime requires a thorough understanding of fluid dynamics, turbulence-chemistry interactions and different approaches to combustion analysis and modelling. Such a study of MILD combustion therefore requires the presentation of relevant concepts in fundamental combustion analysis, and some more detailed background specific to the analysis of MILD combustion.

2.1 Benefits of MILD Combustion

Moderate or intense low oxygen dilution (MILD) combustion technology offers a number of benefits over conventional combustion due to its unique characteristics. Reductions in emissions of nitrogen oxide and soot pollutants, flame-noise and improvements in thermal efficiency are all benefits associated with the use of MILD combustion [14]. These benefits are direct results of characteristics of the MILD combustion regime having a distributed, ‘flameless’ chemical reaction [107].

Nitrogen oxides (NO_x), are key species in formation of photochemical smog [25], and even small concentrations in the atmosphere are highly detrimental to the ozone layer [96]. Thermal NO_x is formed via the Zel’dovich mechanism, with NO formation rates doubling “for every 35 K temperature rise” near 1800 K [8]. Through the Zel’dovich mechanism, therefore, thermal NO_x are most abundant in the hottest regions of a flame. The absence of localised temperature peaks in MILD combustion is, however, a corollary of the MILD combustion requirement for well mixed of fuel and combustion products, resulting in an almost homogeneous reaction zone [14]. These characteristics of MILD combustion burners ultimately result in the most significant reduction of thermal NO_x production of any high temperature combustion technology [7]. Decreases in NO_x of up to 95% from conventional burners have been reported using 8% O_2 coflows [29], with total emissions below 10 ppm in some con-

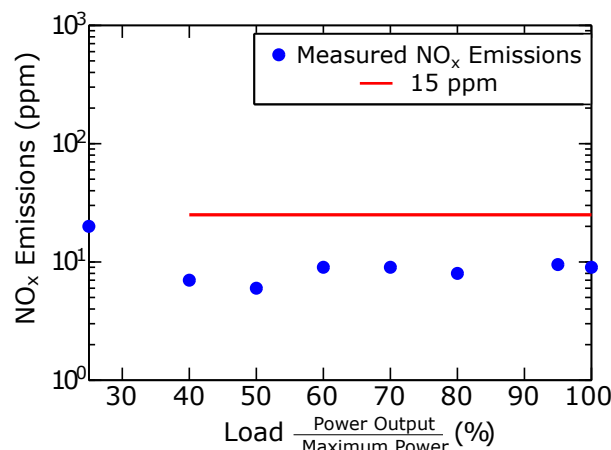


Figure 2.1. NO_x emissions from the Alstom GT24/26 at different operating loads, based on 15% O₂ air [adapted from 26].

figurations [7, 21, 107]. This level of emissions has similarly been achieved in the Alstom GT24/26 sequential gas turbine series. Measurements of emissions from the second stage combustor, operating with a 15% O₂ coflow in conditions resembling MILD, are shown in Figure 2.1. Such low NO_x emissions are characteristic of combustion in hot and diluted environments [85, 102], but may be reduced below 5 ppm using stable, MILD combustion [110]. It is crucial that NO_x pollutants be minimised in industrial and aeronautical exhausts, with MILD combustion technology offering a readily available solution.

Much of the yellow-orange light traditionally associated with fire is characteristic of heated soot particles within the flame. In the flameless MILD combustion regime, soot is not formed, and any already present is effectively ‘cleaned’ from the reacting mixture [14]. The homogeneous reaction zone is not only devoid of light emission [53], it has less acoustic emission than the equivalent, non-reacting fluid flow [107]. This essentially noiseless combustion regime is due to reduced turbulence fluctuations in the reaction zone, and hence less significant pressure undulations. The homogeneity of pressure in the combustion region dramatically reduces downstream, thermoacoustic flame-noise compared to that produced by conventional flames [107]. The clean, low vibration, exhausts extends the life of any subsequent piping and, in gas turbines applications, turbomachinery, resulting in lower equipment maintenance and exhausts devoid of soot and flame-noise.

Heat recovery in combustion processes has been widely researched, following numerous approaches and methodologies, since the nineteen-seventies [105]. This expansive body of research endeavours to increase the thermal, and hence fuel, efficiency of combustion processes. One branch of this research is heat recovery

through exhaust gas recirculation (EGR), satisfying the prerequisite of hot, well-mixed conditions for MILD combustion. Moderate or intense low oxygen dilution combustion offers superior efficiency, and lower fuel consumptions for different industrial applications and may be implemented in applications using different gaseous [54], liquid [3, 86, 87, 106, 110] and/or solid [23, 89, 91, 106] fuels. In furnace applications, MILD combustion has long been known as a higher efficiency, fuel-saving combustion mode [107] and has been successfully implemented as such [14]. Similarly, the implementation of MILD combustion in gas turbine combustors offers potential to lower combustor exit temperatures, thereby increasing the maximum achievable thermal efficiency and reducing thermal loads on turbomachinery.

Combustion with hot and diluted oxidants has been investigated experimentally and numerically in ‘laboratory-scale’ jet-in-hot-cross-/co-flow (JHC) burner, or vitiated coflow burner (VCB), configurations [4–6, 13, 21, 24, 30, 32–35, 46, 50, 55–58, 67–71, 87, 90, 91, 94, 109]. In these configurations, jets of fuel issue into coflows of hot oxidants (usually produced by combustion) with reduced oxygen concentrations compared to air (that is, <21% by volume) [21], emulating the environment of furnaces with EGR or sequential gas turbines. The use of laboratory-scale JHC burners, and VCBs, provide a platform to extend the fundamental understanding of both conventional autoignition and the MILD combustion regime.

Through implementing MILD combustion processes in industrial burners, thermal and fuel efficiencies may be significantly increased. This efficiency increase is beneficial for the operator, demanding lower fuel consumption and reducing overhead costs which may benefit both industry and consumers. The combination of environmental and economic benefits of MILD combustion highlight its compelling advantages for incorporation into the next generation of furnaces and burner systems.

2.2 Fluid Mechanics and Combustion

Jet flames are governed by a combination of fluid mechanics and combustion chemistry. The combination of these aspects results in a complex problem for computational simulation, requiring appropriate modelling of the turbulent fluid flow, the combustion chemistry and their interaction.

2.2.1 Fluid Mechanics, Turbulent Flow and The Reynolds Number

The term ‘fluid’ encompasses two of the states of matter, gases and liquids. As with all matter, fluids are bound by the fundamental physical laws of mass, energy and momentum conservation from which the governing equations of fluid flow, the

Navier-Stokes equations may be derived. The set of three Navier-Stokes equations govern the mechanics of any Newtonian fluid, however, no general, analytical solution is currently known to exist describing any and every applicable fluid under arbitrary conditions. To understand the motion of liquids and gases, therefore, fluid flow is classified into the regimes of laminar and turbulent dynamics. Laminar and turbulent regimes differ by the influence of viscous dissipation on the momentum of the flow, relative to fluid momentum. The ratio of these is given by the non-dimensional parameter, the Reynold number (Re). The Reynolds number may be derived by non-dimensionalising the Navier-Stokes equations, and is defined as:

$$Re \equiv \frac{\rho u D}{\mu} \quad (2.1)$$

or,

$$Re = \frac{uD}{\nu}, \quad (2.2)$$

where D is some characteristic length (such as the diameter of a circular pipe), u the fluid flow speed, ρ the fluid density, μ the dynamic viscosity and ν the kinematic viscosity defined as μ/ρ .

Fluid flow through a length of pipe is generally considered turbulent for $Re \geq 4000$ and laminar for $Re \leq 2100$, or transitional between these values [66]. These values are not universal as, conversely, fluid flow over a flat plate begins to transition from laminar to turbulent at Re of approximately 50 000 [66].

A characteristic of turbulent flows is the formation of rotational eddies within the flow. In these cases, velocity may be described as some fluctuating component (u') about \bar{u} , in a common assumption known as 'Reynolds averaging' [66]. Eddies move chaotically and take a range of sizes from some largest, characteristic scale of a flow (L), to the Kolmogorov length scale [99]. This range is populated by eddies which eventually lose energy to friction through viscous damping, stretch and cascade from lengths of $L = (u'_{rms})^3/\varepsilon$ to the smallest scale eddies. The size of the smallest eddies is referred to as the Kolmogorov length scale, $l_\eta = (\nu^3/\varepsilon)^{1/4}$, and have time scales of $\tau_\eta = (\nu/\varepsilon)^{1/2}$, where ε is the dissipation rate of turbulent eddies [80, 99]. The turbulent kinetic energy of the flow as k equal to the sum of half the mean-squared velocity fluctuations in each direction. With the assumption of isotropic turbulence, this reduces to k being three halves of the mean-square of velocity fluctuation, $\frac{3}{2}(u'_{rms})^2$. A turbulent Reynolds number has subsequently been defined by [80] for eddy length scales, such that:

$$Re_t \equiv \frac{u'_{rms} L}{\nu}, \quad (2.3)$$

which may be written in terms of k , ν and ε as:

$$Re_t = \frac{4}{9} \frac{k^2}{\nu \varepsilon}. \quad (2.4)$$

This non-dimensional relationship may be calculated directly using quantities solved for in the k - ε turbulence model. Turbulence models use approximations for relationships, such as those between k and ε , in fully turbulent flows to simplify the Navier-Stokes equations, facilitating numerical simulation of turbulent fluid flows.

2.2.2 Combustion and the Damköhler Number

The concept of combustion is commonly taken to imply infinitely fast, exothermic reactions of some fuel and oxidiser combination, initiating in a hot environment. Combustion is thus a culmination of the interplay between the physical mixing of matter and the governing chemistry of the associated reactions. The dynamics of combustion vary depending on the state of the fuel, whether it is solid, liquid or gaseous, and the temperature (T) of the resulting reaction zone controlling the rates of different reactions. Turbulent combustion of a fluid fuel is controlled by the time scale of fluctuations in the turbulence field ($\tau_{fluid} \approx L/u'$) and the reaction time-scale (τ_{chem}). The latter time scale may be estimated as phenomenologically the ratio of laminar flame width (δ) to laminar flame speed (s_L^0) [100], or numerically as the time scale of slowest chemical reaction [37, 73]. The dimensionless ratio of these time two scales defines the Damköhler number (Da):

$$Da \equiv \frac{\tau_{fluid}}{\tau_{chem}}. \quad (2.5)$$

Writing this in terms of δ and s_L^0 gives:

$$Da = \frac{L/u'}{\delta/s_L^0}. \quad (2.6)$$

This Da may be related to Re_t through the Karlovitz number (Ka) [80] as:

$$Ka \equiv \left(\frac{L}{\delta}\right)^{-1/2} \left(\frac{u'}{s_L^0}\right)^{3/2} = Re_t^{1/2} Da^{-1} \quad (2.7)$$

or:

$$Re_t = Da^2 Ka^2. \quad (2.8)$$

Combustion regimes may be broadly categorised by $Da \gg 1$, $Da \ll 1$ and $Da \sim 1$. These regimes physically describe fast chemistry compared to turbulence,

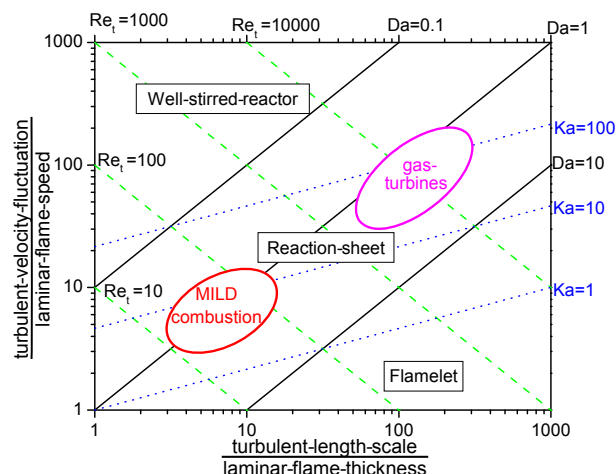


Figure 2.2. Borghi diagram highlighting approximate operating regions for gas turbines, and MILD combustion in a jet-in-hot-coflow (JHC) burner [72], showing combustion regimes and lines of constant Re_t , Da and Ka [adapted from 41].

slow chemistry and combustion heavily dependent on both turbulent and chemical time scales, and may be summarised on a Borghi diagram, as shown in Figure 2.2. This figure shows combustion regimes, where conventional combustion is characterised by flames with $Da \gg 1$ and may be described as a series of laminar flamelets within turbulent structures, each with infinitely fast chemistry, dominated by characteristics of the turbulent flow and hence Re . Many combustion devices typically employ Re_t of 100-2000, where flow mixing is dominated by momentum rather than viscous dissipation [80]. The well-stirred reactor of $Da \ll 1$ is, conversely, completely chemistry dominated with the reactions heavily dependent on the rates of the many chemical reactions in the reaction zone on the assumption that variations in the reactant composition due to turbulent mixing are negligible. Flames in the MILD combustion regime, in contrast, typically lie between these aforementioned domains, with $Da \sim 1$ and $Re_t \sim 10$ [72]. Figure 2.2 shows the strong dependence of reactions in combustion systems such as gas turbines on both chemical and fluid time scales. These similar time scales require that chemistry is represented by finite-rate chemical kinetics, which estimate the time scales of individual chemical reactions (to be discussed in §2.3.2). In cases with $Da \sim 1$, consideration must be given to both the turbulence and chemistry aspects of combustion, indicating that both Re_t and the reaction rates of separate chemical species are crucial to the understanding of combustion in these regimes encompassing both gas turbine and MILD combustion systems.

To analyse combustion at different turbulent length scales in the MILD regime, Mardani *et al.* [50] introduced the turbulence and first Damköhler numbers (Da_T

and Da_f respectively) corresponding to Da at the Kolmogorov length scale and in the large-scale eddies. These are scaled by the reaction rate constant (c_r), defined as the maximum chemical reaction rate divided by fluid density [50]. The dimensionless Da_T and Da_f are defined in Equations 2.9 and 2.10 as:

$$Da_T \equiv \left(\frac{\nu c_r^2}{\varepsilon} \right)^{1/2} \quad (2.9)$$

and

$$Da_f \equiv \frac{c_r}{\text{Local strain rate}}. \quad (2.10)$$

The demarcation of combustion regimes through the use of dimensionless numbers such as Re , Re_t , Da and Ka , allows for the analysis of different modelling approaches and approximations. This expedites the categorisation of tools into those which are, and are not, appropriate for studying flames in the MILD combustion regime.

2.3 Numerical and Analytical Tools for Combustion Research

The interplay between fluid mechanics and chemistry in combustion processes results in a highly non-linear system for which no exact, analytical solutions are available. The complexity of combustion processes subsequently requires analyses through numerical tools, with varying levels of fidelity, or the analytical study of representative, idealised systems.

2.3.1 Computational Fluid Dynamics

Computational fluid dynamics (CFD) is the generic term used for numerical tools for used to predict fluid flows. Various forms of CFD, with different degrees of modelling, are widely used in simulating combustion and combustion research for stand-alone studies, or to complement, and expand upon, experimental research. These range from direct numerical simulations (DNS), which does not include any modelling of terms in the Navier-Stokes equations, to the computationally cheapest form of CFD, which assumes Reynolds-averaged Navier-Stokes (RANS) models of all turbulent fluctuations in a flow.

Direct numerical simulations solve the Navier-Stokes equations starting from an initial flow-field, capturing the entire flow from the macro- to micro-scales. Such DNS tools have been employed in several investigative campaigns of both turbulent flames in hot coflows [59, 111, 112], and well-mixed MILD combustion in isotropic turbulence [60–65]. Although DNS studies provide very high fidelity re-

sults, simulations of jet flames with $Re \sim 10\,000$ require $\sim 10^9$ computational cells [59, 111, 112], and $\sim 10^6$ CPU-hours of computational time [111, 112] to obtain statistically-converged solutions. The minimal modelling implemented in DNS not only requires high fidelity numerical schemes but very fine computational grids. However, the analysis of trends across series of jet flames under a range of different conditions may have the potential to offer additional physical insight over the simulation of a single flame scenario. In such circumstances, where numerous cases are required to understand the effects of changing conditions, the overhead required for DNS results in this technique being prohibitively [computationally] expensive.

Turbulence may be simulated on a wide range of length scales, from momentum driven large eddies which cascade down to eddies at the Kolmogorov scale (recall §2.2.1) which, in turn, are dissipated due to viscosity. The primary approach of directly resolving larger turbulent structures, whilst modelling the subgrid region within computational cells, is large eddy simulation (LES). The accuracy of this approach is heavily dependent on the turbulence-chemistry interaction model implemented, and demonstrates significant sensitivity to both the inlet boundary conditions and the quality of the computational grid. Large eddy simulation has demonstrated reasonable accuracy in modelling the turbulent interactions in jet flames, reproducing velocity and mixing profiles between the jet and oxidant streams with superior accuracy to RANS [9, 36, 40]. Despite this, the results of reacting models using LES have not performed significantly better than RANS models in prediction of temperature and species distributions in the jet near-field [9, 40].

The majority of CFD simulations of MILD and autoignited jet flames have used RANS turbulence models for reasons of computational efficiency. Despite the improved modelling of turbulence in LES, the significantly increased computational demand suggests that this is not a viable alternative to RANS models with complex chemistry. Much research has gone into numerical models of turbulence, with many previous studies of MILD combustion of jet flames successfully validating the modified $k-\varepsilon$ turbulence model of Dally *et al.* [22] for axisymmetric jets [1, 16, 24, 30, 50, 51, 93, 103]. These models of turbulence may be coupled with descriptions of chemical kinetics to provide a range of modelling frameworks for reacting flows with $Da \gg 1$, $Da \ll 1$ or $Da \sim 1$.

2.3.2 Chemical Kinetics

The most simple turbulence-chemistry interaction models use a minimal number of empirically determined, equilibrium-based reactions, sacrificing details of hydrocarbon oxidation for computational speed [100], in what is often referred to as a

'global mechanism'. Global mechanisms typically summarise chemical processes in one to three reactions, and provide estimations of temperature, and major reactant and product species. These simplified chemical mechanisms do not estimate the formation of intermediary chemical species and hence are, by their definition, inappropriate for research of chemical and turbulence-chemistry interactions, being better suited as a preliminary design tool for combustion systems.

Finite-chemical kinetics schemes describe sets of elementary, chemical reactions which form a complex, potentially numerically stiff, highly non-linear system of coupled rate equations [43]. Each elementary reaction is dependent on temperature, local concentration and pressure. Temperature dependence of reaction rates takes the form of an Arrhenius equation, which is then linearly coupled with species concentrations [39]. Additionally, the pressure dependence of elementary reactions may be accounted for through one of several different models [39]. Chemical kinetics schemes describe the roles of intermediary species with different levels of detail, ranging from the most complex detailed mechanisms, to skeletal kinetics schemes. Detailed kinetics mechanisms for hydrocarbons often feature 4-6 reactions per included species, although this number may be as high as 35 in schemes which "lump" a variety of different intermediary species (such as isomers) and reactions for complex fuels [20, 82]. Detailed kinetics schemes may be reduced to form skeletal mechanisms, which target specific fuels and combustion characteristics (such as flame speeds, ignition delays and/or species formation) for a given problem [97], but may not be applicable outside of their target conditions [16]. Examples of detailed kinetics schemes include:

- The "GRI-Mech 3.0" mechanism for high temperature combustion of CH_4 and natural gas (NG), including NO_x formation, with 53 species and 325 reactions [95].
- The "San Diego" (or "UCSD") mechanism for high temperature combustion of C_2H_4 which is updated intermittently (and may be complemented with additional sub-mechanisms for nitrogen and/or larger fuels) – the August 2016 version contains 50 species and 247 reactions [101].
- The "USC-II C_2H_x " mechanism, also for high temperature combustion of C_2H_4 , with 75 species and 529 reactions [104].
- The full "USC-II" mechanism for high temperature combustion of fuels with up to four carbon atoms (per molecule), with 111 species and 784 reactions [104].

- The “POLIMI” mechanism, which is regularly updated and available with or without low temperature chemistry and with or without NO_x reactions – the December 2014 version of the POLIMI C1-C3 scheme for high and low temperature combustion of fuels with up to three carbon atoms (per molecule) contains 107 species and 2642 reactions [83].

The choice of chemical kinetics scheme can have a significant impact on the accuracy of modelled results, especially under MILD combustion conditions [16, 88, 93], and the computational cost required to obtain a solution. Chemical kinetics schemes must therefore be chosen appropriately for different fuels and conditions.

2.3.3 Laminar Flames and Flamelet Theory

Chemical reaction rates may be evaluated numerically in laminar flames, after modelling the transport of species through convection and diffusion in one, two or three dimensions [19, 20]. Details of the process for such an approach is given by Cuoci *et al.* in their descriptions of the ‘laminarSMOKE’ solver developed on the ‘OpenFOAM’ framework [18, 19]. In numerical simulations of flames, the diffusive transport of chemical species may be treated with different degrees of physical accuracy, with the most detailed multicomponent diffusion treatment involving the calculation of a species diffusion coefficient with respect to every other nearby species [19]. This approach to diffusion modelling is also applicable to turbulent combustion. In this sense, laminar flames may be simulated directly in arbitrary configurations, to within the combined accuracy of the numerical, chemical kinetics and molecular transport schemes implemented in the solver.

The simplest configuration for non-premixed combustion is the laminar opposed-flow flame. In this scenario, oxidant (*O*) and fuel (*F*) streams issue from nozzles which are directed at one-another, resulting in laminar, diffusive mixing of the fuel and oxidant. At any given point in the flame, the local composition contains some portion of mass from the fuel stream, and some from the oxidant stream. The mixing of these streams results in the definition of the mixture fraction (*Z*):

$$Z \equiv \frac{m_F}{m_F + m_O} \quad (2.11)$$

which varies across the flame front, where *m* denotes the mass originating from each stream. This *Z*-field is non-trivial to evaluate where the transport of different molecular species are calculated, and reactions occur. As such, *Z* may be estimated by comparing the local atomic mass fractions (for example, *Y_H* or *Y_O*) and their mass fractions in the pure, unmixed fuel and oxidant streams [10, 11]. In the case where

m_F and m_O produce complete combustion (that is, fuel and oxidants may be balanced exactly with H_2O and CO_2), Z is known as the stoichiometric (*st*) mixture fraction (Z_{st}). Owing to the symmetry of this configuration, the centreline of laminar opposed-flow flames may be simulated directly (without restrictions on Da or the treatment of species diffusion) [with software such as 84], or rewritten in terms of a scalar Z . In the laminar opposed-flow flame configuration, Z varies monotonically with distance between the two nozzles, and hence may be used as a coordinate system for the flame [74].

Non-premixed laminar flame behaviour may be described in a Z -space coordinate system. This gives rise to the flamelet equations which couple the temperature (T) and the mass fraction of individual species (Y_i) with Z , the reaction rate of that species (R_i), and the diffusivity of Z (D_Z) [74]. The variable D_Z is taken to be representative of Z , and the term in which it appears in the flamelet equations may be replaced by the scalar dissipation rate (χ) [74], equal to:

$$\chi \equiv 2D_Z|\nabla Z|^2. \quad (2.12)$$

This χ may be considered as the inverse of the fluid residence time (τ_{res}), which may be taken as τ_{fluid} [44, 45]. The temperature and species-distributions may then be solved numerically using numerical packages [such as 77], or approximated analytically – often assuming simplified chemistry and diffusion characteristics [42, 74, 75, 79].

Solving the steady-state reactions for non-premixed flamelets over a range of χ produces a characteristic curve for each variable, with constant Z . In the case of T versus χ , for a simple fuel, this curve resembles a reversed “S” and is termed an “S-shaped curve” [74] (note that T versus τ_{res} would resemble an “S”). An illustration of an S-shaped curve is presented in Figure 2.3, which shows points of autoignition and extinction (which will be described in more detail), the ‘unburnt’, or initial, ‘mixing’ temperature (T_u or T_0) and how the ‘fully burning’ solution approaches the adiabatic flame temperature (T_{ad} or T_b) for very low χ . The S-shaped curve has three branches: the mixing, burning and unstable branches. In such a flamelet, autoignition of an unburnt mixture occurs for any χ less than that of the autoignition point, and the steady-state flamelet solution shifts to the burning branch. Once in a burning state, χ may be increased until the solution reaches the extinction (quenching) point, beyond which the flame extinguishes, and the solution returns to the mixing branch. This illustrates the hysteresis inherent in conventional autoignitive combustion.

Flamelets may be solved numerically, analytically, at steady-state or transiently.

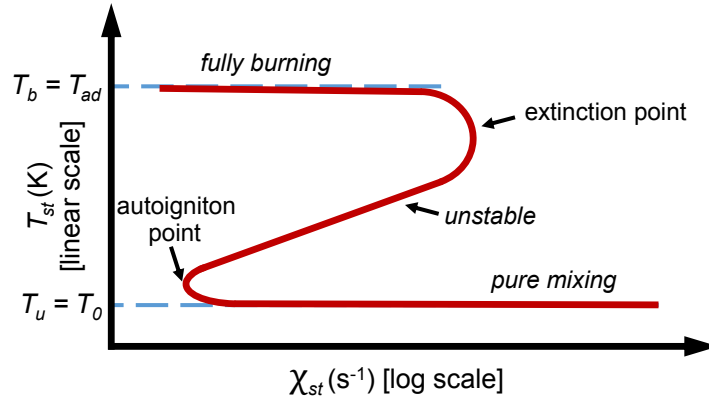


Figure 2.3. An annotated illustration of a stoichiometric S-shaped curve, plotted as T versus χ , showing autoignition and extinction (quenching) points, the temperatures of the ‘pure mixing’ and ‘fully burning’ branches, and the third ‘unstable’ branch. Note that the mixing solution is also referred to as ‘unburnt’ (hence T_u) or initial (T_0) solution, whilst the temperature of the fully burning solution tends towards the adiabatic flame temperature (T_{ad} or T_b) for very low χ .

These approaches may use either an predefined (Z, χ) -field or, more commonly, an empirical relationship between Z and a set of predefined χ calculated using the Chapman gas approximation: $D_Z \sim \rho^{-2}$ [76]. Numerically, solutions may use complex chemical kinetics, and species-specific diffusivities, albeit maintaining a constant ratio of heat to mass diffusivity for a given species – a ratio known as the Lewis number (Le) [80]. This results in a set of temperature and species concentrations calculated for any combination of Z and χ , which may be examined individually, or tabulated of further CFD analyses.

Analytically, flamelets are often examined with the assumption of single-step, global kinetics and Le of unity [12, 78, 79, 92]. Such analyses lead to flamelet equations coupling the consumption of a single fuel and a single oxidant species to the production of a single product species and the resulting temperature [79]. This, in turn, results in an analytical expression for the flamelets, and results in an expression for the S-shaped curve [79]. In this case, χ is a quintic function of T for arbitrary values of Z , however this reduces to a cubic for the stoichiometric flamelet [79]. This simple relationship facilitates algebraic calculation of idealised laminar opposed-flow flames and phenomenological analysis of their behaviour under a range of conditions.

The assumptions required for numerical and analytical flamelet analyses limit the accuracy and validity of this approach, under general conditions. These restrictions impose conditions on the interpretation of flamelet solutions, which must be taken into account when using flamelets as a stand-alone tool, or in conjunction

with CFD modelling.

2.3.4 Modelling Turbulence-Chemistry Interactions

The interactions between turbulence and chemistry in a reacting fluid flow may be modelled using a number of different approaches. In CFD employing RANS or LES, the direct calculation of reaction rates as done in laminar flames is not physically realistic. Different approaches to modelling turbulence-chemistry interactions are therefore required, using global or detailed chemistry, which in turn may use infinitely fast or finite-rate chemistry. Each different modelling technique offers different degrees of accuracy and computational speed, and hence have their own advantages for modelling turbulent combustion.

Conventional combustion is, recalling §2.2.2, driven by fluid turbulence with high Da facilitating the approximation of infinitely fast chemical reaction rates. Computational models of such combustion processes may use this approximation to integrate rudimentary chemistry into the simulated results. Global reactions may be coupled to the flow-field using the “Eddy Dissipation Model” (EDM), developed by Magnussen & Hjertager [47] in 1977. In this model, reactions occur in any computational cell with both fuel and oxidant, and the chemical reaction rate is controlled by a simple relationship of turbulence variables in the flow-field. Subsequently, these reaction rates are empirically limited to avoid excessive temperatures and oversized reaction zones [24]. The EDM approach to combustion modelling is therefore not appropriate for scientific studies on flame stabilisation, due to its simplified approach to modelling combustion processes.

Detailed chemistry offers significant advantages over global mechanisms in the accuracy of the solutions produced by modelling minor species within flows. One approach to modelling detailed, fast chemistry in high Da flames uses the flamelet combustion model, based on the concept of flamelets introduced previously in §2.2.2 and discussed in §2.3.3. Phenomenologically, this treats each small region of a turbulent flame front as the interface between an opposed fuel and oxidant stream. Flamelet combustion models are based on the transport of a scalar Z within a flame (where $Z = 1$ at the fuel inlets and 0 at the oxidant inlets), and the local χ . This approach deconstructs complex combustion interactions into small, individual flamelets governed by local concentrations and strain rates [76]. This approach is not particularly computationally intensive, using tabulated data from pre-calculated flamelets and inherently assumes high Da . This assumption is required to confine reaction zones within individual, independent flamelets which do not interact and are not strongly affected by diffusion [75]. These offer insights

into the composition of minor species with only a slightly greater computational cost than the EDM, without the computational overhead of calculating chemical reaction rates and equilibrium temperatures with each iterative approximation of the flow-field. Derivatives of the flamelet model were shown to predict conditions within a MILD combustion furnace [17], despite significant flamelet-flamelet interactions involved at a micro-scale in MILD combustion [61, 63–65]. Ultimately, however, pre-tabulated flamelet approaches have been shown to be inadequate for use in modelling MILD conditions in a jet-in-hot-coflow (JHC) burner [16, 93] without high fidelity modelling of turbulent structures through the use of LES [35, 36].

In modelling turbulent flames in the MILD combustion regime, Christo & Dally [16] found the EDM and scalar-transport-based combustion models to be inferior to the more sophisticated “Eddy Dissipation Concept” (EDC) combustion model. Notably, the EDC model is sometimes mistaken for its significantly cruder forebear [27, 80] – the EDM [47]. The EDC model, originally presented in 1981 by Magnussen [48] as an advancement of the EDM [47], uses detailed, finite-rate chemical kinetics and a turbulence governed mean reaction rate, to model combustion within small turbulent structures in a fluid. Unlike tabulated flamelets, this approach transports species individually and facilitates a detailed description of multicomponent diffusion. The EDC model therefore better simulates the chemical reaction rates which influence the dynamics of the MILD regime with near unity Da , following the discussion in §2.2.2.

The EDC combustion model assumes reaction rates occur in “fine structures” which may be treated as isobaric, perfectly-stirred reactors [72]. The mean reaction rate (R_i) of a given species, i , within a small turbulent structure is described by Equation 2.13. These fine structures theoretically exist in size scales proportional to, and on the order of magnitude of, the Kolmogorov length scale, l_η [49] (defined in §2.2.1). Equation 2.13 includes the mean residence time (τ^*) spent within fine structures, which is proportional to τ_η , and the length fraction (ξ^*), both of which are scaled by user-changeable parameters C_τ and C_ξ [28], which have default values derived by Magnussen [48, 49]. The equations defining τ^* and ξ^* are shown in Equations 2.14 and 2.15 respectively. The mean R_i is given by:

$$R_i = \frac{\rho(\xi^*)^2}{\tau^*[1 - (\xi^*)^3]}(Y_i^* - Y_i) \quad (2.13)$$

where ρ is density, Y_i the mass fraction of species i in a computational cell, Y_i^* is Y_i within a fine structure. Additionally:

$$\tau^* = C_\tau \left(\frac{\nu}{\varepsilon} \right)^{1/2} \quad (2.14)$$

where $C_\tau = 0.4082$ (default), ν is the kinematic viscosity, ε the turbulent dissipation rate, and:

$$\xi^* = C_\xi \left(\frac{\nu \varepsilon}{k^2} \right)^{1/4} \quad (2.15)$$

where $C_\xi = 2.1377$ (default) and k is the turbulent kinetic energy. Finally, combining these equations, the mean reaction rate may be rewritten as:

$$R_i = \frac{C_\xi^2}{C_\tau} \left[1 - C_\xi^3 \left(\frac{\nu \varepsilon}{k^2} \right)^{3/4} \right]^{-1} \frac{\rho \varepsilon}{k} (Y_i^* - Y_i), \quad (2.16)$$

or, using the definition of turbulent Reynolds number (Re_t) from Equation 2.4:

$$R_i = \frac{C_\xi^2}{C_\tau} \left[1 - C_\xi^3 \left(\frac{9}{4} Re_t \right)^{-3/4} \right]^{-1} \frac{\rho \varepsilon}{k} (Y_i^* - Y_i). \quad (2.17)$$

The finite-rate EDC model was found by Christo & Dally [16] to model combustion of CH_4/H_2 flames in a JHC burner with reasonable accuracy in regions without local extinction or apparent lift-off. The suitability of this turbulence-chemistry model was further confirmed with a later study on a different burner, also operating in the MILD regime [31], whilst more recent work has extended the functionality of the EDC to estimate local extinction with significant success [2]. Further investigations using the EDC model have studied the effects of variation of the EDC parameters, boundary conditions or the detail of chemical kinetics (and will be elaborated on in §3.4.1).

The finite-rate, detailed chemistry, ‘‘Probability Density Function’’ (PDF) transport model of Pope [81], in contrast to the EDC combustion model, estimates paths for reacting species as particles in the flow rather than approximating them as fractions of the fluid. The PDF transport model is directly derived from the Navier-Stokes equations without the requirement of modelling the mean reaction rate of different chemical species. This modelling aspect in the EDC model is a direct result of Reynolds averaging, whereby a flow is separated into time averaged and fluctuating components, and avoidance of this assumption allows ‘‘arbitrarily complicated reactions [to] be treated without approximation’’ [81]. The PDF model is hence devoid of reaction rate equations based on turbulence model, however computational cost is significantly increased by the Eulerian or Lagrangian (which will be used in the current work) tracking a user-set number of reacting particles per compu-

tational cell.

The paths of reacting particles in the PDF transport model are predicted using the flow-field, and particle pairs for reactions selected by different means according to the choice of mixing model [93]. Particle diffusion and pair selection can be determined in a number of ways in PDF transport models, however the most accurate albeit computationally demanding, is the “Euclidean Minimum Spanning Tree” (EMST) method, which determines particle reaction likelihood as a function of proximity within a computational cell [52, 98]. This process is repeated a user-set number of times at each flow-field iteration in order to determine the mean species compositions, and the approximate error in these estimates. Statistical error in this model scales by the inverse square of the number of particles per cell [108], with the number of iterations required for convergence decreasing with increasing number of particles [38]. The number of particles per cell does, of course, subsequently increase the time-taken per iteration and hence computational cost, with the benefit of superior physical representation of species concentrations and hence accuracy. Greater accuracy in modelling MILD combustion in a JHC burner has been shown using the PDF model, as opposed to the EDC model [15, 93], although this comes at the cost of significantly increased computational solver time.

References

- [1] Aminian, J., Galletti, C., Shahhosseini, S., & Tognotti, L. (2012). Numerical Investigation of a MILD Combustion Burner: Analysis of Mixing Field, Chemical Kinetics and Turbulence-Chemistry Interaction. *Flow Turbul. Combust.*, 88(4), 597–623.
- [2] Aminian, J., Galletti, C., & Tognotti, L. (2016). Extended EDC local extinction model accounting finite-rate chemistry for MILD combustion. *Fuel*, 165, 123–133.
- [3] Arghode, V. K., Khalil, A. E., & Gupta, A. K. (2012). Fuel dilution and liquid fuel operational effects on ultra-high thermal intensity distributed combustor. *Appl. Energ.*, 95, 132–138.
- [4] Arndt, C. M., Papageorge, M. J., Fuest, F., Sutton, J. A., Meier, W., & Aigner, M. (2016). The role of temperature, mixture fraction, and scalar dissipation rate on transient methane injection and auto-ignition in a jet in hot coflow burner. *Combust. Flame*, 167, 60–71.
- [5] Arndt, C. M., Schießl, R., Gounder, J. D., Meier, W., & Aigner, M. (2013). Flame

- stabilization and auto-ignition of pulsed methane jets in a hot coflow: Influence of temperature. *Proc. Combust. Inst.*, 34, 1483–1490.
- [6] Arteaga Mendez, L., Tummers, M., van Veen, E., & Roekaerts, D. (2015). Effect of hydrogen addition on the structure of natural-gas jet-in-hot-coflow flames. *Proc. Combust. Inst.*, 35(3), 3557–3564.
- [7] Ayoub, M., Rottier, C., Carpentier, S., Villiermaux, C., Boukhalfa, A., & Honoré, D. (2012). An experimental study of mild flameless combustion of methane/hydrogen mixtures. *Int. J. Hydrogen Energ.*, 37(8), 6912–6921.
- [8] Beér, J. M. (1994). Minimizing NO_x emissions from stationary combustion; reaction engineering methodology. *Chem. Eng. Sci.*, 49(24, Part A), 4067–4083.
- [9] Bhaya, R., De, A., & Yadav, R. (2014). Large Eddy Simulation of MILD combustion using PDF based turbulence-chemistry interaction models. *Combust. Sci. Technol.*, 186(9), 1138–1165.
- [10] Bilger, R. (1989). The structure of turbulent nonpremixed flames. *Proc. Combust. Inst.*, 22(1), 475–488.
- [11] Bilger, R., Stårner, S., & Kee, R. (1990). On reduced mechanisms for methane · air combustion in nonpremixed flames. *Combust. Flame*, 80(2), 135–149.
- [12] Bray, K., Champion, M., & Libby, P. A. (1996). Extinction of premixed flames in turbulent counterflowing streams with unequal enthalpies. *Combust. Flame*, 107(1-2), 53–64.
- [13] Cabra, R., Myhrvold, T., Chen, J., Dibble, R., Karpetis, A., & Barlow, R. (2002). Simultaneous laser raman-rayleigh-lif measurements and numerical modeling results of a lifted turbulent H₂/N₂ jet flame in a vitiated coflow. *Proc. Combust. Inst.*, 29, 1881–1888.
- [14] Cavaliere, A., & de Joannon, M. (2004). Mild Combustion. *Prog. Energ. Combust.*, 30(4), 329–366.
- [15] Christo, F. C., & Dally, B. B. (2004). Application of transport PDF approach for modelling MILD combustion. In *Proceedings of the Fifteenth Australian Fluid Mechanics Conference*. The University of Sydney, Sydney, Australia: The University of Sydney, Sydney, Australia.
- [16] Christo, F. C., & Dally, B. B. (2005). Modeling turbulent reacting jets issuing into a hot and diluted coflow. *Combust. Flame*, 142(1-2), 117–129.

- [17] Coelho, P., & Peters, N. (2001). Numerical simulation of a mild combustion burner. *Combust. Flame*, 124(3), 503–518.
- [18] Cuoci, A., Frassoldati, A., Faravelli, T., & Ranzi, E. (2013). A computational tool for the detailed kinetic modeling of laminar flames: Application to C_2H_4/CH_4 coflow flames. *Combust. Flame*, 160(5), 870–886.
- [19] Cuoci, A., Frassoldati, A., Faravelli, T., & Ranzi, E. (2013). Numerical Modeling of Laminar Flames with Detailed Kinetics Based on the Operator-Splitting Method. *Energy Fuels*, 27(12), 7730–7753.
- [20] Cuoci, A., Frassoldati, A., Faravelli, T., & Ranzi, E. (2015). OpenSMOKE++: An object-oriented framework for the numerical modeling of reactive systems with detailed kinetic mechanisms. *Comput. Phys. Commun.*, 192, 237–264.
- [21] Dally, B., Karpetis, A., & Barlow, R. (2002). Structure of turbulent non-premixed jet flames in a diluted hot coflow. *Proc. Combust. Inst.*, 29, 1147–1154.
- [22] Dally, B. B., Fletcher, D. F., & Masri, A. R. (1998). Flow and mixing fields of turbulent bluff-body jets and flames. *Combust. Theor. Model.*, 2(2), 193–219.
- [23] Dally, B. B., Shim, S. H., Craig, R. A., Ashman, P. J., & Szegö, G. G. (2010). On the Burning of Sawdust in a MILD Combustion Furnace. *Energy Fuels*, 24(6), 3462–3470.
- [24] De, A., Oldenhof, E., Sathiah, P., & Roekaerts, D. (2011). Numerical Simulation of Delft-Jet-in-Hot-Coflow (DJHC) Flames Using the Eddy Dissipation Concept Model for Turbulence-Chemistry Interaction. *Flow Turbul. Combust.*, 87(4), 537–567.
- [25] Dimitriadis, B. (1972). Effects of hydrocarbon and nitrogen oxides on photochemical smog formation. *Environ. Sci. Technol.*, 6(3), 253–260.
- [26] Döbbeling, K., Hellat, J., & Koch, H. (2007). 25 Years of BBC/ABB/Alstom Lean Premix Combustion Technologies. *J. Eng. Gas Turb. Power*, 1, 2–12.
- [27] Echekki, T., & Mastorakos, E. (2011). *Turbulent Combustion Modeling: Advances, New Trends and Perspectives*, vol. 95. Springer Science & Business Media.
- [28] *FLUENT Theory Guide* (2012). ANSYS Inc.

- [29] Flamme, M. (2001). Low NO_x combustion technologies for high temperature applications. *Energ. Convers. Manage.*, 42(15-17), 1919–1935.
- [30] Frassoldati, A., Sharma, P., Cuoci, A., Faravelli, T., & Ranzi, E. (2010). Kinetic and fluid dynamics modeling of methane/hydrogen jet flames in diluted coflow. *Appl. Therm. Eng.*, 30(4), 376–383.
- [31] Galletti, C., Parente, A., & Tognotti, L. (2007). Numerical and experimental investigation of a mild combustion burner. *Combust. Flame*, 151, 649–664.
- [32] Gordon, R. L., Masri, A. R., & Mastorakos, E. (2008). Simultaneous Rayleigh temperature, OH- and CH_2O -LIF imaging of methane jets in a vitiated coflow. *Combust. Flame*, 155(1-2), 181–195.
- [33] Gordon, R. L., Masri, A. R., & Mastorakos, E. (2009). Heat release rate as represented by $[\text{OH}] \times [\text{CH}_2\text{O}]$ and its role in autoignition. *Combust. Theor. Model.*, 13(4), 645–670.
- [34] Gordon, R. L., Masri, A. R., Pope, S. B., & Goldin, G. M. (2007). A numerical study of auto-ignition in turbulent lifted flames issuing into a vitiated co-flow. *Combust. Theor. Model.*, 11(3), 351–376.
- [35] Ihme, M., & See, Y. C. (2011). LES flamelet modeling of a three-stream MILD combustor: Analysis of flame sensitivity to scalar inflow conditions. *Proc. Combust. Inst.*, 33, 1309–1217.
- [36] Ihme, M., Zhang, J., He, G., & Dally, B. B. (2012). Large-Eddy Simulation of a Jet-in-Hot-Coflow Burner Operating in the Oxygen-Diluted Combustion Regime. *Flow, Turbul. Combust.*, 89, 449–464.
- [37] Isaac, B. J., Parente, A., Galletti, C., Thornock, J. N., Smith, P. J., & Tognotti, L. (2013). A Novel Methodology for Chemical Time Scale Evaluation with Detailed Chemical Reaction Kinetics. *Energy Fuels*, 27(4), 2255–2265.
- [38] James, S., Anand, M., & Pope, S. B. (2002). The Lagrangian PDF transport method for simulations of gas turbine combustor flows. In *AIAA/ASME/SAE/ASEE Joint Propulsion Conference & Exhibit*, vol. 38. Indianapolis, Indiana.
- [39] Kee, R. J., Rupley, F. M., Meeks, E., & Miller, J. A. (1996). CHEMKIN-III: A FORTRAN chemical kinetics package for the analysis of gas-phase chemical and plasma kinetics. *Sandia national laboratories report SAND96-8216*.

- [40] Kulkarni, R. M., & Polifke, W. (2013). LES of Delft-Jet-In-Hot-Coflow (DJHC) with tabulated chemistry and stochastic fields combustion model. *Fuel Process. Technol.*, 107, 138–146.
- [41] Li, H., ElKady, A. M., & Evulet, A. T. (2009). Effect of exhaust gas recirculation on NO_x formation in premixed combustion system. *Nat. Gas*, 3.
- [42] Liñán, A. (1974). The asymptotic structure of counterflow diffusion flames for large activation energies. *Acta Astronaut.*, 1(7-8), 1007–1039.
- [43] Lu, T., & Law, C. K. (2009). Toward accommodating realistic fuel chemistry in large-scale computations. *Prog. Energy Combust. Sci.*, 35(2), 192–215.
- [44] Lu, T. F., Yoo, C. S., Chen, J. H., & Law, C. K. (2010). Three-dimensional direct numerical simulation of a turbulent lifted hydrogen jet flame in heated coflow: a chemical explosive mode analysis. *J. Fluid Mech*, 652, 45–64.
- [45] Luo, Z., Yoo, C. S., Richardson, E. S., Chen, J. H., Law, C. K., & Lu, T. (2012). Chemical explosive mode analysis for a turbulent lifted ethylene jet flame in highly-heated coflow. *Combust. Flame*, 159(1), 265–274.
- [46] Ma, L., & Roekaerts, D. (2016). Modeling of spray jet flame under MILD condition with non-adiabatic FGM and a new conditional droplet injection model. *Combust. Flame*, 165, 402–423.
- [47] Magnussen, B., & Hjertager, B. (1977). On mathematical modeling of turbulent combustion with special emphasis on soot formation and combustion. *Proc. Combust. Inst.*, 16(1), 719–729.
- [48] Magnussen, B. F. (1981). On the structure of turbulence and a generalized eddy dissipation concept for chemical reaction in turbulent flow. In *19th AIAA Aerospace Meeting*. St. Louis, USA.
- [49] Magnussen, B. F. (2005). The eddy dissipation concept a bridge between science and technology. In *ECCOMAS thematic conference on computational combustion*. Lisbon, Portugal.
- [50] Mardani, A., Tabejamaat, S., & Ghamari, M. (2010). Numerical study of influence of molecular diffusion in the Mild combustion regime. *Combust. Theor. Model.*, 14(5), 747–774.

-
- [51] Mardani, A., Tabejamaat, S., & Hassanpour, S. (2013). Numerical study of CO and CO₂ formation in CH₄/H₂ blended flame under MILD condition. *Combust. Flame*, 160(9), 1636–1649.
- [52] Masri, A., Subramaniam, S., & Pope, S. (1996). A mixing model to improve the PDF simulation of turbulent diffusion flames. *Proc. Combust. Inst.*, 26(1), 49–57.
- [53] Medwell, P. R. (2007). *Laser Diagnostics in MILD Combustion*. University of Adelaide, School of Mechanical Engineering.
- [54] Medwell, P. R., & Dally, B. B. (2012). Effect of fuel composition on jet flames in a heated and diluted oxidant stream. *Combust. Flame*, 159(10), 3138–3145.
- [55] Medwell, P. R., & Dally, B. B. (2012). Experimental Observation of Lifted Flames in a Heated and Diluted Coflow. *Energy Fuels*, 26(9), 5519–5527.
- [56] Medwell, P. R., Kalt, P. A. M., & Dally, B. B. (2007). Simultaneous imaging of OH, formaldehyde, and temperature of turbulent nonpremixed jet flames in a heated and diluted coflow. *Combust. Flame*, 148(1-2), 48–61.
- [57] Medwell, P. R., Kalt, P. A. M., & Dally, B. B. (2008). Imaging of diluted turbulent ethylene flames stabilized on a Jet in Hot Coflow (JHC) burner. *Combust. Flame*, 152, 100–113.
- [58] Medwell, P. R., Kalt, P. A. M., & Dally, B. B. (2009). Reaction Zone Weakening Effects under Hot and Diluted Oxidant Stream Conditions. *Combust. Sci. Technol.*, 181(7), 937–953.
- [59] Minamoto, Y., & Chen, J. H. (2016). DNS of a turbulent lifted DME jet flame. *Combust. Flame*, 169, 38–50.
- [60] Minamoto, Y., Dunstan, T., Swaminathan, N., & Cant, R. (2013). DNS of EGR-type turbulent flame in MILD condition. *Proc. Combust. Inst.*, 34(2), 3231–3238.
- [61] Minamoto, Y., & Swaminathan, N. (2014). Modelling paradigms for MILD combustion. *Int. J. Adv. Eng. Sci. Appl. Math.*, 6(1), 1–11.
- [62] Minamoto, Y., & Swaminathan, N. (2014). Scalar gradient behaviour in MILD combustion. *Combust. Flame*, 161(4), 1063–1075.

- [63] Minamoto, Y., & Swaminathan, N. (2015). Subgrid scale modelling for MILD combustion. *Proc. Combust. Inst.*, 35(03), 3529–3536.
- [64] Minamoto, Y., Swaminathan, N., Cant, R. S., & Leung, T. (2014). Reaction Zones and Their Structure in MILD Combustion. *Combust. Sci. Technol.*, 186(8), 1075–1096.
- [65] Minamoto, Y., Swaminathan, N., Cant, S. R., & Leung, T. (2014). Morphological and statistical features of reaction zones in MILD and premixed combustion. *Combust. Flame*, 161(11), 2801–2814.
- [66] Munson, B. R., Young, D. F., & Okiishi, T. H. (2006). *Fundamentals of Fluid Mechanics*. John Wiley & Sons, Inc., 5th ed.
- [67] Oldenhof, E., Tummers, M. J., van Veen, E. H., & Roekaerts, D. J. E. M. (2010). Ignition kernel formation and lift-off behaviour of jet-in-hot-coflow flames. *Combust. Flame*, 157(6), 1167–1178.
- [68] Oldenhof, E., Tummers, M. J., van Veen, E. H., & Roekaerts, D. J. E. M. (2011). Role of entrainment in the stabilisation of jet-in-hot-coflow flames. *Combust. Flame*, 158(8), 1553–1563.
- [69] Oldenhof, E., Tummers, M. J., van Veen, E. H., & Roekaerts, D. J. E. M. (2012). Transient response of the Delft jet-in-hot coflow flames. *Combust. Flame*, 159(2), 697–706.
- [70] O’Loughlin, W., & Masri, A. (2011). A new burner for studying auto-ignition in turbulent dilute sprays. *Combust. Flame*, 158(8), 1577–1590.
- [71] O’Loughlin, W., & Masri, A. R. (2012). The Structure of the Auto-Ignition Region of Turbulent Dilute Methanol Sprays Issuing in a Vitiated Co-flow. *Flow, Turbul. Combust.*, 89(1), 13–35.
- [72] Parente, A., Malik, M. R., Contino, E., Cuoci, A., & Dally, B. B. (2016). Extension of the Eddy Dissipation Concept for turbulence/chemistry interactions to MILD combustion. *Fuel*, 163, 98–111.
- [73] Parente, A., Sutherland, J., Dally, B., Tognotti, L., & Smith, P. (2011). Investigation of the MILD combustion regime via Principal Component Analysis. *Proc. Combust. Inst.*, 33(2), 3333–3341.
- [74] Peters, N. (1984). Laminar diffusion flamelet models in non-premixed turbulent combustion. *Prog. Energy Combust. Sci.*, 10(3), 319–339.

- [75] Peters, N. (1988). Laminar flamelet concepts in turbulent combustion. *Proc. Combust. Inst.*, 21(1), 1231–1250.
- [76] Peters, N. (2000). *Turbulent Combustion*. Cambridge University Press.
- [77] Pitsch, H. (1998). FlameMaster: A C++ computer program for 0D combustion and 1D laminar flame calculations. Available at <http://www.itv.rwth-aachen.de/downloads/flamemaster/>.
- [78] Pitsch, H., Chen, M., & Peters, N. (1998). Unsteady flamelet modeling of turbulent hydrogen-air diffusion flames. *Proc. Combust. Inst.*, 27(1), 1057–1064.
- [79] Pitsch, H., & Fedotov, S. (2001). Investigation of scalar dissipation rate fluctuations in non-premixed turbulent combustion using a stochastic approach. *Combust. Theor. Model.*, 5(1), 41–57.
- [80] Poinso, T., & Veynante, D. (2013). *Theoretical and numerical combustion*. Poinso, Thierry and Veynante, Denis, 3rd ed. Purchased July 2015 (3rd ed. updated quarterly).
- [81] Pope, S. (1985). PDF methods for turbulent reactive flows. *Prog. Energy Combust.*, 11(2), 119–192.
- [82] Ranzi, E., Dente, M., Goldaniga, A., Bozzano, G., & Faravelli, T. (2001). Lumping procedures in detailed kinetic modeling of gasification, pyrolysis, partial oxidation and combustion of hydrocarbon mixtures. *Prog. Energy Combust. Sci.*, 27(1), 99–139.
- [83] Ranzi, E., Frassoldati, A., Grana, R., Cuoci, A., Faravelli, T., Kelley, A., & Law, C. (2012). Hierarchical and comparative kinetic modeling of laminar flame speeds of hydrocarbon and oxygenated fuels. *Prog. Energy Combust. Sci.*, 38(4), 468–501. Current version of mechanism available from <http://creckmodeling.chem.polimi.it/>.
- [84] Reaction Design: San Diego (2016). CHEMKIN-PRO 15152.
- [85] Rebola, A., Costa, M., & Coelho, P. J. (2013). Experimental evaluation of the performance of a flameless combustor. *Appl. Therm. Eng.*, 50(1), 805–815.
- [86] Reddy, V. M., Sawant, D., Trivedi, D., & Kumar, S. (2013). Studies on a liquid fuel based two stage flameless combustor. *Proc. Combust. Inst.*, 34(2), 3319–3326.

- [87] Rodrigues, H. C., Tummers, M. J., van Veen, E. H., & Roekaerts, D. J. (2015). Spray flame structure in conventional and hot-diluted combustion regime. *Combust. Flame*, 162(3), 759–773.
- [88] Sabia, P., de Joannon, M., Picarelli, A., Chinnici, A., & Ragucci, R. (2012). Modeling Negative Temperature Coefficient region in methane oxidation. *Fuel*, 91(1), 238–245.
- [89] Saha, M., Chinnici, A., Dally, B. B., & Medwell, P. R. (2015). Numerical Study of Pulverized Coal MILD Combustion in a Self-Recuperative Furnace. *Energy Fuels*, 29(11), 7650–7669.
- [90] Saha, M., Dally, B. B., Medwell, P. R., & Chinnici, A. (2016). Burning characteristics of Victorian brown coal under MILD combustion conditions. *Combust. Flame*, 172, 252–270.
- [91] Saha, M., Dally, B. B., Medwell, P. R., & Chinnici, A. (2016). Effect of particle size on the MILD combustion characteristics of pulverised brown coal. *Fuel Process. Technol.*, 155, 74–87.
- [92] Scholtissek, A., Chan, W. L., Xu, H., Hunger, F., Kolla, H., Chen, J. H., Ihme, M., & Hasse, C. (2015). A multi-scale asymptotic scaling and regime analysis of flamelet equations including tangential diffusion effects for laminar and turbulent flames. *Combust. Flame*, 162(4), 1507–1529.
- [93] Shabanian, S. R., Medwell, P. R., Rahimi, M., Frassoldati, A., & Cuoci, A. (2013). Kinetic and fluid dynamic modeling of ethylene jet flames in diluted and heated oxidant stream combustion conditions. *Appl. Therm. Eng.*, 52, 538–554.
- [94] Sidey, J., & Mastorakos, E. (2015). Visualization of MILD combustion from jets in cross-flow. *Proc. Combust. Inst.*, 35(3), 3537–3545.
- [95] Smith, G. P., Golden, D. M., Frenklach, M., Moriarty, N. W., Eiteneer, B., Goldenberg, M., Bowman, C. T., Hanson, R. K., Song, S., William C. Gardiner, J., Lissianski, V. V., & Qin, Z. (2000). GRI-Mech 3.0. Mechanism available from http://www.me.berkeley.edu/gri_mech/.
- [96] Solomon, S. (1999). Stratospheric ozone depletion: A review of concepts and history. *Rev. Geophys.*, 37(3), 275–316.

- [97] Stagni, A., Frassoldati, A., Cuoci, A., Faravelli, T., & Ranzi, E. (2016). Skeletal mechanism reduction through species-targeted sensitivity analysis. *Combust. Flame*, 163, 382 – 393.
- [98] Subramaniam, S., & Pope, S. (1998). A mixing model for turbulent reactive flows based on Euclidean minimum spanning trees. *Combust. Flame*, 115(4), 487–514.
- [99] Tennekes, H., & Lumley, J. L. (1972). *A First Course in Turbulence*. The MIT Press.
- [100] Turns, S. R. (2000). *Introduction to Combustion*. McGraw-Hill series in mechanical engineering. McGraw-Hill Education, 2nd ed.
- [101] UC San Diego (2016). Chemical-Kinetic Mechanisms for Combustion Applications. Mechanical and Aerospace Engineering (Combustion Research), University of California at San Diego, Current version of mechanism available from: <http://web.eng.ucsd.edu/mae/groups/combustion/mechanism.html>.
- [102] Veríssimo, A. S., Rocha, A. M. A., & Costa, M. (2013). Experimental study on the influence of the thermal input on the reaction zone under flameless oxidation conditions. *Fuel Process. Technol.*, 106, 423–428.
- [103] Wang, F., Mi, J., Li, P., & Zheng, C. (2011). Diffusion flame of a CH₄/H₂ jet in hot low-oxygen coflow. *Int. J. Hydrogen Energ.*, 36(15), 9267–9277.
- [104] Wang, H., You, X., Joshi, A. V., Davis, S. G., Laskin, A., Egolfopoulos, F., & Law, C. K. (2007). USC Mech Version II. High-Temperature Combustion Reaction Model of H₂/CO/C1-C4 Compounds. Mechanism available from http://ignis.usc.edu/USC_Mech_II.htm.
- [105] Weber, R., Orsino, S., Lallemand, N., & Verlaan, A. (2000). Combustion of natural gas with high-temperature air and large quantities of flue gas. *Proc. Combust. Inst.*, 28, 1315–1321.
- [106] Weber, R., Smart, J. P., & vd Kamp, W. (2005). On the (MILD) combustion of gaseous, liquid, and solid fuels in high temperature preheated air. *Proc. Combust. Inst.*, 30(2), 2623–2629.
- [107] Wüning, J. A., & Wüning, J. G. (1997). Flameless oxidation to reduce thermal NO-formation. *Prog. Energ. Combust.*, 23(1), 81–94.

- [108] Xu, J., & Pope, S. B. (1999). Assessment of numerical accuracy of PDF/Monte Carlo methods for turbulent reacting flows. *J. Comput. Phys.*, 152(1), 192–230.
- [109] Ye, J., Medwell, P. R., Dally, B. B., & Evans, M. J. (2016). The transition of ethanol flames from conventional to MILD combustion. *Combust. Flame*, 171, 173–184.
- [110] Ye, J., Medwell, P. R., Varea, E., Kruse, S., Dally, B. B., & Pitsch, H. G. (2015). An experimental study on MILD combustion of prevaporised liquid fuels. *Appl. Energ.*, 151, 93–101.
- [111] Yoo, C. S., Richardson, E. S., Sankaran, R., & Chen, J. H. (2011). A DNS study on the stabilization mechanism of a turbulent lifted ethylene jet flame in highly-heated coflow. *Proc. Combust. Inst.*, 33, 1619–1627.
- [112] Yoo, C. S., Sankaran, R., & Chen, J. H. (2009). Three-dimensional direct numerical simulation of a turbulent lifted hydrogen jet flame in heated coflow: flame stabilization and structure. *J. Fluid Mech*, 640, 453–481.

Chapter 3

Literature Review

Combustion of a fuel and oxidant can occur spontaneously without any external energy input (such as a spark) at sufficiently high temperatures. The minimum temperature at which this can occur is termed the “autoignition temperature” (T_{ai}) of the mixture, and may be estimated numerically using simplified reactors, such as a well-stirred reactor (WSR). In such analyses, a combination of fuel and oxidant in a WSR is mixed with a chosen residence time (τ_{res}) over a range of temperatures. The autoignition temperature is then described as the minimum temperature for which the ignition delay (τ_{ign}) is less than τ_{res} . Both T_{ai} and τ_{ign} are therefore functions of the means by which ignition is defined, the mixture composition and τ_{res} . Although the calculation of T_{ai} using simplified reactors is an accepted practice [19, 81, 130], there is no single, standardised convention for the τ_{res} used or which flame features should be used to identify τ_{ign} .

Autoignition in non-premixed combustion may be defined using laminar flamelet theory. In laminar flamelet theory, autoignition is represented by a turning point in a plot of temperature (T) against scalar-dissipation rate (χ) or τ_{res} [64, 105], as was discussed in §2.3.3. This concept, however, is not applicable to all flame structures [96] and is usually assessed as a steady-state property of the flame and, subsequently, cannot incorporate definitions of τ_{ign} .

Different flame behaviour and features at elevated temperatures have resulted in the classification of combustion into different regimes based on initial temperature (T_0) and composition [83]. Two of these regimes are the moderate or intense low oxygen dilution (MILD) combustion regime, and conventional autoignition [55]. Flames in the transition between these regimes have exhibited unstable behaviour and the boundaries between these two regimes have not yet been clearly defined [31, 83].

3.1 Studies of MILD Combustion

Moderate or intense low oxygen dilution (MILD) combustion, or “flameless oxidation” [134], offers increased thermal efficiency and reduced emissions of pollutants, such as NO_x and soot, over conventional combustion [19]. The MILD combustion regime has been seen to feature well-distributed reaction zones rather than well-defined flame fronts, resulting in a more homogeneous reaction zone without localised temperature peaks associated with conventional combustion [108]. Existing descriptions of MILD combustion have been developed based on premixed or non-premixed combustion, each describing the effects under specific conditions, but have not been used to describe a unified definition of the MILD combustion regime.

3.1.1 Premixed Studies of MILD Combustion

The study of MILD combustion in premixed reactors has been studied in-depth experimentally [30, 31, 36, 115, 117], numerically [30, 31, 35, 36, 117, 125, 130] and analytically [96] to determine thermal, dynamic and chemical descriptions of the MILD combustion regime. These studies of premixed MILD combustion have been primarily undertaken in well-stirred reactor (WSR) [30, 31, 36, 84, 115, 130] or plug-flow (tube) reactor (PFR) [96, 117] configurations. Such reactor configurations facilitate the study of combustion chemistry with the assumption of homogeneity. Explicitly, the mixture in a WSR is considered to be completely homogeneous, whilst perfect mixing is assumed at any given point along the length of the PFR.

The ignition process of MILD combustion in a WSR is consistent with two-stage oxidation with a high initial reactant temperature (T_0) [36]. In such a configuration, MILD combustion has been described as combustion of a preheated and diluted mixture, with a residence time (τ_{res}), which self-ignites, but results in a temperature increase (ΔT) less than the mixture self-ignition temperature (T_{si}) [19]. Following this definition of MILD combustion, different combustion regimes may be demarcated based on the values of T_0 and ΔT with respect to T_{si} . These are presented in Table 3.1. In this description, T_{si} is the minimum T_0 required for a given mixture to result in self-sustained, net heat release and a significant temperature increase at a fixed τ_{res} [19].

Simultaneous reductions of CO and NO_x pollutants are a potential benefit of the MILD combustion regime [60]. Concentrations of CO are reduced under these conditions, due to the recombination of CH_3 , primarily to C_2H_6 [36, 117], whilst NO_x are reduced due to the relatively low temperature increases [19]. Accordingly, the preference of this recombination pathway (over the oxidation pathway

Table 3.1. Combustion regimes in a well-stirred reactor configuration. Based on [19, 83, 113, 130].

	$T_0 < T_{si}$	$T_0 > T_{si}$
$\Delta T < T_{si}$	No combustion/quasi-MILD	MILD combustion
$\Delta T > T_{si}$	Conventional combustion	High temperature/MILD-like combustion

$\text{CH}_3 \rightarrow \text{CH}_3\text{O} \rightarrow \text{CH}_2\text{O}$, which dominates in most CH_4 flames), has been used as a marker to indicate the MILD combustion of CH_4 [116, 117].

The combustion regimes defined by Cavaliere and de Joannon [19] (see Table 3.1), have been extended by chemical analyses of flame ignition characteristics and chemical behaviour. The “quasi-MILD” and “MILD-like” regimes require: forced ignition (that is, $T_0 < T_{si}$), or do not comply with the ‘low oxygen dilution’ condition embedded in the ‘MILD’ acronym, respectively [130]. Despite these substantially different conditions, both “quasi-MILD” and “MILD-like” combustion feature the same chemical pathways and ignition characteristics of MILD combustion when compared numerically in a well-stirred reactor [131]. These conflicting analyses therefore challenge the validity of a regime diagram generated using temperatures alone.

Premixed analyses of MILD combustion have been used to differentiate combustion regimes, not only in well-stirred environments, but in non-premixed flames [2, 84, 86, 124, 129, 130]. Such an approach using the stoichiometric mixture was initially proposed by Cavaliere and de Joannon [19], however has since been superseded by the same authors with descriptions of combustion regimes in different non-premixed configurations [32, 33, 35]. These non-premixed descriptions are associated with subtly different configurations, however their phenomenological descriptions are not inherently consistent with the premixed descriptions of MILD combustion [8, 55, 86, 97]. This highlights the need for a description of the MILD combustion regime based on features common to both premixed and non-premixed configurations.

Premixed MILD combustion in a PFR configuration has been described qualitatively based on the ignition features of MILD combustion as a distributed reaction zone [96]. This description is based on experimental observations of “flameless oxidation” by Plessing *et al.* [108] in a furnace operating in the “well-stirred reactor regime”. This was subsequently termed a “‘mild’ combustion mode” by Oberlack *et al.* [96], having a monotonic transition between unburnt and burning states [96, 108]. The analytical study of the phenomenon in a PFR, using a simple, one-step chemistry approach led to the following criterion for MILD combustion:

$$\frac{E_{eff}}{RT_0} \leq 4 \left(1 + \frac{T_0}{\Delta T} \right) \quad (3.1)$$

where R is the universal gas constant and E_{eff} is the effective activation energy of an equivalent one-step reaction. This is equivalent to defining flameless, MILD combustion as a regime described by a degenerate S-shaped curve, without autoignition or extinction points (refer to §2.3.3), but is not constricted to the temperature limit imposed by Cavaliere and de Joannon [19]. Although this analysis was undertaken specifically for a PFR, this qualitative description of a degenerate S-shaped curve may be analysed in a non-premixed system through further analysis.

The study of combustion in premixed configurations has resulted in an improved understanding of chemical kinetics and flame structure in MILD conditions. Despite this improved understanding of the fundamental aspects of premixed combustion, the accepted descriptions of MILD combustion are not inherently consistent and do not necessarily extend to more complex, non-premixed systems.

3.1.2 Non-Premixed Studies of MILD Combustion

The characteristics and structure of MILD combustion in non-premixed configurations has been studied experimentally in laminar [21–23] and turbulent [28, 83, 85, 86, 122, 124, 136] jet-in-hot-cross-/co-flow (JHC) configurations. Common to all of these studies, is a jet of fresh fuel emanating into a coflow (or crossflow) of hot and diluted oxidant. This coflow may be generated through electrical heating and dilution of air with inert species [2, 21–23] or by an auxiliary burner upstream of the main jet exit plane [28, 83, 85, 86, 121, 122, 124, 136].

Studies of laminar hydrocarbon flames issuing into hot coflows at different temperatures, with different oxygen levels, have revealed different trends between autoignitive, tribrachial edge flames and “lifted flames with MILD combustion” [2, 21–23]. Tribrachial flames have been well-studied in both laminar and turbulent flames in hot coflows, and feature three distinct zones of heat release (lean, rich and diffusion) stemming from a common triple-point at the flame base [2, 14, 20–23, 27, 27, 39, 52, 67, 77, 95, 106, 109]. In turbulent flames, one method flame stabilisation is the manifestation of a triple point outside of the turbulent mixing layer of the jet, from which the flame sheet propagates downstream [67]. In contrast, lifted flames with MILD combustion are not stabilised at a triple-point, nor do they exhibit any form of distinct base [2, 21–23]. These flames are stabilised as lean flames, following a significant pool of precursor species [2]. These findings are consistent with measurements and observations of turbulent flames in similar hot coflows [83, 86]. In these turbulent cases, flames which issue into hot coflows with less than

6% O₂ (by volume), are only weakly luminescent and feature both OH and CH₂O structures, but do not appear to exhibit any distinct flame base [83, 86]. These similarities highlight the direct relevance of laminar flame studies to the understanding the structure of MILD combustion in turbulent coflow flames.

The structure of steady-state, laminar, opposed-flow flames with hot fuel and/or oxidant streams have been studied numerically to understand the characteristics of MILD combustion [32, 33, 35, 37, 87, 124, 135]. Studies of this configuration by de Joannon *et al.* [32, 33, 35, 37] identified key features of the MILD combustion regime in non-premixed flames in Z -space. This body of work identifies the requisite features of MILD combustion as:

1. the disappearance of regions of net negative heat release rate (HRR),
2. thickening of the heat release region, caused by the merger of dual HRR peaks,
3. mismatch between Z_{st} and peak HRR [32, 33, 35, 37].

These features culminate in a broad, low intensity reaction zone, with positive HRR for any Z [33, 35]. This has been termed “Homogeneous Charge Diffusion Ignition” [35, 79], and has been seen in opposed-flow configurations with both hot oxidants [33] and hot fuels [37]. The reduction of reaction zone intensity in opposed-flow flames has been described as “reaction zone weakening” [87], and allows for enhanced diffusion of oxidants [87], producing a homogeneous reaction region in contrast to a “thin” flame front [35]. Reaction zone weakening in this configuration leads to a dependence of HRR on local strain rate, imposed by the mixing field [87]. This has similarly been investigated numerically for ethanol flames with a hot oxidant stream, where results suggested a minimum, critical strain-rate required to meet the conditions of MILD combustion [135]. Although these steady-state analyses have improved the understanding of the structure of MILD combustion, they can only offer limited insight on the transient ignition processes of non-premixed oxidiser and fuel streams in the MILD combustion regime.

Extinction characteristics of opposed-flow flames with hot oxidants have been analysed experimentally [65, 80], analytically [13] and numerically [56, 65, 87, 126]. Experimental work has shown that non-premixed flames with a sufficiently hot oxidant cannot be extinguished, even with oxygen concentrations of 2% by volume [80], consistent with numerical simulations [87], and the premixed and well-stirred classifications of MILD combustion [96, 108]. Analytical work on this in non-premixed combustion, however, (based on criteria derived from the flamelet equations) has inherently assumed a quenching temperature [13], which would bias the

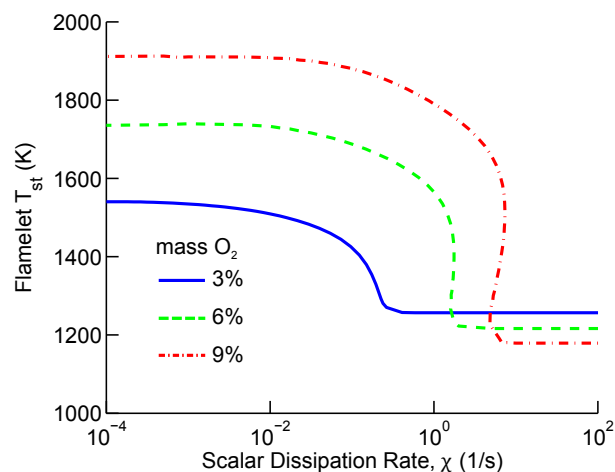


Figure 3.1. S-shaped curves for three stoichiometric flamelets with 1:1 CH_4/H_2 at 300 K as fuel, and 1300 K oxidants with different O_2 concentrations [adapted from 56].

analysis, in contrast to a property of the combustion chemistry. Such analysis has previously been performed in a premixed environment, as was discussed in §3.1.1, culminating in Equation 3.1.

Autoignitive and degenerate S-shaped curves are shown in Figure 3.1. This plot shows an example of a degenerate (MILD) S-shaped curve, representing the stoichiometric flamelet with 1:1 CH_4/H_2 at 300 K as fuel, and an oxidant with 3% O_2 (by mass) at 1300 K. The S-shaped curves representing the stoichiometric flamelets for cases with 6% and 9% O_2 in the oxidants show the autoignition and extinction conditions at the lower and upper turning points of each curve, respectively. These are in contrast to the monotonic change in T and χ in the MILD 3% O_2 case, which does not result in any sharp changes in temperature.

The evidence of a degenerate S-shaped curve was explored numerically in the context of MILD combustion, with the absence of extinction or autoignition correlating with flame thickening and the shift of a single peak in HRR away from the stoichiometric mixture fraction [126]. These results are consistent with the criteria for MILD combustion of CH_4 proposed by de Joannon *et al.* [33] in an opposed-flow configuration. The same study, however, did not observe a shift of peak temperature towards the stoichiometric mixture fraction [126] as described by de Joannon *et al.* [33]. The differences in these studies may be due to a five-fold difference in strain rates between the two studies; or the inclusion of H_2O , H and OH in the oxidant description by Sidey & Mastorakos [126], promoting heat release from the reaction $OH + H_2 \rightleftharpoons H + H_2O$, resulting in a broader HRR region. This comparison, although suggesting that the descriptions of de Joannon *et al.* [33] and Oberlack *et al.* [96]

may be linked, is restricted by the inclusion of minor species in the oxidant composition without accounting for their potential effects on flame structure.

A significant body of work has been generated with the aim of describing non-premixed MILD combustion. This body of work has used a range of approaches to produce phenomenological descriptions of MILD combustion in different non-premixed configurations which have been compared in limited cases [33, 126], however, have not been directly compared by means of generalised criteria. This work cannot be consolidated without first understanding the relevance of major and minor species – present in experimental studies using lean combustion products as an oxidant [28, 34, 83, 85–87, 97–99, 124] and limited numerical studies [126] – on the structure of flames ignited with hot coflows, particularly in the MILD combustion regime.

3.2 Studies of Autoignition

Many practical combustion devices, such as diesel engines and gas-turbine combustors, make use of autoignition [14, 17, 27, 67, 77, 79]. Autoignition is the spontaneous combustion of a fuel and oxidant mixture above its autoignition temperature [79], similar to ignition in the MILD combustion regime. This autoignition temperature is not an intrinsic property of a given fuel, but rather a function of the chemical properties of the local mixture, which are dependent on both composition and ambient pressure. Recalling §2.3.3, the autoignition process may be represented on an S-shaped curve (see Figure 2.3) as the lower turning point, where decreasing χ results in a sudden transition from a ‘mixing’ to a ‘burning’ solution. Similarly, the upper turning point in the S-shaped curve results in the extinction of a flame with increasing χ . This process of autoignition has been the focus of a large body of fundamental research to better the understanding of flame stabilisation in hot coflows [6–8, 15, 16, 22, 24, 27, 39, 52–54, 61, 64, 66, 67, 78, 79, 96–100, 107, 108, 112, 137, 138]. Although sharing the requirement of a hot, ambient environment with MILD combustion, flames in the autoignitive and MILD combustion regimes both have very different flame structures [2, 21, 23, 33, 35, 37, 86, 96, 126]. Despite this, the transition between the two regimes has not been extensively investigated [21, 23, 33, 83, 124, 126].

3.2.1 Autoignitive Flame Stabilisation

Fundamental research of non-premixed autoignition has been undertaken experimentally [6, 8, 15, 16, 21–23, 52, 53, 97–99] and numerically [2, 24, 54, 66, 78, 137, 138]. In these studies, fresh fuel is mixed with a hot oxidant in a coflow configu-

ration. Experimentally, this has been done JHC burners [6, 8, 21–23, 83, 97–99] or in a vitiated-coflow-burner (VCB) [15, 16, 52, 53] configuration. Both burner configurations feature jets of fresh fuel issuing into hot, laminar oxidant streams. The oxidants in these studies typically contain 9-21% O₂ (by volume), at temperatures in excess of 1100 K.

Non-premixed autoignitive flames may be stabilised through several means. In laminar conditions, lifted, autoignitive flames may stabilise following mixing of the fuel and oxidant streams. This premixing gives rise to tribrachial [39, 67, 108] or polybrachial [59] edge flame structures. For non-premixed methane flames, rich and lean wings flank a diffusion-flame, which all stem from a stabilisation point [39, 67, 108]. For more complex fuels, such as dimethyl-ether (DME), additional regions of heat-release may exist upstream or downstream of the stabilisation point (or stem from one of the wings), to form different, polybrachial flame structures [59]. In each scenario, regions of heat release flank the stabilisation point [108], which may be detected by intermediate species which contribute to exothermic reactions [58].

Studies of turbulent flames have indicated that tribrachial flame bases in regions of low turbulence may be one means of jet flame stabilisation [58, 67, 71, 77, 79]. Such edge flame structures have been observed in turbulent, visually lifted flames issuing into a hot coflow, although it could not be determined if they featured tribrachial flame structures [86]. It was hypothesised that this could be due to compression of the reaction zone by turbulent structures [86], although this has not since been confirmed or refuted. Turbulent flames in a hot and vitiated coflow have been studied using combined laser-induced fluorescence (LIF) imaging of OH and CH₂O with planar Rayleigh thermometry [52]. This work identified isolated ignition kernels, surrounded by precursor species, which travel downstream and combine to form a flame-sheet [52]. This means of flame stabilisation has also been identified from DNS studies [137, 138], and through high-speed chemiluminescence imaging [97, 112]. In this process, pockets of mixed fuel and oxidant are confined within large turbulent structures and subsequently ignite. The first of these pockets to ignite are those containing the “most reactive mixture fraction” (Z_{mr}), which is a lean mixture of fuel and hot oxidant [51, 79]. The most reactive mixture fraction is defined as the value of Z “where the reaction rate becomes a maximum” [79]. The value of Z_{mr} is insensitive to the effects of strain rate for a given fuel and oxidiser combination, and is identifiable as the mixture with the shortest ignition delay identified through a series of zero-dimensional reactors [79]. The autoignition and combination of isolated kernels, and laminar edge flames, have both been identified as two means of flame

stabilisation for turbulent jet flames in hot coflows, although the conditions which result in the transition between the two processes have not been identified.

3.2.2 Assessment of Ignition Delay in Autoignitive Flames

Both DNS and optical methods have shown agreement in the dynamics of turbulent flame stabilisation through autoignition of isolated kernels [97, 112, 137, 138], although there is no consensus of the most appropriate metric of τ_{ign} for comparing numerical studies to experimental values. Measures of τ_{ign} have been defined in various ways for simplified reactors. Autoignition has been defined as the onset of thermal runaway [42, 81], as $\dot{T}|_{max}$; peak production rate of OH, $\dot{Y}_{OH}|_{max}$; threshold values of Y_{OH} [16, 137, 138]; or a small, local temperature increase, ΔT [30, 36, 116]. The first two measures are indicative of highly reactive points in a mixture, but may not be equivalent—such as in two-stage ignition processes (correlating to MILD combustion, as discussed in §3.1.1). Threshold values of OH have additionally been compared to this concept of runaway, although these thresholds have been set on case-by-case bases [137, 138]. Finally, the use of a small $\Delta T \sim 5\text{--}10$ K, has previously shown good agreement with experimental observations of CH* in a jet-stirred reactor for a range of different fuels and conditions [30, 36, 116], however this has not been assessed in non-premixed configurations. These metrics have not been assessed across different premixed and non-premixed configurations, or combustion regimes. Determining the validity and appropriateness of these ignition criteria in different cases would serve to identify an appropriate measure for comparing autoignition in experimental flames with simplified models, and serve to better the understanding of how jet flames stabilise in hot coflows.

3.3 Flame Stabilisation in the Transition to MILD Combustion

Jet flames in the MILD and autoignitive combustion regimes both require hot ambient conditions for spontaneous ignition, however have significantly different flame structures and characteristics [21–23, 83, 86]. Visually lifted flames in the transition between the autoignitive and MILD combustion regimes and been studied using laser diagnostics [86, 124] and observations of chemiluminescence [21–23, 83].

3.3.1 Transitional Flame Structure

Lifted, autoignitive flames in hot coflows feature distinct [83], tribrachial [2, 21–24, 124] bases, or may be stabilised by the combination of individual autoignited kernels [52, 112, 137, 138]. Flames in the MILD combustion regime, in contrast, do not feature distinct flame bases, but have well-defined flame bases with significantly

reduced spatial gradients in chemiluminescence [21–23, 83, 86].

Investigation of flames in the transition between autoignitive flames and MILD combustion have been undertaken experimentally and numerically. Experimental studies have reported the presence of two distinct OH structures in visually lifted C_2H_4 flames in 1100-K coflows with 9% O_2 (by volume) [86]. In these “transitional” flames [41, 83, 86], the visual base of the flame (as determined from observations of chemiluminescence) appears to coincide with a transition from “weak” to “strong” OH structures [86]. The strong OH structures in these flames identified using OH-LIF imaging [86] appear similar to the well-defined, tribrachial flame base of a CH_4 flame in a cold air coflow [58]. Unlike flames in cold air streams, however, these strong OH structures appear to stem from weaker OH structures (hereafter referred to as “OH tails”) [86]. These OH tails are associated with low levels of chemiluminescence, which may be observed using long exposure imaging [83], and have been hypothesised to extend to the jet exit plane [83].

The tail structures observed in transitional flames are similar in size and OH number density (n_{OH}) to OH structures seen in MILD C_2H_4 flames issuing into otherwise-identical coflows with 3% O_2 . The presence of these tail structures has resulted in some ambiguity in assessing the lift-off height of transitional flames. The lift-off height of such flames has been defined as either the most upstream evidence of chemiluminescence, or the height of the strong, visible flame-base associated with the (weak-to-strong) transition point [83]. Ultimately, however, the mechanism responsible for the rapid transition between the weak OH tail and the significantly stronger downstream OH structure, is still unknown.

Weak OH tails of jet flames stabilised in hot and diluted coflows have been shown to broaden with reducing coflow oxygen concentrations [86] – in support of the flame thickening effects in simulated flames [33, 35, 37, 92]. This is in contrast to observations of OH structures in jet flames in hot and diluted crossflow [124], but was evident in the subsequent opposed-flow flame study by the same authors [126]. These results suggest that the effects of flame thickening in the transition from autoignitive to MILD combustion are strongly coupled to the underlying flow-field of the burner configuration, in-line with the assertion of similar τ_{chem} and τ_{fluid} , that is $Da \sim 1$, in the MILD combustion regime.

Transitional structures have not only been seen in non-premixed jet flames, but were identified in a LES study of a premixed methane/air flame in a 1650-K coflow with 11.4% O_2 (by mass) [41]. The existence of this “(very) low heat-release zone” prior to the visible flame-base in a premixed flame [41] supports the hypothesis that MILD and transitional flames are stabilised through partial premixing [87].

3.3.2 Species Transport in Non-Premixed Flames in Hot Coflows

The mechanisms of chemical mixing in reactive flows may be separated into turbulent and diffusive transport. Turbulent transport of chemical species occurs when molecules are transported by large fluidic structures, whilst diffusive transport is driven by concentration and thermal gradients. In piloted, partially-premixed jet flames, transport due to molecular diffusion is prevalent near the jet exit plane, whilst turbulent transport has been shown to dominate mixing of jet flames further downstream (beyond $30D$) [10]. This effect of turbulent mixing near the jet exit plane may be more critical in autoignitive flames near the boundary of the MILD combustion regime (in hot coflows with $\sim 9\% \text{ O}_2$), as evidenced by observations of decreasing lift-off heights with increasing bulk flowrate of the jet (u_0) [83, 86, 97, 99]. The most significant reduction in lift-off height, however, occurs over a range of Re near the laminar-turbulent transition for pipe-flow (that is, for $2000 \lesssim Re \lesssim 5000$, based on the flowrates and properties of cold fuel) [83, 86, 97, 99]. To explain this, measurements of the flow-field have revealed the significant impact of turbulence, increasing entrainment of the hot coflow, with a subsequent reduction in lift-off height [99]. This is not consistent with laminar flames, where experimental studies have indicated that lift-off height is proportional to $\tau_{ign}^2 \times u_0 \times Y_{F,0}$, where τ_{ign} is the ignition delay of the stoichiometric mixture, and $Y_{F,0}$ is the mass fraction of fuel in the jet [21–23]. These studies have identified linear trends in the lift-off heights of autoignitive flames, but also shown that this trend is discontinuous across the transition to the MILD combustion regime [21–23].

Appropriate treatment of molecular diffusion is required to model jet flame stabilisation in hot coflows [9, 26, 51, 74, 128]. The effects of molecular diffusion become more apparent in the transition to the MILD combustion regime [74], due to the effects of reaction zone weakening between the hot oxidant and cold fuel streams [87]. Medwell *et al.* [87] demonstrated that, under MILD conditions, the diffusion of oxygen into the fuel stream resulted in partial premixing of the fuel and oxidant to assist in flame stabilisation, whereas other studies have shown that the inclusion of H_2 in the fuel increases the importance of preferential diffusion effects [9, 51, 74, 128]. Although all studies have demonstrated the importance of preferential diffusion in modelling jet flame stabilisation, they have not been able to give a detailed account of what role diffusion plays in stabilising flames in hot coflows and how this effect contributes to the structure of hydrocarbon flames.

3.3.3 Effects of Gaseous Fuel Composition on Flames in Hot Coflows

Studies of jet flames often concentrate on simple hydrocarbon fuels such as CH_4 , the major constituent of natural gas (NG), and C_2H_4 , an important intermediate in the combustion of larger hydrocarbon fuels [133]. To this effect, significant quantities of C_2H_4 have previously been found overlapping regions of CH_4 and C_2H_2 in partially-premixed, autoignitive n-heptane flames [111]. By virtue of their significance, it is therefore not unreasonable that CH_4 and C_2H_4 could be present together in larger concentrations in dual-fuel, MILD combustion systems. The effects of blending CH_4 and C_2H_4 have been studied in the context of flame speed and diluted ignition delays [65, 114], demonstrating that the C_2 chemistry in C_2H_4 oxidation becomes significant for blends with more than 10% C_2H_4 [65]. In such blends, the reaction between C_2H_4 and OH (to form C_2H_3 and H_2O) overwhelms the reaction between CH_4 and OH, which forms CH_3 and H_2O [65]. This balance is further complicated in combustion with hot oxidants, as C_2H_4 and O preferentially react to form CH_3 below 1000 K [63]. Blending these fuels in MILD conditions, therefore, is likely to have a significant effect on the formation and consumption of CH_3 , which plays an important role in both ignition delay and MILD flame structure [116]. The characteristics of CH_4 and C_2H_4 fuel blends are, accordingly, particularly relevant for potential future applications of MILD combustion using a combination of NG and other, more complex, practical fuels.

Hydrogen has been added to assist in stabilising gaseous, hydrocarbon jet flames in JHC burners, and to reduce soot formation to aid laser diagnostics studies [82]. One study found that radial n_{OH} profiles in MILD and transitional flames did not change significantly using any of three different fuels – NG, C_2H_4 and liquefied petroleum gas (LPG) – mixed 1:1 with H_2 (by volume) [82]. Of these flames, the LPG flames demonstrated the lowest flame temperatures and C_2H_4 produced the most CH_2O [82]. In contrast, NG and LPG (predominantly C_3H_8) produced similar concentrations of CH_2O [82]. Although the effects of blending H_2 on DNG [9] and C_2H_4 [131] have been studied in the JHC configuration, the characteristics of other combinations of hydrocarbon fuels – such as CH_4 and C_2H_4 – have not been assessed in the transition to the MILD combustion regime.

3.3.4 Heat Release and Temperature Peaks in Non-Premixed Flames with Hot Oxidants

Heat release is an integral aspect of combustion. It is therefore beneficial to be able to identify regions of peak HRR and peak T in flames in different configurations and regimes.

Local HRR in non-premixed flames have been correlated with region of the HCO radical, which in-turn have been approximated by the instantaneous overlap of the OH and CH₂O species [104]. This has shown very good correlation in lifted, autoignitive flames [53], although this agreement does not hold under MILD combustion conditions [126]. Similarly, peak HRR and Z_{st} are also uncorrelated MILD combustion conditions [33, 35, 37]. Analysis of HRR and peak T in non-premixed configurations have suggested that peak T and HRR profiles may be identified by relatively high concentrations of OH* [126, 135]. In particular, Ye *et al.* [135] showed that the normalised profile of number density of OH* (n_{OH^*}) in non-premixed ethanol flames in the MILD combustion regime corresponds well to the lean edge of HRR profile, for n_{OH^*} and HRR between 20 and 80% of their peak values. In contrast, the profiles of mole fractions of OH* in non-premixed CH₄ flames do not correlate as well with HRR [126], although this may be an artefact of comparing OH* mole fractions [126], rather than number density [135]. Alternatively, the good agreement between OH* and HRR in ethanol flames [135] may be due to reactions involving the OH functional group in ethanol. This does not preclude the effectiveness of n_{OH^*} as an identifier of HRR, however, both studies showed that locations of peak OH* concentrations coincide with peak flame T [126, 135]. These results show that high concentrations of OH*, may be used as a diagnostic to identify regions of peak T in non-premixed flames with hot oxidants.

3.3.5 Response of Lift-off Height to Changes in Coflow

The effect of ambient conditions and oxidants near the boundary between the autoignitive and MILD combustion regimes has been studied chemically [117, 131], and in non-premixed flame conditions [23, 33, 35, 37, 83, 87, 135]. Observations of flames in the transition between these regimes show that the lift-off heights of non-premixed flames do not exhibit continuous, monotonic trends, but demonstrate behaviours which are yet to be explained.

The visual lift-off height of flames in the transition to the MILD combustion regime has been defined as both the height of the first distinguishable chemiluminescence and the transition from strong to weak chemiluminescence intensity [83]. This results in a range of lift-off heights which indicate the low heat-release regions corresponding to the weak OH tail, and the weak-to-strong transition point [83]. Although the mechanisms behind the formation and location of this transition point have not been identified, it has been seen in CH₄ and C₂H₄ flames issuing into hot coflows with more the 6% O₂ (by volume) [83, 86].

The lift-off height of non-premixed flames (of a given fuel) in hot coflows is a

function oxidant temperature, composition and the underlying flow-field. Flames in the MILD combustion regime have been reported as both lifted [21–23] and attached [83, 86], based on the first distinguishable chemiluminescence from long exposure photographs (taken with or without filters centred about blue CH^* emissions at 430 nm [44]). In configurations with visually attached MILD flames, this region of low chemiluminescence intensity diminishes with the transition to the autoignitive flame regime, such that regions of low chemiluminescence intensity can not be seen to extend to the jet exit plane, regardless of exposure time [83]. This was used to provide a minimum estimate of lift-off height, with Medwell & Dally [83] providing a range of visual lift-off heights for flames in different coflows.

Increasing the temperature of a mixture increases its reactivity, decreasing its τ_{ign} [83]. Subsequently, increasing the coflow temperature for an autoignitive jet flame results in a decrease in lift-off height [83]. This may be attributed to increased reactivity of the fuel and oxidant mixture [83]. Increasing the coflow temperature of an attached MILD jet flame, in contrast, has been seen to result in the onset of visual lift-off, suggesting a transition into the autoignitive flame regime [83]. Similar, unstable regions have been seen in recirculating furnaces between conventional and MILD combustion operating modes [43, 134]. The mechanisms behind this behaviour are still yet to be identified, although it has been hypothesised that they are the combined result of chemical and physical (fluidic and thermal) effects [83].

The behaviour of jet flames has been studied in hot coflows with 3–21% O_2 [21–23, 83, 86]. Observations of flames in hot coflows with 3–5% O_2 have suggested that MILD jet flames initiate at the jet exit plane and very gradually intensify with downstream distance [83, 86]. Increasing oxygen concentrations (to $\sim 6\% \text{O}_2$) results in the flames appearing lifted above the jet exit plane, and the appearance of a weak-to-strong transition in chemiluminescence well above the jet exit plane [83]. Further increases in the oxygen concentration in the coflow, monotonically reduce the height of this visual transition point above the jet exit plane [83]. The non-monotonic behaviour of flames in hot coflows of combustion products with 3–12% O_2 is seen for laminar or turbulent, NG or C_2H_4 flames in coflows with temperatures of 1100–1500 K [83]. Similar behaviour has been seen in independent studies of laminar flames in electrically heated, air/ N_2 coflows [21–23]. In these studies, flame of different fuels exhibited two distinct, linear trends in lift-off height for MILD flames, and autoignitive tribrachial flames [21–23]. In both regimes, lift-off height was seen to change linearly with $\tau_{ign}^2 \times u_0 \times Y_{F,0}$ [21–23], and MILD combustion was recorded for oxidants with less than 10% O_2 for CH_4 flames, and less than 6% O_2 for C_2H_4 flames [21]. This critical O_2 concentration decreased further for larger hydrocarbon

fuels [21], but was not greatly affected by the addition of H_2 [23]. This demonstrates the changes the flame structure and ignition behaviour of flames in the transition between the MILD and autoignitive combustion regimes.

Two independent bodies of experimental work have identified different flame structures corresponding to a transition between MILD combustion and autoignitive flames [21–23, 83, 86]. Despite differences in configurations, both bodies of work identified similar conditions for the transition between combustion regimes [21–23, 83], which are consistent with numerical studies under different configurations [35, 126]. Research into the transition between MILD and autoignitive combustion has highlighted the distinct behaviours and characteristics of flames in both regimes. The studies have, however, been undertaken in a range of configurations, with hot oxidants produced through lean combustion (with excess O_2) [83, 86], electrical heating of diluted air [21–23] or numerical idealisations of either [33, 35, 37, 124]. Although these differences have been noted previously [126], the effects of the inherent differences between combustion products, and heated and diluted air have not been studied in non-premixed combustion in the transition between the MILD combustion and autoignitive combustion regimes, which may impact the validity of these comparisons.

Combustion products may include a multitude of different reactant, product and intermediary (minor) species at steady-state or in chemical equilibrium. In lean mixtures, excess amounts O_2 from the reactants remain throughout the combustion process, and are present at steady-state along with the major hydrocarbon combustion products H_2O and CO_2 . In addition to these major species, combustion products also include small concentrations of minor species which may be on the order of parts-per-million, -billion or less. The effects of major species concentrations have been studied in premixed [118–120] and non-premixed [127] configurations. These studies showed that increasing the ratio of CO_2 to H_2O in the oxidant stream decreases the peak flame temperature and overall reactivity [118–120, 127], which serves to enhance CH_3 recombination [119]. This chemical effect dominates the physical effects (due to changes in properties such as density and heat capacity) in turbulent, non-premixed flames in the MILD combustion regime [127], however this study did not extend to similar cases in the autoignitive combustion regime [127].

Intermediary combustion species found in hot combustion products are not easily controlled experimentally, and their importance as boundary conditions are often neither reported nor discussed, despite their importance in flame stabilisation [11, 40, 45, 46, 51, 52, 62, 81, 94, 103, 127, 131]. Previous studies of NO [11, 40, 45, 46],

N_2O [11], OH [81, 84], CH_2O [70, 81], H_2 [131], CO_2 [120, 127] and H_2O_2 [70] doped flames have investigated the effects on ignition and temperatures in different configurations and conditions, however these have not investigated whether concentrations of species at levels expected in combustion products at equilibrium can result in a shift between the MILD and autoignitive combustion regimes. Of these species, OH has been used to define weak-to-strong transition points in a JHC burner [86], but is not seen upstream of turbulent flames in high-temperature air coflows with the same fuel [137]. It has also been shown that OH may significantly reduce ignition delay in a premixed reactor when added in small concentrations [81, 84], however the impact of this species in equilibrium concentrations in non-premixed combustion near the transition between MILD and autoignitive combustion is yet to be assessed.

Despite a large body of already-existing research, the structure of flames and the effects of the ambient environment on flame stabilisation, near the transition between the MILD and autoignitive combustion regimes are still not well understood. An improved understanding of both of these will improve the understanding of processes which dominate MILD and autoignitive combustion, and their relative importance for the purposes of scientific research and engineering design.

3.4 Jet Flame Modelling in MILD Combustion

Numerical studies of MILD and autoignitive combustion have investigated practical and fundamental characteristics of ignition and flame structure [3–5, 15, 18, 25, 26, 29, 32, 33, 37, 47, 48, 55, 56, 72–76, 78, 88–93, 101, 102, 123, 127, 131, 132, 137, 138]. Numerical studies of turbulent flames in the MILD combustion regime have predominantly used experimental data in order to assess the importance of appropriately modelling chemical kinetics and boundary conditions [3, 4, 12, 25, 26, 47, 55, 74, 76] or validate turbulence-chemistry interaction model parameters for low Da and Re_t flames [5, 29, 55, 56, 102]. Several studies have, however, used detailed measurements from a selection of CH_4/H_2 flames in a JHC burner [28] as validation cases prior to undertaking parametric studies or detailed investigations into flame structure [1, 51, 57, 72, 73, 75, 101, 103, 127, 130]. These studies, as well as similar DNS investigations of the same conditions in different configurations [50, 51], have focussed on CH_4/H_2 jet flames in 1300-K coflows. These coflow-stabilised flames are likely to be attached to the jet exit plane [9, 82] (despite being reported to exhibit a “slight” lift-off from a limited set of photographs [28]), as a result of significant preferential diffusion [74] and high-temperature ($T \gtrsim 1120$ K) H_2 branching reactions [38]. In contrast, numerical studies of ethylene-fuelled flames in a JHC burner

have not previously been able to replicate the weak-to-strong transition and visual lift-off of flames in hot coflows [123, 131]. Accurate prediction of this critical feature of the flames in the transition between the MILD and autoignitive combustion regimes is, however, crucial for using CFD to assess – and predict – the structure of flames in hot coflows.

3.4.1 Modelling Jet Flames with the Eddy Dissipation Concept

A significant body modelling work exists with a focus on turbulent jet flames in a JHC burner configuration [3–5, 25, 26, 29, 47, 49, 55, 56, 72–76, 101, 102, 123, 127, 132]. Turbulent flames stabilised in a JHC configuration have $Da \sim 1$ [57, 102], as indicated in Figure 2.2. Accordingly, studies of these flames in RANS simulations have overwhelmingly used the eddy dissipation concept (EDC) combustion model [3–5, 25, 26, 29, 47, 49, 72–76, 101, 102, 123, 127, 132], for its inherent ability to model finite-rate chemistry and molecular species transport, for reasons previously discussed in §2.3.4. Work focussing on Dutch natural gas (DNG) [29] and CH_4/H_2 [3–5, 72–76, 102] flames in JHC burners have identified a need to modify the constants in the standard EDC combustion model of Magnussen [68, 69]. These studies have suggested either the modification of model constants [3, 4, 29, 72–76] or, more recently, extension of the EDC model to account for local extinction [5] or low Re_t [102].

Studies by Aminian *et al.* [4] and Shabanian *et al.* [123], based on an earlier investigation on studies of a JHC burner with a DNG jet flame by De *et al.* [29], found that increasing C_τ in the EDC model to 1.5 [4] or 3 [123] provided better agreement to measurements from a JHC burner [28, 86]. The notable difference between the two aforementioned studies is the fuel involved, with Shabanian *et al.* [123] investigating C_2H_4 -based fuels as opposed to CH_4 -based fuels in De *et al.* [29] and Aminian *et al.* [4]. As a result, Shabanian *et al.* [123] used significantly more detailed chemical models, which are generally accepted to increase accuracy at the cost of computational expenditure [26, 47]. This study [123] also compared the accuracy of a flamelet model and a composition probability density function (PDF) transport model [110] which offers a more elaborate description of reacting species concentrations at a higher computational cost (refer to §2.3.4).

The EDC studies of Aminian *et al.* [4] and Shabanian *et al.* [123] were based on the result of De *et al.* [29] that increasing the EDC parameter C_τ or decreasing C_ξ improves the agreement of the models with experimental measurements. Both of these changes from the default values reduce R_i (see Equation 2.16), in agreement with the observation that the relatively low temperatures and oxygen dilutions of the

MILD combustion regime result in decreased chemical reaction rates [48, 55]. These modifications of the standard EDC model act to improve the predictions of lift-off [29], although this was not particularly apparent by setting $C_\tau = 3$ for C_2H_4 -based fuels in a JHC burner [123]. Aminian *et al.* [4] further justify the modification of C_τ (inversely proportional to R_i from Equation 2.16), by stating that the homogeneity of the MILD reaction region invalidates the assumption that species do not react beyond the confines of fine structures, and that increasing residence times acts to compensate for this. The ratio of chemical and fluid residence times was similarly cited by De *et al.* [29] as a reason for unreliability of the EDC model for flows with low turbulence. De *et al.* [29] showed that the standard value of C_ξ was unreliable for flows with $k^2/(\nu\varepsilon)$ (which was erroneously defined as Re_t) approximately less than 65, or Re_t approximately less than 30. Decreasing the C_ξ parameter decreases the reactions zones in the fluid model, restricting interactions between species and slowing the reaction rates. This emulates smaller interaction regions that could be expected of less reactive species, as would be found in MILD combustion with Damköhler number (Da) of the order of unity. It is apparent from Equation 2.16 that the effects of C_ξ are highly coupled with the fluid flow factors, ν , ε and k and their effects may behave differently at different locations within the flame as characterised by Re_t . The effects of alternate values of C_ξ appears to be a weakness in the literature concerning simulating MILD combustion, hence more research is required to generate an accurate model required to provide further understanding of this combustion regime.

References

- [1] Afarin, Y., & Tabejamaat, S. (2013). The effect of fuel inlet turbulence intensity on H_2/CH_4 flame structure of MILD combustion using the LES method. *Combust. Theor. Model.*, 17(3), 383–410.
- [2] Al-Noman, S. M., Choi, S. K., & Chung, S. H. (2016). Numerical study of laminar nonpremixed methane flames in coflow jets: Autoignited lifted flames with tribrachial edges and MILD combustion at elevated temperatures. *Combust. Flame*, 171, 119–132.
- [3] Aminian, J., Galletti, C., Shahhosseini, S., & Tognotti, L. (2011). Key modeling issues in prediction of minor species in diluted-preheated combustion conditions. *Appl. Therm. Eng.*, 31(16), 3287–3300.
- [4] Aminian, J., Galletti, C., Shahhosseini, S., & Tognotti, L. (2012). Numerical Investigation of a MILD Combustion Burner: Analysis of Mixing Field, Chem-

- ical Kinetics and Turbulence-Chemistry Interaction. *Flow Turbul. Combust.*, *88*(4), 597–623.
- [5] Aminian, J., Galletti, C., & Tognotti, L. (2016). Extended EDC local extinction model accounting finite-rate chemistry for MILD combustion. *Fuel*, *165*, 123–133.
- [6] Arndt, C., Gounder, J., Meier, W., & Aigner, M. (2012). Auto-ignition and flame stabilization of pulsed methane jets in a hot vitiated coflow studied with high-speed laser and imaging techniques. *Appl. Phys. B*, *108*(2), 407–417.
- [7] Arndt, C. M., Papageorge, M. J., Fuest, F., Sutton, J. A., Meier, W., & Aigner, M. (2016). The role of temperature, mixture fraction, and scalar dissipation rate on transient methane injection and auto-ignition in a jet in hot coflow burner. *Combust. Flame*, *167*, 60–71.
- [8] Arndt, C. M., Schießl, R., Gounder, J. D., Meier, W., & Aigner, M. (2013). Flame stabilization and auto-ignition of pulsed methane jets in a hot coflow: Influence of temperature. *Proc. Combust. Inst.*, *34*, 1483–1490.
- [9] Arteaga Mendez, L., Tummers, M., van Veen, E., & Roekaerts, D. (2015). Effect of hydrogen addition on the structure of natural-gas jet-in-hot-coflow flames. *Proc. Combust. Inst.*, *35*(3), 3557–3564.
- [10] Barlow, R., Frank, J., Karpetis, A., & Chen, J.-Y. (2005). Piloted methane/air jet flames: Transport effects and aspects of scalar structure. *Combust. Flame*, *143*(4), 433–449.
- [11] Bendtsen, A. B., Glarborg, P., & Dam-Johansen, K. (2000). Low temperature oxidation of methane: the influence of nitrogen oxides. *Combust. Sci. Technol.*, *151*(1), 31–71.
- [12] Bhaya, R., De, A., & Yadav, R. (2014). Large Eddy Simulation of MILD combustion using PDF based turbulence-chemistry interaction models. *Combust. Sci. Technol.*, *186*(9), 1138–1165.
- [13] Bray, K., Champion, M., & Libby, P. A. (1996). Extinction of premixed flames in turbulent counterflowing streams with unequal enthalpies. *Combust. Flame*, *107*(1-2), 53–64.
- [14] Buckmaster, J. (2002). Edge-flames. *Prog. Energy Combust. Sci.*, *28*(5), 435–475.

- [15] Cabra, R., Chen, J.-Y., Dibble, R., Karpetis, A., & Barlow, R. (2005). Lifted methane-air jet flames in a vitiated coflow. *Combust. Flame*, 143(4), 491–506.
- [16] Cabra, R., Myhrvold, T., Chen, J., Dibble, R., Karpetis, A., & Barlow, R. (2002). Simultaneous laser raman-rayleigh-lif measurements and numerical modeling results of a lifted turbulent H₂/N₂ jet flame in a vitiated coflow. *Proc. Combust. Inst.*, 29, 1881–1888.
- [17] Cai, G., Yen, M., & Abraham, J. (2016). On formulating a simplified soot model for diesel and biodiesel combustion. *Chem. Eng. Sci.*, 144, 249–259.
- [18] Cao, R. R., Pope, S. B., & Masri, A. R. (2005). Turbulent lifted flames in a vitiated coflow investigated using joint PDF calculations. *Combust. Flame*, 142, 438–453.
- [19] Cavaliere, A., & de Joannon, M. (2004). Mild Combustion. *Prog. Energ. Combust.*, 30(4), 329–366.
- [20] Cha, M. S., & Ronney, P. D. (2006). Propagation rates of nonpremixed edge flames. *Combust. Flame*, 146(1-2), 312–328.
- [21] Choi, B., & Chung, S. (2010). Autoignited laminar lifted flames of methane, ethylene, ethane, and n-butane jets in coflow air with elevated temperature. *Combust. Flame*, 157(12), 2348–2356.
- [22] Choi, B., Kim, K., & Chung, S. (2009). Autoignited laminar lifted flames of propane in coflow jets with tribrachial edge and mild combustion. *Combust. Flame*, 156(2), 396–404.
- [23] Choi, B. C., & Chung, S. H. (2012). Autoignited laminar lifted flames of methane/hydrogen mixtures in heated coflow air. *Combust. Flame*, 159(4), 1481–1488.
- [24] Choi, S. K., Kim, J., Chung, S. H., & Kim, J. S. (2009). Structure of the edge flame in a methane-oxygen mixing layer. *Combust. Theor. Model.*, 13(1), 39–56.
- [25] Christo, F. C., & Dally, B. B. (2004). Application of transport PDF approach for modelling MILD combustion. In *Proceedings of the Fifteenth Australian Fluid Mechanics Conference*. The University of Sydney, Sydney, Australia: The University of Sydney, Sydney, Australia.
- [26] Christo, F. C., & Dally, B. B. (2005). Modeling turbulent reacting jets issuing into a hot and diluted coflow. *Combust. Flame*, 142(1-2), 117–129.

- [27] Chung, S. (2007). Stabilization, propagation and instability of tribrachial triple flames. *Proc. Combust. Inst.*, 31(1), 877–892.
- [28] Dally, B., Karpetis, A., & Barlow, R. (2002). Structure of turbulent non-premixed jet flames in a diluted hot coflow. *Proc. Combust. Inst.*, 29, 1147–1154.
- [29] De, A., Oldenhof, E., Sathiah, P., & Roekaerts, D. (2011). Numerical Simulation of Delft-Jet-in-Hot-Coflow (DJHC) Flames Using the Eddy Dissipation Concept Model for Turbulence-Chemistry Interaction. *Flow Turbul. Combust.*, 87(4), 537–567.
- [30] de Joannon, M., Cavaliere, A., Donnarumma, R., & Ragucci, R. (2002). Dependence of autoignition delay on oxygen concentration in mild combustion of high molecular weight paraffin. *Proc. Combust. Inst.*, 29(1), 1139–1146.
- [31] de Joannon, M., Cavaliere, A., Faravelli, T., Ranzi, E., Sabia, P., & Tregrossi, A. (2005). Analysis of process parameters for steady operations in methane mild combustion technology. *Proc. Combust. Inst.*, 30(2), 2605–2612.
- [32] de Joannon, M., Matarazzo, A., Sabia, P., & Cavaliere, A. (2007). Mild Combustion in Homogeneous Charge Diffusion Ignition (HCDI) regime. *Proc. Combust. Inst.*, 31(2), 3409–3416.
- [33] de Joannon, M., Sabia, P., Cozzolino, G., Sorrentino, G., & Cavaliere, A. (2012). Pyrolytic and Oxidative Structures in Hot Oxidant Diluted Oxidant (HODO) MILD Combustion. *Combust. Sci. Technol.*, 184(7-8), 1207–1218.
- [34] de Joannon, M., Sabia, P., Sorrentino, G., Bozza, P., & Ragucci, R. (In Press). Small size burner combustion stabilization by means of strong cyclonic recirculation. *Proc. Combust. Inst.*. DOI: 10.1016/j.proci.2016.06.070.
- [35] de Joannon, M., Sabia, P., Sorrentino, G., & Cavaliere, A. (2009). Numerical study of mild combustion in hot diluted diffusion ignition (HDDI) regime. *Proc. Combust. Inst.*, 32(2), 3147–3154.
- [36] de Joannon, M., Saponaro, A., & Cavaliere, A. (2000). Zero-dimensional analysis of diluted oxidation of methane in rich conditions. *Proc. Comb. Inst.*, 28(2), 1639–1646.
- [37] de Joannon, M., Sorrentino, G., & Cavaliere, A. (2012). MILD combustion in diffusion-controlled regimes of Hot Diluted Fuel. *Combust. Flame*, 159, 1832–1839.

- [38] Derudi, M., Villani, A., & Rota, R. (2007). Sustainability of mild combustion of hydrogen-containing hybrid fuels. *Proc. Combust. Inst.*, 31(2), 3393–3400.
- [39] Domingo, P., & Vervisch, L. (1996). Triple flames and partially premixed combustion in autoignition of non-premixed turbulent mixtures. *Proc. Combust. Inst.*, 26(1), 233–240.
- [40] Dubreuil, A., Foucher, F., Mounaïm-Rousselle, C., Dayma, G., & Dagaut, P. (2007). HCCI combustion: Effect of NO in EGR. *Proc. Combust. Inst.*, 31(2), 2879–2886.
- [41] Duwig, C., & Dunn, M. J. (2013). Large Eddy Simulation of a premixed jet flame stabilized by a vitiated co-flow: Evaluation of auto-ignition tabulated chemistry. *Combust. Flame*, 160(12), 2879–2895.
- [42] Echekki, T., & Chen, J. H. (2003). Direct numerical simulation of autoignition in non-homogeneous hydrogen-air mixtures. *Combust. Flame*, 134(3), 169–191.
- [43] Effuggi, A., Gelosa, D., Derudi, M., & Rota, R. (2008). Mild Combustion of Methane-Derived Fuel Mixtures: Natural Gas and Biogas. *Combustion Science and Technology*, 180(3), 481–493.
- [44] Elsamra, R. M. I., Vranckx, S., & Carl, S. A. (2005). $\text{CH}(\text{A}^2\Delta)$ Formation in Hydrocarbon Combustion: The Temperature Dependence of the Rate Constant of the Reaction $\text{C}_2\text{H} + \text{O}_2 \rightarrow \text{CH}(\text{A}^2\Delta) + \text{CO}_2$. *J. Phys. Chem.*, 109(45), 10287–10293.
- [45] Faravelli, T., Frassoldati, A., & Ranzi, E. (2003). Kinetic modeling of the interactions between NO and hydrocarbons in the oxidation of hydrocarbons at low temperatures. *Combust. Flame*, 132(1-2), 188–207.
- [46] Frassoldati, A., Faravelli, T., & Ranzi, E. (2003). Kinetic modeling of the interactions between NO and hydrocarbons at high temperature. *Combust. Flame*, 135(1-2), 97–112.
- [47] Frassoldati, A., Sharma, P., Cuoci, A., Faravelli, T., & Ranzi, E. (2010). Kinetic and fluid dynamics modeling of methane/hydrogen jet flames in diluted coflow. *Appl. Therm. Eng.*, 30(4), 376–383.
- [48] Galletti, C., Parente, A., & Tognotti, L. (2007). Numerical and experimental investigation of a mild combustion burner. *Combust. Flame*, 151, 649–664.

- [49] Gao, X., Duan, F., Lim, S. C., & Yip, M. S. (2013). NO_x formation in hydrogen-methane turbulent diffusion flame under the moderate or intense low-oxygen dilution conditions. *Energy*, 59, 559–569.
- [50] Göktolga, M. U., van Oijen, J. A., & de Goey, L. H. (In Press). Modeling MILD combustion using a novel multistage FGM method. *Proc. Combust. Inst.*. DOI: 10.1016/j.proci.2016.06.004.
- [51] Göktolga, M. U., van Oijen, J. A., & de Goey, L. P. H. (2015). 3D DNS of MILD combustion: A detailed analysis of heat loss effects, preferential diffusion, and flame formation mechanisms. *Fuel*, 159, 784–795.
- [52] Gordon, R. L., Masri, A. R., & Mastorakos, E. (2008). Simultaneous Rayleigh temperature, OH- and CH₂O-LIF imaging of methane jets in a vitiated coflow. *Combust. Flame*, 155(1-2), 181–195.
- [53] Gordon, R. L., Masri, A. R., & Mastorakos, E. (2009). Heat release rate as represented by [OH] × [CH₂O] and its role in autoignition. *Combust. Theor. Model.*, 13(4), 645–670.
- [54] Gordon, R. L., Masri, A. R., Pope, S. B., & Goldin, G. M. (2007). A numerical study of auto-ignition in turbulent lifted flames issuing into a vitiated co-flow. *Combust. Theor. Model.*, 11(3), 351–376.
- [55] Ihme, M., & See, Y. C. (2011). LES flamelet modeling of a three-stream MILD combustor: Analysis of flame sensitivity to scalar inflow conditions. *Proc. Combust. Inst.*, 33, 1309–1217.
- [56] Ihme, M., Zhang, J., He, G., & Dally, B. B. (2012). Large-Eddy Simulation of a Jet-in-Hot-Coflow Burner Operating in the Oxygen-Diluted Combustion Regime. *Flow, Turbul. Combust.*, 89, 449–464.
- [57] Isaac, B. J., Parente, A., Galletti, C., Thornock, J. N., Smith, P. J., & Tognotti, L. (2013). A Novel Methodology for Chemical Time Scale Evaluation with Detailed Chemical Reaction Kinetics. *Energy Fuels*, 27(4), 2255–2265.
- [58] Joedicke, A., Peters, N., & Mansour, M. (2005). The stabilization mechanism and structure of turbulent hydrocarbon lifted flames. *Proc. Combust. Inst.*, 30(1), 901–909.
- [59] Krisman, A., Tang, J. C., Hawkes, E. R., Lignell, D. O., & Chen, J. H. (2014). A DNS evaluation of mixing models for transported PDF modelling of turbulent nonpremixed flames. *Combust. Flame*, 161(8), 2085–2106.

- [60] Kruse, S., Kerschgens, B., Berger, L., Varea, E., & Pitsch, H. (2015). Experimental and numerical study of MILD combustion for gas turbine applications. *Appl. Energ.*, *148*, 456–465.
- [61] Kulkarni, R. M., & Polifke, W. (2013). LES of Delft-Jet-In-Hot-Coflow (DJHC) with tabulated chemistry and stochastic fields combustion model. *Fuel Process. Technol.*, *107*, 138–146.
- [62] Li, P., Wang, F., Mi, J., Dally, B., Mei, Z., Zhang, J., & Parente, A. (2014). Mechanisms of NO formation in MILD combustion of CH₄/H₂ fuel blends. *Int. J. Hydrogen Energ.*, *39*(33), 19187–19203.
- [63] Li, X., Jasper, A. W., Zádor, J., Miller, J. A., & Klippenstein, S. J. (2016). Theoretical kinetics of O + C₂H₄. *Proc. Combust. Inst.*. DOI: 10.1016/j.proci.2016.06.053.
- [64] Liñán, A. (1974). The asymptotic structure of counterflow diffusion flames for large activation energies. *Acta Astronaut.*, *1*(7-8), 1007–1039.
- [65] Liu, W., Kelley, A., & Law, C. (2010). Flame propagation and counterflow non-premixed ignition of mixtures of methane and ethylene. *Combust. Flame*, *157*(5), 1027–1036.
- [66] Luo, Z., Yoo, C. S., Richardson, E. S., Chen, J. H., Law, C. K., & Lu, T. (2012). Chemical explosive mode analysis for a turbulent lifted ethylene jet flame in highly-heated coflow. *Combust. Flame*, *159*(1), 265–274.
- [67] Lyons, K. M. (2007). Toward an understanding of the stabilization mechanisms of lifted turbulent jet flames: Experiments. *Prog. Energy Combust. Sci.*, *33*(2), 211–231.
- [68] Magnussen, B. F. (1981). On the structure of turbulence and a generalized eddy dissipation concept for chemical reaction in turbulent flow. In *19th AIAA Aerospace Meeting*. St. Louis, USA.
- [69] Magnussen, B. F. (2005). The eddy dissipation concept a bridge between science and technology. In *ECCOMAS thematic conference on computational combustion*. Lisbon, Portugal.
- [70] Manias, D. M., Tingas, E. A., Frouzakis, C. E., Boulouchos, K., & Goussis, D. A. (2016). The mechanism by which CH₂O and H₂O₂ additives affect the autoignition of CH₄/air mixtures. *Combust. Flame*, *164*, 111–125.

- [71] Mansour, M. S. (2003). Stability characteristics of lifted turbulent partially premixed jet flames. *Combust. Flame*, 133(3), 263–274.
- [72] Mardani, A., & Ghomshi, A. F. (2016). Numerical study of oxy-fuel MILD (moderate or intense low-oxygen dilution combustion) combustion for CH₄-H₂ fuel. *Energy*, 99, 136–151.
- [73] Mardani, A., & Tabejamaat, S. (2010). Effect of hydrogen on hydrogen methane turbulent non-premixed flame under MILD condition. *Int. J. Hydrogen Energ.*, 35(20), 11324–11331.
- [74] Mardani, A., Tabejamaat, S., & Ghamari, M. (2010). Numerical study of influence of molecular diffusion in the Mild combustion regime. *Combust. Theor. Model.*, 14(5), 747–774.
- [75] Mardani, A., Tabejamaat, S., & Hassanpour, S. (2013). Numerical study of CO and CO₂ formation in CH₄/H₂ blended flame under MILD condition. *Combust. Flame*, 160(9), 1636–1649.
- [76] Mardani, A., Tabejamaat, S., & Mohammadi, M. B. (2011). Numerical study of the effect of turbulence on rate of reactions in the MILD combustion regime. *Combust. Theor. Model.*, 15(6), 753–772.
- [77] Masri, A. (2015). Partial premixing and stratification in turbulent flames. *Proc. Combust. Inst.*, 35(2), 1115–1136.
- [78] Masri, A. R., Cao, R., Pope, S. B., & Goldin, G. M. (2003). PDF calculations of turbulent lifted flames of H₂/N₂ fuel issuing into a vitiated co-flow. *Combust. Theor. Model.*, 8(1), 1–22.
- [79] Mastorakos, E. (2009). Ignition of turbulent non-premixed flames. *Prog. Energy Combust. Sci.*, 35(1), 57–97.
- [80] Mastorakos, E., Taylor, A., & Whitelaw, J. (1995). Extinction of turbulent counterflow flames with reactants diluted by hot products. *Combust. Flame*, 102(1-2), 101–114.
- [81] Medwell, P. R., Blunck, D. L., & Dally, B. B. (2014). The role of precursors on the stabilisation of jet flames issuing into a hot environment. *Combust. Flame*, 161(2), 465–474.
- [82] Medwell, P. R., & Dally, B. B. (2012). Effect of fuel composition on jet flames in a heated and diluted oxidant stream. *Combust. Flame*, 159(10), 3138–3145.

- [83] Medwell, P. R., & Dally, B. B. (2012). Experimental Observation of Lifted Flames in a Heated and Diluted Coflow. *Energy Fuels*, 26(9), 5519–5527.
- [84] Medwell, P. R., Evans, M. J., Chan, Q. N., & Katta, V. R. (2016). Laminar flame calculations for analysing trends in autoignitive jet flames in a hot and vitiated coflow. *Energy Fuels*, 30(10), 8680–8690.
- [85] Medwell, P. R., Kalt, P. A. M., & Dally, B. B. (2007). Simultaneous imaging of OH, formaldehyde, and temperature of turbulent nonpremixed jet flames in a heated and diluted coflow. *Combust. Flame*, 148(1-2), 48–61.
- [86] Medwell, P. R., Kalt, P. A. M., & Dally, B. B. (2008). Imaging of diluted turbulent ethylene flames stabilized on a Jet in Hot Coflow (JHC) burner. *Combust. Flame*, 152, 100–113.
- [87] Medwell, P. R., Kalt, P. A. M., & Dally, B. B. (2009). Reaction Zone Weakening Effects under Hot and Diluted Oxidant Stream Conditions. *Combust. Sci. Technol.*, 181(7), 937–953.
- [88] Minamoto, Y., Dunstan, T., Swaminathan, N., & Cant, R. (2013). DNS of EGR-type turbulent flame in MILD condition. *Proc. Combust. Inst.*, 34(2), 3231–3238.
- [89] Minamoto, Y., & Swaminathan, N. (2014). Modelling paradigms for MILD combustion. *Int. J. Adv. Eng. Sci. Appl. Math.*, 6(1), 1–11.
- [90] Minamoto, Y., & Swaminathan, N. (2014). Scalar gradient behaviour in MILD combustion. *Combust. Flame*, 161(4), 1063–1075.
- [91] Minamoto, Y., & Swaminathan, N. (2015). Subgrid scale modelling for MILD combustion. *Proc. Combust. Inst.*, 35(03), 3529–3536.
- [92] Minamoto, Y., Swaminathan, N., Cant, R. S., & Leung, T. (2014). Reaction Zones and Their Structure in MILD Combustion. *Combust. Sci. Technol.*, 186(8), 1075–1096.
- [93] Minamoto, Y., Swaminathan, N., Cant, S. R., & Leung, T. (2014). Morphological and statistical features of reaction zones in MILD and premixed combustion. *Combust. Flame*, 161(11), 2801–2814.
- [94] Najafizadeh, S. M., Sadeghi, M., & Sotudeh-Gharebagh, R. (2013). Analysis of autoignition of a turbulent lifted H_2/N_2 jet flame issuing into a vitiated coflow. *Int. J. Hydrogen Energ.*, 38(5), 2510–2522.

- [95] Najm, H. N., Valorani, M., Goussis, D. A., & Prager, J. (2010). Analysis of methane-air edge flame structure. *Combust. Theor. Model.*, 14(2), 257–294.
- [96] Oberlack, M., Arlitt, R., & Peters, N. (2000). On stochastic Damköhler number variations in a homogeneous flow reactor. *Combust. Theor. Model.*, 4(4), 495–510.
- [97] Oldenhof, E., Tummers, M. J., van Veen, E. H., & Roekaerts, D. J. E. M. (2010). Ignition kernel formation and lift-off behaviour of jet-in-hot-coflow flames. *Combust. Flame*, 157(6), 1167–1178.
- [98] Oldenhof, E., Tummers, M. J., van Veen, E. H., & Roekaerts, D. J. E. M. (2011). Role of entrainment in the stabilisation of jet-in-hot-coflow flames. *Combust. Flame*, 158(8), 1553–1563.
- [99] Oldenhof, E., Tummers, M. J., van Veen, E. H., & Roekaerts, D. J. E. M. (2012). Transient response of the Delft jet-in-hot coflow flames. *Combust. Flame*, 159(2), 697–706.
- [100] Papageorge, M., Arndt, C., Fuest, F., Meier, W., & Sutton, J. (2014). High-speed mixture fraction and temperature imaging of pulsed, turbulent fuel jets auto-igniting in high-temperature, vitiated co-flows. *Exp. Fluids*, 55(7).
- [101] Parente, A., Galletti, C., & Tognotti, L. (2011). A simplified approach for predicting NO formation in MILD combustion of CH₄-H₂ mixtures. *Proc. Combust. Inst.*, 33(2), 3343–3350.
- [102] Parente, A., Malik, M. R., Contino, F., Cuoci, A., & Dally, B. B. (2016). Extension of the Eddy Dissipation Concept for turbulence/chemistry interactions to MILD combustion. *Fuel*, 163, 98–111.
- [103] Parente, A., Sutherland, J., Dally, B., Tognotti, L., & Smith, P. (2011). Investigation of the MILD combustion regime via Principal Component Analysis. *Proc. Combust. Inst.*, 33(2), 3333–3341.
- [104] Paul, P. H., & Najm, H. N. (1998). Planar laser-induced fluorescence imaging of flame heat release rate. *Proc. Combust. Inst.*, 27(1), 43–50.
- [105] Peters, N. (1984). Laminar diffusion flamelet models in non-premixed turbulent combustion. *Prog. Energy Combust. Sci.*, 10(3), 319–339.
- [106] Peters, N. (2000). *Turbulent Combustion*. Cambridge University Press.

- [107] Pitsch, H., & Fedotov, S. (2001). Investigation of scalar dissipation rate fluctuations in non-premixed turbulent combustion using a stochastic approach. *Combust. Theor. Model.*, 5(1), 41–57.
- [108] Plessing, T., Peters, N., & Wüning, J. G. (1998). Laseroptical investigation of highly preheated combustion with strong exhaust gas recirculation. *Proc. Combust. Inst.*, 27(2), 3197–3204.
- [109] Plessing, T., Terhoeven, P., Peters, N., & Mansour, M. S. (1998). An experimental and numerical study of a laminar triple flame. *Combust. Flame*, 115(3), 335–353.
- [110] Pope, S. (1985). PDF methods for turbulent reactive flows. *Prog. Energ. Combust.*, 11(2), 119–192.
- [111] Prager, J., Najm, H., Valorani, M., & Goussis, D. (2011). Structure of n-heptane/air triple flames in partially-premixed mixing layers. *Combust. Flame*, 158(11), 2128–2144.
- [112] Ramachandran, A., Tyler, D. A., Patel, P. K., Narayanaswamy, V., & Lyons, K. M. (2015). Global Features of Flame Stabilization in Turbulent Non-premixed Jet Flames in Vitiated Coflow. *45th AIAA Fluid Dynamics Conference*.
- [113] Rao, A. G., & Levy, Y. A. (2010). New combustion methodology for low emission gas turbine engines. In *8th International Symposium on High Temperature Air Combustion and Gasification*, (pp. 177–185). Poznań, Poland.
- [114] Ravi, S., Sikes, T., Morones, A., Keese, C., & Petersen, E. (2015). Comparative study on the laminar flame speed enhancement of methane with ethane and ethylene addition. *Proc. Combust. Inst.*, 35(1), 679 – 686.
- [115] Sabia, P., de Joannon, M., Fierro, S., Tregrossi, A., & Cavaliere, A. (2007). Hydrogen-enriched methane Mild Combustion in a well stirred reactor. *Exp. Therm. Fluid Sci.*, 31(5), 469–475.
- [116] Sabia, P., de Joannon, M., Picarelli, A., Chinnici, A., & Ragucci, R. (2012). Modeling Negative Temperature Coefficient region in methane oxidation. *Fuel*, 91(1), 238–245.
- [117] Sabia, P., de Joannon, M., Picarelli, A., & Ragucci, R. (2013). Methane auto-ignition delay times and oxidation regimes in MILD combustion at atmospheric pressure. *Combust. Flame*, 160(1), 47–55.

- [118] Sabia, P., Lavadera, M. L., Giudicianni, P., Sorrentino, G., Ragucci, R., & de Joannon, M. (2015). CO₂ and H₂O effect on propane auto-ignition delay times under mild combustion operative conditions. *Combust. Flame*, 162(3), 533–543.
- [119] Sabia, P., Lubrano Lavadera, M., Sorrentino, G., Giudicianni, P., Ragucci, R., & de Joannon, M. (2016). H₂O and CO₂ Dilution in MILD Combustion of Simple Hydrocarbons. *Flow, Turbul. Combust.*, 96(2), 433–448.
- [120] Sabia, P., Sorrentino, G., Chinnici, A., Cavaliere, A., & Ragucci, R. (2015). Dynamic Behaviors in Methane MILD and Oxy-Fuel Combustion. Chemical Effect of CO₂. *Energy Fuels*, 29(3), 1978–1986.
- [121] Saha, M., Chinnici, A., Dally, B. B., & Medwell, P. R. (2015). Numerical Study of Pulverized Coal MILD Combustion in a Self-Recuperative Furnace. *Energy Fuels*, 29(11), 7650–7669.
- [122] Saha, M., Dally, B. B., Medwell, P. R., & Chinnici, A. (2016). Effect of particle size on the MILD combustion characteristics of pulverised brown coal. *Fuel Process. Technol.*, 155, 74–87.
- [123] Shabanian, S. R., Medwell, P. R., Rahimi, M., Frassoldati, A., & Cuoci, A. (2013). Kinetic and fluid dynamic modeling of ethylene jet flames in diluted and heated oxidant stream combustion conditions. *Appl. Therm. Eng.*, 52, 538–554.
- [124] Sidey, J., & Mastorakos, E. (2015). Visualization of MILD combustion from jets in cross-flow. *Proc. Combust. Inst.*, 35(3), 3537–3545.
- [125] Sidey, J., Mastorakos, E., & Gordon, R. L. (2014). Simulations of Autoignition and Laminar Premixed Flames in Methane/Air Mixtures Diluted with Hot Products. *Combust. Sci. Technol.*, 186(4-5), 453–465.
- [126] Sidey, J. A., & Mastorakos, E. (2016). Simulations of laminar non-premixed flames of methane with hot combustion products as oxidiser. *Combust. Flame*, 163, 1–11.
- [127] Tu, Y., Su, K., Liu, H., Chen, S., Liu, Z., & Zheng, C. (2016). Physical and chemical effects of CO₂ addition on CH₄/H₂ flames on a Jet in Hot Coflow (JHC) burner. *Energy Fuels*, 30(2), 1390–1399.

- [128] van Oijen, J. (2013). Direct numerical simulation of autoigniting mixing layers in MILD combustion. *Proc. Combust. Inst.*, 34(1), 1163–1171.
- [129] Wada, T., Lefkowitz, J. K., & Ju, Y. (2015). Plasma Assisted MILD Combustion. *53rd AIAA Aerospace Sciences Meeting*.
- [130] Wang, F., Li, P., Mei, Z., Zhang, J., & Mi, J. (2014). Combustion of CH₄/O₂/N₂ in a well stirred reactor. *Energy*, 72, 242–253.
- [131] Wang, F., Li, P., Mi, J., Wang, J., & Xu, M. (2015). Chemical kinetic effect of hydrogen addition on ethylene jet flames in a hot and diluted coflow. *Int. J. Hydrogen Energ.*, 40(46), 16634–16648.
- [132] Wang, F., Mi, J., & Li, P. (2013). Combustion Regimes of a Jet Diffusion Flame in Hot Co-flow. *Energy Fuels*, 27(6), 3488–3498.
- [133] Westbrook, C. K., & Dryer, F. L. (1984). Chemical kinetic modeling of hydrocarbon combustion. *Prog. Energy Combust. Sci.*, 10(1), 1–57.
- [134] Wüning, J. A., & Wüning, J. G. (1997). Flameless oxidation to reduce thermal no-formation. *Prog. Energy Combust.*, 23(1), 81–94.
- [135] Ye, J., Medwell, P. R., Dally, B. B., & Evans, M. J. (2016). The transition of ethanol flames from conventional to MILD combustion. *Combust. Flame*, 171, 173–184.
- [136] Ye, J., Medwell, P. R., Varea, E., Kruse, S., Dally, B. B., & Pitsch, H. G. (2015). An experimental study on MILD combustion of prevaporised liquid fuels. *Appl. Energ.*, 151, 93–101.
- [137] Yoo, C. S., Richardson, E. S., Sankaran, R., & Chen, J. H. (2011). A DNS study on the stabilization mechanism of a turbulent lifted ethylene jet flame in highly-heated coflow. *Proc. Combust. Inst.*, 33, 1619–1627.
- [138] Yoo, C. S., Sankaran, R., & Chen, J. H. (2009). Three-dimensional direct numerical simulation of a turbulent lifted hydrogen jet flame in heated coflow: flame stabilization and structure. *J. Fluid Mech*, 640, 453–481.

Chapter 4

Classification and Lift-Off Height

Prediction of Non-Premixed MILD and Autoignitive Flames

Statement of Authorship

Title of Paper	Classification and Lift-Off Height Prediction of Non-Premixed MILD and Autoignitive Flames
Publication Status	<input type="checkbox"/> Published <input checked="" type="checkbox"/> Accepted for Publication <input type="checkbox"/> Submitted for Publication <input type="checkbox"/> Unpublished and Unsubmitted work written in manuscript style
Publication Details	Evans, MJ , Medwell, PR, Wu, H, Stagni, A, Ihme, M (2016). "Classification and Lift-Off Height Prediction of Non-Premixed MILD and Autoignitive Flames". <i>Proceedings of the Combustion Institute</i> , DOI: 10.1016/j.proci.2016.06.013

Principal Author

Name of Principal Author (Candidate)	Michael John Evans
Contribution to the Paper	Designed research concept, planned analytical approach, generation and analysis of all numerical data, co-designed and undertook experiments, interpreted data, wrote manuscript and acted as corresponding author.
Overall percentage (%)	70
Certification:	This paper reports on original research I conducted during the period of my Higher Degree by Research candidature and is not subject to any obligations or contractual agreements with a third party that would constrain its inclusion in this thesis. I am the primary author of this paper.
Signature	<div style="display: flex; justify-content: space-between;"> <div>Digitally signed by Michael Evans Date: 2016.10.18 16:52:27 +10'30'</div> <div>Date</div> <div>18-Oct-2016</div> </div>

Co-Author Contributions

By signing the Statement of Authorship, each author certifies that:

- i. the candidate's stated contribution to the publication is accurate (as detailed above);
- ii. permission is granted for the candidate to include the publication in the thesis; and
- iii. the sum of all co-author contributions is equal to 100% less the candidate's stated contribution.

Name of Co-Author	Paul Ross Medwell
Contribution to the Paper	Co-supervised development of the work, co-designed and undertook experiments, helped to evaluate and edit the manuscript.
Signature	<div style="display: flex; justify-content: space-between;"> <div>Paul Medwell 2016.10.18 17:16:19 +10'30'</div> <div>Date</div> <div>18-OCT-2016</div> </div>

Name of Co-Author	Hao Wu
Contribution to the Paper	Co-designed analytical approach and chemical data.
Signature	<div style="display: flex; justify-content: space-between;"> <div>Digitally signed by Hao Wu Date: 2016.10.18 15:19:43 -07'00'</div> <div>Date</div> <div>18-OCT-2016</div> </div>

Name of Co-Author	Alessandro Stagni
-------------------	-------------------

Contribution to the Paper	Helped to analyse chemical data, helped to evaluate and edit the manuscript.		
Signature	<small>Firmato digitalmente da Alessandro Stagni DN: cn=Alessandro Stagni, o=Università di Milano, email=Alessandro.Stagni@polimi.it, c=IT Date: 2016.10.19 17:57:03 +02'00'</small>	Date	19-OCT-2016

Name of Co-Author	Matthias Ihme		
Contribution to the Paper	Co-supervised development of the work, helped to evaluate and edit the manuscript.		
Signature	<small>Digitally signed by Matthias Ihme DN: cn=Matthias Ihme, o=Stanford University, ou, email=mihme@stanford.edu, c=US Date: 2016.10.18 06:09:09 -06'00'</small>	Date	



ELSEVIER

Available online at www.sciencedirect.com

ScienceDirect

Proceedings of the Combustion Institute 000 (2016) 1–8

Proceedings
of the
Combustion
Institutewww.elsevier.com/locate/proci

Classification and lift-off height prediction of non-premixed MILD and autoignitive flames

M.J. Evans^{a,b,*}, P.R. Medwell^a, H. Wu^b, A. Stagni^{b,c}, M. Ihme^b^a School of Mechanical Engineering, The University of Adelaide, South Australia 5005, Australia^b Department of Mechanical Engineering, Stanford University, California 94305, USA^c Dipartimento di Chimica, Materiali ed Ingegneria Chimica "G. Natta", Politecnico di Milano, 20133 Milan, Italy

Received 4 December 2015; accepted 1 June 2016

Available online xxx

Abstract

Moderate or intense low oxygen dilution (MILD) combustion has been the subject of numerous studies in recent years. An issue remains, however, in the definition of the boundaries of the MILD combustion regime with respect to non-premixed configurations without predefined reference temperatures. A flamelet definition is applied to non-premixed configurations to better understand the MILD combustion regime and classify previous experimental investigations. Through a simplified analysis, a new definition for the non-premixed MILD combustion regime is derived. This new definition is a function of initial and final temperatures, and the effective activation energy of an equivalent one-step chemical reaction. This inherently agrees with the features of the premixed flamelet definition and provides insight into previous attempts to reconcile premixed and non-premixed classifications of MILD combustion. Previously studied turbulent flames are classified using the new definition of MILD combustion and are compared to experimental observations. The new definition of MILD combustion is subsequently compared to the ignition characteristics of opposed-flow ethylene flames, showing good agreement. Finally, transient flamelets are solved for a modelled flow-field to successfully reproduce non-monotonic trends in the lift-off that is observed experimentally in a series of MILD and autoignitive, turbulent ethylene flames in hot, diluted coflows.

© 2016 by The Combustion Institute. Published by Elsevier Inc.

Keywords: MILD combustion; Non-premixed flames; Lifted flames; Autoignition; Flamelet theory

1. Introduction

Moderate or intense low oxygen dilution (MILD) combustion features reduced pollutant emissions and efficiency improvements over conventional combustion [1]. Operation in the MILD, or flameless, combustion regime is generally achieved by burning fuel in hot, low oxygen environments. This reduces chemical reaction rates,

* Corresponding author at: School of Mechanical Engineering, The University of Adelaide, South Australia, 5005, Australia. Fax: +61 8 8313 4367.

E-mail address: m.evans@adelaide.edu.au (M.J. Evans).

Nomenclature

α	Heat release parameter
χ	Scalar dissipation rate
ΔT	Temperature increase
ω	Reaction rate
ρ	Density
τ	Non-dimensional time
θ	Non-dimensional temperature
D	Jet exit diameter
Da	Global Damköhler number
E_{eff}	Effective one-step activation energy
R	Universal gas constant
r	Radius (cylindrical polar coordinates)
Sc_t	Turbulent Schmidt number
T	Temperature
u_0	Jet bulk velocity relative to coflow velocity
x	Axial distance from jet exit plane
Subscripts	
0	Reference value
b	Fully burnt mixture
$cofl$	Coflow conditions
ex	Extinction condition
ign	Steady-state autoignition condition
in	Initial condition
mr	Most reactive mixture
si	Self-ignition condition
st	Stoichiometric mixture
u	Unburnt (fresh) mixture

resulting in distributed reaction zones as opposed to the high temperature peaks in conventional flames [1]. As a result, jet flames in the MILD regime feature a global Damköhler number (Da) near unity, such that finite-rate chemistry becomes important [2,3]. Despite numerous investigations into the unique characteristics of MILD combustion, the boundaries of the MILD regime have not been thoroughly defined in non-premixed configurations.

Ignition and combustion stability of the MILD combustion regime have been investigated experimentally [4] and numerically [4–7] in premixed reactors [1]. These analyses have been based on initial temperature (T_{in}) and temperature increase (ΔT), relative to a self-ignition temperature (T_{si}) [1]. This T_{si} is defined as the minimum inlet temperature required for ignition in a perfectly-stirred reactor (PSR) within one second [1]. This definition has since formed the basis of premixed [4–6] and non-premixed [8] analyses of MILD combustion.

The MILD combustion regime in a premixed reactor has been defined independently to T_{si} [1,5]. By this definition, MILD combustion implies that the S-shaped curve of temperature as a function of the characteristic time is monotonic, and without

ignition or extinction points [5,9–11]. This definition leads to a criterion for premixed MILD combustion, which, assuming constant specific heat at constant pressure, may be approximated as [1]:

$$E_{eff}/(RT_{in}) \leq 4(1 + T_{in}/\Delta T) \quad (1)$$

where R is the universal gas constant and E_{eff} is the effective activation energy of an equivalent one-step reaction. This definition separates gradually igniting MILD flames from conventional autoignitive flames, which feature ignition and extinction points on the S-shaped curve. This is consistent with the “flameless” description of MILD combustion [1,5]. The two alternate premixed classifications of MILD combustion both propose distinct definitions of the MILD regime, based on a critical temperature, T_{si} , [1] or the global ignition process, E_{eff} [5].

The definition of MILD combustion based on the S-shaped curve has previously been applied in analytical [9] and numerical [10,11] studies. A previous analytical study combined the monotonic S-shaped curve with a pre-defined quenching temperature, to enforce an extinction condition [9]. The S-shaped curve concept has additionally been used to classify results in a numerical study, with extinction disappearing with sufficient preheating and dilution [11].

Experimental studies of non-premixed ethylene (C_2H_4) flames in a jet-in-hot-coflow (JHC) burner indicate that apparently attached flames undergo gradual ignition in low oxygen coflows, corresponding to MILD combustion [12,13]. Increasing oxygen concentration leads to a transition to a conventional autoignitive flame structure [12–14]. Both flame structures were observed by Medwell et al. [12] in two flames meeting the PSR definition of MILD combustion, despite their different ignition characteristics.

The numerical investigation of MILD combustion in a JHC configuration added “quasi-MILD” and “MILD-like” regimes [8] to the PSR definition of Cavaliere and de Joannon [1]. Both regimes keep the condition $\Delta T < T_{si}$, however, the former describes cases requiring forced ignition and the latter does not meet the imposed “low oxygen dilution” criterion [8]. Neither [8], nor the subsequent chemical kinetics analysis [6] offer further distinctions between MILD combustion and these two regimes. These classifications expand the PSR definition, however are unable to distinguish gradual MILD combustion from conventional autoignition.

The definitions of MILD combustion based on temperatures are not consistent between premixed and non-premixed configurations. The current work aims to use an idealised, one-dimensional flamelet analysis to define non-premixed MILD combustion without the requirement for composition-dependent reference temperatures, by including a fuel-specific E_{eff} . This definition is based on the S-shaped curve

concept [5,9] which is applied to non-premixed configurations through analysis similar to that by Pitsch and Fedotov [15]. This new definition for non-premixed MILD combustion is quantified through an opposed-flow flamelet analysis, to produce a criterion for non-premixed MILD combustion, which is compared to premixed regime classifications. This definition is subsequently used to classify previous experiments, and compare flamelet simulations to new experimental observations in a JHC burner.

2. Numerical analysis

2.1. Non-premixed flamelet analysis

The one-dimensional, opposed-flow flamelet equations for a non-premixed system with an irreversible, one-step reaction were analysed by Pitsch and Fedotov [15]. This analysis couples the reaction rate (ω), scalar dissipation rate (χ), mixture fraction (Z) and normalised time (τ). At stoichiometric conditions (st), the flamelet solution was shown to yield the following equation relating normalised temperature (θ_{st}) and χ along the S-shaped curve [15]:

$$\frac{d\theta_{st}}{d\tau} + (\chi_{st}/\chi_{st,0})\theta_{st} - \omega(\theta_{st}) = 0 \quad (2)$$

with $\theta = (T - T_{st,u})/\Delta T$ and:

$$\omega = Da(1 - \theta_{st})^2 \frac{(1 - \alpha)\exp(\beta_0 - \beta)}{1 - \alpha(1 - \theta_{st})} \times \exp\left(-\alpha\beta \frac{1 - \theta_{st}}{1 - \alpha(1 - \theta_{st})}\right) \quad (3)$$

where $\alpha = \Delta T_{st}/T_{st,b}$ is the heat release parameter, $\beta = E_{eff}/(RT_{st,b})$ is the activation temperature ratio, u refers to the unburnt (fresh) mixture, b indicates fully-burnt, 0 indicates a reference value and Da is constant for any given fuel and oxidant combination. Differentiation of Eq. (3) with respect to θ_{st} , at steady-state, produces the condition for turning points in the S-shaped curve ($\frac{\partial \chi_{st}}{\partial \theta_{st}} = 0$), on the interval $0 < \theta_{st} < 1$:

$$\zeta = (\beta^2 + 6\beta + 1)\alpha^2 - (6\beta - 2)\alpha + 1 \geq 0 \quad (4)$$

Satisfying this condition implies turning points exist in the curve χ_{st} versus θ_{st} , corresponding to ignition (ig) and extinction (ex) given by:

$$\theta_{st} = 1 - \frac{1 + (3 + \beta)\alpha \pm \zeta^{1/2}}{2(\alpha^2 + (1 + \beta)\alpha)}, \quad \theta_{st,ex} \geq \theta_{st,ign} \quad (5)$$

If $\theta_{st,ign}$ and $\theta_{st,ex}$ are real, the S-shaped curve features autoignition and extinction. If these are complex, $\zeta < 0$, then χ_{st} versus θ_{st} is monotonic, indicating MILD combustion [5]. Finally, negative values indicate no physical solution.

2.2. S-Shaped curve generation

Sixty-three S-shaped curves with C_2H_4 fuel were simulated in FlameMaster [16]. The FlameMaster code uses a finite difference method solved on an adaptive mesh with a second-order, implicit backward difference formula. These S-shaped curve solutions were used to form a map of $\theta_{st,ex} - \theta_{st,ign}$ (see Eq. (5)), with MILD combustion identified if $\theta_{st,ex} - \theta_{st,ign}$ was zero or could not be evaluated. Oxidisers ranged from 1000 K to 1600 K, at intervals of 100 K, and composed of 2–15% O_2 by volume, at increments of 1% from 2–9% and then every 2% to 15%. The oxidisers consisted of 10% H_2O and 3% CO_2 , balanced by N_2 [12]. These were solved using the C1–C3 sub-mechanism from the December 2014 version of the detailed POLIMI mechanism for hydrocarbon combustion [17].

2.3. Transient flamelet analysis

The ignition of MILD and conventional autoignitive flames was analysed using two-dimensional profiles for Z and χ . This procedure is similar to previous analyses of turbulent jet flames using transient, opposed-flow flamelets [18]. A conical potential core was imposed for the mixture fraction with a length of $7x/D$. Further downstream ($x/D \geq 7$), the Z profile was taken from the self-similar analysis by [19]:

$x/D < 7$:

$$Z = \begin{cases} 1, & R(x) < 0 \\ (1 + [\gamma R_\eta(x)]^2/4)^{-2Sc_t}, & R(x) \geq 0 \end{cases} \quad (6)$$

$x/D \geq 7$:

$$Z = \frac{70}{32} \frac{(1 + 2Sc_t)D}{(x + x_0)(\rho_0\rho_{st})^{1/2}} \left(1 + \frac{[\gamma\eta]^2}{4}\right)^{-2Sc_t}$$

where $\gamma = [3 \times 70^2 / (64\rho_{st})]^{1/2}$ [19]; $\eta = r_\rho D / (x + x_0)$ [19]; $x_0 = [70/32(1 + 2Sc_t)\rho_{st} - 7]D$; $R(x) = [1 - x/(7D)]/2$ and:

$$R_\eta(x) = \frac{[r_\rho - R(x)]D}{x + [1 - x/(7D)]x_0} \quad (7)$$

$$r_\rho = D^{-1} \left(2 \int_0^r \frac{\rho}{\rho_{cofl}} r' dr'\right)^{1/2} \quad (8)$$

with $Sc_t = 0.71$ [19]. Values of $D = 4.6$ mm, $\rho_0 = 1.26$ kg/m³, $\rho_{cofl} = 0.31$ kg/m³ and $\rho_{st} = 0.20$ kg/m³ and $u_0 = 15.2$ m/s were taken from experimental conditions. Density was taken to be the linear mixture of the fuel and oxidant streams. Finally, the profile of χ was taken as [18,20]:

$$\chi = u_0 / (35Sc_t D) (\rho_0/\rho)^2 \left| \frac{dZ}{dr_\rho} \right|^2 \quad (9)$$

Fuel and oxidiser streams were matched to the current experimental C_2H_4 flames in 1250-K coflows of 3%, 6% and 9% O_2 by volume with $Z_{st} = 0.01$,

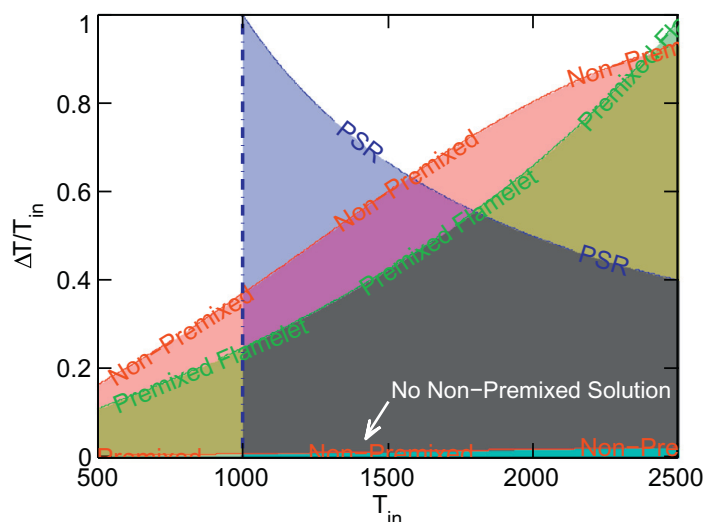


Fig. 1. Combined regime map for MILD combustion according to three different definitions: PSR [1] (blue), premixed flamelet [5] (green), and non-premixed flamelet (red). With $T_{st} = 1000$ K, $E_{eff} = 1.67 \times 10^8$ J/kmol [1] and $T_{in} = T_{st, u}$. (For interpretation of the references to colour in this figure legend, the reader is referred to the web version of this article).

0.02 and 0.03, respectively. Flames with hot oxidisers initially ignite at the most-reactive mixture fraction (Z_{mr}) $< Z_{st}$, with the maximum reaction rate [21]. Although Z_{mr} is not strongly dependent on χ , higher χ increase ignition delays [21]. Changes in the reactant streams may shift Z_{mr} and the ignition location, resulting in significantly different ignition delays. The flamelets were solved using the USC-II C1-C4 chemical kinetics mechanism [22]. A stoichiometric flamelet velocity described the downstream motion of Z_{st} in time [18], based on a self-similar jet velocity profile [19]. Higher values of Z_{st} are closer to the faster fuel jet, and hence have higher flamelet velocities. The stoichiometric flamelet velocity was subsequently used to remap times to corresponding x/D for analysis.

3. Experimental details

Chemiluminescence images were taken of C_2H_4 flames in a previously studied JHC burner [12]. Chemiluminescence of OH^* is spontaneous UV emission from excited OH. The peak intensity of OH^* concentration has been shown to correspond to peak flame temperatures in laminar flames [11]. Imaging of OH^* chemiluminescence may be therefore used to qualitatively identify the highest temperature regions of a flame.

Fuel issues from a 4.6-mm diameter central jet at a Reynolds number near 10,000 into 2.8 m/s coflows with measured coflow temperatures (T_{cofl}) of 1250 K and 3–11% O_2 . These coflows also include 10.7% H_2O and 3.6% CO_2 by volume, balanced with N_2 . These compositions are similar to previous experiments [12], which are used for the C_2H_4 regime map. This configuration provides a controlled environment for approximately 100 mm

downstream of the coflow exit plane. Flames are imaged using a pco.pixelfly camera with a Lambert Instruments intensifier. An f-number 3.5, UV transmissive lens is fitted with a 310 nm optical filter with a bandwidth of 10 nm. Mean images are formed from a series of 50 images, each taken with a gate time of 1 ms and corrected for background.

4. Results and discussion

4.1. MILD combustion definitions

Different definitions of MILD combustion are shown overlaid in Fig. 1. The values of $T_{st} = 1000$ K and $E_{eff} = 1.67 \times 10^8$ J/kmol (40 kcal/mol) are chosen from reference [1]. The blue region indicates the PSR definition of Cavaliere and de Joannon [1], bounded by $\Delta T \leq T_{st}$; the premixed S-shaped curve definition of Oberlack et al. [5], where Eq. (1) holds, is in green; and the current non-premixed study, where the condition in Eq. (4) is not met, is shown in red. The overlap between the domains indicates that both gradual ignition and conventional autoignition flame structures exist within the boundaries of the PSR defined regime. This indicates that the PSR regime includes flames featuring instabilities due to local autoignition and extinction, and those which are devoid of local extinction or sharp peaks in flame temperature, which are consistent with the physical description of MILD combustion [1]. This is consistent with previous experimental investigations of ethylene 3% O_2 and 9% O_2 oxidants which exhibit significant differences in structure [12], despite both conditions meeting the PSR definition of MILD combustion [1]. The PSR definition simply limits the maximum flame temperature to $T_{in} + T_{st}$, whereas

the definitions based on the S-shaped curves indicate the shift from gradual ignition to autoignition. The maximum flame temperature of the S-shaped curve-based MILD regimes, however, increase with T_{in} , highlighting inconsistency between $\Delta T = T_{st,b} - T_{st,u} \leq T_{si}$ and the flame ignition characteristics. This supports the use of the new MILD combustion definition for predicting ignition behaviour of non-premixed flames.

Combustion is apparent well below the pre-defined $T_{in} = 1000$ K PSR threshold [1] shown in Fig. 1. This region exhibits what Wang et al. [6,8] term “quasi-MILD” combustion, which requires an external ignition source. This indicates MILD combustion occurring under forced ignition [6,8], in contrast to the $T_{in} \geq T_{si}$ requirement of the PSR definition [1]. In this sense, the new MILD definition predicts “quasi-MILD” behaviour suggested by Wang et al. [6,8]. The region of “MILD-like” combustion [6,8] cannot, however, be determined from this generalised figure which makes no reference to oxygen levels.

Of the flamelet regimes in Fig. 1, the non-premixed MILD regime allows for greater ΔT compared to the premixed case for most T_{in} . At higher T_{in} , however, the non-premixed limit begins to approach a limiting value whilst the maximum $\Delta T/T_{in}$ for the premixed MILD regime continues to increase. Additionally, the analysis features a region of low $\Delta T/T_{in}$ where a non-premixed solution does not exist. These effects demonstrate the differences between premixed and non-premixed flames, despite qualitatively similar trends and descriptions of MILD combustion. These different trends show that for a given fuel of some E_{eff} , there is a limiting value of $\Delta T/T_{in}$ for non-premixed MILD flames which does not exist in premixed configurations.

4.2. Non-premixed regime maps

The MILD regime map in Fig. 1 may be expanded to arbitrary fuel and oxidant combinations on the α and β axes. The regime diagram in Fig. 2 shows shaded contours of $\theta_{st,ign}$, defined by Eq. (5), in the three distinct regions for different fuels with specific E_{eff} .

A selection of experimental cases are included in Fig. 2 to classify flames as either MILD or autoignitive flames. E_{eff} is taken to be 2.51×10^8 J/kmol (60 kcal/mol) [23] for all cases using CH₄-based fuels. These are HM1-3 cases using a CH₄-H₂ blend [24], the Delft JHC (DJHC) using Dutch natural gas [25], the F1, F4 and F7 cases using pure CH₄ [26] and CH₄-air flame of Cabra et al. [27]. One set of data for pure C₂H₄ fuels is included [12] with $E_{eff} = 1.26 \times 10^8$ J/kmol (30 kcal/mol) [28]. The classification of the HM1-3 flames agrees with previously simulated S-shaped curves, which indicate autoignition in the two cases with the greatest %O₂ coflows [10]. The cases for oxidants with 3% O₂ in the studies from Med-

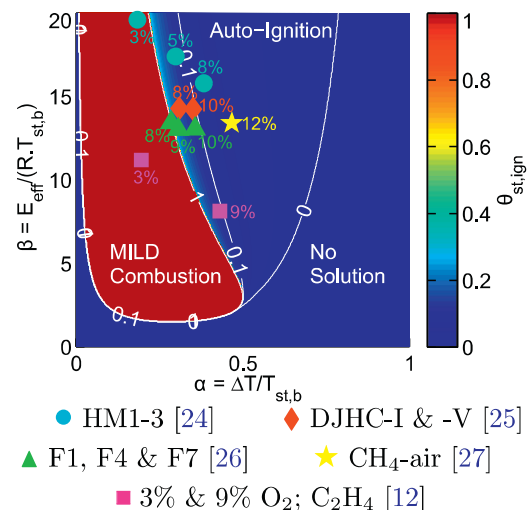


Fig. 2. Normalised autoignition temperature, $\theta_{st,ign}$, for a range of α and β and showing experimental cases with coflow O₂ concentrations as percentage of volume.

well et al. [12] and Dally et al. [24] are within the MILD regime, whereas the remaining flames with oxidant O₂ ~ 7–10%, are autoignitive. This is consistent with the experimentally observed structures of these flames [12,24–27]. This is in spite of some of these flames [12,25] meeting the PSR conditions of MILD combustion [1].

The regime diagram in Fig. 2 separates MILD and autoignitive flames and may be used to predict the structure of flames from evaluation of the initial mixing temperature $T_{st,u}$, adiabatic flame temperature $T_{st,b}$ and E_{eff} for a given fuel. This regime map shows the limited achievable range of α with almost constant β using CH₄/air coflows [25,26]. Both the HM1-3 and C₂H₄ sets of flames, ignite at almost constant $T_{st,u}$ with varying concentrations of O₂. This highlights the necessity of studying ignition in coflows with different fuels and diluents which can access a wider range of operating conditions [12,24].

The regime diagram in Fig. 2 shows a region of significant temperature increase followed by autoignition ($\theta_{st,ign} > 10\%$), which may be indicative of the “transitional” flames described by Medwell et al. [12]. The width of this region increases with β , implying precursor reactions with significant heat release are more prominent for high β , or low $T_{st,b}$. Additionally, increasing $T_{st,u}$ with constant ΔT results in lower β . This shows that MILD combustion is most readily achievable for high $T_{st,u}$, however may be achieved at any $T_{st,u}$ with sufficiently low ΔT , consistent with the premixed definition [5] and the regimes of Wang et al. [6,8].

Figure 3 presents regimes of stoichiometric ethylene combustion as a function of oxidant O₂ molar concentration and initial mixture temperature. This figure shows a pair of previously studied flames [12], and flame conditions to be

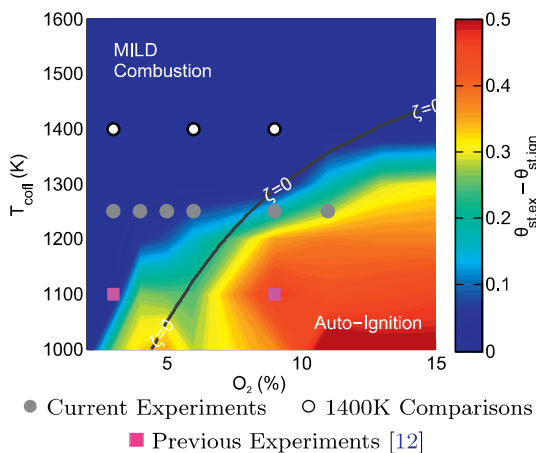


Fig. 3. Contours of $\theta_{st,ex} - \theta_{st,ign}$ for C_2H_4 flamelets on T_{coff} and O_2 axes, with the boundary between MILD and autoignition regimes ($\zeta = 0$) from Eq. (4).

examined in the next section. The line of $\zeta = 0$ (see Eq. (4)) with $E_{eff} = 1.26 \times 10^8$ J/kmol [28] is plotted over these contours, and shows very good agreement in the location of the MILD combustion regime boundary. Discrepancies in the lower-left corner of the figure are due to small $\theta_{st,ex} - \theta_{st,ign} < 100$ K. These ignition events are the result of two-stage ignition processes not captured by the cubic S-shaped curve of the analytical model. In these flames, autoignition occurs after significant, gradual increases in temperature, which are reminiscent of gradual MILD ignition. Additionally, this may be indicative of non-unity Lewis number effects in the flamelet analyses, neglected in deriving ζ .

The good agreement between regime boundaries in Fig. 3 implies that both autoignition and MILD combustion may be analysed with single-step reactions. In such analyses, different conditions and chemical pathways could be accounted for with rate coefficients which are functions of the fuel and oxidant compositions, and the local mixture fraction. This is in contrast to previous modelling of similar flames which stressed the importance of multi-step kinetics [2]. These results suggest the potential effectiveness of one-step reaction models, using functions as rate coefficients, near the limits of autoignition.

4.3. Chemiluminescence of jet flames

Chemiluminescence of excited hydroxyl from a series of turbulent C_2H_4 jet flames issuing into hot and diluted coflows are shown in Fig. 4. The regime diagram in Fig. 3 indicates that the flames issuing into the 9% and 11% O_2 coflows should be autoignitive, with the remainder in the MILD regime. These images show strong OH^* emissions near the base of the autoignitive flames which are not apparent in the MILD flames. The OH^* signal may be used as a qualitative indicator of regions of peak temperatures [11]. Well-defined lift-off heights of 8 mm and

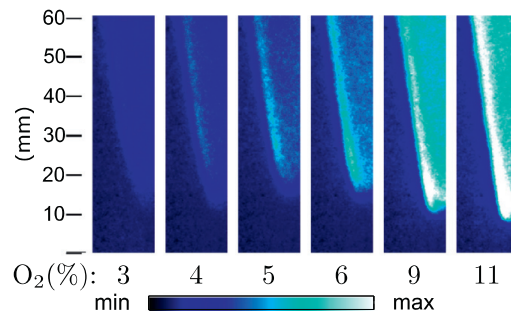


Fig. 4. Images of OH^* emissions from turbulent C_2H_4 flames in 1250-K coflows with different % O_2 (by vol.) averaged over 50×1 ms images. The height is given in millimetres, with the lower edge of the images at the jet exit plane. Images are 16 mm \times 60 mm and corrected for background.

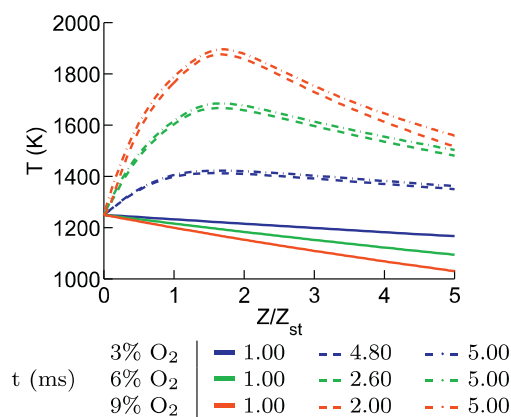


Fig. 5. T vs. Z/Z_{st} profiles of transient flamelets at different times for C_2H_4 fuel in 1250-K coflows.

11 mm ($x/D = 1.7$ and 2.4) are seen for the flames in 11% and 9% O_2 coflows, with less distinct lift-off heights of approximately 14 mm ($x/D = 3.0$) in 5% and 6% O_2 coflows. No OH^* chemiluminescence is detectable below these points for any camera and intensifier exposure times. Chemiluminescent emissions are discernible in the 3% and 4% O_2 cases from 11 mm downstream of the jet exit, following adjustments of the colour-scale (not shown for brevity). Below these locations, any OH^* emission is below the measurement threshold of the equipment. This trend in lift-off heights demonstrate gradual ignition in MILD combustion in low O_2 coflows, and the transition to conventional autoignition with increasing O_2 concentration.

4.4. Transient flamelet analyses

Transient flamelet profiles of the MILD and autoignitive flames from Fig. 4 are presented in Fig. 5. These results indicate that all flames begin to ignite at approximately 1.2 ms. This corresponds to initial ignition at 1.6, 1.8 and 2.0 x/D in the 3%, 6% and 9% O_2 coflows respectively, after this time is remapped to x/D using the stoichiometric flamelet

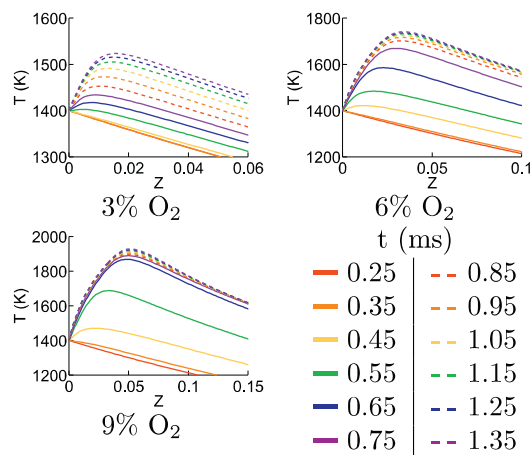


Fig. 6. T vs. Z profiles of transient flamelets at different times for C_2H_4 fuel in 1400-K coflows.

velocities for the respective values of Z_{st} [18]. The increasing heights with increasing O_2 are due to Z_{st} shifting towards regions of higher χ , delaying ignition. Following initial ignition, the flamelet in the 9% O_2 coflow reaches its maximum temperature by 2 ms, which is remapped to x/D of 2.6. This is shorter than the 6% O_2 case which takes 2.6 ms, corresponding to x/D of 2.7. The 3% O_2 case does not reach a steady temperature until approximately 5 ms, at x/D of 3.0, undergoing a significantly more gradual ignition process. These results replicate the experimentally observed trend, where the maximum chemiluminescence of flame in the 6% O_2 coflow appears higher than that in the 9% O_2 coflow and the flame in the 3% O_2 coflow initiates gradually, initially appearing closest to the jet exit plane. This is representative of the MILD combustion behaviour in the 3% O_2 case transitioning to autoignitive behaviour in the 9% O_2 case.

The effects of increased temperature on MILD flame stabilisation were assessed using transient flamelets with 1400-K oxidants. Fig. 3 indicates that all of these flames are within the MILD combustion regime. Temperature profiles from the transient analyses are shown in Fig. 6 with lines on each plot indicating increments of 0.10 ms from 0.25 ms to 1.35 ms. The profiles indicate ignition initiating after approximately 0.5 ms, 0.4 ms and 0.35 ms in the 3%, 6% and 9% O_2 oxidants, respectively. Flame temperatures reach steady-state values by 1.65 ms, 1.05 ms and 0.65 ms, at 1.9, 1.7 and 1.3 x/D , in the 3%, 6% and 9% O_2 oxidants, respectively. This shows that increases in coflow O_2 decrease the heights of both the initial ignition and the distance to reach a steady temperature and do not indicate any non-monotonic trend in lift-off height. In contrast, the flames in 1250-K coflows exhibit increasing heights before initial temperature increases with increasing O_2 concentration, demonstrating the effects of temperature, coupled with the imposed Z and χ fields. In the cooler 1250-K coflow, Z_{mr} shifts towards Z_{st} in regions of higher

χ and lower velocity (described in the analysis of Fig. 5). Lower χ at Z_{mr} allows the flame in 3% O_2 coflow to stabilise closer to the jet exit plane than in the 6% O_2 case. With the increase to 9% O_2 , the increased reactivity at Z_{mr} overcomes higher χ and the flame-base moves closer to the jet exit plane, as seen experimentally. This suggests that the non-monotonic trend in lift-off height seen experimentally indicates Z_{mr} shifts away from the coflow, into the high shear mixing layer, where autoignitive flames ignite more readily than MILD flames. This additionally explains the wider reaction zones under MILD conditions seen in previous work at lower temperatures [12], as the burning mixtures are confined by the low Z flammability limit and the high χ turbulent mixing layer.

5. Conclusions

A new non-premixed definition for MILD combustion, based on an equivalent activation energy rather than prior assessment of a reference temperature, was derived and shown to be consistent with previous experimental observations of gradual ignition. This definition incorporates, and consolidates, previous definitions of the MILD combustion conditions and the suggested combustion regimes which exhibit similar ignition behaviours. The new definition has shown good agreement with steady-state flamelet simulations, demonstrating better agreement than previous classifications between the simulated and predicted boundaries between the non-premixed MILD and autoignitive regimes. These boundaries show that non-premixed MILD combustion is achievable by minimising the overall temperature increase, or increasing initial temperatures and may be achieved following forced ignition.

Time-averaged chemiluminescent images of a series of flames showed that autoignitive flames exhibit peak temperatures at the flame-base, in contrast to the gradual ignition predicted and observed in MILD jet flames. Transient flamelet modelling indicated that the shift in ignition location from regions of low scalar dissipation rate towards the jet shear layer is responsible for the observed non-monotonic trend in flame lift-off heights. This shift towards shear layer is driven by decreasing temperature and increasing oxidant O_2 levels. This may also explain the decreasing reaction zone width in the transition to conventional autoignition. These results provide a better understanding of the boundaries and stabilisation of non-premixed flames in, and near, the MILD combustion regime.

Acknowledgements

The authors thank Ms Jingjing Ye for her assistance during experimental setup and flame imaging. The authors acknowledge support from

The University of Adelaide, Stanford University and the Politecnico di Milano. M.J.E. acknowledges financial support from the Endeavour Scholarships and Fellowship grant programme; P.R.M. and M.J.E. acknowledge financial support [Australian Research Council](#) (ARC) Discovery (DP and DECRA) grant scheme and the United States Asian Office for Aerospace Research and Development (AOARD); and H.W. and M.I. acknowledge financial support through [NASA](#) with award number [NNX15AV04A](#).

References

- [1] A. Cavaliere, M. de Joannon, *Prog. Energy Combust.* 30 (4) (2004) 329–366, doi:[10.1016/j.pecs.2004.02.003](#).
- [2] F.C. Christo, B.B. Dally, *Combust. Flame* 142 (1–2) (2005) 117–129, doi:[10.1016/j.combustflame.2005.03.002](#).
- [3] M. Ihme, Y.C. See, *Proc. Combust. Inst.* 33 (1) (2011) 1309–1317, doi:[10.1016/j.proci.2010.05.019](#).
- [4] P. Sabia, M. de Joannon, A. Picarelli, R. Ragucci, *Combust. Flame* 160 (1) (2013) 47–55, doi:[10.1016/j.combustflame.2012.09.015](#).
- [5] M. Oberlack, R. Arlitt, N. Peters, *Combust. Theor. Model.* 4 (4) (2000) 495–510, doi:[10.1088/1364-7830/4/4/307](#).
- [6] F. Wang, P. Li, Z. Mei, J. Zhang, J. Mi, *Energy* 72 (2014) 242–253, doi:[10.1016/j.energy.2014.05.029](#).
- [7] M.J. Evans, P.R. Medwell, Z.F. Tian, A. Frassoldati, A. Cuoci, A. Stagni, *AIAA J.* (2016). In Press, doi:[10.2514/1.J054958](#).
- [8] F. Wang, J. Mi, P. Li, *Energy Fuels* 27 (6) (2013) 3488–3498, doi:[10.1021/ef400500w](#).
- [9] K. Bray, M. Champion, P.A. Libby, *Combust. Flame* 107 (1–2) (1996) 53–64, doi:[10.1016/0010-2180\(96\)00014-4](#).
- [10] M. Ihme, J. Zhang, G. He, B.B. Dally, *Flow Turbul. Combust.* 89 (2012) 449–464, doi:[10.1007/s10494-012-9399-7](#).
- [11] J.A. Sidey, E. Mastorakos, *Combust. Flame* 163 (2016) 1–11, doi:[10.1016/j.combustflame.2015.07.034](#).
- [12] P.R. Medwell, P.A.M. Kalt, B.B. Dally, *Combust. Flame* 152 (2008) 100–113, doi:[10.1016/j.combustflame.2007.09.003](#).
- [13] B. Choi, S. Chung, *Combust. Flame* 157 (12) (2010) 2348–2356, doi:[10.1016/j.combustflame.2010.06.011](#).
- [14] M.J. Evans, P.R. Medwell, Z.F. Tian, *Combust. Sci. Technol.* 187 (7) (2015) 1093–1109, doi:[10.1080/00102202.2014.1002836](#).
- [15] H. Pitsch, S. Fedotov, *Combust. Theor. Model.* 5 (1) (2001) 41–57, doi:[10.1088/1364-7830/5/1/303](#).
- [16] H. Pitsch, 1998. FlameMaster: A C++ computer program for 0D combustion and 1D laminar flame calculations. Available at URL: <http://www.itv.rwth-aachen.de/downloads/flamemaster/>.
- [17] E. Ranzi, A. Frassoldati, R. Grana, et al., *Prog. Energy Combust. Sci.* 38 (4) (2012) 468–501, doi:[10.1016/j.pecs.2012.03.004](#). Version: Dec. 2015. Current version of mechanism available from URL: <http://creckmodeling.chem.polimi.it/>
- [18] H. Pitsch, M. Chen, N. Peters, *Proc. Combust. Inst.* 27 (1) (1998) 1057–1064, doi:[10.1016/S0082-0784\(98\)80506-7](#).
- [19] N. Peters, *Turbulent Combustion*, Cambridge University Press, 2000.
- [20] N. Peters, F.A. Williams, *AIAA J.* 21 (3) (1983) 423–429, doi:[10.2514/3.8089](#).
- [21] E. Mastorakos, *Prog. Energy Combust. Sci.* 35 (1) (2009) 57–97, doi:[10.1016/j.pecs.2008.07.002](#).
- [22] H. Wang, X. You, A. V. Joshi, et al. 2007. USC Mech Version II. High-Temperature Combustion Reaction Model of H₂/CO/C₁-C₄ Compounds. Mechanism available from URL: http://ignis.usc.edu/USC_Mech_II.htm.
- [23] N. Peters, F. Williams, *Combust. Flame* 68 (2) (1987) 185–207, doi:[10.1016/0010-2180\(87\)90057-5](#).
- [24] B. Dally, A. Karpetis, R. Barlow, *Proc. Combust. Inst.* 29 (1) (2002) 1147–1154, doi:[10.1016/S1540-7489\(02\)80145-6](#).
- [25] E. Oldenhof, M.J. Tummers, E.H. van Veen, D.J.E.M. Roekaerts, *Combust. Flame* 157 (6) (2010) 1167–1178, doi:[10.1016/j.combustflame.2010.01.002](#).
- [26] C.M. Arndt, R. Schießl, J.D. Gounder, W. Meier, M. Aigner, *Proc. Combust. Inst.* 34 (1) (2013) 1483–1490, doi:[10.1016/j.proci.2012.05.082](#).
- [27] R. Cabra, J.-Y. Chen, R. Dibble, A. Karpetis, R. Barlow, *Combust. Flame* 143 (4) (2005) 491–506, doi:[10.1016/j.combustflame.2005.08.019](#).
- [28] C.K. Westbrook, F.L. Dryer, *Prog. Energy Combust. Sci.* 10 (1) (1984) 1–57, doi:[10.1016/0360-1285\(84\)90118-7](#).

Chapter 5

Effects of Oxidant Stream Composition on Non-Premixed, Laminar Flames with Heated and Diluted Coflows

Statement of Authorship

Title of Paper	Effects of Oxidant Stream Composition on Non-Premixed Laminar Flames with Heated and Diluted Coflows
Publication Status	<input type="checkbox"/> Published <input type="checkbox"/> Accepted for Publication <input checked="" type="checkbox"/> Submitted for Publication <input type="checkbox"/> Unpublished and Unsubmitted work written in manuscript style
Publication Details	Evans, MJ , Medwell, PR, Tian, ZF, Ye, J, Frassoldati, A, & Cuoci, A. "Effects of Oxidant Stream Composition on Non-Premixed Laminar Flames with Heated and Diluted Coflows". Submitted to: <i>Combustion and Flame</i> .

Principal Author

Name of Principal Author (Candidate)	Michael John Evans
Contribution to the Paper	Designed research concept, planned numerical approach, generation and analysis of all numerical data, co-designed and undertook experiments, interpreted data, wrote manuscript and acted as corresponding author.
Overall percentage (%)	75
Certification:	This paper reports on original research I conducted during the period of my Higher Degree by Research candidature and is not subject to any obligations or contractual agreements with a third party that would constrain its inclusion in this thesis. I am the primary author of this paper.
Signature	<div style="display: flex; justify-content: space-between; align-items: center;"> <div style="text-align: center;"> <small>Digitally signed by Michael Evans Date: 2016.10.18 16:51:50 +10'30'</small> </div> <div style="border-left: 1px solid black; padding-left: 10px;"> <small>Date</small> 18-Oct-2016 </div> </div>

Co-Author Contributions

By signing the Statement of Authorship, each author certifies that:

- i. the candidate's stated contribution to the publication is accurate (as detailed above);
- ii. permission is granted for the candidate to include the publication in the thesis; and
- iii. the sum of all co-author contributions is equal to 100% less the candidate's stated contribution.

Name of Co-Author	Paul Ross Medwell
Contribution to the Paper	Co-supervised development of the work, helped to evaluate and edit the manuscript.
Signature	<div style="display: flex; justify-content: space-between; align-items: center;"> <div style="text-align: center;"> <small>Paul Medwell Date: 2016.10.18 17:13:22 +10'30'</small> </div> <div style="border-left: 1px solid black; padding-left: 10px;"> <small>Date</small> 18-OCT-2016 </div> </div>

Name of Co-Author	Zhao Feng Tian
Contribution to the Paper	Co-supervised development of the work, helped to evaluate and edit the manuscript.
Signature	<div style="display: flex; justify-content: space-between; align-items: center;"> <div style="text-align: center;"> <small>Digitally signed by Zhao Feng Tian Date: 2016.10.24 12:03:30 +10'30'</small> </div> <div style="border-left: 1px solid black; padding-left: 10px;"> <small>Date</small> 24-Oct-2016 </div> </div>

Name of Co-Author	
-------------------	--

Contribution to the Paper	helped to evaluate and edit the manuscript.		
Signature	Digitally signed by JINGJING YE Date: 2016.10.19 14:39:46 +10'30'	Date	19-OCT-2016

Name of Co-Author	Alessio Frassoldati		
Contribution to the Paper	Co-supervised development of the work, helped to evaluate and edit the manuscript.		
Signature	10070207@polimi.it 2016.10.18 13:15:05 +02'00'	Date	18-OCT-2016

Name of Co-Author	Alberto Cuoci		
Contribution to the Paper	Wrote the numerical codes used in the study, co-supervised development of the work, helped to evaluate and edit the manuscript.		
Signature	Alberto Cuoci 2016.10.18 18:01:53 +02'00'	Date	18-OCT-2016

Manuscript Number: CNF-D-16-00395R1

Title: Effects of Oxidant Stream Composition on Non-Premixed Laminar
Flames with Heated and Diluted Coflows

Article Type: Full Length Article

Keywords: MILD combustion; Tribrachial flames; Lifted flames; JHC burner;
Autoignition

Corresponding Author: Mr. Michael John Evans,

Corresponding Author's Institution: The University of Adelaide

First Author: Michael John Evans

Order of Authors: Michael John Evans; Paul R Medwell; Zhao F Tian;
Jingjing Ye; Alessio Frassoldati; Alberto Cuoci

Abstract: The moderate or intense low oxygen dilution (MILD) combustion regime offers reductions in pollutant emissions and improvements in efficiency. The implementation of MILD combustion in non-premixed systems, however, still requires a significantly improved understanding of the effects of the oxidant stream composition in both the MILD combustion regime, and in the transition from MILD combustion to conventional spontaneous-ignition. New experimental observations of laminar flames in the transition between MILD combustion and conventional spontaneous-ignition demonstrate a non-monotonic change in lift-off height with changing oxidant O₂ concentration. This occurs in conjunction with a transition from spatially gradual ignition to well-defined flame bases, with increasing coflow O₂ level. A numerical study of two-dimensional flames near this transition is performed with a detailed kinetic mechanism, using the laminarSMOKE code, to complement these experimental observations and provide insight into the chemical structure of flames with a hot and diluted coflow. The simulated flames are compared to a previous definition of MILD combustion in a hot coflow as an edge flame without a tribrachial flame structure. The different structures of simulated CH₄ flames are consistent with the observed experimental behaviour under similar conditions, however comparisons between experimental observations and simulations of C₂H₄ flames highlight the importance of the flow-field, even in a simple streaming flow. The simulations show that equilibrium levels of the hydroxyl radical (<10 ppm) in the oxidant stream significantly intensifies a MILD CH₄ reaction zone, by increasing methyl oxidation, however such levels have little effect on tribrachial, spontaneously-igniting flames. Conversely, increasing the ratio of CO₂ to H₂O in the coflow reduces the intensity of a MILD CH₄ reaction zone. Neither the inclusion of equilibrium concentrations of OH, nor the change in CO₂ to H₂O ratio, in the oxidant results in a transition between MILD reaction zones to tribrachial spontaneously-igniting flames, despite significantly affecting the temperature of reaction zones in the MILD combustion regime. The results show that the intensity of MILD combustion is strongly dependent on the different chemical species in the oxidant

stream. Tribrachial spontaneously-igniting flames are, in contrast, relatively resilient against changes other than temperature and O₂ level.

Effects of Oxidant Stream Composition on Non-Premixed Laminar Flames with Heated and Diluted Coflows

M.J. Evans^{a,*}, P.R. Medwell^a, Z.F. Tian^a, J. Ye^a, A. Frassoldati^b, A. Cuoci^b

^a*School of Mechanical Engineering, The University of Adelaide, South Australia, 5005, AUSTRALIA*

^b*Dipartimento di Chimica, Materiali ed Ingegneria Chimica "G. Natta", Politecnico di Milano, 20133, Milan, ITALY*

Abstract

The moderate or intense low oxygen dilution (MILD) combustion regime offers reductions in pollutant emissions and improvements in efficiency. The implementation of MILD combustion in non-premixed systems, however, still requires a significantly improved understanding of the effects of the oxidant stream composition in both the MILD combustion regime, and in the transition from MILD combustion to conventional spontaneous-ignition. New experimental observations of laminar flames in the transition between MILD combustion and conventional spontaneous-ignition demonstrate a non-monotonic change in lift-off height with changing oxidant O₂ concentration. This occurs in conjunction with a transition from spatially gradual ignition to well-defined flame bases, with increasing coflow O₂ level. A numerical study of two-dimensional flames near this transition is performed with a detailed kinetic mechanism, using the laminarSMOKE code, to complement these experimental observations and provide insight into the chemical structure of flames with a hot and diluted coflow. The simulated flames are compared to a previous definition of MILD combustion in a hot coflow as an edge flame without a tribrachial flame structure. The different structures of simulated CH₄ flames are consistent with the observed experimental behaviour under similar conditions, however comparisons between experimental observations and simulations of C₂H₄ flames highlight the importance of the flow-field, even in a simple streaming flow. The simulations show that equilibrium levels of the hydroxyl radical (<10 ppm) in the oxidant stream significantly intensifies a MILD CH₄ reaction zone, by increasing methyl oxidation, however such levels have little effect on tribrachial, spontaneously-igniting flames. Conversely, increasing the ratio of CO₂ to H₂O in the coflow reduces the intensity of a MILD CH₄ reaction zone. Neither the inclusion of equilibrium concentrations of OH, nor the change in CO₂ to H₂O ratio, in the oxidant results in a transition between MILD reaction zones to tribrachial spontaneously-igniting flames, despite significantly affecting the temperature of reaction zones in the MILD combustion regime. The results show that the intensity of MILD combustion is strongly dependent on the different chemical species in the oxidant stream. Tribrachial spontaneously-igniting flames are, in contrast, relatively resilient against changes other than temperature and O₂ level.

Keywords: MILD combustion, Tribrachial flames, Lifted flames, JHC burner, Autoignition

*Corresponding author. Tel.: +61 8 8313 5460, Fax: +61 8 8313 4367.
Email address: m.evans@adelaide.edu.au (M.J. Evans)

1. Introduction

Requirements for improved efficiency and reduced pollutant emissions have driven research into novel combustion systems. Potential applications for new combustion technologies range from more fuel-efficient industrial furnace applications [1], to low-emissions aero-engines [2]. One aspect of research into this contemporary problem, explores combustion stabilised through exhaust gas recirculation (EGR) [1, 3, 4], staged combustion [2, 5], or the recirculation of hot combustion products in confined burners [6–8]. Fundamentally, these systems may be described as non-premixed combustion with hot and diluted oxidants. One proposed technology to meet the targets for next-generation combustion systems, is moderate or intense low oxygen dilution (MILD) combustion [9].

The MILD combustion regime offers both reduced pollutant emissions and improved thermal efficiency over conventional combustion [1, 9]. Characteristic features of MILD combustion – otherwise referred to as “flameless oxidation” or “colourless” combustion – include low peak temperatures, low luminosity, reduced thermal gradients, and reduced soot production compared with conventional combustion [9]. The MILD combustion regime has been successfully implemented in furnaces [1, 3, 10], and similar combustion regimes consisting of a fuel stream issuing into a hot, low oxygen environment have been suggested for further applications [2, 11–14]. Such configurations have been the foci of recent research [15–18] to better the understanding of the boundaries of MILD combustion, and the sensitivity of flame behaviour and structure to operating conditions, required for future applications of MILD combustion.

Significant experimental research into non-premixed MILD combustion has been undertaken using jet-in-hot-co-/cross-flow (JHC) burners [16–25]. These experiments have focussed on understanding the ignition and stabilisation of simple hydrocarbon fuels with combustion products used to produce hot, low oxygen environments encountered in EGR, and required for MILD combustion. These experimental studies have used different combinations of laser diagnostics, photographs and chemiluminescence imaging to reveal the structure of MILD jet flames, and have been supplemented by computational investigations [26–30].

Combustion under MILD conditions has been previously described as exhibiting gradual ignition, in both a spatial and temporal sense, without a distinct flame base [22, 23, 27–31]. This configuration has been specifically studied in the context of combustion of fresh fuel with a hot [oxidant], diluted oxidant (HODO) stream [32, 33] providing increased initial enthalpy to the reactant mixture [34], and extending the flammability limits [35]. This is consistent with studies of combustion in porous media [36]; confined, swirl-stabilised flames [37, 38] (where flames are stabilised through recirculation of hot combustion products) [8, 39]; and insights into bluff-body flames [40]. Research into these combustion applications [36, 40] are consistent with fundamental studies of opposed-flow flames, which suggested that CH_4 flames could not be extinguished by decreasing O_2 concentrations in HODO streams in excess of approximately 1550 K [35]. It has been concluded that laminar MILD counterflow CH_4 flames are stabilised due to partial premixing from the diffusion of O_2 from the oxidant stream into the fuel through reaction zone weakening [26]. Although this explains the presence of CH_2O near the jet centreline in flames in JHC burners [22, 41], it cannot be concluded that the diffusion effects are unilateral or that the mechanism for stabilising flames in the MILD combustion regime is a direct result of the diffusion of O_2 into the fuel alone.

Conventional autoignition of non-premixed flames has, similar to MILD combustion, been studied in JHC [12, 15, 20, 21, 42–45] and vitiated coflow burner (VCB) [46–48] configurations. Although most of these experimental studies investigated non-premixed turbulent flames, laminar ‘autoignitive’ flames in hot and vitiated coflows have been observed to have distinct, lifted, tribrachial flame bases [20, 21, 49]. This phenomenon of tribrachial flames has been used to describe non-premixed ‘autoignition’ in experimental studies [50–52] and has been discussed at length (with detailed figures) elsewhere [49, 53, 54]. This work will use the terminology ‘spontaneous-ignition’ [55] to describe the ignition of an arbitrary mixture (outside of the MILD combustion regime), which may or may not be affected by the transport of combustion precursors or products from other parts of the reaction zone.

Methane (CH_4) and ethylene (C_2H_4) have been the subject of studies of the ignition and structure of laminar [21, 56] and turbulent [15–17, 19, 22, 23, 42–44, 46–48, 57] flames in hot and diluted (HODO) coflows. Identifying the ignition process of these fuels is critical for understanding the combustion of larger hydrocarbons under MILD combustion conditions, with C_2H_4 found in significant quantities in both rich and lean regions of more complex hydrocarbon flames, encompassing “layers” of acetylene (C_2H_2) and CH_4 [58]. Both MILD combustion and conventional spontaneous-ignition require hot environments to stabilise jet flames, generally considered to be above a pre-defined autoignition temperature [9]. Despite the similarities in the conditions for spontaneously-igniting flames and MILD combustion, the two regimes have been shown to feature very different ignition characteristics and flame structures: experimentally [18, 22, 23, 30, 59]; in zero-dimensional reactors [60]; one-dimensional flame analyses [16, 28–31, 61]; and direct numerical simulations of reaction zone structures in EGR configurations [62–64].

At a given oxidant temperature, increasing the concentration of coflow O_2 results in a shift from spatially gradual ignition of MILD combustion towards lifted, spontaneously-igniting flames with a well-defined flame-base [18, 22, 23, 30]. This transition away from the MILD combustion regime, has been described both as a transition to an edge flame stabilised at a triple point in non-premixed laminar flames [20, 21], and the initiation of a region of net negative heat release rate across the reaction zone [32]. This transition away from the MILD combustion regime has also been described (in homogeneous reactors) as the conditions where methyl (CH_3) oxidation becomes dominant over recombination [61].

Laser-based imaging of turbulent, lifted, C_2H_4 flames has been unable to identify any evidence of tribrachial structures, although such structures may collapse due to interactions with turbulent vortices [22]. Observations of such structures would facilitate comparisons against separate studies of laminar flames [20, 21], which exhibit a transition between two distinct flame behaviours with changing coflow O_2 levels, similar to the turbulent flames [20–23]. The differences between laminar and turbulent flow regimes demonstrate the need for a systematic experimental and numerical investigation into the structure of laminar flames, without the effects of turbulence, in both the MILD and conventional spontaneous-ignition regimes.

Minor species, such as OH, are inherent in hot coflows due to the presence of combustion products. Such minor species cannot be easily controlled experimentally and are neither generally reported as boundary conditions nor taken in account during discussion of experimental observations or computational modelling. However, some previous studies of flames with hot and diluted oxidants have indicated the importance of precursor and radical species to flame stabilisation [17, 41, 48, 65–73]. Previous studies have investigated the addition of species such as NO [65–68], N_2O [66], OH [17, 74], CH_2O [17, 75], H_2 [72],

CO₂ [73, 76] and H₂O₂ [75] on flame ignition and temperature, across a range of different configurations and conditions.

The formation of OH upstream of a visually defined flame base has previously been observed in C₂H₄ flames in a JHC burner [22]. Additionally, low concentrations of OH have been shown to significantly reduce ignition delay times when added to a premixed reactor [17]. To complement these findings, a previous investigation of equilibrium OH concentrations (~ 10 ppm) in a turbulent flame issuing into a hot coflow with 9% O₂ demonstrated negligible effects in Reynolds-averaged Navier-Stokes (RANS) simulations [74]. The small impact of equilibrium OH was in agreement with the premixed reactor simulations of CH₄ flames, which showed only slight reductions in ignition delay for oxidants with less than 10 ppm of OH [17]. The RANS study, however, did not investigate other fuel mixtures or coflows with as little as 3% O₂ (by volume) [74].

Improved understanding of MILD combustion is critical for its implementation in practical combustion systems. This study builds on the understanding of the effects of oxidant oxygen concentration and oxidant temperature in the transition to MILD combustion by further investigating the effects of coflow composition on flame stabilisation in, and the transition to, the MILD combustion regime. This study presents experimental observations of laminar flames in a JHC burner to establish a distinction between the MILD and conventional spontaneously-igniting combustion regimes. In the numerical component of this work, the use of two-dimensional, laminar simulations to predict the structure of previously measured turbulent flames [19] will first be assessed. The effects of including equilibrium levels of OH in the oxidant description on the structure of CH₄ and C₂H₄ flames issuing into hot and diluted environments will then be evaluated to determine whether equilibrium amounts of minor species must be accounted for in MILD combustion for future practical systems.

2. Methodology

2.1. Experimental details

Photographs and chemiluminescence images were taken of laminar natural gas (NG) ($\gtrsim 92\%$ vol./vol. CH₄) and C₂H₄ flames in a JHC burner, which has been used for previous studies of turbulent flames [17, 22, 23, 57]. More recently, the same burner was used for studies of pre-vaporised ethanol flames [18]. This burner features a 4.6-mm diameter central fuel jet which issues into a hot coflow of products from a premixed burner upstream of the jet exit plane. The central jet pipe is in excess of 100 diameters long, to ensure fully-developed pipe flow.

Bulk velocities of both the jet and coflow were held at 2.4 m/s throughout this study. The jet flowrate was controlled using a rotameter, whilst coflow flowrates were controlled using Alicat mass flow controllers with a specified accuracy of less than 1%. Coflows were produced using a premixed flame of H₂, NG, O₂ and N₂, in order to emulate environments encountered using EGR. The coflows are at temperatures (T_{cofl}) of 1250 K, 1315 K and 1385 K, and 3-9% O₂ by volume. Heat loss was minimised by encasing the external faces of the burner in fibrous insulation. Coflow compositions include 10.7% H₂O and 3.6% CO₂ by volume, and they are balanced with N₂, similar to previous studies [18, 22, 57]. These flame conditions are summarised in Table 1. This configuration provides a controlled environment to approximately 100 mm downstream of the coflow exit plane. Beyond this distance, entrainment of surrounding air creates a condition where the local environment is not defined.

Table 1. Fuel and oxidant stream compositions (as percent vol./vol.) and temperatures (K) used for experiments. All streams are held at 2.4 m/s.

Case description	Fuel stream composition	Coflow streams				
		T_{cofl} (K)	O ₂	N ₂	CO ₂	H ₂ O
3% O ₂	NG, C ₂ H ₄	1250, 1315, 1385	3.0	82.7	3.6	10.7
6% O ₂	NG, C ₂ H ₄	1250, 1315, 1385	6.0	79.7	3.6	10.7
9% O ₂	NG, C ₂ H ₄	1250, 1315, 1385	9.0	76.7	3.6	10.7

Chemiluminescence images were taken of NG and C₂H₄ flames. Chemiluminescence imaging of OH* was performed at 310 nm. Flames were imaged using a pco.pixelfly camera with a Lambert Instruments intensifier. This was fitted with an $f_{\#}3.5$ UV transmissive lens and a 310 nm optical filter with a bandwidth of 10 nm. Mean images were formed from a series of 50 images, each taken with a gate time of 1 ms and corrected for background.

Photographs were taken using a Canon EOS 60D SLR camera fitted with a 50 mm, $f_{\#}1.8$ lens at $f/4$ using manual white balance. Photographs show the first 120 mm downstream of the jet exit plane and, hence, the top region of each photograph cannot be considered as coflow-controlled. All photographs of NG flames, and C₂H₄ flames issuing into coflows with 3% O₂, were taken with 4 s exposure times with ISO 100. The photographs of C₂H₄ flames issuing into coflows with 9% O₂ were taken with exposure times of 0.5 s to avoid saturation near the flame base. Further analysis of the flame photographs used the inverse of the blue channel of the images, this is taken to be indicative of (blue) chemiluminescence of CH* around 430 nm [77].

2.2. Numerical approach

Two-dimensional simulations of CH₄/H₂, CH₄ and C₂H₄ flames were performed using the laminarSMOKE code [78, 79]. The simulated flames are similar cases to those investigated experimentally. These numerical cases feature different flow-fields and geometries to the experiments. Accordingly, the simulations cannot be directly compared to the experimental observations, but are designed to focus on the chemical aspects of flame structure to complement the experiments.

The laminarSMOKE code is a CFD solver, based on the OpenFOAM platform, for multidimensional laminar reacting flows specifically conceived for detailed kinetic mechanisms incorporating the OpenSMOKE++ libraries [78–80]. The laminarSMOKE code is based on the operator-splitting method, and is discussed extensively elsewhere [78, 79], as is the object-orientated OpenSMOKE++ framework [80]. Flames were simulated using laminarSMOKE version 0.15, with OpenFOAM version 2.2.0 used to solve the fluid flow-field. The approach and mesh in these simulations are similar to a previous study of the non-premixed ignition delay of C₂H₄ in hot and diluted coflows [29]. One advantage of the planar, coflowing, laminar configuration is the very low strain rates between the fuel and oxidant streams (due to the absence of velocity deficits or curvature effects). Therefore, data taken at any horizontal sample height of a completely burning flame represents a steady-state, low strain-rate, opposed-flow laminar flame. Data along any of these sample heights should, therefore, be identical in mixture-fraction-space. The domain size was chosen to capture the mechanics of visual lift-off phenomena observed in Figs. 2-4 (should they be an artefact of the combustion chemistry alone). The measurement height of 30 mm was subsequently chosen as it was estimated to correspond to interesting phenomena near the bases of the experimental flames (discussed later in §3.1). Additionally, this measurement height was sufficiently far

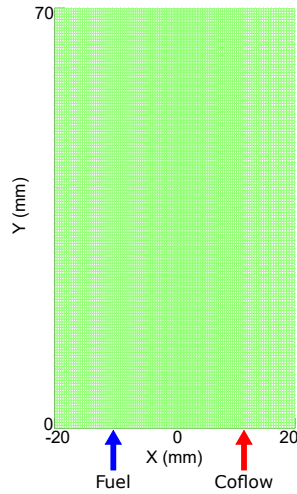


Fig. 1. Two-dimensional, planar domain and mesh for non-premixed, laminar flame simulations. Dimensions are given in millimetres.

downstream of the inlet to allow for mixing of the fuel and oxidant streams, and for the stabilisation of all but one case (discussed later in §4.2).

Cases were run on a single node of an AMD-Opteron cluster, with each node having 48 logical processing cores and 128 GB of both physical and virtual memory. The flow-field was solved using a second-order upwind numerical scheme, with first-order, bounded, implicit time-stepping. Similarly, species transport was solved using an implicit Euler method [80]. Species transport is calculated based on multicomponent diffusion coefficients, based on the molecular theory of gases, and includes the Soret effect. Chemical kinetics were solved using the RADAU5 solver, which is an implicit Runge-Kutta method of order five. Residuals at each step met a relative tolerance of 10^{-7} .

The computational domain represents a planar jet with a coflowing HODO stream and is shown in Figure 1. This domain extends 70 mm downstream (in the Y-direction) with a total width of 40 mm separated into the two equally sized inlets. The fuel inlet is on the X-axis for negative values of X, and the oxidant inlet on the X-axis for positive X. The thickness of the wall between the two streams (in a physical burner) was neglected. The X and Y extents of the domain were varied to ensure that any effects of the boundaries were negligible and the results were independent of the domain size. The domain is meshed by 18 000 elements, with 150 uniformly-spaced stream-wise elements, and with 120 elements in the transverse direction, with finest grid spacing at the fuel/oxidant interface and an expansion ratio of 2 from the largest to smallest elements. This was selected for all cases following a grid independence study.

Fuel and oxidant enter the computational domain with uniform velocities of 1 m/s, where the different compositions of these streams are given in Table 2. The concentrations of OH given in Table 2 were evaluated through chemical equilibrium calculations, which result in the major oxidant species being produced at the oxidant temperature. Simulations were run until steady-state with transient time-steps of the order of $10 \mu\text{s}$. Such small time steps were necessary due to the numerically stiff chemical kinetics required for the problem, with a maximum Courant number of 0.05 enforced for each simulation time-step. Each chemistry step took approximately 1.85 s of CPU-time to converge. The simulation approach was validated against experimental data of the HM1-3 flames measured by Dally *et al.* [19], which has been used as validation data for numerous modelling studies [81–87].

The GRI-Mech 3.0 kinetics mechanism was used for the chemistry in all of the simulations [88]. The

Table 2. Fuel and oxidant stream compositions (as percent vol./vol. except for HM1-3 flames, which are as percent mass) and temperatures (K) used for simulations, all fuel streams are at 305 K.

Case description	Fuel stream composition	T_{cofl} (K)	Oxidant streams				
			O ₂	N ₂	CO ₂ ^a	H ₂ O ^a	OH (ppm) ^b
3% O ₂	CH ₄ , C ₂ H ₄	1100, 1300, 1500	3	84	3	10	8
6% O ₂	CH ₄ , C ₂ H ₄	1100, 1300, 1500	6	81	3	10	9
9% O ₂	CH ₄ , C ₂ H ₄	1100, 1300, 1500	9	78	3	10	9
HM1 ^c [19]	1:1 CH ₄ /H ₂	1300	3	85	6.5	5.5	-
HM2 ^c [19]	1:1 CH ₄ /H ₂	1300	6	82	6.5	5.5	-
HM3 ^c [19]	1:1 CH ₄ /H ₂	1300	9	79	6.5	5.5	-

^aCO₂ and H₂O concentrations were swapped to test the effects of CO₂ to H₂O ratio (see §4.4).

^bsimulations performed with and without OH, with N₂ adjusted to keep the sum of concentrations at 100% (see §4.2).

^ccoflow concentrations given as percentage mass rather than percentage volume.

GRI-Mech 3.0 mechanism has previously shown good agreement with the significantly more detailed C1-C3 kinetics mechanism of Ranzi *et al.* [89] in qualitatively describing the reaction zone profile of C₂H₄ flames in MILD and lifted, spontaneously-igniting turbulent jet flames [90]. Both of these mechanisms feature similar pathways for non-premixed combustion of C₂H₄ and dilute oxidants, as described in a previous modelling campaign [90]. This finding was verified in this study with both mechanisms producing almost identical temperature profiles and qualitatively similar profiles of hydroxyl (OH), formaldehyde (CH₂O) and hydroperoxyl (HO₂) 30 mm downstream of the domain inlet (not shown for brevity).

3. Experimental Observations

3.1. Experimental observations of laminar flames

Figures 2 and 3 show images of six, laminar NG and C₂H₄ flames, respectively. These are labelled as flames (a)-(f) for both fuels. The jet and coflow bulk velocities were held constant at 2.4 m/s, resulting in similar flow-fields for all flames. The coflow temperature and O₂ level were varied independently. The flames presented were stabilised in 1250-, 1315- and 1385-K coflows, with 3-9% O₂ (refer to Table 1). No indication of NG flames were observable in the 1250-K coflows, irrespective of O₂ content, although C₂H₄ flames could be stabilised. This is consistent with C₂H₄ being significantly more reactive than NG. This is further evidenced by the decreased lift-off heights of all C₂H₄ flames in comparison to NG flames.

Photographs of the flames in Figs. 2 and 3 are divided vertically along the jet centreline. The left-hand side of each image is a raw photograph of the laminar flame, however the low luminosity of the flames in coflows with 3% O₂, and the limited dynamic range of the images, make the base of these flames difficult to distinguish (particularly NG flames (a) and (d) in Fig. 2). The right-hand side of each photograph has therefore been altered to show only the blue channel of the original image, in inverse grey-scale. The intensity of these ‘inverse-blue’ images is taken to be indicative of CH* chemiluminescence (centred about 430 nm), in locations where the photographs of the flames indicate a blue colour (hence, a region devoid of soot). The complementary photographs and inverse-blue images allow for easier identification and comparison of the flame base shapes and structures.

The inverse blue images of NG flames (a)-(c) in Fig. 2 appear to show that the maximum lift-off height occurs in the 6% O₂ coflow. This trend is consistent with previous observations of NG flames in hot and diluted (HODO) coflows [23]. The non-monotonic change in lift-off height with changing coflow O₂ levels

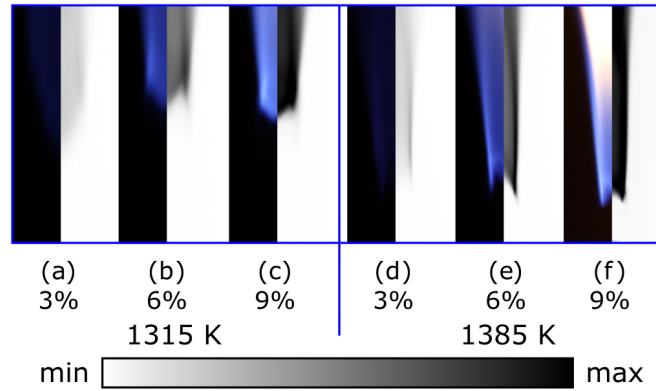


Fig. 2. Laminar NG flames in the JHC burner showing visible chemiluminescence in coflows of different temperatures and oxygen concentrations. The right-hand side of each photograph shows only the inverse of the blue channel, to better show the effect of coflow on lift-off height. The lower edge of the images is at the jet exit plane. Images are 50 mm \times 120 mm, with 4 s exposure with an $f_{\#}1.8$ lens at $f/4$ and ISO-100.

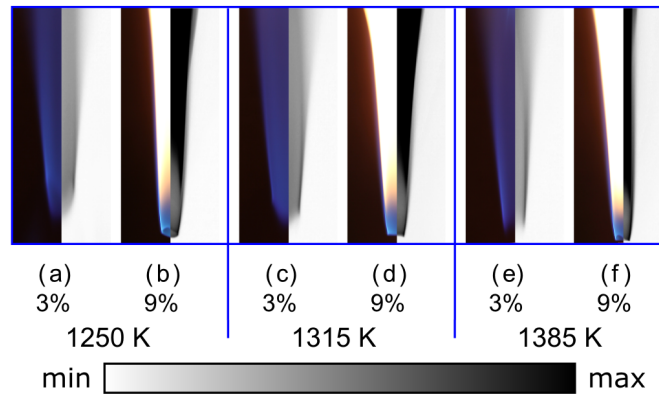


Fig. 3. Laminar C_2H_4 flames in the JHC burner showing visible chemiluminescence in coflows of different temperatures and oxygen concentrations. The right-hand side of each photograph shows only the inverse of the blue channel, to better show the effect of coflow on lift-off height. The lower edge of the images is at the jet exit plane. Images are 50 mm \times 120 mm, with an $f_{\#}1.8$ lens at $f/4$ and ISO-100. Exposure times for flames in coflows with 3% O_2 is 4 s, and 0.5 s for flames in coflows with 9% O_2 .

indicates a difference in the flame stabilisation mechanism between laminar NG flames in 1315-K coflows with 3% O_2 , and those with 6% O_2 or greater.

The shape of the bases of the flames issuing into coflows with 3% O_2 differ from those in coflows with more than 6% O_2 (Figs. 2 and 3). The images of chemiluminescence of flames issuing into coflows with 3% O_2 indicate significantly reduced spatial gradients than those in the coflows with 9% O_2 , which feature very distinct flame bases with very well defined stabilisation heights. Flames in coflows with 6% O_2 have similar bases to those in 9% O_2 , but appear more lifted (in all cases).

The NG flame (a) in the 1315-K coflow with 3% O_2 features a broader flame base than any other flames in Figs. 2 or 3. This is in contrast to the significantly narrower base of NG flame (d), stabilised in a 1385-K coflow with the same O_2 level. This demonstrates that the NG flame base shape and spatial gradients of chemiluminescence are significantly affected by the coflow temperature, although this is not seen for C_2H_4 flames across different temperatures. These observations suggest similar stabilisation mechanisms between all the NG flames issuing into 1385-K coflows, independent of oxygen concentration, but a different mechanism for the NG flame in the 1315-K coflow with 3% O_2 . These effects of temperature on the structure of CH_4 flames will be simulated numerically (refer to §4.5) to compare the chemical structure of these flames.

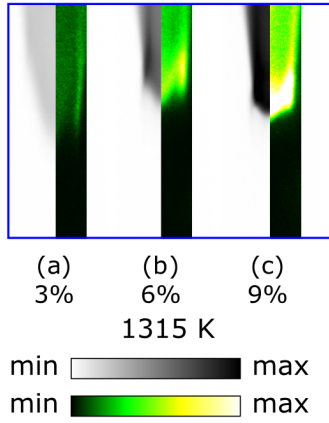


Fig. 4. False-colour, time-averaged, intensified OH* images of laminar NG flames (right-hand side), presented with the inverse of the blue channel of photographs (left-hand side). Flames issue into hot coflows of 1315 K with different O₂ concentrations (given in percentage volume). Images of OH* were taken with 2 ms exposure time, are 16 mm × 120 mm and the lower edge of the images is at the jet exit plane. Photographs are taken from Fig. 2, originally 50 mm × 120 mm, with 4 s exposure with an $f_{\#}1.8$ lens at $f/4$ and ISO-100.

3.2. Comparison of visible and UV chemiluminescence imaging

The relative strength of OH* chemiluminescence has been identified as an indicator of peak temperatures in non-premixed hydrocarbon flames in, and in the transition to, the MILD combustion regime [18, 91]. Images of OH* chemiluminescence of NG flames issuing into 1315-K coflows are shown in Fig. 4, next to the inverse-blue images of the same flame. Images of OH* have been reversed about the jet centreline and are presented in false colour.

The OH* images indicate a more spatially distributed ignition process in the 3% O₂ case (Fig. 4). These figures demonstrate that the temperature of the CH₄ flame in the 3% O₂ coflow increases gradually with downstream distance, without a clear flame base defining a lift-off height. This is consistent with previous descriptions and definitions of gradual ignition in MILD combustion [22, 23, 27, 28, 30, 31]. Comparisons between the inverse-blue and OH* imaging both indicate the same trends in flame shape and spatial-gradients of chemiluminescence, suggesting that the inverse-blue images may be used as a surrogate for locating the peak flame temperatures.

As the oxygen content in the hot coflow increases, the flame bases become more well-defined and the OH* chemiluminescence becomes more intense (see Fig. 4). This suggests a different structure between NG flame (a), and NG flames (b) and (c). This analysis, however, uses line-of-sight measurements of chemiluminescence. As such, it cannot provide insight into the structure of the reaction zone through a cross-section of the flames. The differences between the flame structures in coflows with different O₂ levels, along with the inability to derive further insight from the current observations, further support the need for the investigation of this transition through numerical simulations.

4. Simulations of Laminar Flames with Hot Coflows

4.1. CH₄/H₂ flames with hot and diluted coflows

Laminar flame simulations have been compared, in mixture-fraction-space, to experimentally measured profiles of temperature and species in turbulent flames, to better understand flame structure and behaviour [19, 46]. Figure 5 shows a comparison of data extracted from laminarSMOKE simulations against those from experimental measurements of turbulent flames studied by Dally *et al.* [19], with conditions summarised in Table 2. The data from the simulations are taken at 30 mm downstream from

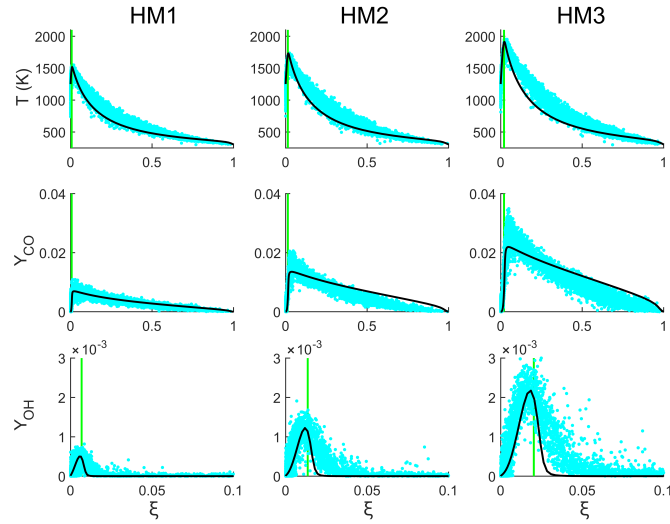


Fig. 5. Comparison of experimental data of HM1-3 flames [19]. Scatter plot shows experimental point measurements, overlaid with solid curves from laminarSMOKE. The vertical line indicates the stoichiometric mixture fraction.

the domain inlets and are representative of data in mixture-fraction-space at other downstream locations following initial ignition. This suggests a stable, developed flame in each case at this axial location. These data are in reasonably good agreement with each other, with the simulated data falling within the experimental data set measured in the turbulent jet flames [19]. The discrepancies between the simulated data and experimental measurements are not unexpected. Some potential reasons for this are: physical effects such as different strain rates and turbulent fluctuations, or omission of effects such as heat loss and turbulent mixing, although this is not an exhaustive list.

Figure 6 shows the OH, CH₂O and HO₂ distributions in the simulated, laminar HM1 and HM3 flames (see Table 2). The species concentrations in each case demonstrate the effect of the oxygen concentration on the overall structure of the flame. The relative distributions of OH, CH₂O, HO₂ are similar in both the HM1 and HM3 flames (Fig. 6). The build-up of CH₂O has been shown to be important in CH₄ combustion [41, 48], whilst HO₂ is a precursor in the combustion of H₂ [92]. Both flames indicate a build-up of HO₂ and CH₂O precursors on the fuel-rich and -lean wings of the flames. The build-up of CH₂O is much less significant in the HM1 case, with peak concentrations of CH₂O on the lean-side of the flame an order of magnitude less than in the HM3 flame. The concentrations of HO₂, however, are of similar magnitude for both flames, on both sides of the reaction zone. Conversely, the peak concentrations of CH₂O on the lean side of the flames are significantly less than those on the rich side. The lean CH₂O peak suggests carbon transport across the reaction zone as a result of diffusive mixing, similar to the O₂ diffusion into the fuel stream which has been shown in previous work [26].

The presence of precursors on either side of the OH region suggests two separate locations of heat release across the flame. This heat release is due to lean, exothermic reactions between OH, H and HO₂, specifically, in the HM1 (3% O₂) case:

- $\text{H} + \text{O}_2 + \text{H}_2\text{O} \rightleftharpoons \text{HO}_2 + \text{H}_2\text{O}$,
- $\text{OH} + \text{HO}_2 \rightleftharpoons \text{O}_2 + \text{H}_2\text{O}$,
- $\text{H} + \text{HO}_2 \rightleftharpoons 2\text{OH}$,
- $\text{H} + \text{O}_2 + \text{N}_2 \rightleftharpoons \text{HO}_2 + \text{N}_2$,

and, in the HM3 (9% O₂) case:

- OH + HO₂ ⇌ O₂ + H₂O,
- H + O₂ + H₂O ⇌ HO₂ + H₂O,
- 2OH (+M) ⇌ O + H₂O (+M) [backwards],
- OH + H₂O₂ ⇌ HO₂ + H₂O.

These reactions are exothermic in the forwards direction, unless explicitly indicated otherwise. The increase in available O₂ in the HM3 case promotes the backwards reaction-rate of OH + HO₂ ⇌ O₂ + H₂O and 2OH (+M) ⇌ O + H₂O (+M), and decreases the influence of the (forward) third-body reaction involving N₂: H + O₂ + N₂ ⇌ HO₂ + N₂. For both cases, heat release in the rich region of the flame is dominated by the reaction: H + CH₃ (+M) ⇌ CH₄ (+M). The net reaction rate is forwards, and is exothermic, in the HM1 case, but has an endothermic effect in the HM3 case. Additionally, OH × CH₂O is often regarded as a marker for heat release rate (and HCO) in non-premixed flames [26, 91, 93, 94]. Reactions which contribute most to the positive heat release rate near the stoichiometric mixture are, for both flames, OH + H₂ ⇌ H + H₂O and H + OH (+M) ⇌ H₂O (+M). Profiles of the relative contributions of heat release in these flames, and their net reaction-rates, are included as §S1 in the Supplementary Data, showing the dominant reactions responsible for heat release in rich, lean and near stoichiometric regions of the steady-state flame. Note that these regions degenerate under these hot oxidant conditions to produce a bimodal heat release zone at steady-state conditions. The presence of precursor wings either side of the peak OH indicates that these flames exhibit tribrachial flame structures [51], which have been associated with spontaneously-igniting flames [20, 21]. This is consistent with a previous simulation of a similar configuration, which indicated that the “primary flame reaction zone” of a tribrachial CH₄-air flame coincides with the region of peak HO₂ in stoichiometric and rich mixtures, although these regions do not align in the lean wing of the flame, suggesting that the region of HO₂ may be indicative of heat release in these flames [95].

Tribrachial spontaneously-igniting flames have demonstrated different trends and appearance to edge flames without triple points in coflows with reduced O₂ concentrations [20, 21]. This has led to the classification of edge flames without triple points in HODO coflows as lean flames with MILD combustion [20, 21, 49], and without a “conspicuous transition” between ignition and propagation [49]. The description of non-premixed MILD reaction zones as having a single peak in heat release rate is consistent with another description of non-premixed MILD combustion, as having no regions of net negative heat release rate [32]. This combined classification of both HM1 and HM3 as conventional spontaneously-igniting flames is in direct contrast to their classification as combustion in the MILD regime based on low luminosity and temperature profiles [9, 19]. The former reaction zone structure description of MILD combustion is, however, based on lifted flames which do not include H₂ in the fuel stream (which may result in flame attachment [96]), whereas the latter definition is based on a well-stirred reactor analysis that cannot account for non-premixed flame structure [9].

4.2. Structure of CH₄ flames with hot and diluted coflows

Results of simulations of the laminar CH₄ flames with 1300-K coflows, with and without equilibrium concentrations of OH, are shown in Figs. 7-9. The plots in Fig. 7 show profiles for flames with coflows

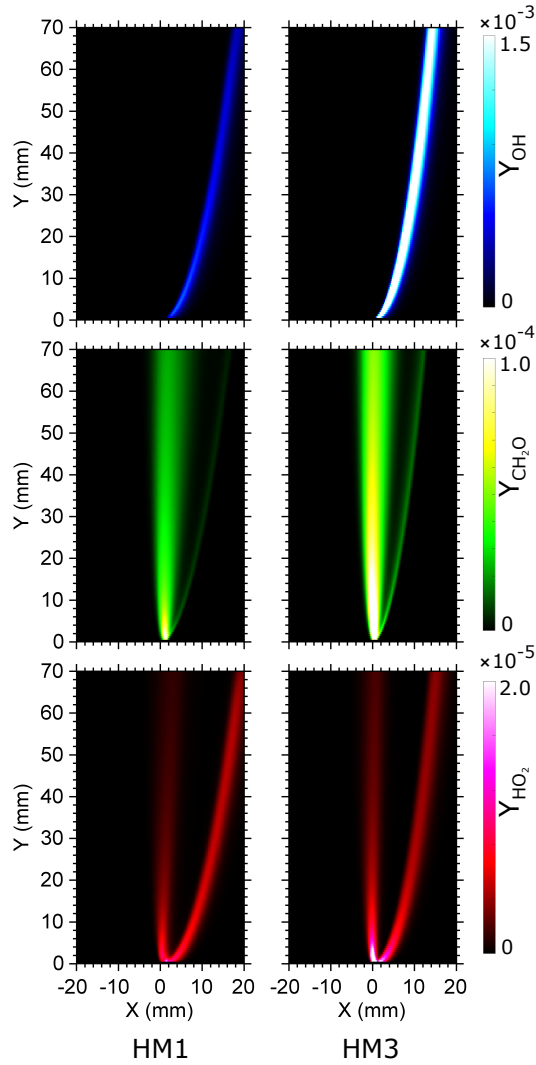


Fig. 6. Distributions of OH, CH₂O and HO₂ in laminar CH₄/H₂ flames (1:1 vol.) with coflowing oxidiser streams specified in Table 2.

with 3, 6 and 9% O₂, whereas distributions of species and temperature presented for coflows with 3 (Fig. 8) and 9% (Fig. 9) O₂. The 6% O₂ case is omitted as the results are qualitatively very similar to the flame with the 9% O₂ coflow. The detailed composition of each oxidant is given in Table 2. Figure 7 shows plots of species and temperatures profiles 30 mm from the jet exit plane. Left- and right-hand columns in Figs. 8 and 9 present images of the whole domain, neglecting and including equilibrium OH in the coflow description, respectively.

The plots in Fig. 7 and images in Figs. 8 and 9 show the effects of coflow O₂ level on CH₄ flames. The species and temperature distributions in these figures demonstrate the different structures of flames in 1300-K coflows with 3 and 9% O₂. The flame in the coflow with 3% O₂ appears lifted from inspection of the left-hand column of images in Fig. 8. The lift-off of this flame is confirmed by the profiles in Fig. 7, which show the absence of any OH or temperature increases 30 mm downstream of the domain inlets. In this case, the flame does not reach a completely burning state at any point within the computational domain, and as such the steady-state cannot be represented with data along any cross-section. Nevertheless, Fig. 7 reveals the distribution of species during the initial stages of ignition, and is well situated to provide insight into the relevance of different intermediate and radical species in the precursor pool. This shows a significant build-up of the CH₂O and HO₂ precursor species 30 mm downstream, which precede

the flame-base, consistent with previous studies [48, 97]. This is in contrast to the flame in the coflow with 9% O₂ which appears to have a lift-off of less than 1 mm (seen in Fig. 9).

The build-up of precursor species may be used to interpret the structure of the CH₄ reaction zones. At steady-state, the dominant exothermic reactions (in the forwards direction) shared by both the CH₄ flames with 1300-K coflows with 3 and 9% O₂ are:

- $\text{O} + \text{CH}_3 \rightleftharpoons \text{H} + \text{CH}_2\text{O}$,
- $\text{H} + \text{CH}_3 (+\text{M}) \rightleftharpoons \text{CH}_4 (+\text{M})$,
- $\text{OH} + \text{H}_2 \rightleftharpoons \text{H} + \text{H}_2\text{O}$,
- $\text{OH} + \text{CO} \rightleftharpoons \text{H} + \text{CO}_2$,
- $\text{OH} + \text{CH}_2\text{O} \rightleftharpoons \text{HCO} + \text{H}_2\text{O}$.

The relative importance of these reactions rates do not change at steady-state (that is, infinitely far downstream) with the inclusion of equilibrium OH in the coflow, however with the increase from 3 to 9% O₂ in coflow:

- $\text{H} + \text{O}_2 + \text{H}_2\text{O} \rightleftharpoons \text{HO}_2 + \text{H}_2\text{O}$,
- $\text{CH} + \text{H}_2\text{O} \rightleftharpoons \text{H} + \text{CH}_2\text{O}$,
- $\text{OH} + \text{HO}_2 \rightleftharpoons \text{O}_2 + \text{H}_2\text{O}$

become more important, whilst,

- $\text{OH} + \text{CH}_4 \rightleftharpoons \text{CH}_3 + \text{H}_2\text{O}$,
- $2\text{CH}_3 (+\text{M}) \rightleftharpoons \text{C}_2\text{H}_6 (+\text{M})$,
- $\text{O} + \text{CH}_3 \rightleftharpoons \text{H} + \text{H}_2 + \text{CO}$

become less influential. This is due to the increased availability of O₂ and higher temperatures in the reaction zone, and the subsequently decreased concentrations of CH₃ in the shift away from MILD combustion. Additionally, at steady-state, three distinct regions of heat release (rich, lean, near-stoichiometric) are identifiable with the 9% O₂ oxidant stream, whereas the peaks of these profiles collapse towards the stoichiometric mixture fraction with oxidants with 3% O₂. In the former (9% O₂) case, heat release rates in richer mixture fractions are dominated by the endothermic (reverse) reaction $\text{H} + \text{CH}_3 (+\text{M}) \rightleftharpoons \text{CH}_4 (+\text{M})$. In contrast, the dominant heat release reaction is exothermic (forwards reaction of $2\text{CH}_3 (+\text{M}) \rightleftharpoons \text{C}_2\text{H}_6 (+\text{M})$) for rich mixtures with an oxidant with 3% O₂. In this 3% O₂ case, there is no indication of negative heat release rate in the rich mixture, consistent previous descriptions of MILD reaction zones [18, 32]. Profiles of these heat release rates in mixture-fraction-space, and their net reaction-rates, are included as figures in §S1 of the Supplementary Data.

The structure of CH₄ flames in the 1300-K coflow without minor species may be inferred from Fig. 7 and the left-hand column of images in Figs. 8 and 9. The left-hand column in Fig. 8 indicates only a single peak in either CH₂O or HO₂ distributions around the region of OH in the reaction zone of the CH₄ flame in the coflow with 3% O₂. This suggests that the flame with the 3% O₂ oxidant is an edge

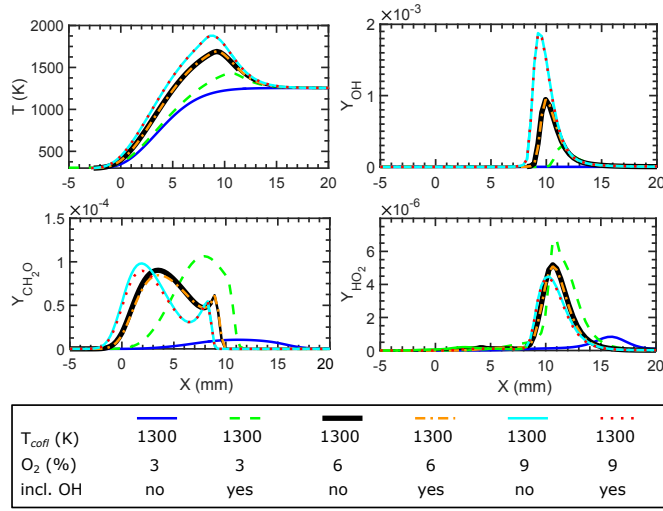


Fig. 7. The effects of including equilibrium OH in the coflow description. Plots show profiles of CH₄ flame temperature (in Kelvin), OH, CH₂O and HO₂ mass fractions against X (refer to Fig. 1) 30 mm downstream of the inlet plane, for 1300-K oxidants with 3, 6 and 9% O₂ (vol./vol.) (see Table 2).

flame, without a triple point, which has been previously used to define non-premixed MILD combustion in laminar coflows [20, 21, 49].

In contrast to the flame in the 3% O₂ coflow, both lean and rich peaks in the CH₂O distribution are seen for the flame with the 9% O₂ oxidant stream (see Figs. 7 and 9). This suggests partial premixing through diffusion of oxygen into the fuel stream (as identified previously [26]) and carbon into the oxygen stream. This double CH₂O peak suggests that this is a triple flame, which stabilises through conventional spontaneous-ignition [20, 21].

The differences in structure between the simulated CH₄ flames in 1300-K coflows with 3 and 9% O₂ demonstrate a similar transition in flame structure to the experimental observations in §3.1. This is in agreement with previous studies hypothesising different stabilisation mechanisms in a JHC burner configuration [23], suggesting this may be a transition from MILD reaction zones to conventional spontaneously-igniting flames with tribrachial flame bases.

A dominant single peak is seen in the HO₂ distribution of Fig. 9, rather than dual peaks as seen in the HM1-3 cases in Fig. 6. This suggests that the strong HO₂ peaks are evidence of the fuel H₂ reaction pathway in the HM1-3 flames. A significantly smaller HO₂ peak on the rich side of the reaction zone supports the classification of the CH₄ flame as a tribrachial flame.

The plots in Fig. 7 demonstrate the effects of including equilibrium concentrations of OH in the simulated coflow. Peak values from these plots are summarised for comparison in Table 3. It is apparent from Table 3 that the inclusion of equilibrium concentrations of OH has the most significant effect in the case of the 3% O₂ coflow. This is confirmed in Fig. 7 and comparisons between the left- and right-hand columns in Figs. 8 and 9. These show that the CH₄ flame in the coflow with 3% O₂ becomes much more intense with addition of equilibrium OH, although the effect is negligible on flames in coflows with more than 6% O₂. Additionally, the inclusion of equilibrium OH in the oxidant description had a negligible effect on C₂H₄ flames in the same configuration and 1100-1500-K coflows (not shown for brevity). This result shows that a detailed description of the oxidant is critical in simulations of CH₄ flames in HODO configurations. For this reason, all simulations presented hereafter include equilibrium concentrations of OH.

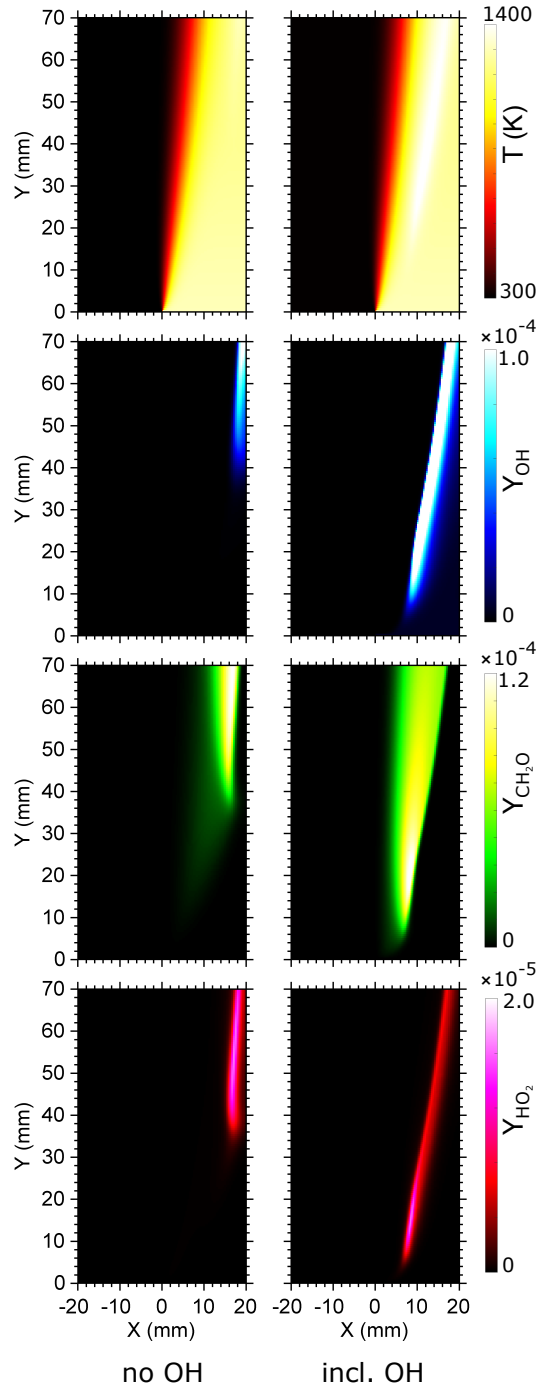


Fig. 8. Temperature and species mass fraction distributions in CH_4 flames stabilised in 1300-K coflows with 3% O_2 (vol./vol.), neglecting (left) and including (right) equilibrium OH in the coflow description.

The inclusion of minor species has little effect on the intensity, lift-off, or structure of CH_4 flames in coflows with more than 6% O_2 . The inclusion of equilibrium OH causes the CH_4 flame in the 3% O_2 coflow to ignite much closer to the domain inlet (refer to Fig. 8). This ignition is gradual and does not suddenly initiate at a distinct location, consistent with previous phenomenological descriptions of MILD combustion [22, 23, 27, 28, 30, 31, 91]. This is a result of increased precursor formation due to the added OH, resulting in large peaks of CH_2O and HO_2 . Unlike the 6% and 9% O_2 cases, these precursors are confined to single peaks in the CH_4 flame in the coflow with 3% O_2 . These single peaks, and unchanged profiles of heat release rate (see §4.2) indicate that this is still a MILD reaction zone despite the inclusion of equilibrium OH, promoting oxidation of the methyl radical, and resulting in OH production initiating

Table 3. Effects of equilibrium OH concentrations on a planar, laminar CH₄ jet with a 1300-K coflow, 30 mm downstream from the inlet.

% O ₂ (mol/mol)	Without minor species in coflow			With equilibrium OH		
	Y _{CH₂O} _{peak}	Y _{OH} _{peak}	T _{peak} (K)	Y _{CH₂O} _{peak}	Y _{OH} _{peak}	T _{peak} (K)
3	1.0×10 ⁻⁵	1.5×10 ⁻⁶	1300	1.1×10 ⁻⁴	2.7×10 ⁻⁴	1425
6	9.0×10 ⁻⁵	9.4×10 ⁻⁴	1691	8.5×10 ⁻⁵	9.5×10 ⁻⁴	1693
9	9.8×10 ⁻⁵	1.9×10 ⁻³	1878	9.0×10 ⁻⁵	1.8×10 ⁻³	1878

much closer to the domain inlet plane. The same effects were seen with super-equilibrium concentrations of OH of 80, and 800 ppm (10 and 100× equilibrium levels), although the latter resulted in an attached flame. Accounting for equilibrium OH in the oxidant does not change the qualitative structure of the CH₄ flame in the coflow with 3% O₂ and is still consistent with the previous classification as a MILD flame [20, 21].

Figure 9 indicates the tribrachial structures of CH₄ flames in coflows with 6 and 9% O₂ at 1300 K. These flames feature precursor wings on either side of the reaction zones. Investigation of the CH₂O and HO₂ production rates and diffusion fluxes in the 9% O₂ case indicates that these precursor wings are the result of downstream transport from the precursor pool near the domain inlet. These results are presented as images in §S2 of the Supplementary Data, showing broad regions of CH₂O diffusion, but only single peaks of CH₂O formation, across the reaction zone.

The precursor wings in the tribrachial CH₄ flames indicate a build-up of precursors in the initial precursor pool. The transport of species from this pool across the reaction zone indicates that not all the precursor species are consumed below the flame base. This is consistent with the previous analysis of reaction zone weakening resulting in O₂ transport under high strain rates in opposed-flow flames [26]. In contrast to the dominant transport of O₂ in the fuel stream, these coflow conditions lead to a partial premixing effect by transporting oxygen into the fuel stream, and carbon and hydrogen into the oxidant stream as radicals. This is consistent with the transport of fuel and coflow species in the preheating zone of non-premixed spontaneously-igniting flames, which becomes more important with slow chemical time-scales [95], such as those previously identified in MILD combustion [98].

The peak concentration of the precursor species in the 3% O₂ case exceeds those for higher O₂ levels at the 30 mm downstream location in Fig. 7. Despite their differences, the similar magnitudes are consistent with measurements of CH₄/H₂ flames [57] and previous simulations of opposed CH₄ flames [26]. By including equilibrium OH, similar to concentrations expected experimentally, in the 3% O₂ case, the peak concentration of OH in Fig. 7 increases by over a factor of 100, and results in HCO concentrations comparable to the 6 and 9% O₂ cases (not shown for brevity).

In the 3% O₂ case, the equilibrium concentrations of OH react directly with CH₄ to form CH₃ in lean mixtures. The OH continues to react with CH₃ to directly form CH₂(S), H₂O, CH₂O and atomic H. Additional CH₂O and CO is produced via CH₂(S). Atomic H reacts with O₂ and H₂O to form additional OH and HO₂. The formation of HO₂ is further enhanced via OH recombination (through the pathway: OH → H₂O₂ → HO₂). These processes increases HO₂ in the reaction zone by nearly an order of magnitude (recall Fig. 7). Supporting results of this description from rate of production and sensitivity analyses are included in §S3 of the Supplementary Data.

In rich mixtures HO₂ reacts directly with CH₃ to form CH₃O which is the main precursor to CH₂O

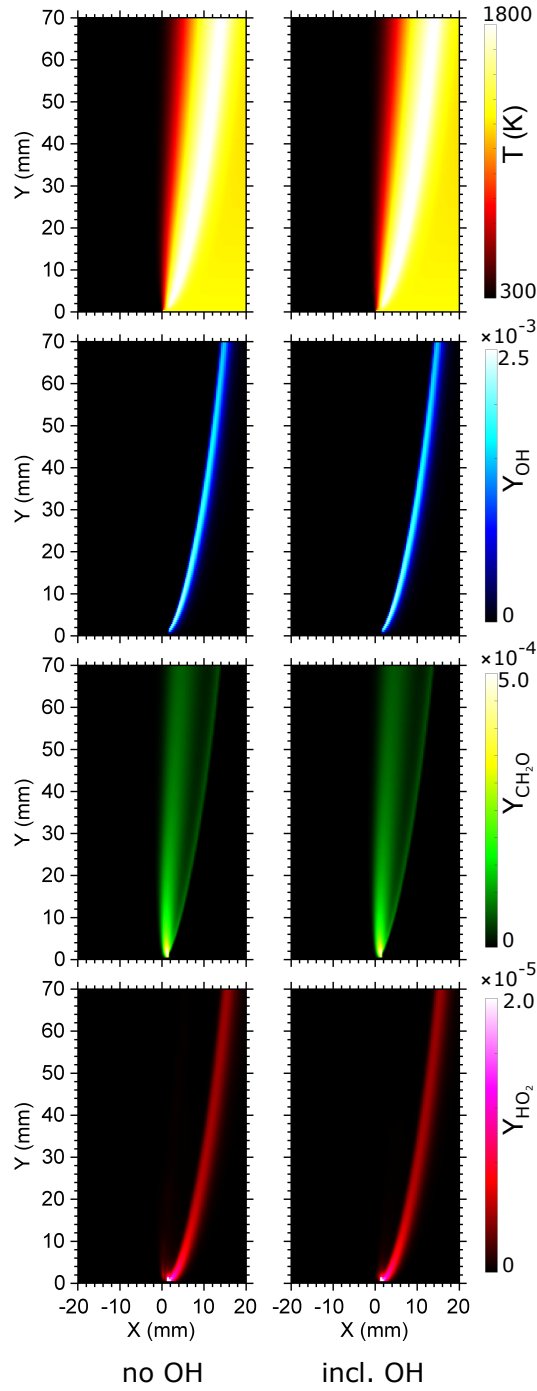


Fig. 9. Temperature and species mass fraction distributions in CH_4 flames stabilised in 1300-K coflows with 9% O_2 (vol./vol.), neglecting (left) and including (right) equilibrium OH in the coflow description.

in the flame. This reaction pathway promotes short ignition delays and increased consumption of O_2 prior to thermal runaway [99], decreasing CH_3 recombination to C_2H_6 [61]. This is consistent with the dominant CH_3 consumption path identified in a previous study of a tribrachial CH_4 flame [95], and a study of CH_4/air mixtures in a 900-K simulated homogeneous reactor. These studies suggested the same effect when lean and stoichiometric mixtures were doped with either H_2O_2 or CH_2O at concentrations between 0.1% and 3.0% [75]. The concentrations of H_2O_2 and CH_2O in the latter study [75] far exceed their equilibrium values, with equilibrium mole fractions of H_2O_2 on the order of 10^{-9} and CH_2O on the order of 10^{-22} . Their results indicated, however, the impact of these species on the ignition delay of a homogeneous mixture of hot CH_4/air is qualitatively similar to the results seen in this study when

accounting for equilibrium OH in the simulation of CH₄ with a 1300-K coflow with 3% O₂ [75]. The effect of OH inclusion is less prevalent in the 6 and 9% O₂ cases or at higher temperatures, in which the CH₃ radical is more readily oxidised by the increased concentration of oxygen, and is less susceptible to recombination [61, 100]. These results highlight the critical importance of the inclusion of OH in ignition analyses and modelling of MILD CH₄ combustion.

4.3. The effects of oxidant composition on C₂H₄ flames

The reaction zone structure of C₂H₄ flames in 1300-K coflows with 3 and 9% O₂ is significantly different to CH₄ flames. Figures 10 and 11 show temperature and species distributions in two-dimensions and at a height of 30 mm respectively. Noticeably, lean peaks of CH₂O are not as prominent in the CH₄ flames (refer to Fig. 7), but in contrast, feature two similar-sized peaks of HO₂ on the rich and lean wings of the reaction zone. These profiles are similar in shape for reaction zones with coflows with both 3 and 9% O₂, in contrast to the differences seen experimentally (see Fig. 3), suggesting that these flames may be significantly dependent on the underlying flow- and mixing-fields. This is consistent with an analysis of ethanol flames in the transition between MILD combustion and conventional spontaneous-ignition [18], and supports defining the boundaries of non-premixed MILD combustion in terms of both oxidant and flow-field characteristics.

The double peaks of HO₂ suggest tribrachial structures in the C₂H₄ flames. This is indicative of free H from the rich side of the flame, from the decomposition of C₂H₄ to C₂H₃ and C₂H₂, and eventually to CH₂O and HCCO. The exothermic reactions which dominate this positive heat release in the rich regions of the flame are associated with this decomposition of C₂H₄ in the flame with 9% O₂ in the oxidant, whilst heat release from the forwards reaction $\text{H} + \text{CH}_3 (+\text{M}) \rightleftharpoons \text{CH}_4 (+\text{M})$ is significantly promoted in the 3% O₂ case – dominating heat release rates in the rich side of the reaction zone. The (forwards) reaction $\text{H} + \text{O}_2 + \text{H}_2\text{O} \rightleftharpoons \text{HO}_2 + \text{H}_2\text{O}$ is responsible for heat release on the lean side of the reaction zone in both cases, however the forwards reaction $\text{OH} + \text{HO}_2 \rightleftharpoons \text{O}_2 + \text{H}_2\text{O}$ is promoted in the 9% O₂ case. Profiles of heat release rate for these flames, and relevant net reaction-rates, are included as figures in §S1 of the Supplementary Data.

Distributions of HO₂ and CH₂O precursors in C₂H₄ flames are shown in Fig. 10. These images do not appear to indicate any significant build-up of CH₂O on the lean side of the reaction zone. This suggests that oxygen is transported into the fuel stream, as previously identified [26], but carbon is not transported into the oxidant stream, as seen with the CH₄ flames. The absence of the CH₂O intermediary species in the lean wing of these flames suggests that, unlike the CH₄ flames, diffusion across the reaction zone is unilateral.

The absence of dual CH₂O peaks serves to explain why triple flame structures could not be seen in experimental measurements at the base of turbulent C₂H₄ flames in 1100-K coflows [22], despite being observable in CH₄ flames in a similar configuration [48]. At the time, this was explained as the possible compression of the triple flame structure due to turbulence, such that the lean CH₂O wing became undetectable [22]. The current results, however, suggest that HO₂ is the more important precursor in C₂H₄ ignition in hot and diluted coflows.

The HO₂ species has been shown to be an important precursor in C₂H₄ combustion in hot air [92] and, from the current study, in diluted oxidants. This increased concentration of HO₂ is due to H abstraction

in the initial stages of C_2H_4 ignition (with $C_2H_4 \rightarrow C_2H_3 \rightarrow C_2H_2$ [90, 101]). This produces HO_2 through the reactions between H or H_2 released from the fuel and O_2 from the oxidant stream, whilst the endothermic process of H abstraction from C_2H_3 is responsible of significant negative heat release on the rich side of the reaction zone. Although the different pathways in C_2H_4 ignition have previously been assessed in hot and diluted coflows [90], the current work shows the relative importance of HO_2 and CH_2O in the stabilisation of C_2H_4 flames through H/ H_2 and C_2H_2 reaction pathways, respectively.

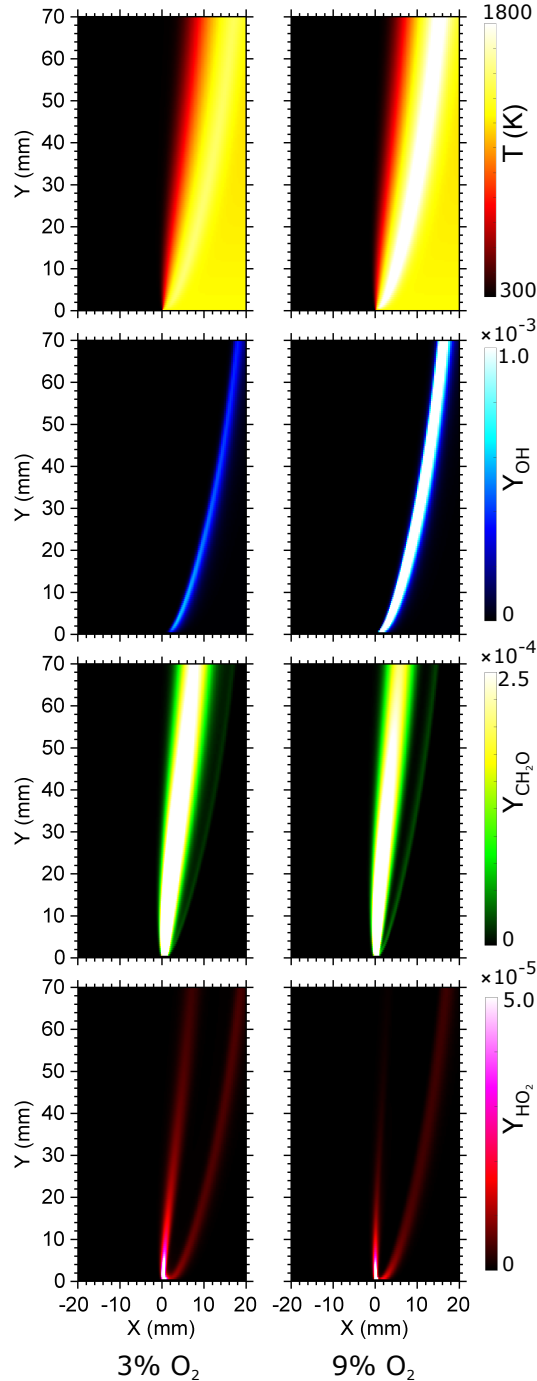


Fig. 10. Temperature and species mass fraction distributions in C_2H_4 flames stabilised in 1300-K coflows with 3 (left) and 9% (right) O_2 (vol./vol.). Both cases include equilibrium OH in the coflow description.

4.4. The effects of relative oxidant C/H concentration on CH_4 flames

The oxidants in Figs. 7-9 include 10% H_2O and 3% CO_2 by volume. Swapping these concentrations, to 3% H_2O and 10% CO_2 , has a significant effect on the temperature profile of the flame in the 3% O_2

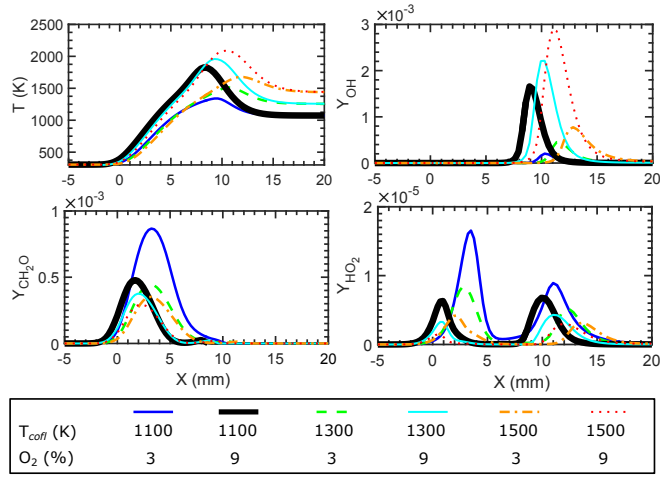


Fig. 11. The effects of coflow temperature on C_2H_4 flames. Plots show profiles of flame temperature (in Kelvin), OH, CH_2O and HO_2 mass fractions against X (refer to Fig. 1) 30 mm downstream of the inlet plane, for 1300-K oxidants with 3 and 9% O_2 (vol./vol.) (see Table 2).

case, but results in a negligible difference in the 9% O_2 case (shown in Fig. 12). This change in H_2O to CO_2 ratio results in a 6% increase in mean molecular weight of the oxidant, but a negligible change in heat capacity. This change will therefore only exhibit a minimal physical effect (due to changes in heat capacity and momentum) on the flames. This change also affects the species profiles in the 3% O_2 case more than the 9% O_2 case (included as figures in §S4 of the Supplementary Data).

Increasing the relative concentration of CO_2 in the oxidant causes a significant decrease in peak temperature of the MILD reaction zone in the coflow with 3% O_2 . The causes of this effect have been studied in previous investigations into MILD combustion in homogeneous [76, 102, 103] and non-premixed [73] configurations. These studies found that increased concentrations of CO_2 in MILD combustion lead to reduced reactivity [73, 103] by enhancing the CH_3 recombination pathway, particularly at temperatures above 1250 K [103]. Additionally, CO_2 competes with O_2 and CH_4 for H consumption through the reaction $CO_2 + H \rightleftharpoons CO + OH$ [76, 104], reducing reaction-rates, although this was studied in CH_4/O_2 systems which are “highly diluted in CO_2 ” [76] with more than 75% CO_2 [104]. In the current study, however, the major diluent in all cases is N_2 , which would reduce the relative influence of this reaction. This is consistent with the conclusion drawn from analyses of CH_4/H_2 flames in coflows with 3% O_2 , where this chemical effect was demonstrated to be more significant than the physical effect of increasing CO_2 concentrations [73].

The CH_4 flame with the coflow with 9% O_2 is not as significantly affected by the change in H_2O to CO_2 ratio as the 3% O_2 case (see Fig. 12). Under these conditions, there is a slight decrease in flame temperature on the lean side of the reaction zone accompanied by a decrease in OH concentration. The change in H_2O to CO_2 ratio does not have a significant impact on the rich side of the reaction zone (refer to Fig. 12 as well as the figures in §S4 of the Supplementary Data). This indicates that the rich chemistry is not greatly affected by the change in oxidant C/H ratio, suggesting that the CO_2 transported into the fuel stream is not present in sufficient quantities to effect H abstraction from CH_4 or CH_3 recombination. Further to this, the recombination of CH_3 is less influential on the combustion process in the (tribranchial) 9% O_2 case than the (MILD) 3% O_2 case, as discussed in §4.2 and in previous studies [61].

The combined results highlight the sensitivity of the MILD combustion of CH_4 to oxidant compo-

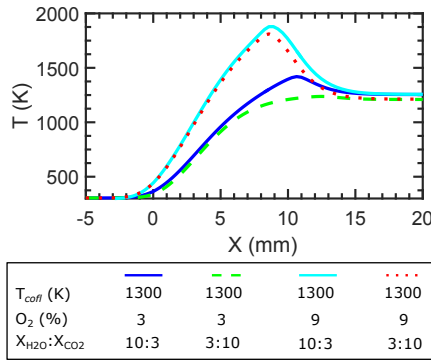


Fig. 12. The effects of changing H_2O and CO_2 concentrations in the coflow from 10 and 3% to 3 and 10% (vol./vol.), respectively. Plots show profiles of CH_4 flame temperature (in Kelvin) against X (refer to Fig. 1) 30 mm downstream of the inlet plane, for 1300-K oxidants with 3 and 9% O_2 (vol./vol.) (see Table 2).

sitions, in stark contrast to the tribrachial spontaneously-igniting flames. These results reinforce the previous conclusion from S4.2 that oxidant compositions must be accurately described in attempts to understand the structure of non-premixed, MILD CH_4 reaction zones, and in their subsequent modelling.

4.5. Effects of oxidant temperature on CH_4 and C_2H_4 flames

Simulations of CH_4 flames in §4.2 show that the composition of 1300-K oxidants have a significant effect on reaction zone structure in the MILD combustion regime. Figure 13 shows differences between CH_4 flames with different oxidants at 1300 and 1500 K with either 3, 6 or 9% O_2 . No ignition occurred with 1100-K oxidants for any diluted O_2 level.

The profiles of CH_2O in Fig. 13 show that only the CH_4 flame with the 1300-K oxidant with 3% O_2 has a non-tribrachial, MILD reaction zone structure. CH_4 flames with this oxidant composition transition from MILD to tribrachial structures as oxidant temperature increases from 1300 to 1500 K. This is consistent with the experimental observations of flames in coflows below 1500 K, shown in Fig. 2. Such a change in structure was not seen in C_2H_4 flames, where the HODO coflow temperature did not change the location(s) of peaks in species profiles (see Fig. 11). This indicates that the presence of MILD reaction zones in CH_4 combustion is confined to a very limited range of oxidant temperatures and O_2 levels, as has been previously been noted for the MILD combustion regime [20, 21, 56].

Simulations of non-premixed CH_4 flames with HODO coflows demonstrate two distinct reaction zone structures. Despite this, each CH_4 flame exhibits temperature increases below its stoichiometric self-ignition temperature [9, 105]. This supports the conclusions of de Joannon *et al.* [27, 32, 106], Ye *et al.* [18], Evans *et al.* [30] and Medwell *et al.* [105] that an appropriate definition of MILD combustion in non-premixed HODO configurations cannot be based on temperature alone, but should incorporate both thermal and chemical structure elements of MILD combustion. Although this is directly relevant to the analysis of non-premixed, lab-scale flames [19, 22, 23, 26, 42, 57], it is not the focus of this work to consolidate the regime descriptions proposed in these studies.

5. Conclusions

Analysis of experimental photographs and simulations have investigated differences between MILD reaction zones and conventional spontaneously-igniting flames in hot and diluted (HODO) coflows, with the following conclusions:

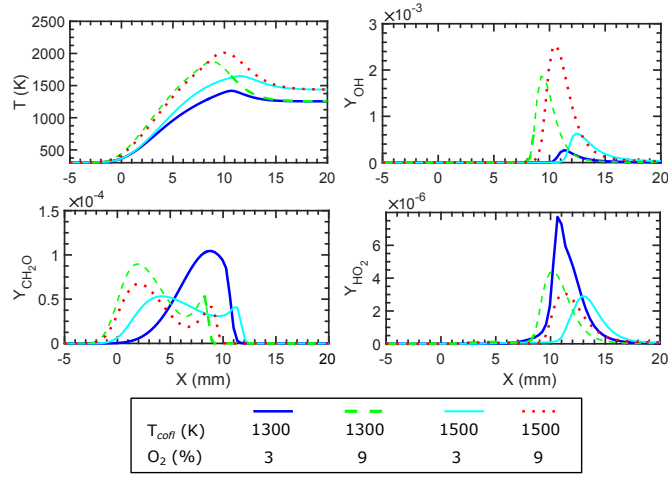


Fig. 13. The effects of coflow temperature on CH_4 flames. Plots show profiles of flame temperature (in Kelvin), OH, CH_2O and HO_2 mass fractions against X (refer to Fig. 1) 30 mm downstream of the inlet plane, for 1300-K oxidants with 3 and 9% O_2 (vol./vol.) (see Table 2).

- Only one of the simulated CH_4 flames investigated (1300-K oxidant with 3% O_2) meets the criteria for MILD combustion as an edge flame without a triple point [18, 21, 32], consistent with experimental observations.
- Classifications of simulated C_2H_4 flames as MILD or tribrachial are inconsistent with experimental observations.
- Changing in relative C/H concentrations in HODO coflows affects the intensity of MILD reaction zones more than conventional spontaneously-igniting flames.
- Equilibrium levels of OH (<10 ppm) significantly increase the reactivity of MILD, CH_4 reaction zones – resulting in the attachment of the reaction zone and increasing peak temperatures – but not tribrachial CH_4 or C_2H_4 flames or steady-state, opposed-flow flames.
- The HO_2 radical is a more appropriate indicator of a tribrachial structure for non-premixed C_2H_4 flames in HODO coflows than CH_2O .

The conclusions highlight the importance of the oxidant description in numerical simulations of MILD CH_4 combustion. They imply that the transition between the MILD and conventional spontaneously-ignitive combustion regimes is dominated by temperature and oxidant O_2 levels, despite the remainder of the coflow composition having a significant impact on the intensity of MILD reaction zones.

6. Acknowledgements

The authors thank Prof. Bassam Dally for sharing previously published experimental data, and thank Dr. Alfonso Chinnici for useful discussions on MILD combustion. The authors acknowledge the support of the Centre for Energy Technology (CET), The University of Adelaide and the Politecnico di Milano, as well as eResearch SA for high-performance computing services. Funding support from the United States Asian Office for Aerospace Research and Development (AOARD) and the Australian Research Council (ARC) is acknowledged.

References

- [1] J. A. Wüning, J. G. Wüning, Flameless oxidation to reduce thermal no-formation, *Prog. Energ. Combust.* 23 (1) (1997) 81–94.
- [2] K. Döbbeling, J. Hellat, H. Koch, 25 Years of BBC/ABB/Alstom Lean Premix Combustion Technologies, *J. Eng. Gas Turb. Power* 1 (2007) 2–12.
- [3] B. Dally, E. Riesmeier, N. Peters, Effect of fuel mixture on moderate and intense low oxygen dilution combustion, *Combust. Flame* 137 (4) (2004) 418–431.
- [4] B. B. Dally, S. H. Shim, R. A. Craig, P. J. Ashman, G. G. Szegö, On the Burning of Sawdust in a MILD Combustion Furnace, *Energy Fuels* 24 (6) (2010) 3462–3470.
- [5] M. Flamme, Low NO_x combustion technologies for high temperature applications, *Energ. Convers. Manage.* 42 (15-17) (2001) 1919–1935.
- [6] R. Lückerrath, W. Meier, M. Aigner, FLOX[®] combustion at high pressure with different fuel compositions, *J. Eng. Gas Turb. Power* 130 (1) (2008) 011505.
- [7] O. Lammel, H. Schütz, G. Schmitz, R. Lückerrath, M. Stöhr, B. Noll, M. Aigner, M. Hase, W. Krebs, FLOX[®] combustion at high power density and high flame temperatures, *J. Eng. Gas Turb. Power* 132 (12) (2010) 121503.
- [8] M. Stöhr, I. Boxx, C. D. Carter, W. Meier, Experimental study of vortex-flame interaction in a gas turbine model combustor, *Combust. Flame* 159 (8) (2012) 2636–2649.
- [9] A. Cavaliere, M. de Joannon, Mild Combustion, *Prog. Energ. Combust.* 30 (4) (2004) 329–366.
- [10] M. Saha, A. Chinnici, B. B. Dally, P. R. Medwell, Numerical Study of Pulverized Coal MILD Combustion in a Self-Recuperative Furnace, *Energy Fuels* 29 (11) (2015) 7650–7669.
- [11] G. Sturgess, J. Zelina, D. T. Shouse, W. Roquemore, Emissions reduction technologies for military gas turbine engines, *J. Propul. Power* 21 (2) (2005) 193–217.
- [12] C. Prathap, F. C. C. Galeazzo, P. Kasabov, P. Habisreuther, N. Zarzalis, C. Beck, W. Krebs, B. Wegner, Analysis of NO_x Formation in an Axially Staged Combustion System at Elevated Pressure Conditions, *J. Eng. Gas Turb. Power* 134 (3) (2012) 031507.
- [13] S. Can Gülen, Étude on Gas Turbine Combined Cycle Power Plant–Next 20 Years, *J. Eng. Gas Turb. Power* 138 (5) (2015) 051701.
- [14] D. Guyot, G. Tea, C. Appel, Low NO_x Lean Premix Reheat Combustion in Alstom GT24 Gas Turbines, *J. Eng. Gas Turb. Power* 138 (5) (2015) 051503.
- [15] C. M. Arndt, R. Schießl, J. D. Gounder, W. Meier, M. Aigner, Flame stabilization and auto-ignition of pulsed methane jets in a hot coflow: Influence of temperature, *Proc. Combust. Inst.* 34 (2013) 1483–1490.
- [16] J. Sidey, E. Mastorakos, Visualization of MILD combustion from jets in cross-flow, *Proc. Combust. Inst.* 35 (3) (2015) 3537–3545.
- [17] P. R. Medwell, D. L. Blunck, B. B. Dally, The role of precursors on the stabilisation of jet flames issuing into a hot environment, *Combust. Flame* 161 (2) (2014) 465–474.
- [18] J. Ye, P. R. Medwell, B. B. Dally, M. J. Evans, The transition of ethanol flames from conventional to MILD combustion, *Combust. Flame* 171 (2016) 173–184.
- [19] B. Dally, A. Karpetsis, R. Barlow, Structure of turbulent non-premixed jet flames in a diluted hot coflow, *Proc. Combust. Inst.* 29 (2002) 1147–1154.
- [20] B. Choi, K. Kim, S. Chung, Autoignited laminar lifted flames of propane in coflow jets with tribrachial edge and mild combustion, *Combust. Flame* 156 (2) (2009) 396–404.
- [21] B. Choi, S. Chung, Autoignited laminar lifted flames of methane, ethylene, ethane, and n-butane jets in coflow air with elevated temperature, *Combust. Flame* 157 (12) (2010) 2348–2356.
- [22] P. R. Medwell, P. A. M. Kalt, B. B. Dally, Imaging of diluted turbulent ethylene flames stabilized on a Jet in Hot Coflow (JHC) burner, *Combust. Flame* 152 (2008) 100–113.
- [23] P. R. Medwell, B. B. Dally, Experimental Observation of Lifted Flames in a Heated and Diluted Coflow, *Energy Fuels* 26 (9) (2012) 5519–5527.
- [24] M. Saha, B. B. Dally, P. R. Medwell, A. Chinnici, Effect of particle size on the MILD combustion characteristics of pulverised brown coal, *Fuel Process. Technol.* DOI: 10.1016/j.fuproc.2016.04.003.
- [25] M. Saha, B. B. Dally, P. R. Medwell, A. Chinnici, Burning characteristics of Victorian brown coal under MILD combustion conditions, *Combust. Flame* 172 (2016) 252–270.
- [26] P. R. Medwell, P. A. M. Kalt, B. B. Dally, Reaction Zone Weakening Effects under Hot and Diluted Oxidant Stream Conditions, *Combust. Sci. Technol.* 181 (7) (2009) 937–953.
- [27] M. de Joannon, A. Matarazzo, P. Sabia, A. Cavaliere, Mild Combustion in Homogeneous Charge Diffusion Ignition (HCDI) regime, *Proc. Combust. Inst.* 31 (2) (2007) 3409–3416.
- [28] M. de Joannon, P. Sabia, G. Sorrentino, A. Cavaliere, Numerical study of mild combustion in hot diluted diffusion ignition (HDDI) regime, *Proc. Combust. Inst.* 32 (2) (2009) 3147–3154.
- [29] M. J. Evans, P. R. Medwell, Z. F. Tian, A. Frassoldati, A. Cuoci, A. Stagni, Ignition Characteristics in Spatially Zero-, One- and Two-Dimensional Laminar Ethylene Flames, *AIAA J.* 54 (10) (2016) 3255–3264.
- [30] M. J. Evans, P. R. Medwell, H. Wu, A. Stagni, M. Ihme, Classification and Lift-Off Height Prediction of Non-Premixed MILD and Autoignitive Flames, *Proc. Combust. Inst.* DOI: 10.1016/j.proci.2016.06.013.
- [31] M. Oberlack, R. Arlitt, N. Peters, On stochastic Damköhler number variations in a homogeneous flow reactor, *Combust. Theor. Model.* 4 (4) (2000) 495–510.
- [32] M. de Joannon, P. Sabia, G. Cozzolino, G. Sorrentino, A. Cavaliere, Pyrolytic and Oxidative Structures in Hot Oxidant Diluted Oxidant (HODO) MILD Combustion, *Combust. Sci. Technol.* 184 (7-8) (2012) 1207–1218.
- [33] G. Sorrentino, D. Scarpa, A. Cavaliere, Transient inception of MILD combustion in hot diluted diffusion ignition (HDDI) regime: A numerical study, *Proc. Combust. Inst.* 34 (2) (2013) 3239–3247.
- [34] K. Bray, M. Champion, P. A. Libby, Extinction of premixed flames in turbulent counterflowing streams with unequal enthalpies, *Combust. Flame* 107 (1-2) (1996) 53–64.
- [35] E. Mastorakos, A. Taylor, J. Whitelaw, Extinction of turbulent counterflow flames with reactants diluted by hot products, *Combust. Flame* 102 (1-2) (1995) 101–114.
- [36] D. J. Diamantis, E. Mastorakos, D. A. Goussis, Simulations of premixed combustion in porous media, *Combust. Theor. Model.* 6 (3) (2002) 383–411.
- [37] S. Taamallah, S. J. Shanbhogue, A. F. Ghoniem, Turbulent flame stabilization modes in premixed swirl combustion: Physical mechanism and Karlovitz number-based criterion, *Combust. Flame* 166 (2016) 19–33.
- [38] S. Taamallah, N. W. Chakroun, H. Watanabe, S. J. Shanbhogue, A. F. Ghoniem, On the characteristic flow and

- flame times for scaling oxy and air flame stabilization modes in premixed swirl combustion, *Proc. Combust. Inst.* DOI: 10.1016/j.proci.2016.07.022.
- [39] I. Chtereve, C. W. Foley, D. Foti, S. Kostka, A. W. Caswell, N. Jiang, A. Lynch, D. R. Noble, S. Menon, J. M. Seitzman, T. C. Lieuwen, Flame and Flow Topologies in an Annular Swirling Flow, *Combust. Sci. Technol.* 186 (8) (2014) 1041–1074.
- [40] S. J. Shanbhogue, S. Husain, T. Lieuwen, Lean blowoff of bluff body stabilized flames: Scaling and dynamics, *Prog. Energy Combust. Sci.* 35 (1) (2009) 98–120.
- [41] M. U. Göktolga, J. A. van Oijen, L. P. H. de Goey, 3D DNS of MILD combustion: A detailed analysis of heat loss effects, preferential diffusion, and flame formation mechanisms, *Fuel* 159 (2015) 784–795.
- [42] E. Oldenhof, M. J. Tummers, E. H. van Veen, D. J. E. M. Roekaerts, Ignition kernel formation and lift-off behaviour of jet-in-hot-coflow flames, *Combust. Flame* 157 (6) (2010) 1167–1178.
- [43] E. Oldenhof, M. J. Tummers, E. H. van Veen, D. J. E. M. Roekaerts, Role of entrainment in the stabilisation of jet-in-hot-coflow flames, *Combust. Flame* 158 (8) (2011) 1553–1563.
- [44] M. Papageorge, C. Arndt, F. Fuest, W. Meier, J. Sutton, High-speed mixture fraction and temperature imaging of pulsed, turbulent fuel jets auto-igniting in high-temperature, vitiated co-flows, *Exp. Fluids* 55 (7) 1763.
- [45] C. M. Arndt, M. J. Papageorge, F. Fuest, J. A. Sutton, W. Meier, M. Aigner, The role of temperature, mixture fraction, and scalar dissipation rate on transient methane injection and auto-ignition in a jet in hot coflow burner, *Combust. Flame* 167 (2016) 60–71.
- [46] R. Cabra, T. Myhrvold, J. Chen, R. Dibble, A. Karpetsis, R. Barlow, Simultaneous laser raman-rayleigh-lif measurements and numerical modeling results of a lifted turbulent H_2/N_2 jet flame in a vitiated coflow, *Proc. Combust. Inst.* 29 (2002) 1881–1888.
- [47] R. Cabra, J.-Y. Chen, R. Dibble, A. Karpetsis, R. Barlow, Lifted methane-air jet flames in a vitiated coflow, *Combust. Flame* 143 (4) (2005) 491–506.
- [48] R. L. Gordon, A. R. Masri, E. Mastorakos, Simultaneous Rayleigh temperature, OH- and CH_2O -LIF imaging of methane jets in a vitiated coflow, *Combust. Flame* 155 (1-2) (2008) 181–195.
- [49] S. M. Al-Noman, S. K. Choi, S. H. Chung, Numerical study of laminar nonpremixed methane flames in coflow jets: Autoignited lifted flames with tribrachial edges and MILD combustion at elevated temperatures, *Combust. Flame* 171 (2016) 119–132.
- [50] P. Domingo, L. Vervisch, Triple flames and partially premixed combustion in autoignition of non-premixed turbulent mixtures, *Proc. Combust. Inst.* 26 (1) (1996) 233–240.
- [51] T. Plessing, P. Terhoeven, N. Peters, M. S. Mansour, An experimental and numerical study of a laminar triple flame, *Combust. Flame* 115 (3) (1998) 335–353.
- [52] A. Joedicke, N. Peters, M. Mansour, The stabilization mechanism and structure of turbulent hydrocarbon lifted flames, *Proc. Combust. Inst.* 30 (1) (2005) 901–909.
- [53] K. M. Lyons, Toward an understanding of the stabilization mechanisms of lifted turbulent jet flames: Experiments, *Prog. Energy Combust. Sci.* 33 (2) (2007) 211–231.
- [54] A. Masri, Partial premixing and stratification in turbulent flames, *Proc. Combust. Inst.* 35 (2) (2015) 1115–1136.
- [55] E. Mastorakos, Ignition of turbulent non-premixed flames, *Prog. Energy Combust. Sci.* 35 (1) (2009) 57–97.
- [56] S. K. Choi, J. Kim, S. H. Chung, J. S. Kim, Structure of the edge flame in a methane-oxygen mixing layer, *Combust. Theor. Model.* 13 (1) (2009) 39–56.
- [57] P. R. Medwell, P. A. M. Kalt, B. B. Dally, Simultaneous imaging of OH, formaldehyde, and temperature of turbulent nonpremixed jet flames in a heated and diluted coflow, *Combust. Flame* 148 (1-2) (2007) 48–61.
- [58] J. Prager, H. Najm, M. Valorani, D. Goussis, Structure of n-heptane/air triple flames in partially-premixed mixing layers, *Combust. Flame* 158 (11) (2011) 2128–2144.
- [59] T. Plessing, N. Peters, J. G. Wüning, Laseroptical investigation of highly preheated combustion with strong exhaust gas recirculation, *Proc. Combust. Inst.* 27 (2) (1998) 3197–3204.
- [60] F. Wang, P. Li, Z. Mei, J. Zhang, J. Mi, Combustion of $CH_4/O_2/N_2$ in a well stirred reactor, *Energy* 72 (2014) 242–253.
- [61] P. Sabia, M. de Joannon, A. Picarelli, R. Ragucci, Methane auto-ignition delay times and oxidation regimes in MILD combustion at atmospheric pressure, *Combust. Flame* 160 (1) (2013) 47–55.
- [62] Y. Minamoto, T. Dunstan, N. Swaminathan, R. Cant, DNS of EGR-type turbulent flame in MILD condition, *Proc. Combust. Inst.* 34 (2) (2013) 3231–3238.
- [63] Y. Minamoto, N. Swaminathan, R. S. Cant, T. Leung, Reaction Zones and Their Structure in MILD Combustion, *Combust. Sci. Technol.* 186 (8) (2014) 1075–1096.
- [64] Y. Minamoto, N. Swaminathan, S. R. Cant, T. Leung, Morphological and statistical features of reaction zones in MILD and premixed combustion, *Combust. Flame* 161 (11) (2014) 2801–2814.
- [65] A. Dubreuil, F. Foucher, C. Mounaïm-Rousselle, G. Dayma, P. Dagaut, HCCI combustion: Effect of NO in EGR, *Proc. Combust. Inst.* 31 (2) (2007) 2879–2886.
- [66] A. B. Bendtsen, P. Glarborg, K. Dam-Johansen, Low temperature oxidation of methane: the influence of nitrogen oxides, *Combust. Sci. Technol.* 151 (1) (2000) 31–71.
- [67] T. Faravelli, A. Frassoldati, E. Ranzi, Kinetic modeling of the interactions between NO and hydrocarbons in the oxidation of hydrocarbons at low temperatures, *Combust. Flame* 132 (1-2) (2003) 188–207.
- [68] A. Frassoldati, T. Faravelli, E. Ranzi, Kinetic modeling of the interactions between NO and hydrocarbons at high temperature, *Combust. Flame* 135 (1-2) (2003) 97–112.
- [69] A. Parente, J. Sutherland, B. Dally, L. Tognotti, P. Smith, Investigation of the MILD combustion regime via Principal Component Analysis, *Proc. Combust. Inst.* 33 (2) (2011) 3333–3341.
- [70] S. M. Najafzadeh, M. Sadeghi, R. Sotudeh-Gharebagh, Analysis of autoignition of a turbulent lifted H_2/N_2 jet flame issuing into a vitiated coflow, *Int. J. Hydrogen Energ.* 38 (5) (2013) 2510–2522.
- [71] P. Li, F. Wang, J. Mi, B. Dally, Z. Mei, J. Zhang, A. Parente, Mechanisms of NO formation in MILD combustion of CH_4/H_2 fuel blends, *Int. J. Hydrogen Energ.* 39 (33) (2014) 19187–19203.
- [72] F. Wang, P. Li, J. Mi, J. Wang, M. Xu, Chemical kinetic effect of hydrogen addition on ethylene jet flames in a hot and diluted coflow, *Int. J. Hydrogen Energ.* 40 (46) (2015) 16634–16648.
- [73] Y. Tu, K. Su, H. Liu, S. Chen, Z. Liu, C. Zheng, Physical and chemical effects of CO_2 addition on CH_4/H_2 flames on a Jet in Hot Coflow (JHC) burner, *Energy Fuels* 30 (2) (2016) 1390–1399.
- [74] M. J. Evans, P. R. Medwell, Z. F. Tian, Modeling Lifted Jet Flames in a Heated Coflow using an Optimized Eddy Dissipation Concept Model, *Combust. Sci. Technol.* 187 (7) (2015) 1093–1109.

- [75] D. M. Manias, E. A. Tingas, C. E. Frouzakis, K. Boulouchos, D. A. Goussis, The mechanism by which CH_2O and H_2O_2 additives affect the autoignition of CH_4 /air mixtures, *Combust. Flame* 164 (2016) 111–125.
- [76] P. Sabia, G. Sorrentino, A. Chinnici, A. Cavaliere, R. Ragucci, Dynamic Behaviors in Methane MILD and Oxy-Fuel Combustion. Chemical Effect of CO_2 , *Energy Fuels* 29 (3) (2015) 1978–1986.
- [77] R. M. I. Elsamra, S. Vranckx, S. A. Carl, $\text{CH}(\text{A}^2\Delta)$ Formation in Hydrocarbon Combustion: The Temperature Dependence of the Rate Constant of the Reaction $\text{C}_2\text{H} + \text{O}_2 \rightarrow \text{CH}(\text{A}^2\Delta) + \text{CO}_2$, *J. Phys. Chem.* 109 (45) (2005) 10287–10293.
- [78] A. Cuoci, A. Frassoldati, T. Faravelli, E. Ranzi, A computational tool for the detailed kinetic modeling of laminar flames: Application to $\text{C}_2\text{H}_4/\text{CH}_4$ coflow flames, *Combust. Flame* 160 (5) (2013) 870–886.
- [79] A. Cuoci, A. Frassoldati, T. Faravelli, E. Ranzi, Numerical Modeling of Laminar Flames with Detailed Kinetics Based on the Operator-Splitting Method, *Energy Fuels* 27 (12) (2013) 7730–7753.
- [80] A. Cuoci, A. Frassoldati, T. Faravelli, E. Ranzi, OpenSMOKE++: An object-oriented framework for the numerical modeling of reactive systems with detailed kinetic mechanisms, *Comput. Phys. Commun.* 192 (2015) 237–264.
- [81] F. C. Christo, B. B. Dally, Modeling turbulent reacting jets issuing into a hot and diluted coflow, *Combust. Flame* 142 (1–2) (2005) 117–129.
- [82] J. Aminian, C. Galletti, S. Shahhosseini, L. Tognotti, Key modeling issues in prediction of minor species in diluted-preheated combustion conditions, *Appl. Therm. Eng.* 31 (16) (2011) 3287–3300.
- [83] A. Frassoldati, P. Sharma, A. Cuoci, T. Faravelli, E. Ranzi, Kinetic and fluid dynamics modeling of methane/hydrogen jet flames in diluted coflow, *Appl. Therm. Eng.* 30 (4) (2010) 376–383.
- [84] A. Mardani, S. Tabejamaat, M. Ghamari, Numerical study of influence of molecular diffusion in the Mild combustion regime, *Combust. Theor. Model.* 14 (5) (2010) 747–774.
- [85] M. Ihme, Y. C. See, LES flamelet modeling of a three-stream MILD combustor: Analysis of flame sensitivity to scalar inflow conditions, *Proc. Combust. Inst.* 33 (2011) 1309–1217.
- [86] A. Parente, M. R. Malik, F. Contino, A. Cuoci, B. B. Dally, Extension of the Eddy Dissipation Concept for turbulence/chemistry interactions to MILD combustion, *Fuel* 163 (2016) 98–111.
- [87] F. Wang, J. Mi, P. Li, C. Zheng, Diffusion flame of a CH_4/H_2 jet in hot low-oxygen coflow, *Int. J. Hydrogen Energ.* 36 (15) (2011) 9267–9277.
- [88] G. P. Smith, D. M. Golden, M. Frenklach, N. W. Moriarty, B. Eiteneer, M. Goldenberg, C. T. Bowman, R. K. Hanson, S. Song, J. William C. Gardiner, V. V. Lissianski, Z. Qin, GRI-Mech 3.0, mechanism available from http://www.me.berkeley.edu/gri_mech/, 2000.
- [89] E. Ranzi, A. Frassoldati, R. Grana, A. Cuoci, T. Faravelli, A. Kelley, C. Law, Hierarchical and comparative kinetic modeling of laminar flame speeds of hydrocarbon and oxygenated fuels, *Prog. Energy Combust. Sci.* 38 (4) (2012) 468–501, current version of mechanism available from <http://creckmodeling.chem.polimi.it/>.
- [90] S. R. Shabaniyan, P. R. Medwell, M. Rahimi, A. Frassoldati, A. Cuoci, Kinetic and fluid dynamic modeling of ethylene jet flames in diluted and heated oxidant stream combustion conditions, *Appl. Therm. Eng.* 52 (2013) 538–554.
- [91] J. A. Sidey, E. Mastorakos, Simulations of laminar non-premixed flames of methane with hot combustion products as oxidiser, *Combust. Flame* 163 (2016) 1–11.
- [92] C. S. Yoo, R. Sankaran, J. H. Chen, Three-dimensional direct numerical simulation of a turbulent lifted hydrogen jet flame in heated coflow: flame stabilization and structure, *J. Fluid Mech* 640 (2009) 453–481.
- [93] H. N. Najm, P. H. Paul, C. J. Mueller, P. S. Wyckoff, On the Adequacy of Certain Experimental Observables as Measurements of Flame Burning Rate, *Combustion and Flame* 113 (3) (1998) 312–332.
- [94] R. L. Gordon, A. R. Masri, E. Mastorakos, Heat release rate as represented by $[\text{OH}] \times [\text{CH}_2\text{O}]$ and its role in autoignition, *Combust. Theor. Model.* 13 (4) (2009) 645–670.
- [95] H. N. Najm, M. Valorani, D. A. Goussis, J. Prager, Analysis of methane-air edge flame structure, *Combust. Theor. Model.* 14 (2) (2010) 257–294.
- [96] L. Arteaga Mendez, M. Tummers, E. van Veen, D. Roekaerts, Effect of hydrogen addition on the structure of natural-gas jet-in-hot-coflow flames, *Proc. Combust. Inst.* 35 (3) (2015) 3557–3564.
- [97] C. S. Yoo, E. S. Richardson, R. Sankaran, J. H. Chen, A DNS study on the stabilization mechanism of a turbulent lifted ethylene jet flame in highly-heated coflow, *Proc. Combust. Inst.* 33 (2011) 1619–1627.
- [98] B. J. Isaac, A. Parente, C. Galletti, J. N. Thornock, P. J. Smith, L. Tognotti, A Novel Methodology for Chemical Time Scale Evaluation with Detailed Chemical Reaction Kinetics, *Energy Fuels* 27 (4) (2013) 2255–2265.
- [99] D. J. Diamantis, D. C. Kyritsis, D. A. Goussis, The reactions supporting or opposing the development of explosive modes: Auto-ignition of a homogeneous methane/air mixture, *Proc. Combust. Inst.* 35 (1) (2015) 267–274.
- [100] P. Sabia, M. de Joannon, A. Picarelli, A. Chinnici, R. Ragucci, Modeling Negative Temperature Coefficient region in methane oxidation, *Fuel* 91 (1) (2012) 238–245.
- [101] C. K. Westbrook, F. L. Dryer, Chemical kinetic modeling of hydrocarbon combustion, *Prog. Energy Combust. Sci.* 10 (1) (1984) 1–57.
- [102] P. Sabia, M. L. Lavadera, P. Giudicianni, G. Sorrentino, R. Ragucci, M. de Joannon, CO_2 and H_2O effect on propane auto-ignition delay times under mild combustion operative conditions, *Combust. Flame* 162 (3) (2015) 533–543.
- [103] P. Sabia, M. Lubrano Lavadera, G. Sorrentino, P. Giudicianni, R. Ragucci, M. de Joannon, H_2O and CO_2 Dilution in MILD Combustion of Simple Hydrocarbons, *Flow, Turbul. Combust.* 96 (2) (2016) 433–448.
- [104] P. Glarborg, L. L. B. Bentzen, Chemical Effects of a High CO_2 Concentration in Oxy-Fuel Combustion of Methane, *Energy Fuels* 22 (1) (2008) 291–296.
- [105] P. R. Medwell, M. J. Evans, Q. N. Chan, V. R. Katta, Laminar flame calculations for analysing trends in autoignitive jet flames in a hot and vitiated coflow, *Energy Fuels* DOI: 10.1021/acs.energyfuels.6b01264.
- [106] M. de Joannon, G. Sorrentino, A. Cavaliere, MILD combustion in diffusion-controlled regimes of Hot Diluted Fuel, *Combust. Flame* 159 (2012) 1832–1839.

Chapter 6

Ignition Characteristics in Spatially Zero-, One- and Two-Dimensional Laminar Ethylene Flames

Statement of Authorship

Title of Paper	Ignition Characteristics in Spatially Zero-, One- and Two-Dimensional Laminar Ethylene Flames
Publication Status	<input checked="" type="checkbox"/> Published <input type="checkbox"/> Accepted for Publication <input type="checkbox"/> Submitted for Publication <input type="checkbox"/> Unpublished and Unsubmitted work written in manuscript style
Publication Details	Evans, MJ , Medwell, PR, Tian, ZF, Frassoldati, A, Cuoci, A & Stagni, A (2016). "Ignition Characteristics in Spatially Zero-, One- and Two-Dimensional Laminar Ethylene Flames". <i>AIAA Journal</i> , vol 54, no 10, pp 3255–3264.

Principal Author

Name of Principal Author (Candidate)	Michael John Evans			
Contribution to the Paper	Designed research concept, planned numerical approach, generation and analysis of all data, interpreted data, wrote manuscript and acted as corresponding author.			
Overall percentage (%)	75			
Certification:	This paper reports on original research I conducted during the period of my Higher Degree by Research candidature and is not subject to any obligations or contractual agreements with a third party that would constrain its inclusion in this thesis. I am the primary author of this paper.			
Signature	<table border="1"> <tr> <td>Digitally signed by Michael Evans Date: 2016.10.18 16:50:58 +10'30'</td> <td>Date</td> <td>18-Oct-2016</td> </tr> </table>	Digitally signed by Michael Evans Date: 2016.10.18 16:50:58 +10'30'	Date	18-Oct-2016
Digitally signed by Michael Evans Date: 2016.10.18 16:50:58 +10'30'	Date	18-Oct-2016		

Co-Author Contributions

By signing the Statement of Authorship, each author certifies that:

- the candidate's stated contribution to the publication is accurate (as detailed above);
- permission is granted for the candidate to include the publication in the thesis; and
- the sum of all co-author contributions is equal to 100% less the candidate's stated contribution.

Name of Co-Author	Paul Ross Medwell			
Contribution to the Paper	Co-supervised development of the work, helped to evaluate and edit the manuscript.			
Signature	<table border="1"> <tr> <td>Paul Medwell Date: 2016.10.18 17:12:28 +10'30'</td> <td>Date</td> <td>18-OCT-2016</td> </tr> </table>	Paul Medwell Date: 2016.10.18 17:12:28 +10'30'	Date	18-OCT-2016
Paul Medwell Date: 2016.10.18 17:12:28 +10'30'	Date	18-OCT-2016		

Name of Co-Author	Zhao Feng Tian			
Contribution to the Paper	Co-supervised development of the work, helped to evaluate and edit the manuscript.			
Signature	<table border="1"> <tr> <td>Digitally signed by Zhao Feng Tian Date: 2016.10.24 12:01:47 +10'30'</td> <td>Date</td> <td>24-OCT-2016</td> </tr> </table>	Digitally signed by Zhao Feng Tian Date: 2016.10.24 12:01:47 +10'30'	Date	24-OCT-2016
Digitally signed by Zhao Feng Tian Date: 2016.10.24 12:01:47 +10'30'	Date	24-OCT-2016		

Name of Co-Author	Alessio Frassoldati
-------------------	---------------------

Contribution to the Paper	Co-supervised development of the work, helped to evaluate and edit the manuscript.		
Signature	10070207@polimi.it 2016.10.18 13:16:09 +02'00'	Date	18-OCT-2016

Name of Co-Author	Alberto Cuoci		
Contribution to the Paper	Wrote the numerical codes used in the study, co-supervised development of the work, helped to evaluate and edit the manuscript.		
Signature	Alberto Cuoci 2016.10.18 18:00:59 +02'00'	Date	18-OCT-2016

Name of Co-Author	Alessandro Stagni		
Contribution to the Paper	Generated reduced chemical kinetics mechanism, helped to evaluate and edit the manuscript.		
Signature	<small>Firma di Alessandro Stagni Alessandro Stagni, email:astagni@polimi.it Mail: a.stagni@polimi.it Date: 2016.10.19 17:52:45+02'00'</small>	Date	19-OCT-2016

Ignition Characteristics in Spatially Zero-, One- and Two-Dimensional Laminar Ethylene Flames

Michael J. Evans,* Paul R. Medwell,[†] and Zhao F. Tian[†]
University of Adelaide, Adelaide, South Australia 5005, Australia
and

Alessio Frassoldati,[‡] Alberto Cuoci,[‡] and Alessandro Stagni[§]
Politecnico di Milano, 20133 Milan, Italy

DOI: 10.2514/1.J054958

In the continual effort to reduce emissions and improve efficiency, moderate or intense low-oxygen dilution combustion has been suggested for aeroengine applications. This new application of moderate or intense low-oxygen dilution combustion requires further insight in applying the knowledge from conventional analyses of well-mixed systems to non-premixed flames. The ignition of ethylene, a key species in hydrocarbon oxidation, is simulated in simplified combustion systems with three different hot oxidants using detailed chemical kinetics. Zero-dimensional batch reactors, one-dimensional opposed-flow flame simulations, and planar two-dimensional laminar coflowing slot flame simulations are used to compare different ignition metrics across the autoignitive and moderate or intense low-oxygen dilution combustion regimes. It is found that the autoignition of ethylene with hot air may be described in two dimensions as the intersection of a critical hydroxyl fraction and the most reactive mixture fraction. Although this provides a reasonable prediction of the flame base for ignition with hot air, this becomes less reliable in the approach to the moderate or intense low-oxygen dilution combustion regime. For the cases in, and in the transition to, the moderate or intense low-oxygen dilution combustion regime, a good agreement is seen between a 10 K rise above the oxidant temperature and the onset of strong chemiluminescence seen experimentally.

Nomenclature

\bar{U}_0	=	mean jet exit velocity
ΔT	=	temperature increase
h_{LOH}	=	flame base lift-off height
0-D	=	zero-dimensional batch reactor
1-D	=	one-dimensional opposed-flow flame
2-D	=	two-dimensional laminar flame
T	=	temperature
Y	=	mass fraction
Z	=	fuel mixture fraction
ϕ	=	equivalence ratio
τ_{ign}	=	autoignition delay

Subscripts

coflow	=	relative to the coflow
max	=	maximum value (in time)
st	=	stoichiometric condition

I. Introduction

THE focus toward high-fuel-efficiency low-emissions systems for modern aeroengines presents numerous design and scientific challenges for researchers in the implementation and understanding

of combustion. One proposed method to achieve these targets is through the implementation of two-stage combustion systems incorporating moderate or intense low-oxygen dilution (MILD) combustion [1]. The MILD combustion, or flameless oxidation [2], regime has been described as combustion occurring in distributed reaction zones of hot and diluted mixtures. Under these MILD conditions, combustion does not occur in intense flame fronts but rather in reaction zones with significantly reduced temperatures [1], thermal gradients [2–4], and resistance to high strain rates without extinction [5–7]. The subsequent advantages of MILD combustion therefore include increased thermal efficiency, more complete combustion, reduced carbon monoxide (CO) and nitrogen oxides (NO_x) emissions, negligible direct combustion noise, and soot and pollutant elimination [1].

Moderate or intense low-oxygen dilution combustion bears several similarities with autoignitive flames, which occur in higher-oxygen environments than MILD combustion [8] and are encountered in gas turbine combustors and diesel engines. Both combustion regimes require elevated temperatures, exceeding some autoignition temperature, for flame ignition and stabilization, and have both been studied experimentally in jet-in-hot-coflow (JHC), or vitiated coflow, burners [4,9–22]. The stabilization of turbulent, autoignitive jet flames in hot-air coflows has additionally been studied through direct numerical simulations (DNS) [23–26]. Autoignitive flames are reported to be sensitive to small variations in ambient conditions [27], and therefore may not provide the same efficiency and reduced pollutant benefits as MILD combustion.

The reduced oxygen content in the hot coflows required for MILD combustion results in reduced chemical reaction rates compared to conventional flames [28,29]. This effect complicates the turbulence–chemistry interactions within the flame, and their coupling presents significant challenges for numerical predictions of flame behavior. In such conditions, chemical reaction rates cannot be assumed to be infinitely fast but occur over similar timescales to the turbulence flowfield, such that the Damköhler number (Da) is of order unity [30]. These comparable timescales cannot be accounted for by simple combustion models, and they require computationally expensive finite-rate chemistry modeling [28]. Detailed finite-rate chemistry in zero- and one-dimensional simulations are therefore used to provide insight into the differences and boundaries of the MILD combustion

Received 16 December 2015; revision received 8 March 2016; accepted for publication 5 April 2016; published online 16 June 2016. Copyright © 2016 by the American Institute of Aeronautics and Astronautics, Inc. All rights reserved. Copies of this paper may be made for personal and internal use, on condition that the copier pay the per-copy fee to the Copyright Clearance Center (CCC). All requests for copying and permission to reprint should be submitted to CCC at www.copyright.com; employ the ISSN 0001-1452 (print) or 1533-385X (online) to initiate your request.

*Postgraduate Student, School of Mechanical Engineering, Student Member AIAA.

[†]Senior Lecturer, School of Mechanical Engineering.

[‡]Associate Professor, Dipartimento di Chimica, Materiali ed Ingegneria Chimica “G. Natta,” Lombardy.

[§]Ph.D. Candidate, Dipartimento di Chimica, Materiali ed Ingegneria Chimica “G. Natta,” Lombardy.

regime. Correlations between these types of simulations and the ignition behavior of jet flames in the transition between the MILD and autoignitive combustion regimes will assist in classifying and evaluating ignition characteristics under different ambient, or operating, conditions.

Current distinctions between autoignitive and MILD flames have been based on the visual appearance of jet flames [4,18], the rate of the ignition process in an ideal premixed flame [7], or the temperature increase in an ideal well-stirred reactor [1]. These definitions have been used to distinguish the two different regimes based on different ignition process and flame properties in different configurations. These different flames display distinct visual characteristics in JHC configurations, with faint MILD flames appearing to initiate and stabilize close to, or at, the fuel jet exit plane — upstream of stronger chemiluminescence [18]. This is in contrast to conventional autoignitive flames, which are stabilized by the rapid ignition of isolated reacting kernels and their combination to form a flame sheet [15]. Identifying the onset ignition in models of both of these different combustion regimes with a robust metric therefore presents a challenge for comparison with experimental observations and numerical investigations. The ignition of reactive mixtures occurs at some most reactive mixture, which is the most reactive combination of the temperature and fuel-to-oxidant ratio [15]. This has been shown to be the mode of ignition for the turbulent DNS comparison case [24] and for MILD combustion of 1:1 methane (CH_4) and hydrogen (H_2) jets [26]. The basis for this paper is the study of autoignitive flames, where the initial temperature exceeds the autoignition temperature of the mixture, and this work will be applicable to applications where this is the case. The identification of the stabilization location and ignition delay (τ_{ign}) for both of these types of flames is critical for the understanding of the behavior of flames in hot, vitiated environments.

The onset of autoignition has previously been defined in batch reactors by thermal runaway, which may be indicated by the maximum rate of temperature increase ($\dot{T}|_{\text{max}}$) [20,31] in the reactor. Peak concentrations of the hydroxyl (OH) radical and the maximum rate of OH production ($\dot{Y}_{\text{OH}}|_{\text{max}}$) have additionally been used in batch reactor simulations to complement the measure of $\dot{T}|_{\text{max}}$. These two measures both indicate highly reactive points in time during ignition, and hence are expected to give similar results for autoignition delay. These two measures are not universal for all flame conditions, and thus discrepancies may occur, such as in the event of two-stage ignition. In non-premixed flames, threshold levels of the OH radical in experiments [10,32] and DNS [24] have been used to identify autoignition, whereas small increases in temperature (ΔT) have previously shown correlations between CH^* in a jet-stirred reactor [33–36]. The validity and appropriateness of these common criteria used to define ignition delay, however, are yet to be assessed across different flames across the MILD and autoignitive regimes. This study will compare these different criteria in an idealized batch reactor; a one-dimensional laminar, simulated opposed-flow flame; a two-dimensional laminar, non-premixed coflowing flame; and between the three different configurations. The purpose of the simulations chosen is to gradually increase the complexity of the flow physics (from isolated batch to coflowing streams), and this mixing process is captured (with minimal strain rate) in the two-dimensional (2-D) simulation. Finally, these criteria are compared against estimates of ignition delay in experimental observations [18] and DNS [24] to find a suitable measure for estimating autoignition in simplified kinetic simulations for comparison to real flames.

II. Methods and Models

A. Case Descriptions

The fuel of interest in this work is ethylene (C_2H_4). Ethylene has been the subject of investigations in a variety of different heated coflows from 3 to 21% oxygen (O_2) [18,24] and is recognized as a key species in the oxidation of larger hydrocarbon fuels. The three cases investigated are chosen for qualitative comparison with previously published experimental [18] and turbulent DNS [24] studies of ethylene-fueled flames. The DNS study used a 22-species skeletal mechanism with mixture-averaged transport properties based on the kinetic theory of individual gases [24,37]. Both of the previous studies featured ethylene-based jets at $Re = 10,000$ issuing into hot, laminar coflows with bulk flow velocities approximately 10% of the mean jet exit velocity. The chemical compositions and temperatures of the three cases under investigation are provided in Table 1, and they are expected to encompass jet flames from the MILD combustion regime (3% O_2 coflow) to autoigniting, lifted flames (21% O_2 coflow). The intermediate case (9% O_2 coflow) represents an autoigniting jet flame near the suspected boundary of the MILD combustion regime, which has been experimentally observed to contain features of both MILD and autoigniting jet flames [4,18].

The combustion of ethylene is modeled using two forms of the C1-C3 submechanism—for fuels containing 1 to 3 carbon atoms (C)—from the July 2014 version of the detailed mechanism developed at Politecnico di Milano (POLIMI) for hydrocarbon combustion [38]. In this study, the full 106-species submechanism is used for the zero- and one-dimensional calculations. A second 31-species skeletal mechanism is for used the two-dimensional non-premixed simulations to reduce the required computational time. This significantly reduced mechanism is generated using a combined chemical reduction approach, based on a reacting flux analysis [39]. The OpenSMOKE++ suite [40,41] and the laminarSMOKE reacting flow solver based on the OpenFOAM framework [42,43] are used to simulate the complex chemical kinetics of ignition across a wide range of operating conditions. The OpenSMOKE++ suite is a collection of zero- and one-dimensional reacting flow solvers that may be used to efficiently model a range of laboratory combustors, such as batch well-stirred reactors and laminar opposed-flow flames [40,41].

B. Premixed Analysis

This study uses a series of batch reactors for each flow case of different fuels and oxidants, referred to in the following sections as the zero-dimensional (0-D) analyses. The idealized zero-dimensional batch reactor represents a constant-volume combustion chamber with a homogeneous mixture of fuel and oxidant at given initial conditions. The following analysis of the flame base as isolated batch reactors may be considered as a simplified analogy to fluid kernels formed through turbulent mixing between the coflowing fuel and hot-air streams, neglecting heat transfer and diffusion between the surrounding fluids.

For each different fuel and oxidant case, a series of batch reactors is prescribed with unique mass fractions of fuel (Z). The mixture fractions are then expressed in terms of the stoichiometric mixture fraction (Z_{st}) for the particular fuel and oxidizer combinations. In this manner, the initial batch reactor temperature may be described as a function of the equivalence ratio (ϕ), which is equal to one at stoichiometric conditions. The relationship between (Z) and (ϕ) in a given reactor is given in Eq. (1), such that

Table 1 Fuel and oxidant stream compositions (as percent volume per volume) and temperatures (in Kelvin) used for batch reactor, opposed-flow, and two-dimensional simulations of C_2H_4 combustion for comparison against previous experiments [18] and DNS [24]

Case description	Fuel stream			Oxidant stream					
	T_f , K	C_2H_4	N_2	T_{coflow} , K	O_2	N_2	CO_2	H_2O	Stoichiometric mixture fraction
3% O_2 [18]	300	100	0	1300	3	84	3	10	0.010
9% O_2 [18]	300	100	0	1300	9	78	3	10	0.030
21% O_2 [24]	550	18	82	1550	21	79	0	0	0.274

$$\phi(Z) = \left(\frac{Z}{1-Z} \right) \left(\frac{1-Z_{st}}{Z_{st}} \right) \quad (1)$$

The individual values of ϕ describe unique batch reactor initial conditions for a given case and Z . For each reactor, the ratio of the fuel and oxidizer species are directly specified by ϕ . The values of ϕ in these individual batch reactors range from 0.05 to 2 in increments of 0.05. Subsequently, the initial reactor temperature is defined as the mixed temperature of the two streams in the same ratio. As a result, the high temperature of the oxidant streams implies higher temperatures for leaner reactors, with values of ϕ closer to zero. The higher temperatures in lean reactors promote increased reaction rates and, as such, they may react faster than stoichiometric mixtures at some "most reactive" mixture fraction.

C. Non-Premixed Analyses

Simulated opposed-flow flames facilitate the analysis of the fuel and oxidant streams in non-premixed conditions, and they will be referred to as the one-dimensional (1-D) analyses. This approach has successfully been used to compare experimentally measured turbulent flame compositions to simulated opposed flames at low-to-moderate strain rates [9,14]. The opposed-flow flame model simulates the centerline of an axisymmetric non-premixed flame supplied by laminar counterflowing jets of fuel and oxidant, with strain rates of 55–60 s⁻¹ at the stagnation plane [44]. These relatively low strain rates are similar to those previously found to show best agreement with previously studied turbulent flames in a JHC burner [4,13]. It has previously been shown that the flame structure is insensitive to strain rate in this range [20], whereas high strain rates have been shown to significantly increase ignition delay [15]. Additionally, this low strain rate reduces the physical differences between opposed-flow flames and both the batch reactor and the coflowing, laminar simulation analysis, which was designed for minimal strain rates between the two streams. Species diffusion transport is based on the molecular theory of gases, and it includes the Soret effect. These cases are initialized with a steady-state non-reacting mixture, which is then used as the initial profile for transient ignition. The initial field is assumed to be unreacted, as this is consistent with the lifted flame behavior of these flames, such that fuel and oxidizer are mixed before the initiation of combustion, via auto-ignition. In contrast to the series of premixed batch reactor simulations, this model adds complexity through species mixing effects from strain and diffusivity, which affect species residence times and local concentrations. To compare the results of the opposed-flow flame to the batch reactors, each of which has an individual value of Z , the mixture fraction at every point in the spatial and temporal domain is evaluated through Bilger's formula [45]. This formulation of a local Z allows for the analysis of non-premixed flames in terms of a local mixture fraction, and hence a local ϕ that can account for diffusive mass transfer.

The two-dimensional simulations were performed using the laminarSMOKE code [42,43], referred to as the 2-D analyses. The laminarSMOKE code is a computational fluid dynamics (CFD) solver, based on the OpenFOAM platform, for multidimensional laminar reacting flows specifically conceived for detailed kinetic mechanisms incorporating the OpenSMOKE++ libraries [42,43]. The computational domain for the 2-D simulation used to assess the validity of the zero- and one-dimensional analyses is shown in Fig. 1. The domain extends 5 mm downstream (in the Y direction) and is 4 mm wide, with two 2 mm inlets where fluid enters the domain with uniform velocities of 10 ms⁻¹. This results in very small, bulk velocity components in the transverse direction, minimizing any velocity-induced strain between the two streams. The domain is meshed with 16,000 elements, with a uniform streamwise element length of 25 μ m and a mean transverse element length of 50 μ m. Simulations were run until steady state with transient time steps on the order of 0.1 μ s. Such small time steps were necessary due to the numerically stiff chemical kinetics required for the problem, with a maximum Courant number of 0.05 enforced for each simulation time step. These flames add yet another spatial dimension to the flame

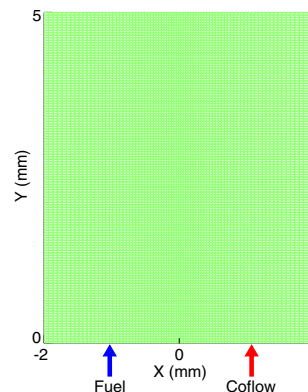


Fig. 1 Planar computational domain for the two-dimensional laminarSMOKE simulations used in this study.

analysis, simulating real laminar flames and providing further insight into practical flames without the effects of turbulence.

D. Description of Ignition Criteria

Autoignition has previously been assessed via several different criteria in different studies of turbulent jet flames, although these have not been directly compared for different cases. The measures of ignition compared in this work are 1) a set increase in local temperature above the local initial conditions (ΔT); 2) a temperature increase of 10 K ($\Delta T_{\text{coflow}} = 10$ K) above the initial oxidant stream temperature (T_{coflow}) [36]; 3) the maximum rate of change in temperature (\dot{T}_{max}) [20,31]; 4) the maximum rate of hydroxyl production ($\dot{Y}_{\text{OH}}|_{\text{max}}$); and 5) a critical value of OH mass fraction (Y_{OH}), previously taken as 2×10^{-4} [10].

The time-derivative-based metrics of the maximum rate of change in temperature and OH production are only evaluated in the closed 0-D systems, which assume no transport of species through diffusion or convection. Local ΔT increases are not used in the two-dimensional non-premixed analyses, as these metrics cannot easily be identified in a physical flame. The scalar thresholds are set in each 0-D series and assessed in the context of an opposed-flow flame and non-premixed coflowing flames. In the batch reactor series, τ_{ign} is estimated by evaluating the time derivatives of temperature and Y_{OH} , with ignition defined as the point in time when these derivatives reach their maximum value during the simulation. The threshold values of Y_{OH} and ΔT are then selected such that they provide the best agreement with the corresponding time-derivative-based ignition indicators. Comparisons between the zero- and one-dimensional ignition results facilitate the identification and description of an ignition point at the stabilized flame base of the 2-D simulation. Autoignition delay is additionally compared with the reported liftoff height (h_{LOH}) of the previous experimental and turbulent DNS studies by approximating τ_{ign} as h_{LOH} normalized by the mean jet exit velocity (\bar{U}_0), such that

$$\tau_{\text{ign}} = h_{\text{LOH}} / \bar{U}_0 \quad (2)$$

The comparisons to the turbulent DNS and experimental observations through Eq. (2) are only a first-order approximation to the ignition delay time in the absence of flowfield velocity measurements. The liftoff heights in the turbulent DNS study range from four to seven slot widths, whereas liftoff in the experimental flames is less than two jet diameters. In all cases, the turbulent flames are stabilized before the end of the jet potential core. In all cases, the liftoff height is within or close to the potential core and, over this range, the velocity decay is sufficiently small to be neglected for the purposes of this study.

III. Results and Discussion

A. Analysis of a Diluted Ethylene Flame in a Hot-Air Coflow

The ignition of diluted ethylene in hot air has been previously studied through DNS to investigate the structure of typical auto-

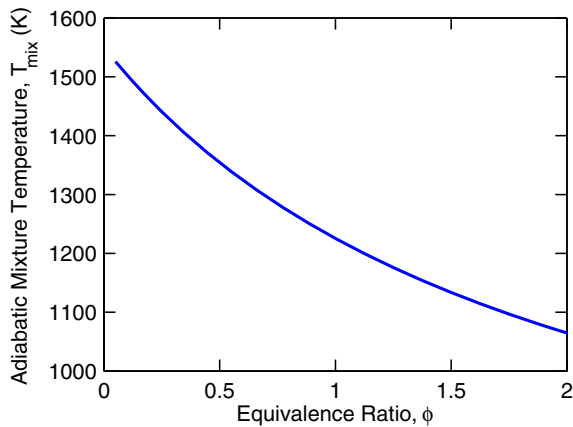


Fig. 2 Adiabatic mixture temperature of ethylene diluted with 82% N₂ by volume at 550 K and air at 1550 K, as a function of equivalence ratio.

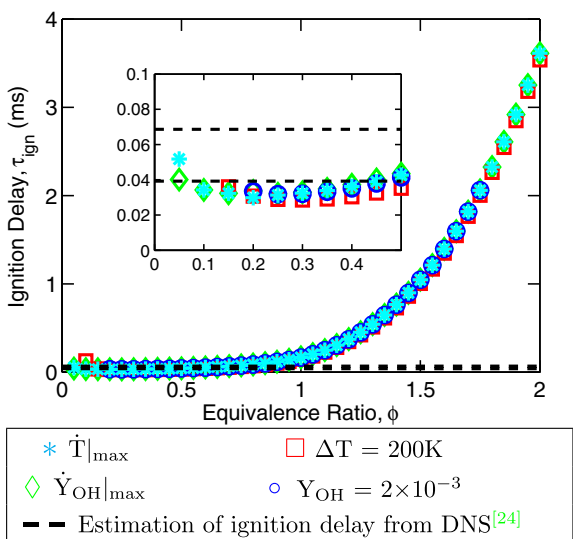


Fig. 3 Ignition delay profiles of diluted ethylene with hot air at different ϕ .

ignitive, hydrocarbon flames [24,25]. This simulation investigated the autoignition of a turbulent ethylene slot flame, diluted with 82% nitrogen (N₂) by volume, at 550 K in a 1550 K air coflow. This study found isolated kernels of autoignitive mixture occurring in the mixing layer and combining downstream to form a continuous turbulent flame front. Based on these stream conditions, the initial temperature profile of the diluted ethylene and hot-air streams for the individual 0-D reactors is shown in Fig. 2. This figure shows the increased temperature of the lean mixtures in the reactor, with increased fractions of hot oxidant in the reactors of reduced ϕ .

The ignition delays of diluted ethylene in hot air for different ϕ in 0-D reactors, and subsequently different reactant temperatures, are shown in Fig. 3. This figure shows the ignition delay τ_{ign} assessed through four different metrics of $\dot{T}|_{\text{max}}$ and $\dot{Y}_{\text{OH}}|_{\text{max}}$, with Y_{OH} and ΔT subsequently chosen for best agreement. The most reactive mixture is identified using the time-derivative metrics as $\phi \approx 0.25$, which results in the minimum value of τ_{ign} . The features of these curves were subsequently matched using scalar thresholds of $Y_{\text{OH}} = 2 \times 10^{-3}$ and $\Delta T = 200$ K to give τ_{ign} of 0.030–0.032 ms. Comparison to the original turbulent DNS results indicate the validity of these values, with a 200 K increase in mean temperature at the liftoff height corresponding to ignition kernels with Y_{OH} between 1.5×10^{-3} and 2.5×10^{-3} [24]. The previous turbulent DNS gives an estimated range of $0.039 \leq \tau_{\text{ign}} \leq 0.069$ ms [24], which is slightly in excess of the minimum predicted τ_{ign} in this study. The underestimation of τ_{ign} by this simplified analysis may be explained by diffusive mass transfer in the jet mixing field, the finite mixing time between the streams, heat transfer, and non-zero strain rates that are all inherent in

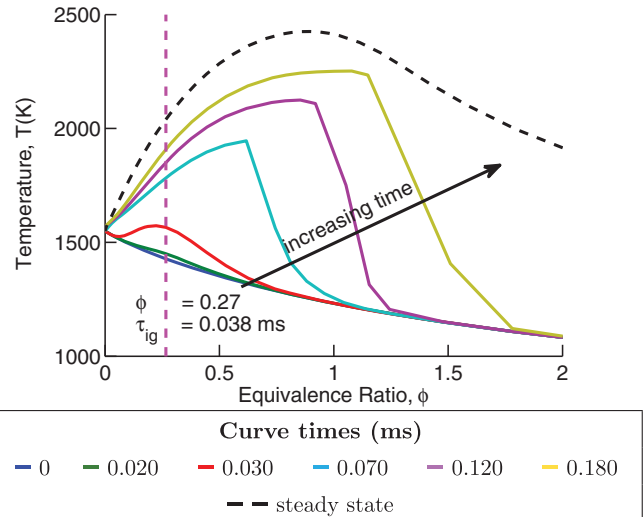


Fig. 4 Transient temperature profiles of a 1-D flame with diluted ethylene and hot air.

the original DNS. The data in Fig. 3 show excellent agreement between the two derivative-based metrics for ϕ at ignition and near stoichiometry. The agreement between the four metrics does not hold for very lean or rich mixtures, away from $\phi = 1$. In these regions, at least one of the scalar metrics of Y_{OH} and ΔT fail to predict ignition, as they do not achieve the set threshold values. This is an indication that the simple scalar metrics may not be able to identify ignition in very lean or very rich mixtures where there is some increase in temperature and OH production.

Figure 4 shows the transient temperature profile of the ignition of 1-D opposing, laminar 550 K diluted fuel and 1550 K coflow air streams. Ignition is defined using the criteria that $Y_{\text{OH}} = 2 \times 10^{-3}$, which shows excellent agreement with the time-derivative-based markers of thermal runaway in the 0-D analysis. The 1-D simulation has a strain rate of approximately 55 s^{-1} ; however, similar results (not shown for brevity) are found for a strain rate increased by a factor of five. The ignition delay of 0.038 ms indicated in Fig. 4 is slightly longer than that predicted by the 0-D simulation but very close to the minimum τ_{ign} of 0.039 ms determined by the turbulent DNS [24]. The minor discrepancies between the 1-D simulation and the turbulent DNS [24] are due to the different configurations, and therefore different strain rates across the reaction zone. These are similar to previous comparisons of 1-D flames against experimental data [9,14], verifying the use of these simulations for predicting turbulent flame behavior.

Table 2 summarizes the minimum global τ_{ign} for both the 0-D and 1-D simulations calculated using a variety of different criteria. This table includes τ_{ign} corresponding to the different ignition criteria visualized in Fig. 3 and from previously published studies [10,20,31,32,35,36]. The table features a 10 K temperature increase above that of the coflow ΔT_{coflow} , which has previously been used to

Table 2 Ignition delay τ_{ign} corresponding to different combustion criteria in different fundamental reactors^a

Criterion	0-D batch reactor τ_{ign} , ms	1-D opposed flame τ_{ign} , ms ^b
$\dot{T} _{\text{max}}$ ^b	0.031	N/A
$\dot{Y}_{\text{OH}} _{\text{max}}$	0.032	N/A
$Y_{\text{OH}} = 2 \times 10^{-3}$	0.032	0.038
$Y_{\text{OH}} = 1.6 \times 10^{-3}$	0.030	0.036
$Y_{\text{OH}} = 2 \times 10^{-4}$	0.016	0.021
$\Delta T = 200$ K	0.029	0.034
$\Delta T_{\text{coflow}} = 10$ K ^c	0.017	0.021

^aNote three-dimensional DNS estimates τ_{ign} of 0.039–0.069 ms [24].

^bPreviously published metric [20,31].

^cN/A does, indeed, denote “not applicable.”

^dPreviously published metric [10,32].

^ePreviously published metric [35,36].

define a minimum temperature increase for MILD combustion [35,36]. This is in contrast to the 200 K local ΔT , which demonstrated good agreement with thermal runaway for isolated 0-D reactors in Fig. 3. The combination of 0-D and 1-D simulations of τ_{ign} indicate the validity of describing autoignition in the most reactive mixture occurring at $\phi = 0.27$ and a set level of Y_{OH} . Additionally, the metrics of $Y_{\text{OH}} = 2 \times 10^{-4}$ and $\Delta T_{\text{coflow}} = 10$ K, which have both been used for correlation with the minimum threshold of CH^* chemiluminescence in simple hydrocarbon flames [10,32,34–36], are in very good agreement with each other for both the 0-D and 1-D flames but are not in agreement with the other metrics or the DNS findings.

Figures 5a–5c show results of the 2-D simulation of the diluted C_2H_4 fuel jet with a hot-air coflow. These figures show the characteristics of the coflow flames to complement the 0-D and 1-D simulations. Figure 5a shows isocontours of ϕ and Y_{OH} . These contour lines are overlaid on the shaded region of $T \geq T_{\text{coflow}} + \Delta T_{\text{coflow}}$; that is, $T \geq 1560$ K. This is adjacent to Figs. 5b and 5c, which show contours of the formaldehyde CH_2O mass fraction ($Y_{\text{CH}_2\text{O}}$), which is an important combustion precursor species for flame stabilization in hot coflows [4,13,14,20]; and the magnitude of the temperature gradient vector ($|\nabla T|$), respectively. The ignition point is defined as the intersection of the isocontours $\phi = 0.27$ and $Y_{\text{OH}} = 2 \times 10^{-3}$, as previously identified in the 0-D simulation. This intersection is marked in Fig. 5a, and it is the most upstream point on the $Y_{\text{OH}} = 2 \times 10^{-3}$ isocontour, which supports the choice of this location as the flame ignition point. This point is located 0.28 mm downstream of the inlet boundary, corresponding to τ_{ign} of 0.028 ms after normalization by the bulk flow velocity. This is in reasonably good agreement with the 0.030–0.032 ms from the 0-D simulations; however, it is somewhat less than the 0.038 ms predicted by the 1-D flame. This is due to the equal and parallel inlet velocities, eliminating velocity-induced strain between the fuel and oxidant. These results support the use of simple 0-D reactors, rather than 1-D simulations, for the initial estimation of ignition delay in non-premixed systems with low velocity-induced strain rates.

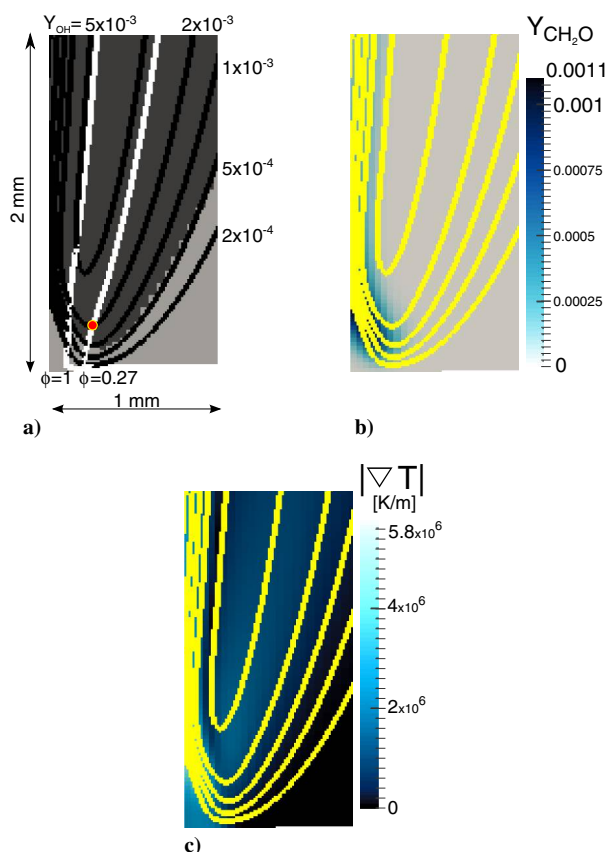


Fig. 5 Contours of a 2-D ethylene flame with high-temperature air coflow.

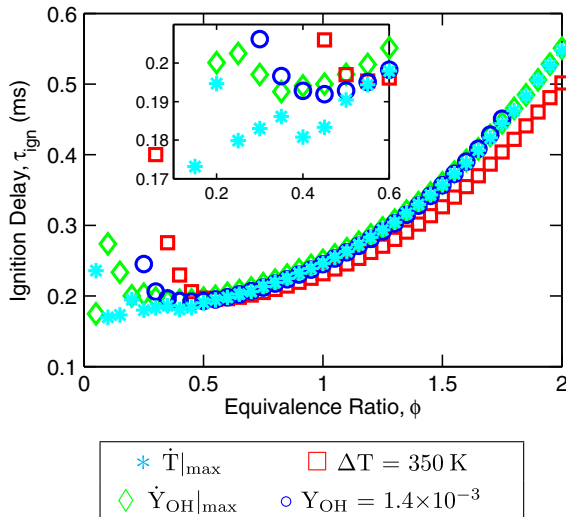
The identified ignition point corresponds to a region of high $|\nabla T|$, shown in Fig. 5c. This gradient of the T contour closely follows the shape of the $Y_{\text{OH,max}}$ contours on the lean side of the flame. The most upstream location of $T \geq T_{\text{coflow}} + \Delta T_{\text{coflow}}$ indicates a τ_{ign} of 0.015 ms and correlates to rapid consumption of the CH_2O precursor species and significant heat release. This point is in good agreement with τ_{ign} based on ΔT_{coflow} , which is evaluated in the 0-D simulations. This demonstrates a gradual temperature rise associated with precursor buildup before thermal runaway is observed in the 0-D simulations downstream. This phenomenon indicates that this system features two distinct metrics that may be taken as autoignition delay: one associated with a global temperature rise (ΔT_{coflow}) and the other associated with thermal runaway ($\dot{T}|_{\text{max}}$), located by a combination of ϕ and a chosen Y_{OH} .

B. Ethylene Fuel and 1300-Kelvin Oxidizer with Nine-Percent Oxygen

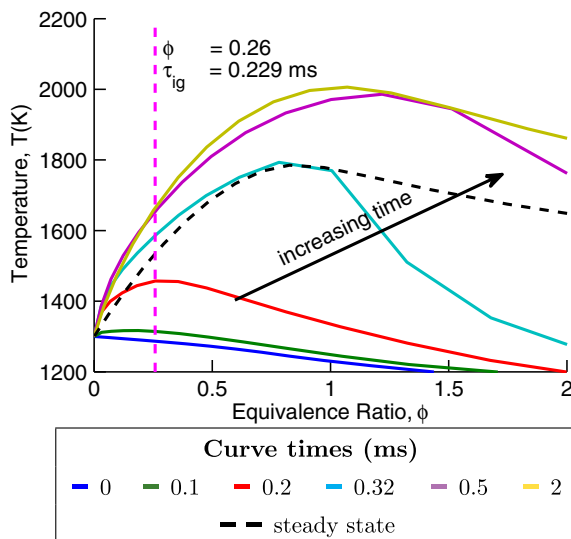
Previous experimental studies of the transition from autoignitive to MILD flames have focused on the liftoff and autoignition of ethylene fuel jet flames [4,18]. The ignition of 300 K ethylene and hot combustion products with 9% O_2 at 1300 K has previously been assessed to belong to the autoignitive flame regime, experimentally appearing as a lifted flame [18]. Calculated ignition delays for this case are shown in Figs. 6a and 6b for 0- and 1-D simulations, respectively. The analysis of the 0-D simulations shows that, with the exception of ΔT , ignition is predicted in mixtures of $\phi = 0.35 - 0.45$ with τ_{ign} of 0.17–0.19 ms, which is an order of magnitude slower than the diluted ethylene and hot-air flame. Despite the poor agreement between $\Delta T = 350$ K and the time derivative at low and high ϕ , this choice of ΔT best follows the shape of the $\dot{T}|_{\text{max}}$ and $\dot{Y}_{\text{OH}}|_{\text{max}}$ curves near the minimum τ_{ign} . The scalar value of $Y_{\text{OH}} = 1.4 \times 10^{-3}$, however, demonstrates a superior estimation of τ_{ign} , reasonably following the profile of \dot{Y}_{OH} for $0.30 \leq \phi \leq 1.75$. The scatter seen in very lean mixtures, approximately $\phi < 0.25$ in this case, is due to very gradual ignition processes, which do not have distinct ignition events. Under these circumstances, the detection of ignition by either $\dot{T}|_{\text{max}}$ or \dot{Y}_{OH} is very sensitive to numerical differentiation with respect to time. Points in this region are not of significant interest, as they are too lean, and not sufficiently reactive, to result in combustion. Figure 6a repeats the absence of a Y_{OH} threshold for high ϕ , previously observed in Fig. 3, as the required concentrations of OH are not produced during ignition. Additionally, the disagreement between $\dot{T}|_{\text{max}}$ and all other measures becomes significant for $\phi < 0.5$, where the four different metrics deviate significantly. This corresponds to a less rapid temperature increase after the initial precursor buildup during the OH production phase. This is the result of a two-stage ignition process where the maximum production rate of OH no longer occurs at the same time as $\dot{T}|_{\text{max}}$. This has the effect of shifting the peaks of \dot{T} and \dot{Y}_{OH} away from each other in very lean mixtures but does not have a significant impact on the minimum ignition delay time.

The value of τ_{ign} predicted by the 1-D flame, shown in Fig. 6b, is significantly longer than evaluated in the 0-D analysis. This figure indicates a slow initial reaction followed by thermal runaway after 0.23 ms, after which the system approaches steady-state temperatures. This is indicative of the “transitional behavior” previously seen in ethylene flames in 1100 K coflows with 9% O_2 [4]. In this case, thin regions of OH are recorded upstream of the visible, strongly reacting the flame base [4]. In both this intermediate 1-D flame and the diluted ethylene/hot-air flame, ignition occurs at $\phi \approx 0.25$ in accordance with the Y_{OH} threshold metric matched to the peak \dot{Y}_{OH} . In contrast, the ΔT criterion (not shown graphically) indicates ignition at $\phi = 0.47$ for the 9% O_2 case and 0.20 for the diluted ethylene/hot-air flame. This is consistent with the disparity noticed in the 0-D analysis of the 9% O_2 case, presented in Fig. 6a, where the ΔT metric also predicts ignition at higher values of ϕ . Significantly, this indicates the peak threshold of Y_{OH} occurs significantly later than the rise in temperature rather than being equivalent markers of ignition as the flame approaches MILD conditions.

The values of τ_{ign} from 0-D and 1-D simulations are summarized in Table 3. This table displays the good agreement between $Y_{\text{OH}} = 2 \times 10^{-4}$ and $\Delta T_{\text{coflow}} = 10$ K between the two different reactors.



a) Ignition delay from 0-D simulations, with τ_{ign} defined by four different criteria over a range of equivalence ratios



b) Transient temperatures from a 1-D simulation; strain rate $\approx 60 \text{ s}^{-1}$. The dashed vertical line represents ignition according to the criterion $Y_{\text{OH}} = 1 \times 10^{-3}$

Fig. 6 Zero- and one-dimensional analyses of ignition delay of ethylene at 300 K and combustion products with 9% O_2 at 1300 K.

This indicates that these metrics are resistant to the effects of strain and heat transfer, which is inherent in the 1-D flame but absent in the isolated 0-D reactors. These values may be compared to experi-

Table 3 Ignition delay τ_{ign} corresponding to different combustion criteria in different fundamental reactors with streams of ethylene at 300 K and combustion products with 9% O_2 at 1300 K

Criterion	0-D batch reactor $\tau_{\text{ign}}, \text{ms}$	1-D opposed flame $\tau_{\text{ign}}, \text{ms}$
$\dot{T} _{\text{max}}^a$	0.17	N/A
$\dot{Y}_{\text{OH}} _{\text{max}}$	0.19	N/A
$Y_{\text{OH}} = 1.4 \times 10^{-3}$	0.19	0.23
$Y_{\text{OH}} = 2 \times 10^{-4b}$	0.14	0.16
$\Delta T = 350 \text{ K}$	0.20	0.26
$\Delta T_{\text{coflow}} = 10 \text{ K}^c$	0.092	0.098

^aPreviously published metric [20,31].

^bPreviously published metric [10,32].

^cPreviously published metric [35,36].

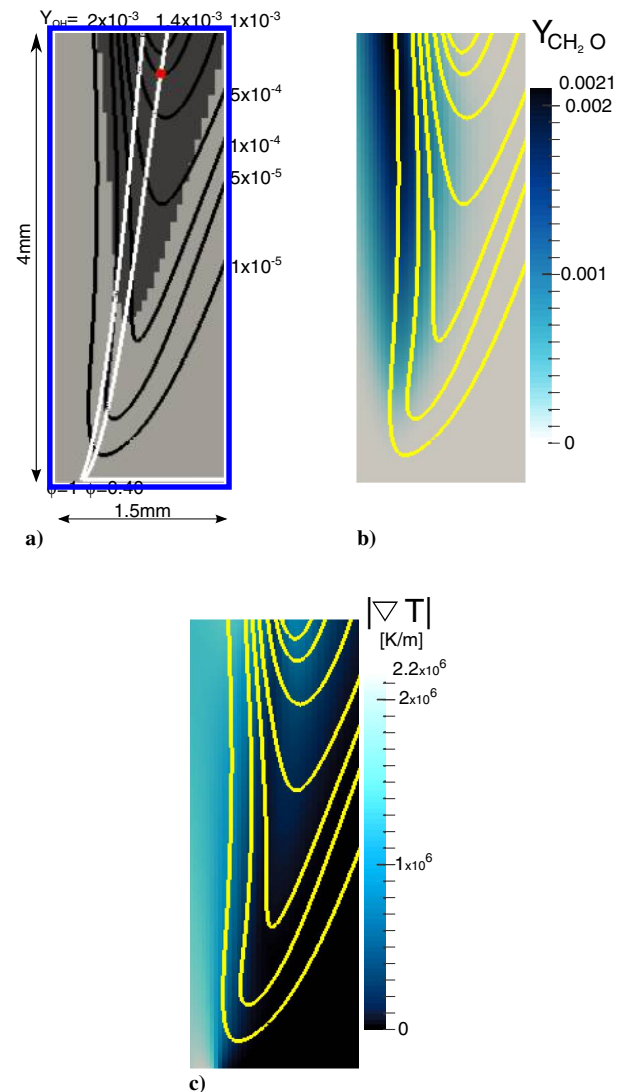
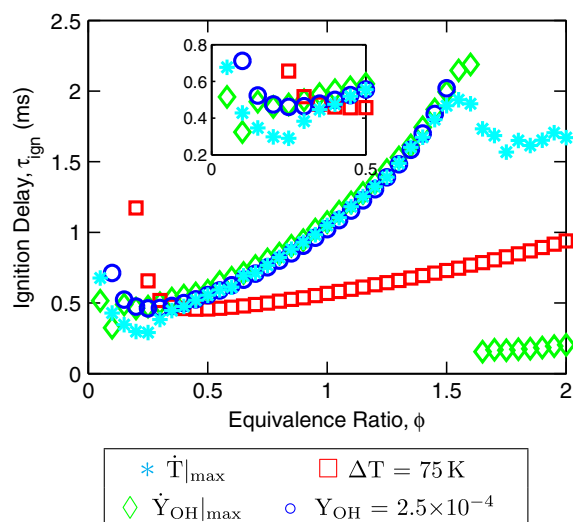


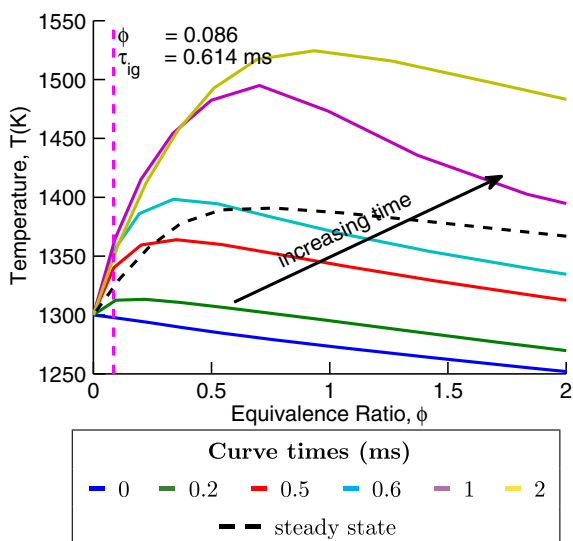
Fig. 7 Contours of a 2-D ethylene flame with a 1300 K coflow with 9% O_2 .

mentally observed liftoff heights based on CH^* measurements [18] after normalization by the bulk jet velocity through Eq. (2). The ignition delay defined by CH^* in the experimental flame ranges between 0.17 to 0.22 ms [18]. It is evident from Table 3 that the time-derivative-based metrics derived from temperature and Y_{OH} are both able to provide estimations of time for the minimum visual liftoff seen experimentally. Noticeably, however, there is a significant difference between the ΔT_{coflow} and the $Y_{\text{OH}} = 2 \times 10^{-4}$ thresholds, which have both previously been proposed as locations for the minimum CH^* threshold [10,32,35,36]. The best agreement between the metrics and experimental observation in either reactor, is given by the $Y_{\text{OH}} = 1.4 \times 10^{-3}$ criterion chosen to match $\dot{T}|_{\text{max}}$ for ϕ near one.

Figures 7a–7c show results from a 2-D simulation of the ethylene fuel and 9% O_2 oxidant in a non-premixed coflowing configuration. The figures present isocontours of Y_{OH} plotted with lines of constant ϕ and contours of $\Delta T_{\text{coflow}} = 10 \text{ K}$, $Y_{\text{CH}_2\text{O}}$ and $|VT|$, respectively. The intersection of the lines $\phi = 0.4$ and $Y_{\text{OH}} = 1.4 \times 10^{-3}$ occurs 3.7 mm downstream of the inlets. This region is associated with a high-temperature gradient that, unlike the temperature gradients in Fig. 5c, does not follow the contours of Y_{OH} . The disparity between the temperature gradients and contours of Y_{OH} is similar to the diverging trends at ignition noted in Fig. 6a, in contrast to the exceptional agreement between criteria in Fig. 3. In Fig. 7a, the first temperature increase of $\Delta T_{\text{coflow}} = 10 \text{ K}$ initiates in a richer mixture than predicted in 0-D simulations, 1.6 mm downstream of the domain inlets. This indicates an ignition delay of 0.16 ms, which is in very good agreement with the minimum value of observed visual liftoff corresponding to 0.17 ms [18]. These correlations support the global



a) Ignition delay from 0-D simulations, with τ_{ign} defined by four different criteria over a range of equivalence ratios.



b) Transient temperatures from a 1-D simulation; strain rate $\approx 60 \text{ s}^{-1}$. The dashed vertical line represents ignition according to the criterion $Y_{\text{OH}} = 2.5 \times 10^{-4}$

Fig. 8 Zero- and one-dimensional analyses of ignition delay of ethylene at 300 K and combustion products with 3% O_2 at 1300 K.

temperature increase definition of ignition as a measure of the chemiluminescent flame base [34] in preference to a Y_{OH} threshold [10]. The increase in temperature occurs far upstream of the 0-D defined ignition point without significant $|\nabla T|$, in accordance to the arrested temperature increase in the 0-D simulations. The combined contours indicate that the initial less-intense ignition reactions occur shortly following the presence of CH_2O into the lean mixture, beyond which the first instance of autoignition flame occurs.

C. Ethylene Fuel and 1300-Kelvin Oxidizer with Three-Percent Oxygen

Turbulent jet flames in hot coflows with as little as 3% O_2 have been studied extensively as examples of MILD combustion [4,6,9,13,18–20,22,28]. This classification has been based on low maximum temperatures in stoichiometric 0-D simulations [1], combustion without the presence of sudden extinction conditions [7], and experimental observations of very faint flames with indistinct flame bases [4,9,18]. Figures 8a and 8b show the ignition of ethylene

and combustion products with 3% O_2 at 1300 K in 0-D and 1-D simulations. Figure 8a shows good agreement between the two time-derivative-based metrics and the scalar criterion $Y_{\text{OH}} = 2.5 \times 10^{-4}$ over most of the ϕ domain, centered near $\phi = 1$. The mass fraction of Y_{OH} does not reach 2.5×10^{-4} within a 100 ms simulation time, for rich and very lean 0-D reactors. The \dot{T}_{max} , $\dot{Y}_{\text{OH}|_{\text{max}}}$, and Y_{OH} ignition criteria result in τ_{ign} of 0.29–0.46 ms across a range of ϕ from 0.1 to 0.25. In these simulations, the \dot{T}_{max} criterion exhibits a minimum range for τ_{ign} and a plateau above $\phi \geq 1.5$. The $\Delta T = 75 \text{ K}$ metric predicts smooth changes in τ_{ign} over the entire range; although it exhibits a significantly flatter curve than the other τ_{ign} criteria and overpredicts ϕ at ignition. This is consistent with similar features observed in Fig. 6a, indicating that local values of ΔT demonstrate deteriorating agreement with \dot{T}_{max} and $\dot{Y}_{\text{OH}|_{\text{max}}}$ profiles in the transition to MILD combustion.

Transient temperature profiles from a 1-D simulation of ethylene with a 3% O_2 oxidant at 1300 K are shown in Fig. 8b. This plot indicates a very slow, lean ignition after 0.614 ms at $\phi = 0.086$. This is both significantly slower and leaner than predictions from the 0-D analysis. The temperature profiles, additionally, increase steadily with a less well-defined ignition location or time of thermal runaway. This is in agreement with the relatively flat τ_{ign} versus ϕ curve indicated by the ΔT in the 0-D analysis. The temperature increases in the 1-D flame are more distributed than in the isolated 0-D reactors, due to diffusion between different local mixture fractions over timescales on the order of τ_{ign} , which blurs the standard definition of combustion. These features are consistent with MILD combustion being defined as distributed reactions without distinct ignition or extinction conditions [7]. The rate of temperature increase in this condition is not homogeneous; however, the transient solution tends toward an almost uniform temperature at steady state. At steady state, there is a less than 50 K difference between any mixtures in the range $0.20 \leq \phi \leq 4.25$.

Measures of autoignition in this flame and the corresponding 0-D reactor are summarized in Table 4. This table summarizes the relevant ignition metrics for fuel and oxidant streams of ethylene at 300 K and combustion products with 3% O_2 at 1300 K, respectively. Noticeably, there is poor agreement between the 0-D and 1-D values of τ_{ign} as defined by $Y_{\text{OH}} = 2 \times 10^{-4}$ and $\Delta T_{\text{coflow}} = 10 \text{ K}$, which was not seen in the previous cases. These values may additionally be compared to the experimental observation of a strong CH^* transition, normalized to τ_{ign} of 0.44 ms using Eq. (2) after an extended, faint flame base [18]. This experimental value is in very good agreement with the 0-D prediction of $\dot{Y}_{\text{OH}|_{\text{max}}}$ (taking the minimum of the continuous curve), $Y_{\text{OH}} = 2.5 \times 10^{-4}$, and $\Delta T = 75 \text{ K}$. The experimental value is, however, significantly greater than the time of \dot{T}_{max} , which was not observed for the previous cases and indicates significant reactions occurring before this transition point. In this regard, the $\dot{Y}_{\text{OH}|_{\text{max}}}$ metric appears to be a more appropriate measure of ignition than \dot{T}_{max} in a 0-D reactor for the prediction of experimentally observed liftoff or ignition transition. The best agreement between the metrics and experimental observation, in either simulation, is similar to the 9% O_2 case, given by the minimum in the curve of Y_{OH} chosen to match \dot{T}_{max} for mixtures near stoichiometry.

Table 4 Ignition delay τ_{ign} corresponding to different combustion criteria in different fundamental reactors with streams of ethylene at 300 K and combustion products with 3% O_2 at 1300 K

Criterion	0-D batch reactor τ_{ign} , ms	1-D opposed flame τ_{ign} , ms
\dot{T}_{max}^a	0.29	N/A
$\dot{Y}_{\text{OH} _{\text{max}}}$	0.32 ^a	N/A
$Y_{\text{OH}} = 2.5 \times 10^{-4}$	0.46	0.61
$Y_{\text{OH}} = 2 \times 10^{-4}$ ^b	0.43	0.55
$\Delta T = 75 \text{ K}$	0.46	0.47
$\Delta T_{\text{coflow}} = 10 \text{ K}^c$	0.30	0.19

^aPreviously published metric [20,31].

^bPreviously published metric [10,32].

^cPreviously published metric [35,36].

^dThis point at $\phi = 0.10$ lies below the curve predicting τ_{ign} of 0.46 ms.

Figures 9a–9c show results from a 2-D simulation of the ethylene fuel and 3% O₂ oxidant in a non-premixed coflowing configuration. These images show significant similarities to those in Figs. 7a and 7b; however, they indicate much weaker reactions before autoignition. These figures clearly show the broadened reaction zone predicted under MILD conditions with decreasing O₂ levels [6]. Figure 9a demonstrates a further shift of $T \geq T_{\text{coflow}} + \Delta T_{\text{coflow}}$ away from the Y_{OH} isocontours in comparison to previous cases. In this case, the initial ignition point defined by $T \geq T_{\text{coflow}} + \Delta T_{\text{coflow}}$ lies on $\phi = 0.5$, with the most upstream point of the nearest Y_{OH} isocontour initiating at $\phi = 0.15$. These values of ϕ are not in good agreement with the predictions from the 0-D and 1-D models, with ignition in the 2-D simulation occurring under richer conditions. This flame exhibits a slow OH production before the initial location of $T \geq T_{\text{coflow}} + \Delta T_{\text{coflow}}$ without, however, a significant increase in temperature gradient, seen in Fig. 9c. This could be indicative of the MILD reaction zone, with fuel conversion without a strong flame front. Finally, the autoignition delay defined by the liftoff height defined by $\Delta T_{\text{coflow}} = 10$ K is 0.42 ms. This is in very good agreement with the first region of strong CH* occurring after approximately 0.44 ms in experimental flames with the same stream compositions [18]. This would indicate a visible flame front in regions where $Y_{\text{OH}} > 2 \times 10^{-3}$, which has previously been used as a lower limit for an autoigniting, lifted flame [10,32]. This OH threshold, like the previously defined threshold of $Y_{\text{OH}} = 2.5 \times 10^{-4}$, does not however occur at any point within the computational domain, whereas the

presence of both OH and CH₂O indicates flameless combustion well below the visible, or thermal, flame base.

IV. Conclusions

Criteria for ignition in autoignitive and MILD flames have been compared in simplified reactors, using the metrics of temperature rise (local ΔT and ΔT_{coflow}) and Y_{OH} and their time derivatives \dot{T} and \dot{Y}_{OH} . These different criteria were assessed as markers of ignition in simplified simulations of autoignitive and MILD flames. Good agreement was seen in the case of an autoignitive, diluted ethylene flame with a hot-air oxidant between all the different metrics in 0-D batch reactor simulations. In contrast, there were significant disparities in the local ΔT metric and the other criteria for the autoignitive ethylene flame with 9% O₂ oxidant, as well as MILD ethylene flame with 3% O₂ oxidant. In these reduced O₂ cases, the use of \dot{T} and \dot{Y}_{OH} as an ignition metric was not suitable for predicting τ_{ign} in very lean mixtures. The slower, more uniform temperature increase of the MILD flame, however, resulted in the prediction of a very lean, most reactive ϕ and much slower τ_{ign} .

Matching a threshold value of Y_{OH} to thermal runaway for ϕ near one provided a good estimate of τ_{ign} in the most reactive fuel and oxidant mixture in each case. Extension of the simulations to two-dimensional laminar simulations demonstrated that the 0-D analysis could identify an appropriate flame base for an autoignitive ethylene flame in heated air based on a Y_{OH} threshold and ϕ . Such agreement was not seen in a similar analysis of ethylene flames in, or in the transition to, the MILD combustion regime with 3 or 9% O₂ oxidants. In these two cases, the point where $\Delta T_{\text{coflow}} = 10$ K demonstrated good agreement with the visual liftoff and transition based on previous CH* measurements.

The results promote the use of a Y_{OH} threshold, matched to \dot{Y}_{OH} for ϕ near one, to predict τ_{ign} through analysis of a series of 0-D batch reactors. Additionally, a 10 K increase above the coflow temperature is shown to be a more appropriate marker of chemiluminescence in a two-dimensional laminar diffusion flame. The results indicate the appropriateness of these ignition metrics for comparison between simulations and experimentally observed flame bases of turbulent autoignitive or MILD jet flames.

Acknowledgments

The authors wish to acknowledge the support of the Centre for Energy Technology, eResearch SA, the University of Adelaide, and the Politecnico di Milano. The authors acknowledge funding support from the Australian Research Council through the Discovery Project (DP) and Discovery Early Career Researcher Award (DECRA) grant scheme, the U.S. Asian Office for Aerospace Research and Development, and the Australian-Government-funded Endeavour Scholarships and Fellowship grant program.

References

- [1] Cavaliere, A., and de Joannon, M., "Mild Combustion," *Progress in Energy and Combustion Science*, Vol. 30, No. 4, 2004, pp. 329–366. doi:10.1016/j.pecs.2004.02.003
- [2] Wünnig, J. A., and Wünnig, J. G., "Flameless Oxidation to Reduce Thermal NO-Formation," *Progress in Energy and Combustion Science*, Vol. 23, No. 1, 1997, pp. 81–94. doi:10.1016/S0360-1285(97)00006-3
- [3] Dally, B., Riesmeier, E., and Peters, N., "Effect of Fuel Mixture on Moderate and Intense Low Oxygen Dilution Combustion," *Combustion and Flame*, Vol. 137, No. 4, 2004, pp. 418–431. doi:10.1016/j.combustflame.2004.02.011
- [4] Medwell, P. R., Kalt, P. A. M., and Dally, B. B., "Imaging of Diluted Turbulent Ethylene Flames Stabilized on a JET in Hot Coflow (JHC) Burner," *Combustion and Flame*, Vol. 152, Nos. 1–2, 2008, pp. 100–113. doi:10.1016/j.combustflame.2007.09.003
- [5] de Joannon, M., Sabia, P., Sorrentino, G., and Cavaliere, A., "Numerical Study of Mild Combustion in Hot Diluted Diffusion Ignition (HDDI) Regime," *Proceedings of the Combustion Institute*, Vol. 32, No. 2, 2009, pp. 3147–3154. doi:10.1016/j.proci.2008.09.003

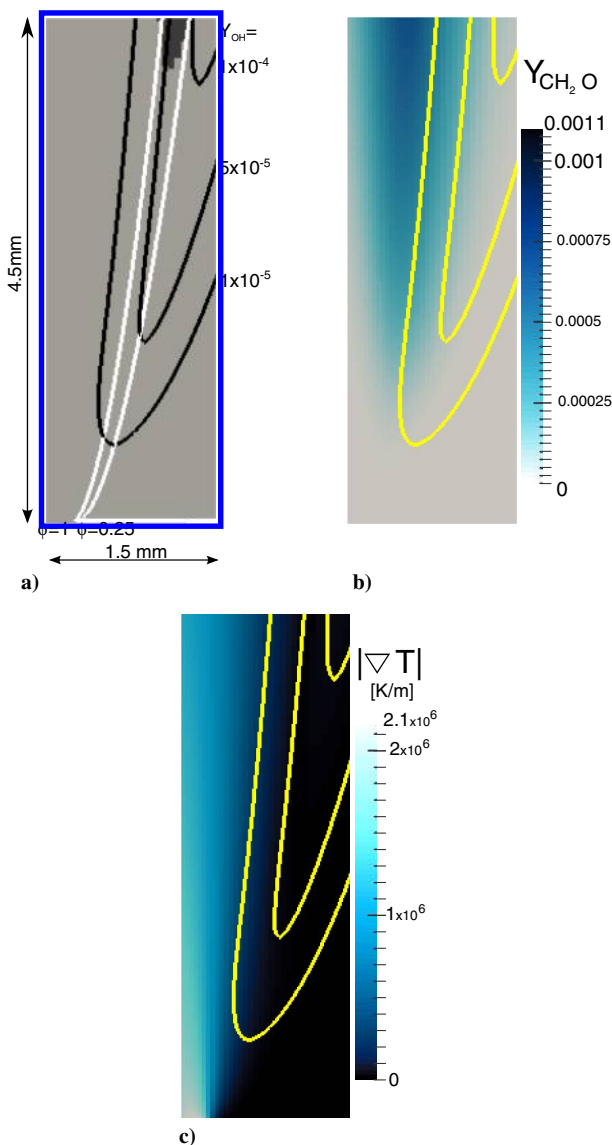


Fig. 9 Contours of a 2-D ethylene flame with a 1300 K coflow with 3% O₂.

- [6] Medwell, P. R., Kalt, P. A. M., and Dally, B. B., "Reaction Zone Weakening Effects Under Hot and Diluted Oxidant Stream Conditions," *Combustion Science and Technology*, Vol. 181, No. 7, 2009, pp. 937–953.
doi:10.1080/00102200902904138
- [7] Oberlack, M., Arlitt, R., and Peters, N., "On Stochastic Damkohler Number Variations in a Homogeneous Flow Reactor," *Combustion Theory and Modelling*, Vol. 4, No. 4, 2000, pp. 495–509.
doi:10.1088/1364-7830/4/4/307
- [8] Rao, A. G., and Levy, Y. A., "New Combustion Methodology for Low Emission Gas Turbine Engines," *8th International Symposium on High Temperature Air Combustion and Gasification*, Poznań Univ. of Technology, Poznań, Poland, 2010, pp. 177–185.
- [9] Dally, B., Karpetsis, A., and Barlow, R., "Structure of Turbulent Non-Premixed Jet Flames in a Diluted Hot Coflow," *Proceedings of the Combustion Institute*, Vol. 29, No. 1, 2002, pp. 1147–1154.
doi:10.1016/S1540-7489(02)80145-6
- [10] Cabra, R., Myhrvold, T., Chen, J., Dibble, R., Karpetsis, A., and Barlow, R., "Simultaneous Laser Raman-Rayleigh-Lif Measurements and Numerical Modeling Results of a Lifted Turbulent H₂/N₂ Jet Flame in a Vitiated Coflow," *Proceedings of the Combustion Institute*, Vol. 29, No. 2, 2002, pp. 1881–1888.
doi:10.1016/S1540-7489(02)80228-0
- [11] Cabra, R., Chen, J.-Y., Dibble, R., Karpetsis, A., and Barlow, R., "Lifted Methane-Air Jet Flames in a Vitiated Coflow," *Combustion and Flame*, Vol. 143, No. 4, 2005, pp. 491–506.
doi:10.1016/j.combustflame.2005.08.019
- [12] Chung, S., "Stabilization, Propagation and Instability of Tribraichal Triple Flames," *Proceedings of the Combustion Institute*, Vol. 31, No. 1, 2007, pp. 877–892.
doi:10.1016/j.proci.2006.08.117
- [13] Medwell, P. R., Kalt, P. A. M., and Dally, B. B., "Simultaneous Imaging of OH, Formaldehyde, and Temperature of Turbulent Nonpremixed Jet Flames in a Heated and Diluted Coflow," *Combustion and Flame*, Vol. 148, Nos. 1–2, 2007, pp. 48–61.
doi:10.1016/j.combustflame.2006.10.002
- [14] Gordon, R. L., Masri, A. R., and Mastorakos, E., "Simultaneous Rayleigh Temperature, OH- and CH₂O-LIF Imaging of Methane Jets in a Vitiated Coflow," *Combustion and Flame*, Vol. 155, Nos. 1–2, 2008, pp. 181–195.
doi:10.1016/j.combustflame.2008.07.001
- [15] Mastorakos, E., "Ignition of Turbulent Non-Premixed Flames," *Progress in Energy and Combustion Science*, Vol. 35, No. 1, 2009, pp. 57–97.
doi:10.1016/j.pecs.2008.07.002
- [16] Choi, B., and Chung, S., "Autoignited Laminar Lifted Flames of Methane, Ethylene, Ethane, and N-Butane Jets in Coflow Air with Elevated Temperature," *Combustion and Flame*, Vol. 157, No. 12, 2010, pp. 2348–2356.
doi:10.1016/j.combustflame.2010.06.011
- [17] Arndt, C., Gounder, J., Meier, W., and Aigner, M., "Auto-Ignition and Flame Stabilization of Pulsed Methane Jets in a Hot Vitiated Coflow Studied with High-Speed Laser and Imaging Techniques," *Applied Physics B*, Vol. 108, No. 2, 2012, pp. 407–417.
doi:10.1007/s00340-012-4945-5
- [18] Medwell, P. R., and Dally, B. B., "Experimental Observation of Lifted Flames in a Heated and Diluted Coflow," *Energy Fuels*, Vol. 26, No. 9, 2012, pp. 5519–5527.
doi:10.1021/ef301029u
- [19] Arndt, C. M., Schießl, R., Gounder, J. D., Meier, W., and Aigner, M., "Flame Stabilization and Auto-Ignition of Pulsed Methane Jets in a Hot Coflow: Influence of Temperature," *Proceedings of the Combustion Institute*, Vol. 34, No. 1, 2013, pp. 1483–1490.
doi:10.1016/j.proci.2012.05.082
- [20] Medwell, P. R., Blunck, D. L., and Dally, B. B., "The Role of Precursors on the Stabilisation of Jet Flames Issuing Into a Hot Environment," *Combustion and Flame*, Vol. 161, No. 2, 2014, pp. 465–474.
doi:10.1016/j.combustflame.2013.08.028
- [21] Papageorge, M., Arndt, C., Fuest, F., Meier, W., and Sutton, J., "High-Speed Mixture Fraction and Temperature Imaging of Pulsed, Turbulent Fuel Jets Auto-Igniting in High-Temperature, Vitiated Co-Flows," *Experiments in Fluids*, Vol. 55, No. 7, 2014, Paper 1763.
doi:10.1007/s00348-014-1763-z
- [22] Sidey, J., and Mastorakos, E., "Visualization of MILD Combustion From Jets in Cross-Flow," *Proceedings of the Combustion Institute*, Vol. 35, No. 3, 2015, pp. 3537–3545.
doi:10.1016/j.proci.2014.07.028
- [23] Lu, T. F., Yoo, C. S., Chen, J. H., and Law, C. K., "Three-Dimensional Direct Numerical Simulation of a Turbulent Lifted Hydrogen Jet Flame in Heated Coflow: A Chemical Explosive Mode Analysis," *Journal of Fluid Mechanics*, Vol. 652, June 2010, pp. 45–64.
doi:10.1017/S002211201000039X
- [24] Yoo, C. S., Richardson, E. S., Sankaran, R., and Chen, J. H., "A DNS Study on the Stabilization Mechanism of a Turbulent Lifted Ethylene Jet Flame in Highly-Heated Coflow," *Proceedings of the Combustion Institute*, Vol. 33, No. 1, 2011, pp. 1619–1627.
doi:10.1016/j.proci.2010.06.147
- [25] Luo, Z., Yoo, C. S., Richardson, E. S., Chen, J. H., Law, C. K., and Lu, T., "Chemical Explosive Mode Analysis for a Turbulent Lifted Ethylene Jet Flame in Highly-Heated Coflow," *Combustion and Flame*, Vol. 159, No. 1, 2012, pp. 265–274.
doi:10.1016/j.combustflame.2011.05.023
- [26] Göktolga, M. U., van Oijen, J. A., and de Goey, L. P. H., "3D DNS of MILD Combustion: A Detailed Analysis of Heat Loss Effects, Preferential Diffusion, and Flame Formation Mechanisms," *Fuel*, Vol. 159, Nov. 2015, pp. 784–795.
doi:10.1016/j.fuel.2015.07.049
- [27] Oldenhof, E., Tummers, M. J., van Veen, E. H., and Roekaerts, D. J. E. M., "Ignition Kernel Formation and Lift-Off Behaviour of Jet-in-Hot-Coflow Flames," *Combustion and Flame*, Vol. 157, No. 6, 2010, pp. 1167–1178.
doi:10.1016/j.combustflame.2010.01.002
- [28] Christo, F. C., and Dally, B. B., "Application of Transport PDF Approach for Modelling MILD Combustion," *Proceedings of the Fifteenth Australian Fluid Mechanics Conference*, Univ. of Sydney, Sydney, NSW, Australia, Dec. 2004.
- [29] Mardani, A., Tabejamaat, S., and Ghamari, M., "Numerical Study of Influence of Molecular Diffusion in the Mild Combustion Regime," *Combustion Theory and Modelling*, Vol. 14, No. 5, 2010, pp. 747–774.
doi:10.1080/13647830.2010.512959
- [30] Galletti, C., Parente, A., and Tognotti, L., "Numerical and Experimental Investigation of a Mild Combustion Burner," *Combustion and Flame*, Vol. 151, No. 4, 2007, pp. 649–664.
doi:10.1016/j.combustflame.2007.07.016
- [31] Echehki, T., and Chen, J. H., "Direct Numerical Simulation of Auto-ignition in Non-Homogeneous Hydrogen-Air Mixtures," *Combustion and Flame*, Vol. 134, No. 3, 2003, pp. 169–191.
doi:10.1016/S0010-2180(03)00088-9
- [32] Cao, R. R., Pope, S. B., and Masri, A. R., "Turbulent Lifted Flames in a Vitiated Coflow Investigated Using Joint PDF Calculations," *Combustion and Flame*, Vol. 142, No. 4, 2005, pp. 438–453.
doi:10.1016/j.combustflame.2005.04.005
- [33] de Joannon, M., Saponaro, A., and Cavaliere, A., "Zero-Dimensional Analysis of Diluted Oxidation of Methane in rich Conditions," *Proceedings of the Combustion Institute*, Vol. 28, No. 2, 2000, pp. 1639–1646.
doi:10.1016/S0082-0784(00)80562-7
- [34] de Joannon, M., Cavaliere, A., Donnarumma, R., and Ragucci, R., "Dependence of Autoignition Delay on Oxygen Concentration in Mild Combustion of High Molecular Weight Paraffin," *Proceedings of the Combustion Institute*, Vol. 29, No. 1, 2002, pp. 1139–1146.
doi:10.1016/S1540-7489(02)80144-4
- [35] Sabia, P., de Joannon, M., Picarelli, A., Chinnici, A., and Ragucci, R., "Modeling Negative Temperature Coefficient Region in Methane Oxidation," *Fuel*, Vol. 91, No. 1, 2012, pp. 238–245.
doi:10.1016/j.fuel.2011.07.026
- [36] Sabia, P., de Joannon, M., Picarelli, A., and Ragucci, R., "Methane Auto-Ignition Delay Times and Oxidation Regimes in MILD Combustion at Atmospheric Pressure," *Combustion and Flame*, Vol. 160, No. 1, 2013, pp. 47–55.
doi:10.1016/j.combustflame.2012.09.015
- [37] Kee, R. J., Dixon-Lewis, G., Warnatz, J., Coltrin, M. E., and Miller, J. A., *A Fortran Computer Code Package for the Evaluation of Gas-Phase, Multicomponent Transport Properties*, Sandia National Labs. Rept. SAND86-8246, Livermore, CA, 1988.
- [38] Ranzi, E., Frassoldati, A., Grana, R., Cuoci, A., Faravelli, T., Kelley, A., and Law, C., "Hierarchical and Comparative Kinetic Modeling of Laminar Flame Speeds of Hydrocarbon and Oxygenated Fuels," *Progress in Energy and Combustion Science*, Vol. 38, No. 4, 2012, pp. 468–501.
doi:10.1016/j.pecs.2012.03.004
- [39] Stagni, A., Cuoci, A., Frassoldati, A., Faravelli, T., and Ranzi, E., "Lumping and Reduction of Detailed Kinetic Schemes: An Effective Coupling," *Industrial and Engineering Chemistry Research*, Vol. 53, No. 22, 2013, pp. 9004–9016.
doi:10.1021/ie403272f
- [40] Cuoci, A., Frassoldati, A., Faravelli, T., and Ranzi, E., "Formation of Soot and Nitrogen Oxides in Unsteady Counterflow Diffusion Flames,"

- Combustion and Flame*, Vol. 156, No. 10, 2009, pp. 2010–2022.
doi:10.1016/j.combustflame.2009.06.023
- [41] Cuoci, A., Frassoldati, A., Faravelli, T., and Ranzi, E., “OpenSMOKE+: An Object-Oriented Framework for the Numerical Modeling of Reactive Systems with Detailed Kinetic Mechanisms,” *Computer Physics Communications*, Vol. 192, July 2015, pp. 237–264.
doi:10.1016/j.cpc.2015.02.014
- [42] Cuoci, A., Frassoldati, A., Faravelli, T., and Ranzi, E., “A Computational Tool for the Detailed Kinetic Modeling of Laminar Flames: Application to C₂H₄/CH₄ Coflow Flames,” *Combustion and Flame*, Vol. 160, No. 5, 2013, pp. 870–886.
doi:10.1016/j.combustflame.2013.01.011
- [43] Cuoci, A., Frassoldati, A., Faravelli, T., and Ranzi, E., “Numerical Modeling of Laminar Flames with Detailed Kinetics Based on the Operator-Splitting Method,” *Energy Fuels*, Vol. 27, No. 12, 2013, pp. 7730–7753.
doi:10.1021/ef4016334
- [44] Fisher, E. M., Williams, B. A., and Fleming, J. W., “Determination of the Strain in Counterflow Diffusion Flames From Flow Conditions,” *Proceedings of the Eastern States Section of the Combustion Institute*, Combustion Inst., 1997, pp. 191–194.
- [45] Bilger, R., Stärner, S., and Kee, R., “On Reduced Mechanisms for Methane Air Combustion in Nonpremixed Flames,” *Combustion and Flame*, Vol. 80, No. 2, 1990, pp. 135–149.
doi:10.1016/0010-2180(90)90122-8

J. P. Drummond
Associate Editor

This article has been cited by:

1. Paul R. Medwell, Michael J. Evans, Qing N. Chan, Viswanath R. Katta. 2016. Laminar Flame Calculations for Analyzing Trends in Autoignitive Jet Flames in a Hot and Vitiated Coflow. *Energy & Fuels* . [[CrossRef](#)]

Chapter 7

Modelling Lifted Jet Flames in a Heated Coflow using an Optimised Eddy Dissipation Concept Model

Statement of Authorship

Title of Paper	Modelling Lifted Jet Flames in a Heated Coflow using an Optimised Eddy Dissipation Concept Model
Publication Status	<input checked="" type="checkbox"/> Published <input type="checkbox"/> Accepted for Publication <input type="checkbox"/> Submitted for Publication <input type="checkbox"/> Unpublished and Unsubmitted work written in manuscript style
Publication Details	Evans, MJ , Medwell, PR & Tian, ZF (2015). "Modelling Lifted Jet Flames in a Heated Coflow using an Optimised Eddy Dissipation Concept Model". <i>Combustion Science and Technology</i> , vol 187, no 7, pp 1093–1109.

Principal Author

Name of Principal Author (Candidate)	Michael John Evans
Contribution to the Paper	Designed research concept, planned numerical approach, generation and analysis of all data, interpreted data, wrote manuscript and acted as corresponding author.
Overall percentage (%)	75
Certification:	This paper reports on original research I conducted during the period of my Higher Degree by Research candidature and is not subject to any obligations or contractual agreements with a third party that would constrain its inclusion in this thesis. I am the primary author of this paper.
Signature	<div style="display: flex; justify-content: space-between; align-items: center;"> <div style="text-align: right; font-size: small;"> Digitally signed by Michael Evans Date: 2016.10.18 16:49:54 +10'30' </div> <div style="border-left: 1px solid black; padding-left: 10px;">Date</div> <div style="border-left: 1px solid black; padding-left: 10px;">18-Oct-2016</div> </div>

Co-Author Contributions

By signing the Statement of Authorship, each author certifies that:

- i. the candidate's stated contribution to the publication is accurate (as detailed above);
- ii. permission is granted for the candidate to include the publication in the thesis; and
- iii. the sum of all co-author contributions is equal to 100% less the candidate's stated contribution.

Name of Co-Author	Paul Ross Medwell
Contribution to the Paper	Co-supervised development of the work, helped to evaluate and edit the manuscript.
Signature	<div style="display: flex; justify-content: space-between; align-items: center;"> <div style="text-align: right; font-size: small;"> Paul Medwell Date: 2016.10.18 17:14:26 +10'30' </div> <div style="border-left: 1px solid black; padding-left: 10px;">Date</div> <div style="border-left: 1px solid black; padding-left: 10px;">18-OCT-2016</div> </div>

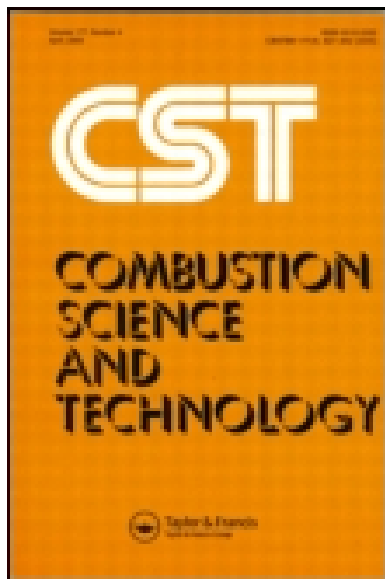
Name of Co-Author	Zhao Feng Tian
Contribution to the Paper	Co-supervised development of the work, helped to evaluate and edit the manuscript.
Signature	<div style="display: flex; justify-content: space-between; align-items: center;"> <div style="text-align: right; font-size: small;"> Digitally signed by Zhao Feng Tian Date: 2016.10.24 12:05:20 +10'30' </div> <div style="border-left: 1px solid black; padding-left: 10px;">Date</div> <div style="border-left: 1px solid black; padding-left: 10px;">24-Oct-2016</div> </div>

This article was downloaded by: [171.66.208.10]

On: 14 April 2015, At: 08:32

Publisher: Taylor & Francis

Informa Ltd Registered in England and Wales Registered Number: 1072954 Registered office: Mortimer House, 37-41 Mortimer Street, London W1T 3JH, UK



Combustion Science and Technology

Publication details, including instructions for authors and subscription information:

<http://www.tandfonline.com/loi/gcst20>

Modeling Lifted Jet Flames in a Heated Coflow using an Optimized Eddy Dissipation Concept Model

M. J. Evans^a, P. R. Medwell^a & Z. F. Tian^a

^a School of Mechanical Engineering, The University of Adelaide, Adelaide, South Australia, Australia

Accepted author version posted online: 06 Jan 2015.



CrossMark

[Click for updates](#)

To cite this article: M. J. Evans, P. R. Medwell & Z. F. Tian (2015) Modeling Lifted Jet Flames in a Heated Coflow using an Optimized Eddy Dissipation Concept Model, Combustion Science and Technology, 187:7, 1093-1109, DOI: [10.1080/00102202.2014.1002836](https://doi.org/10.1080/00102202.2014.1002836)

To link to this article: <http://dx.doi.org/10.1080/00102202.2014.1002836>

PLEASE SCROLL DOWN FOR ARTICLE

Taylor & Francis makes every effort to ensure the accuracy of all the information (the "Content") contained in the publications on our platform. However, Taylor & Francis, our agents, and our licensors make no representations or warranties whatsoever as to the accuracy, completeness, or suitability for any purpose of the Content. Any opinions and views expressed in this publication are the opinions and views of the authors, and are not the views of or endorsed by Taylor & Francis. The accuracy of the Content should not be relied upon and should be independently verified with primary sources of information. Taylor and Francis shall not be liable for any losses, actions, claims, proceedings, demands, costs, expenses, damages, and other liabilities whatsoever or howsoever caused arising directly or indirectly in connection with, in relation to or arising out of the use of the Content.

This article may be used for research, teaching, and private study purposes. Any substantial or systematic reproduction, redistribution, reselling, loan, sub-licensing, systematic supply, or distribution in any form to anyone is expressly forbidden. Terms &

Conditions of access and use can be found at <http://www.tandfonline.com/page/terms-and-conditions>

MODELING LIFTED JET FLAMES IN A HEATED COFLOW USING AN OPTIMIZED EDDY DISSIPATION CONCEPT MODEL

M. J. Evans,^{ID} P. R. Medwell,^{ID} and Z. F. Tian^{ID}

School of Mechanical Engineering, The University of Adelaide, Adelaide, South Australia, Australia

Moderate or intense low oxygen dilution (MILD) combustion has been established as a combustion regime with improved thermal efficiency and decreased pollutant emissions, including NO_x and soot. MILD combustion has been the subject of numerous experimental studies, and presents a challenge for computational modeling due to the strong turbulence–chemistry coupling within the homogeneous reaction zone. Models of flames in the jet in hot coflow (JHC) burner have typically had limited success using the eddy dissipation concept (EDC) combustion model, which incorporates finite-rate kinetics at low computational expense. A modified EDC model is presented, which successfully simulates an ethylene–nitrogen flame in a 9% O_2 coflow. It is found by means of a systematic study in which adjusting the parameters C_τ and C_ξ from the default 0.4082 and 2.1377 to 3.0 and 1.0 gives significantly improved performance of the EDC model under these conditions. This modified EDC model has subsequently been applied to other ethylene- and methane-based fuel jets in a range of coflow oxidant stream conditions. The modified EDC offers results comparable to the more sophisticated, and computationally expensive, transport probability density function (PDF) approach. The optimized EDC models give better agreement with experimental measurements of temperature, hydroxyl (OH), and formaldehyde (CH_2O) profiles. The visual boundary of a chosen flame is subsequently defined using a kinetic mechanism for OH^ and CH^* , showing good agreement with experimental observations. This model also appears more robust to variations in the fuel jet inlet temperature and turbulence intensity than the standard EDC model trialed in previous studies. The sensitivity of the newly modified model to the chemical composition of the heated coflow boundary also demonstrates robustness and qualitative agreement with previous works. The presented modified EDC model offers improved agreement with experimental data profiles than has been achieved previously, and offers a viable alternative to significantly more computationally expensive modeling methods for lifted flames in a heated and vitiated coflow. Finally, the visually lifted flame behavior observed experimentally in this configuration is replicated, a phenomenon that has not been successfully reproduced using the EDC model in the past.*

Keywords: Eddy dissipation concept (EDC); Jet in hot coflow (JHC) burner; Lifted flames; Moderate or intense low oxygen dilution (MILD) combustion; Turbulent flames

Received 13 April 2014; revised 22 December 2014; accepted 23 December 2014.

Address correspondence to M. J. Evans, School of Mechanical Engineering, The University of Adelaide, Adelaide, SA 5005, Australia. E-mail: m.evans@adelaide.edu.au

Color versions of one or more of the figures in the article can be found online at www.tandfonline.com/gcst.

INTRODUCTION

The moderate or intense low oxygen dilution (MILD) combustion regime offers improved thermal efficiency and reduction of nitrogen oxides (NO_x) pollutants and soot, facilitating lower fuel consumption and cleaner exhaust gases (Cavaliere and de Joannon, 2004). A characteristic of the MILD regime is a distributed, homogeneous reaction zone, without flame temperature peaks and reduced pressure variations. Under these conditions, the Damköhler number (Da) is near unity in the reaction region (Galletti et al., 2007), indicating that both chemical and turbulence time scales are important in describing the MILD regime. A number of experimental studies into the mechanics of the MILD combustion regime have been performed using simplified jet flames in low oxygen, heated coflows. The jet in hot coflow (JHC) burner, shown in Figure 1 and described by Medwell et al. (2007), consists of a central jet emanating into a coflow of combustion products. The 4.6-mm-diameter central jet of the JHC burner issues into an 82-mm-diameter concentric coflow of combustion products from an up-stream secondary burner. The JHC burner has been used to provide experimental data for numerous fuel and Reynolds number combinations (Dally et al., 2002; Medwell and Dally, 2012; Medwell et al., 2007, 2008; Oldenhof et al., 2010, 2011, 2012), as has the similarly configured vitiated coflow burner (VCB) (Cabra et al., 2002, 2005; Gordon et al., 2008).

Numerous computational studies of the JHC burner have been made using Reynolds averaged Navier–Stokes (RANS) modeling (Aminian et al., 2011, 2012; Christo and Dally, 2005; De et al., 2011; Frassoldati et al., 2010; Gao et al., 2013; Mardani et al., 2011, 2013; Wang et al., 2013) and large-eddy simulations (LES) (Afarin and Tabejaamat, 2013; Ihme and See, 2011; Ihme et al., 2012; Kulkarni and Polifke, 2013), focusing on CH_4/H_2 fuel cases. Subsequent findings of these studies have been extended by recent modeling efforts

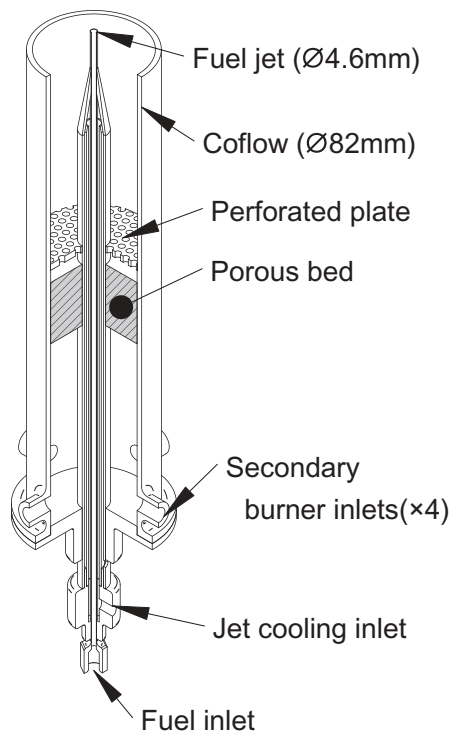


Figure 1 Schematic of the JHC burner used for MILD combustion experiments.

of the more complex C_2H_4 -based fuel experiments (Shabanian et al., 2013). This work, trialing a number of different turbulence and combustion models, found best agreement with the experimental results of Medwell et al. (2008) using the modified standard $k-\varepsilon$ (SKE) turbulence model of Dally et al. (1998) and a modified eddy dissipation concept (EDC) finite-rate reaction model with the parameter C_τ increased from the default 0.4082 to 3 (Shabanian et al., 2013). The modified SKE and modified EDC model combination generally agreed well with the experimental data; however, in most cases, the temperature distributions modeled downstream of the jet were in excess of those measured and the radial peaks in minor species distributions were not accurately predicted (Shabanian et al., 2013). These simulations also did not exhibit any lifted behavior, in contrast to the C_2H_4 -based flames measured by Medwell et al. (2008). The particle density function (PDF) modeling approach of Shabanian et al. (2013) was, however, in good agreement with this apparent lift-off phenomenon not captured by the computationally cheaper EDC model, especially in the C_2H_4/N_2 fuel case. The good agreement of PDF models with experimental measurements from the JHC is consistent with RANS modeling efforts of the VCB (Cabra et al., 2005; Cao et al., 2005; Gkagkas and Lindstedt, 2007; Gordon et al., 2007; Masri et al., 2003; Najafizadeh et al., 2013; Ren and Pope, 2009). In light of the limited success of the RANS-EDC models, the objective of this article is to systematically determine an approach for improving the performance of CFD modeling to capture lifted jet flame behavior in a heated coflow using the ANSYS FLUENT 14.0 software package. The commercial FLUENT 14.0 code was adopted in the absence of any suitable alternative research code with similar capabilities, appropriate for modeling turbulent flames in the MILD regime without requiring excessive customization. The desire to develop the capabilities of RANS-EDC modeling of these flames is driven by the desire for reduced computational cost.

Flames in the transition to MILD combustion have been reported as appearing visually lifted in the JHC burner for ethylene (C_2H_4)-based fuel streams (Medwell et al., 2008). Long exposure images of such flames, shown in Figure 2, demonstrate the apparent

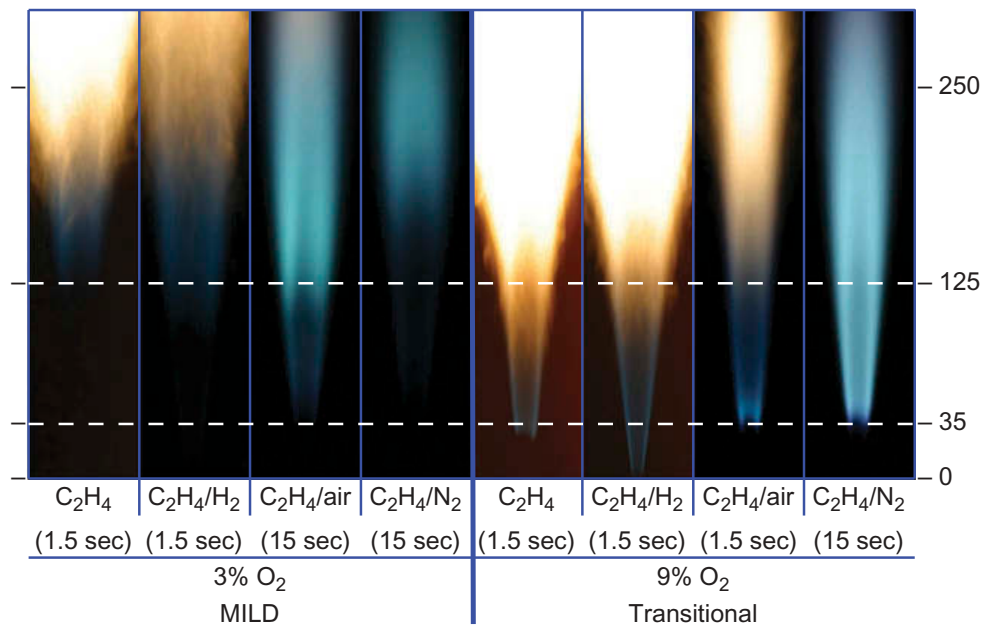


Figure 2 Visual comparison of different C_2H_4 -based flames at $Re_{jet} = 10,000$ in the JHC burner up to 300 mm above jet exit plane, showing heights in millimeters; labeled with exposure times and O_2 coflow conditions.

visual lift-off of these transitional flames in comparison to MILD flames. Despite visually resembling lifted flames, laser diagnostic imaging has revealed the occurrence of reactions upstream of the apparent lift-off height, as evident by measurements of formaldehyde (CH_2O) and the hydroxyl radical (OH) (Medwell et al., 2008). This is the case for C_2H_4 , $\text{C}_2\text{H}_4/\text{air}$, and $\text{C}_2\text{H}_4/\text{N}_2$ fueled jet flames with $\text{Re}_{\text{jet}} = 10,000$ in a 1100 K, 9% O_2 mol/mol coflow. Simplified one-dimensional (1D) modeling of these flames indicates that, despite the depleted oxygen concentration in the oxidant stream, under these conditions O_2 penetrates across the reaction zone to the fuel-rich side, which facilitates a radical pool build-up (Medwell et al., 2009). This observation is consistent with previous observations in similar lifted flames in a hot and vitiated coflow (Gordon et al., 2008). These flames present a particularly interesting test case for investigating the finite-rate chemistry effects under depleted oxygen conditions. Such effects have been modeled using 2D PDF models (Cabra et al., 2005; Cao et al., 2005; Gkagkas and Lindstedt, 2007; Gordon et al., 2007; Masri et al., 2003; Najafizadeh et al., 2013; Ren and Pope, 2009) and 3D direct numerical simulations (DNS) (Kerkemeier et al., 2013; Luo et al., 2012; Yoo et al., 2011). The objective of this article is to improve the performance of the computationally cheaper RANS-EDC models for lifted flames in a heated and depleted oxygen environment.

MODEL DEVELOPMENT

Domain and Boundary Conditions

The computational domain for the JHC burner was chosen to be a 2D rectangular region downstream of the jet plane exit. The geometry for this study was based on computational domains previously employed in similar studies of the JHC burner (Frassoldati et al., 2010; Shabaniyan et al., 2013). The study of MILD combustion using the JHC burner is only valid where the fuel jet is entrained by the controlled coflow, up to ~ 100 mm (or ~ 22 jet diameters) downstream of the jet exit plane, after which the ambient air becomes influential. The near jet region is therefore the focus of the modeling effort for optimization of the EDC model, with the focus of the work targeting the relationships between empirical parameters in the model and their effect on species reaction rates. The 400 mm (~ 85 jet diameters) downstream extent of the computational domain from the jet exit plane captures the experimental measurement locations of 30 mm (Dally et al., 2002) and 35 mm (Medwell et al., 2008) downstream of the jet exit plane. Although the radiation model has previously been shown to have a negligible effect on these essentially soot-free flames (Aminian et al., 2011; Frassoldati et al., 2010; Mardani et al., 2010; Shabaniyan et al., 2013), the 'P1' radiation model was implemented to retain accuracy at a minimal computational cost. The simplest implementation of the 'P1' model assumes a basic grey-band model for gases with constant absorption and scattering coefficients.

The boundaries of the domain were a combination of walls, pressure outlets, velocity inlets, and the axis of cylindrical symmetry through the center of the coaxial jets. Adiabatic, no-slip boundaries were used to describe the pipe walls in the JHC burner. Pressure outlets specify the ambient surrounds to be simplified air, with 21% O_2 and 79% N_2 mol/mol, at zero gauge pressure and a temperature of 300 K. A coflowing wind tunnel velocity of 3.3 m/s was also included in models of the flames measured by Dally et al. (2002). The computational domain was divided into a structured, quadrilateral, computational mesh with 53,610 elements based on mesh independence studies using the C_2H_4 and $\text{C}_2\text{H}_4/\text{H}_2$ fuel cases and additional meshes of 149,060 and 251,916 elements.

Previous attempts to model combustion in JHC burners have used experimentally measured inlet profiles (De et al., 2011), assumed constant velocity across the domain inlet (Aminian et al., 2012; Frassoldati et al., 2010; Shabanian et al., 2013), or modeled the jet and coflow exit profiles (Christo and Dally, 2005; Mardani et al., 2011). Previous modeling of the C₂H₄-based JHC flames made the assumption of constant velocity profiles, although did not investigate any sensitivity to inlet boundary conditions (Shabanian et al., 2013). For the current study the fuel pipe geometry was computationally modeled separately as a constant 4.6-mm-diameter tube, 100 diameters in length, in order to ensure fully developed flow in the pipe. This was modified to 4.25 mm for the Dally et al. (2002) simulated cases for consistency with the experiments. To determine the coflow velocity profile, an additional model of the secondary burner and outer annulus was generated, with the flow emanating with a uniform velocity of combustion products at the perforated plate 160 mm upstream of the coflow exit plane.

Turbulence and Turbulence-Chemistry Interaction Models

The modified k - ε turbulence model is adjusted from the standard k - ε model by changing the common default value of $C_{1\varepsilon}$ from 1.44 to 1.6, as recommended and verified for 2D axisymmetric flows (Dally et al., 1998). The anisotropic Reynolds stress model (RSM), featuring the same modification to $C_{1\varepsilon}$, has been previously verified for non-reacting jets (Dally et al., 1998) and was also implemented in selected cases for comparison. In modeling the MILD regime in the JHC burner, simple global-chemistry and scalar-based combustion models are unable to provide the accuracy of the more sophisticated eddy dissipation concept (EDC) combustion model (Christo and Dally, 2005; Shabanian et al., 2013). The EDC model allows for the implementation of finite-rate chemical kinetics mechanisms, such as GRI-Mech 3.0 (Smith et al., 2000). A reduced, 36 species, form of the GRI-Mech 3.0 kinetics mechanism, excluding N-O reactions, was used after a similar GRI-Mech 3.0 mechanism demonstrated success in CH₄-based fuels in the JHC (Christo and Dally, 2005) and good agreement with a separately reduced kinetics scheme for both CH₄- (Frassoldati et al., 2010) and C₂H₄-based fuels (Shabanian et al., 2013).

Analysis of excited, chemiluminescent species and the effect of minor species in the coflow required the use of additional kinetic mechanisms. Additional reactions for the excited species mechanism was implemented using a combination of kinetics rates and reactions (Elsamra et al., 2005; Hall and Petersen, 2006; Hidaka et al., 1985; Petersen et al., 2003; Tamura et al., 1998) and a 50-species modified GRI-Mech 3.0 mechanism was used for the inclusion of minor species in the coflow. OH* and CH* denote excited OH and CH molecules, respectively, and emit light in the blue and ultraviolet regions of the light spectrum upon relaxation to their ground states. Therefore, concentrations of the excited CH* species indicate a blue colored flame, and the lack of CH* in regions with OH species concentration may be interpreted as evidence of MILD (flameless) combustion. The distributions of these excited species were evaluated in post-processing using a combination of OH* excitation reactions by Petersen et al. (2003) and Hall and Petersen (2006), CH* reactions by Elsamra et al. (2005), and quenching rates by Hidaka et al. (1985) and Tamura et al. (1998). The combined mechanism consisted of an additional 21 reactions, which were chosen to be evaluated in post-processing rather than incorporated into the existing modified GRI-Mech 3.0 in the interest of brevity. Kinetics post-processing was employed with the expectation that the populations of OH and CH species would contain only a negligible fraction of excited molecules, which would therefore have little impact on

the combustion chemistry. This assumption was later confirmed through inspection of the results. The effects of minor species were additionally investigated by adding equilibrium concentrations of OH and NO to the coflow composition, both separately and simultaneously, using a further modified 50 species GRI-Mech 3.0 mechanism, which included N–O reactions while excluding argon and C_3H_x species. The addition of 0.001% mol/mol OH and 0.03% mol/mol NO in the coflow, separately and simultaneously, were investigated for change of peak temperature and apparent lift-off height. The effects of a 1% concentration of OH in the coflow on the same parameters was similarly considered following recent work on the effect of minor species in reducing ignition delay (Medwell et al., 2014).

The mean reaction rate in the EDC combustion model, R_i , of species i is assumed to occur only within small turbulent structures, as described by Eq. (1) (Magnussen, 1981). Both the mean residence time (τ^*) spent within fine structures with length fraction (ξ^*), are scaled by C_τ and C_ξ , with default values originally derived from an extensive control volume analysis of isotropic turbulent structures (Magnussen, 1981). The equations defining τ^* and ξ^* are shown in Eqs. (2) and (3), respectively.

$$R_i = \frac{\rho(\xi^*)^2}{\tau^*[1 - (\xi^*)^3]}(Y_i^* - Y_i) \quad (1)$$

where ρ is density, Y_i the mass fraction of species i in a computational cell, and Y_i^* within fine scales,

$$\tau^* = C_\tau \left(\frac{\nu}{\varepsilon}\right)^{1/2} \quad (2)$$

where $C_\tau = 0.4082$ (default), ν is the kinematic viscosity, and ε the turbulent dissipation rate,

$$\xi^* = C_\xi \left(\frac{\nu\varepsilon}{k^2}\right)^{1/4} \quad (3)$$

where $C_\xi = 2.1377$ (default) and k is the turbulent kinetic energy. Finally, combining these equations, the mean reaction rate may be rewritten as:

$$R_i = \frac{C_\xi^2}{C_\tau} \left[1 - C_\xi^3 \left(\frac{\nu\varepsilon}{k^2}\right)^{3/4}\right]^{-1} \frac{\rho\varepsilon}{k}(Y_i^* - Y_i) \quad (4)$$

Recent studies (Aminian et al., 2012; Shabaniyan et al., 2013), based on an earlier investigation on the Delft jet in hot coflow burner (De et al., 2011), found that increasing C_τ in the EDC model to 1.5 (Aminian et al., 2012) or 3 (Aminian et al., 2012; Shabaniyan et al., 2013) provided better agreement to measurements from the JHC burner.

The results of the Delft jet in hot coflow modeling (De et al., 2011) indicate that these variations of the standard EDC model act to improve the predictions of lift-off, although this was not particularly apparent by setting $C_\tau = 3$ for ethylene fuels in the JHC burner (Shabaniyan et al., 2013). This is in agreement with the observation that in the MILD combustion regime there is a decrease in chemical reaction rates (Galletti et al., 2007; Ihme and See, 2011). The modification of C_τ (inversely proportional to R_i , from Eq. (4)) has been further justified by stating that the homogeneity of the MILD reaction region invalidates the assumption that species do not react beyond the confines of fine structures, and that

increasing residence times act to compensate for this (Aminian et al., 2012). The near unity Damköhler number was similarly cited as a reason for unreliability of the EDC model for flows with low turbulence (De et al., 2011). It was shown that the standard value of C_ξ was unreliable for flows with $k^2/(\nu\varepsilon)$ less than 65 (De et al., 2011). Decreasing the C_ξ parameter decreases the reaction zone volume fraction in the fluid model, restricting interactions between species and slowing the reaction rates (De et al., 2011). In spite of this detailed discussion, the work of De et al. (2011) does not quantify the effects of changing the parameter C_ξ on species profiles or rigorously investigate the effects of this empirical parameter on temperature profiles.

The effects of changing C_ξ on R_i are not immediately apparent due to the strong coupling of R_i , C_ξ , and the flow variables ν , ε , and k . The relationship can be seen by taking the partial derivative of R_i with respect to C_ξ , as shown in Eq. (5):

$$\frac{\partial R_i}{\partial C_\xi} = \left(\frac{2}{C_\xi} + \frac{3C_\xi^2 \left(\frac{\nu\varepsilon}{k^2}\right)^{3/4}}{\left[1 - C_\xi^2 \left(\frac{\nu\varepsilon}{k^2}\right)^{3/4}\right]} \right) R_i \quad (5)$$

This highlights the complex interplay between R_i , C_ξ , and the ratio $\nu\varepsilon/k^2$. In comparison, Eq. (6) shows the comparatively simple coupling between C_τ and the rate of change of R_i where:

$$\frac{\partial R_i}{\partial C_\tau} = -\frac{R_i}{C_\tau} \quad (6)$$

It is hypothesised that decreasing R_i would result in a more accurate model, thus a parametric study using the combinations of C_ξ and C_τ summarized in Table 1, for the case of a C_2H_4/N_2 jet flame with Reynolds number (Re_{jet}) of 10,000 in a 1100 K, 9% O_2 mol/mol coflow. The C_ξ parameter was varied with both the default and most successful value of C_τ from previous studies of jet flames in the transition to the MILD regime (Aminian et al., 2012; De et al., 2011; Shabaniyan et al., 2013) in order to gain an insight into the effect of each individual parameter on the accuracy of simulation results. The computational results of species and temperature distributions at 35 mm downstream from the jet exit and any apparent lift-off indicated from the CH^* and OH distributions were then compared to experimental measurements for each combination of parameters and the results of simulations

Table 1 Parameters and values chosen for parametric study, with combinations of six different C_ξ using both the default (0.4082) and previously most successful value of C_τ (3.0)

C_τ	C_ξ
0.4082 ^a	0.5
	0.75
	1
	1.5
3.0	2.1377 ^a
	2.5

^aDefault parameter value.

Table 2 Fuel jet and coflow stream operating conditions

Composition description Fuel (temperature)	Mean inlet velocity (m/s)	Composition (% vol/vol)			
		C ₂ H ₄	CH ₄	N ₂	H ₂
C ₂ H ₄ (305 K)	17.7	100	0	0	0
C ₂ H ₄ /H ₂ (305 K)	30.6	50	0	0	50
C ₂ H ₄ /N ₂ (305 K)	27.3	25	0	75	0
CH ₄ /H ₂ (305 K)	58.7	0	50	0	50
Coflow (temperature)		O ₂	CO ₂	N ₂	H ₂ O
Y = 3% O ₂ coflow (1300 K) ^a	3.2	2.6	3.5	83.9	10
Y = 9% O ₂ coflow (1300 K) ^a	3.2	7.8	3.5	78.7	10
X = 9% O ₂ coflow (1100 K)	2.3	9	3	78	10

^aWithin a coflowing wind tunnel with air velocity of 3.2 m/s and temperature assumed to be 300 K.

Sources: Dally et al., 2002; Medwell et al., 2008.

using the more sophisticated, and computationally expensive, composition probability density function (PDF) combustion model using an Euclidean minimum spanning tree (EMST) mixing model.

The combination of EDC parameters and velocity boundary conditions, which provided the best agreement to the measurements of the C₂H₄/N₂ flame in a 9% mol/mol O₂ coflow, was then compared to other fuel cases, all summarized in Table 2. Note that coflow compositions specified by mass fraction (Y) correspond to methane-based studies by Dally et al. (2002), with remaining cases measured experimentally by Medwell et al. (2008).

RESULTS AND DISCUSSION

Results of the parametric study into the effects of C_ξ in the EDC combustion model were obtained for the C₂H₄/N₂ in a 9% mol/mol O₂ coflow. This produced a set of results from the previously listed parameter combinations for comparison against experimental temperature, OH and CH₂O profiles, in addition to visible lift-off behavior. These results indicated best agreement using the modified SKE turbulence model (Dally et al., 1998) and a newly modified EDC model with the parameters $C_\tau = 3$ and $C_\xi = 1$, compared to the default $C_\tau = 0.4082$ and $C_\xi = 2.1377$, and recently used modified values $C_\tau = 3$ and $C_\xi = 2.1377$ (Shabanian et al., 2013). The newly modified EDC model required approximately 1500 CPU hours for an individual computational case using ANSYS FLUENT 14.0. This lengthy time required for convergence highlights the complexity of using the EDC model with the modified GRI-Mech 3.0 and a simple, 2D geometry, while the PDF-EMST model simulations notably required an order of magnitude greater computational time. The profiles of temperature, hydroxyl (OH), and formaldehyde (CH₂O) concentrations of these selected EDC parameter combinations, and the results of simulation using the PDF-EMST model, are compared with the experimental data in Figure 3. Both the newly modified EDC and PDF-EMST models show excellent agreement with the temperature distribution and the profile shapes of species distributions, despite a significant difference in peak magnitude. The best agreement with experimental data were found to require fully developed velocity profiles of the fuel jet at the jet exit. The combinations of developed velocity and uniform profiles were assessed for the most successful combination in the literature, $C_\tau = 3.0$ and

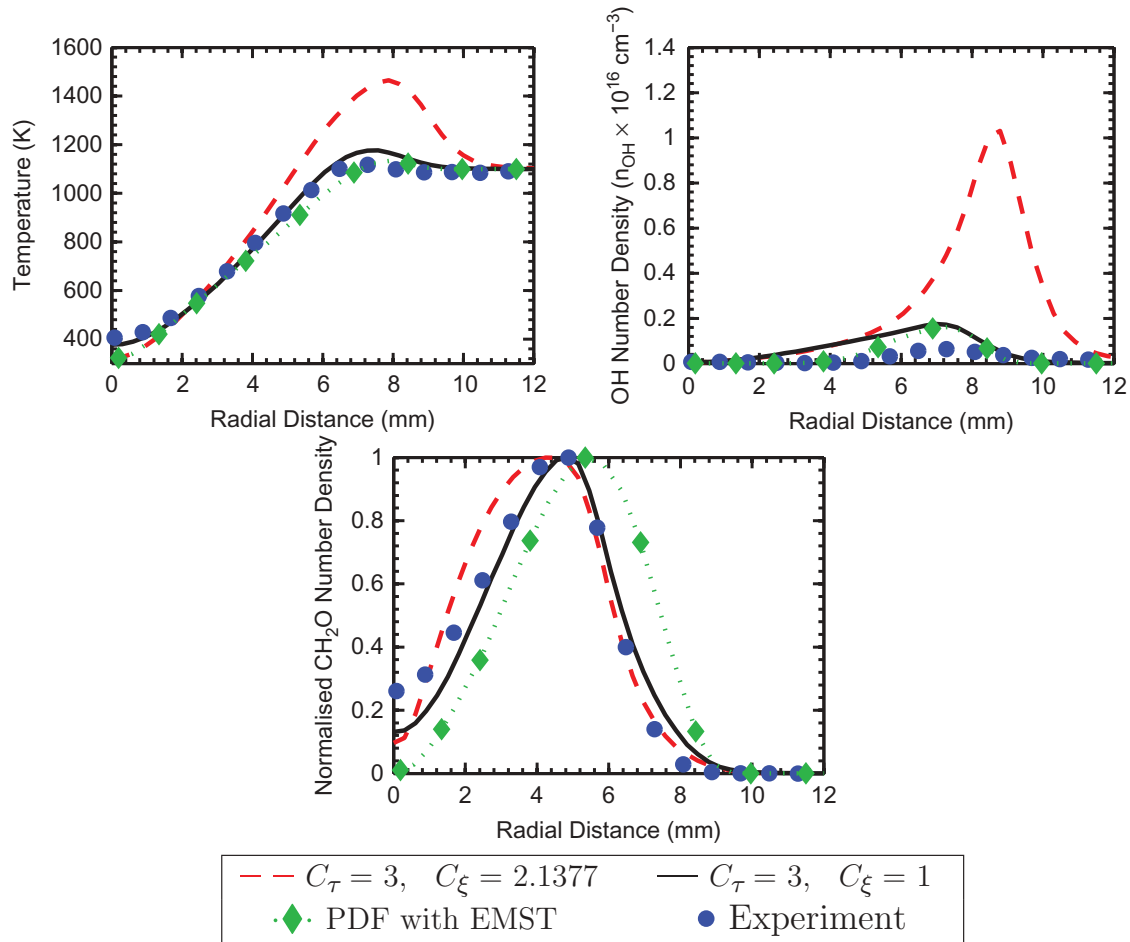


Figure 3 Temperature and species profiles 35 mm downstream from jet exit for C_2H_4/N_2 fuel in a 9% mol/mol O_2 coflow, showing two modified EDC models, PDF with EMST model and experimental measurements (experimental data from Medwell et al., 2008).

$C_\xi = 2.1377$, in addition to $C_\tau = 3.0$ with $C_\xi = 1$ and $C_\tau = 0.4082$ with $C_\xi = 1.5$, which demonstrated the best agreement with experimental measurements among all the parameter combinations. The influence of the coflow profile, jet turbulent intensity (in contrast to previous findings for CH_4/H_2 jets (Christo and Dally, 2005)) and variations in jet temperature ~ 100 K were seen to have an insignificant impact on the shape and magnitude of temperature and species distribution peaks. This could imply that the optimized EDC parameter combination of $C_\tau = 3$ and $C_\xi = 1$ offers a more robust model, or that the effects of turbulence intensity on the axisymmetric C_2H_4 -based jets are less significant than the effects on CH_4/H_2 when issuing into a heated coflow.

With apparent lift-off height an interest for investigation of flame stability and autoignition, the CH^* distribution was compared to visual measurements by Medwell et al. (2008). The initial downstream formation locations of CH^* were then subsequently used to define the visible flame base for further analysis and comparison with experimental cases (Medwell et al., 2008). The combination of $C_\tau = 3$ and $C_\xi = 1$ demonstrated the best agreement with visual lift-off height while maintaining a reaction zone near the jet exit, and is shown using the developed jet and coflow profiles in Figure 4. The simulated number densities of OH and CH^* species are shown for this case in Figure 4, showing both sets

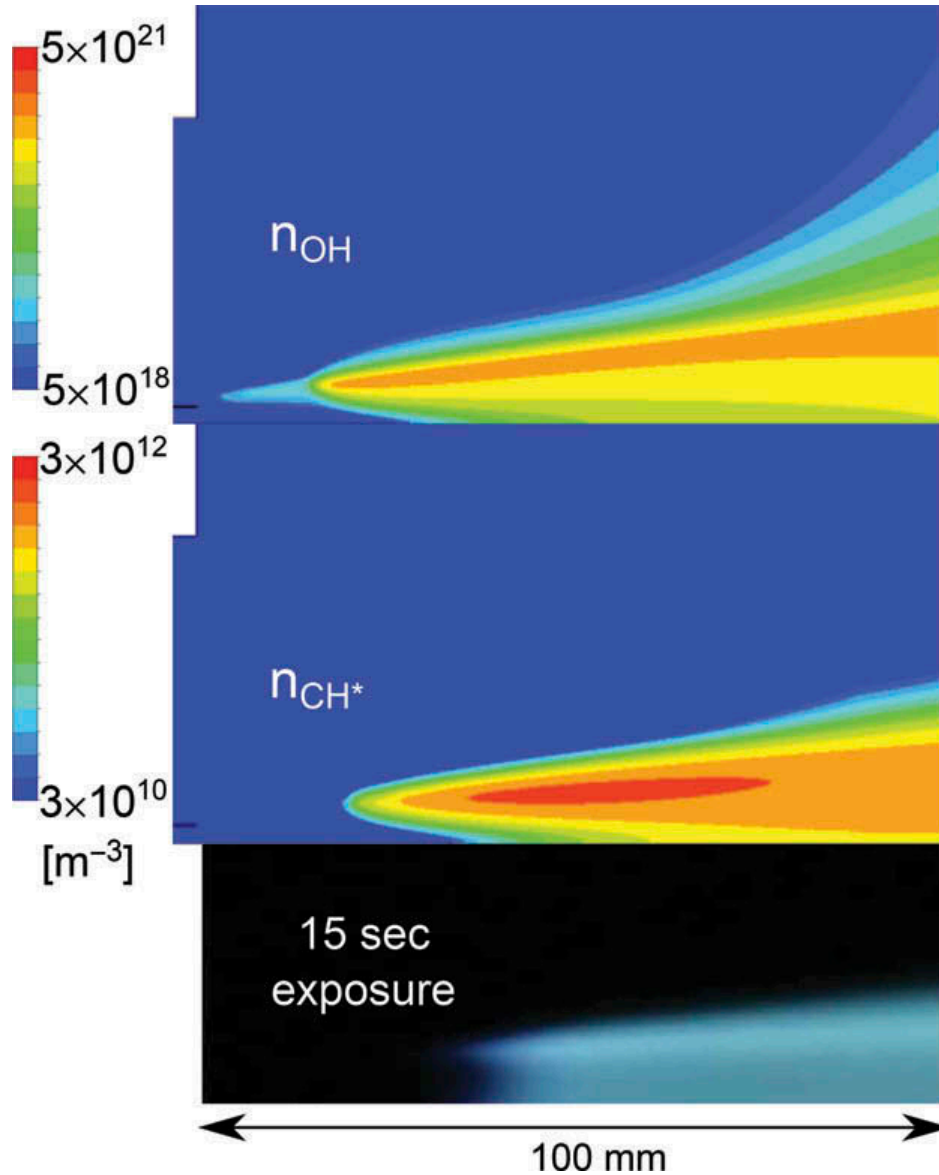


Figure 4 Number densities (in m^{-3}) of OH and CH* species near the jet exit with logarithmic scales compared to experiment (Medwell et al., 2008). Modeled using the EDC combustion model with $C_T = 3$ and $C_\xi = 1$ for $\text{C}_2\text{H}_4/\text{N}_2$ fuel in a 9% O_2 coflow, appearing to simulate flameless combustion near the jet exit. Model results show jet and coflow radii, omitted from photographic image.

of results near the jet exit with a logarithmic scales in comparison to experimental observations. The logarithmic scale was chosen due to the proportional relationship between light intensity and the total light energy flux squared, and thus preserving a linear relationship between the logs of the species concentrations and the intensity of the emitted light. Similar contours were produced using the PDF-EMST model, including the same general features clearly showing a difference of orders of magnitude between OH and excited species concentrations. A difference of several orders of magnitude between the excited and base CH and OH concentrations additionally justified the assumption that CH* and OH* reactions may be neglected in determining the overall structure of the flame, and that the time-saving post-processing stage is an effective means of defining a visible flame boundary. This figure

clearly demonstrates a transitional flame with a jet flame visually detached from the jet exit (as indicated by CH^*), yet showing evidence of minor species (OH) almost to the jet exit plane. Such results, clearly replicating the visually lifted description of these flames, have not been previously demonstrated for this series of cases in the JHC burner using EDC combustion models, but are consistent with experimental measurements.

The combination of $C_\tau = 3$ and $C_\xi = 1$ results in better agreement with measured data than the default EDC parameters, and accordingly replicates the visual lift-off seen experimentally, which had not previously been achieved for these jet flames using the EDC combustion model, or any other Reynolds averaged method. These parameters were then assessed for accuracy in modeling the remaining C_2H_4 , $\text{C}_2\text{H}_4/\text{H}_2$ jet flames in identical coflow conditions and the CH_4/H_2 flames as listed in Table 2. These results are presented as Figures 5–7, and demonstrate the good agreement between the $C_\tau = 3$ and $C_\xi = 1$ EDC model and the value of peak temperature in the C_2H_4 and both CH_4/H_2 flames, and in predicting the radial location of peak CH_2O species for all cases. The newly modified EDC with $C_\tau = 3$ and $C_\xi = 1$ offers an improved temperature prediction compared to previously attempted parameter combinations with $C_\xi = 2.1377$ and varying C_τ (Aminian et al., 2012). In their comparison of fine-scale time constants, Aminian et al. (2012) found an ‘optimal’ value of $C_\xi = 1.5$ resulting in relative errors in peak temperatures (with respect

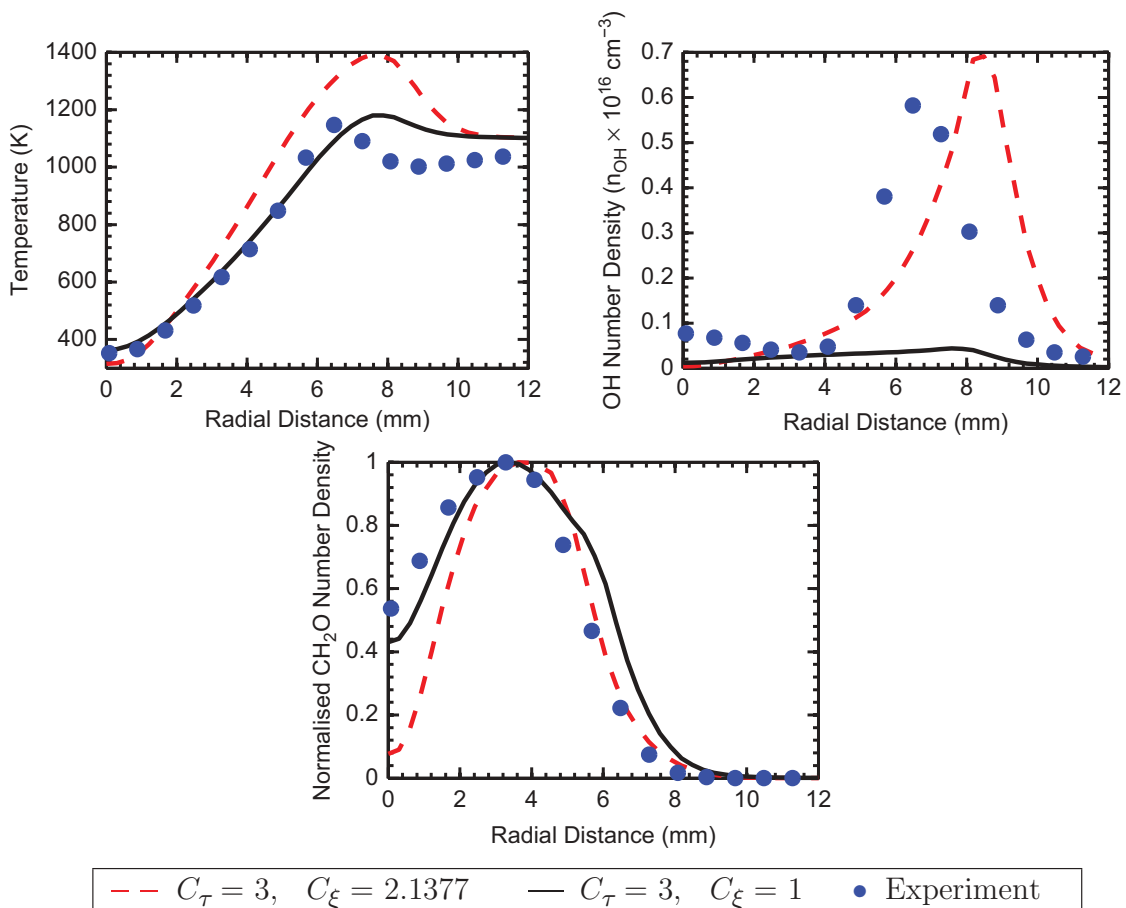


Figure 5 Temperature and species profiles 35 mm downstream from jet exit for C_2H_4 fuel in a 9% mol/mol O_2 coflow, showing two modified EDC models and experimental measurements (experimental data from Medwell et al., 2008).

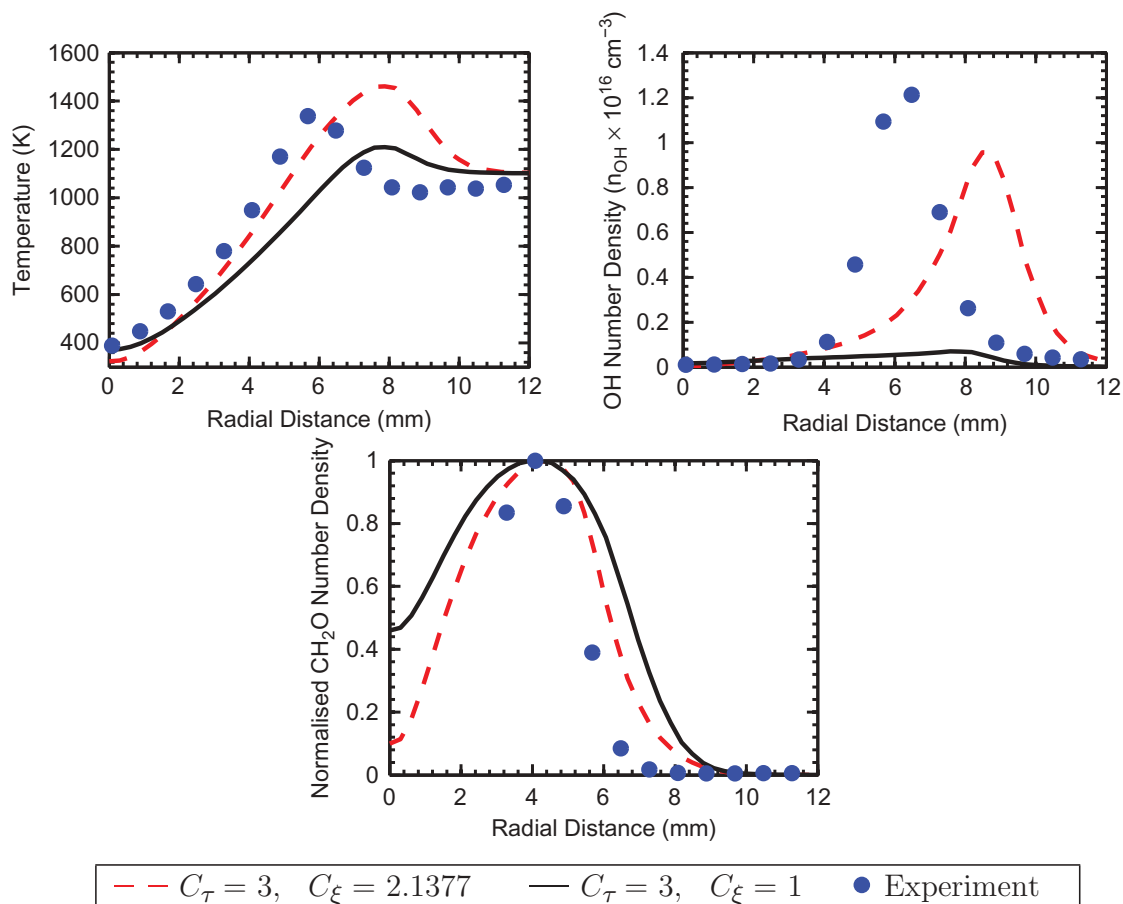


Figure 6 Temperature and species profiles 35 mm downstream from jet exit for C_2H_4/H_2 fuel in a 9% mol/mol O_2 coflow, showing two modified EDC models and experimental measurements (experimental data from Medwell et al., 2008).

to the experimental peak) of 2.0% and 3.7% for the CH_4/H_2 fuel flames in 9% and 3% O_2 coflows respectively. In comparison, the new EDC parameter set offers an improved overall agreement with the two of these peak temperatures with relative errors of 2.7% and 1.7% for the same CH_4/H_2 fuel flames in 9% and 3% O_2 coflows, respectively. These errors are shown alongside other fuel cases in Table 3, which shows significantly better consistency in prediction of peak temperature for all flames in comparison to previously ‘optimized’ EDC parameters.

The effects of minor species in the coflow were investigated as a possible source of influence in modeling the visual lift-off of flames in the transition to the MILD regime. The effect of the alternate 50 species GRI-Mech 3.0 kinetics using the newly modified EDC, and inclusion of reactions involving nitrogen was a total peak temperature difference of 11.2 K, demonstrating the robustness of the solution to the inclusion of nitrogen reactions. Additionally the inclusion of equilibrium OH and NO did not significantly increase the peak temperatures 35 mm downstream or alter the apparent lift-off, resulting only in 0.3 K and 12.4 K increases, respectively, and 12.5 K when both were included. These results justify the removal of N–O reactions in the GRI-Mech 3.0 mechanism and the simplification of the chemical composition at the coflow boundary. The increased concentration of 1% OH, however, resulted in an increase in peak temperature of 65.5 K at

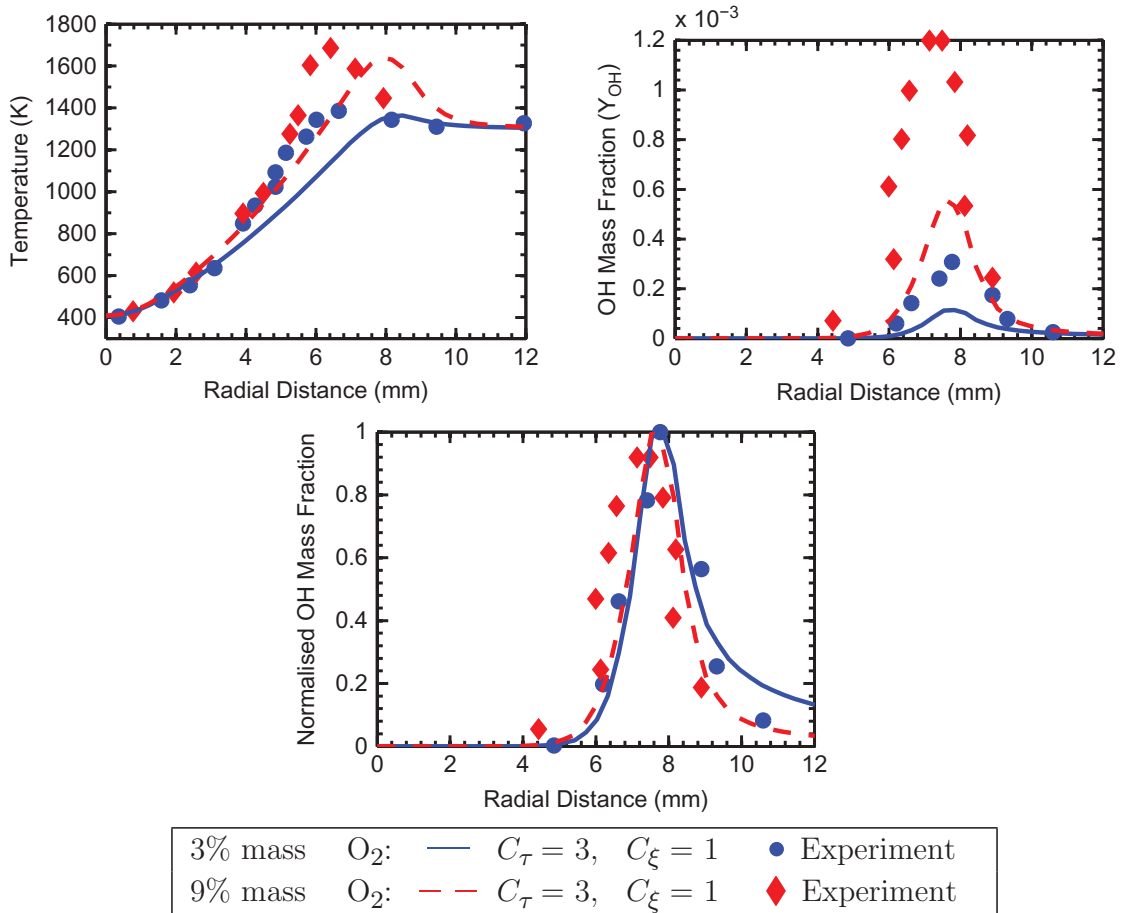


Figure 7 Temperature and species profiles 30 mm downstream from jet exit for CH_4/H_2 fuel, showing modified EDC models with $C_\tau = 3$ and $C_\xi = 1$ (lines), and experimental measurements (markers) for 3% and 9% mass O_2 coflows (experimental data from Dally et al., 2002).

Table 3 Comparison of relative error in peak temperatures at 30 (CH_4/H_2 flames only) or 35 mm downstream of jet exit plane, as a percentage of experimental peak temperature (Dally et al., 2002; Medwell et al., 2008), coflows contain 9% mol/mol O_2 unless stated otherwise (Aminian et al., 2012; Shabanian et al., 2013)

EDC parameters	Relative error (%)				
	CH_4/H_2 (3%) ^b	CH_4/H_2 (9%) ^b	C_2H_4	$\text{C}_2\text{H}_4/\text{H}_2$	$\text{C}_2\text{H}_4/\text{N}_2$
$C_\tau = 1.5^a$	3.7	2.0	—	—	—
$C_\tau = 3^a$	—	7.9	14.9	9.2	28.6
$C_\tau = 3, C_\xi = 1^c$	1.7	2.7	2.7	9.6	3.3
PDF-EMST ^a	—	—	10.3	9.6	0.5 ^c

^aCFD results for CH_4/H_2 flames by Aminian et al. (2012); otherwise Shabanian et al. (2013).

^bPercentage coflow O_2 by mass.

^cCurrent study.

Note: Dashes indicate no available CFD results.

35 mm downstream of the jet exit plane, and resulted in the flame attaching to the jet exit plane, eliminating any form of lift-off. This is in accordance with previous findings where OH at similar concentrations was shown to significantly reduce ignition delay of jet flames

in a hot environment (Medwell et al., 2014). The newly modified EDC model, in this sense, behaves as anticipated with altered inlet compositions and verifies the importance of OH in flame stabilization.

The new, modified EDC under-predicts the number density of OH in all cases except the C_2H_4/N_2 fuel, where it is in good agreement with the PDF-EMST model. The modeling deficiencies resulting in under-prediction of OH have previously been seen using the PDF-EMST model for the C_2H_4/H_2 fuel case (Shabnian et al., 2013), and CH_4/H_2 cases (Aminian et al., 2012; Christo and Dally, 2004), reporting peak magnitudes reduced by a factor of four in the 3% O_2 coflow at the 30 mm measurement location with the PDF-EMST model and a factor of three assigning $C_\xi = 1.5$ (Aminian et al., 2012). These three- (Aminian et al., 2012) and four-fold errors (Christo and Dally, 2004) are significantly greater than the factor of two predicted by the newly modified EDC model in the same fuel case after optimization of both the C_τ and C_ξ parameters. The normalized OH distribution, however, agrees very well with measurement for the C_2H_4/N_2 and both CH_4/H_2 flames. In comparison, the standard EDC model significantly over-predicts OH concentrations in both the C_2H_4/N_2 and CH_4/H_2 flames. The radial location of peak temperatures are over-predicted for all cases except the C_2H_4/N_2 fuel; however, this location is very dependent on the choice of turbulence model. The combination of modified RSM and EDC with $C_\tau = 3$ and $C_\xi = 2.1377$ (not shown) shows excellent agreement with experimental measurements for the C_2H_4/H_2 fuel case, but results in significant discrepancies compared to the C_2H_4/N_2 case. This deficiency may therefore be attributed to the modified SKE model, and hence, implies the need for a more robust 2D turbulence model in order to accurately capture the detail of temperature and species distributions.

A possible explanation for the improvement of both modified EDC models may be due to the decreased fine structure sizes for $C_\xi = 1$ and increased residence times more appropriately emulating the conditions of transitional jet flames in the JHC burner. This is consistent with reduced temperatures observed in MILD combustion (Cavaliere and de Joannon, 2004), which are indicative of reduced reaction rates resulting from the low oxygen dilution in the reaction zone. In contrast to conventional combustion, the MILD and, similarly transitional, regimes may be categorized such that fluid and chemical time scales are similar and turbulent time scales are reduced compared to conventional combustion. Similarly, Eq. (3) shows that C_ξ is a monotonically decreasing function of the ratio $k^2 / (\nu \epsilon)$, which is, in turn, proportional to the square of the turbulent kinetic energy of the fluid. This relationship implies that reacting fine structure scales increase in size with less energetic fluids, resulting in extended residence times in larger fine structures, serving to decrease the chemical time scale. In such circumstances, the combustion regime of a large control volume, such as a furnace, would tend towards emulating a well-stirred reactor where all products are completely mixed. The JHC burner, however, drives fluid motion downstream of the jet exit and dictates mixing between the ambient temperature, fast moving jet, and heated, slow, low oxygen coflow. The laminarizing, viscous shear effects between these streams may result in limited interaction regions between the fuel and oxidizer, reducing the boundaries for interactions between species while simultaneously increasing the time a fluid particle is encapsulated within a fine structure. Such viscous fluid effects may not be captured accurately by the EDC model due its assumption of isotropic Reynolds averaging (Magnussen, 2005), and numerical unreliability at low turbulence (De et al., 2011). Turbulent fine scales within the flow therefore need to be adjusted, through the parameters C_τ and C_ξ , in order to account for these viscous effects to better predict the mixing and chemical interactions between species in this region.

CONCLUSION

Lifted jet flames in a heated and depleted oxygen coflow stream in the transition to MILD combustion present an interesting test case for models. The use of RANS-based EDC models is particularly attractive due to the low computation cost yet retaining the capacity to model finite-rate chemical kinetics. However, previous RANS-EDC modeling efforts of the JHC burner have failed to accurately predict the experimental observations of transitional flames. These flames are characterized by measurements of combustion reactions in a region that visually appears lifted. Through a parametric investigation, it has been demonstrated that adopting the EDC constants $C_\tau = 3$ and $C_\xi = 1$ enable the behavior of these transitional flames to be recreated as shown through CH^* contours of a visually lifted flame. It is also shown that this pair of constants similarly improves the EDC model capabilities in predicting peak temperatures, OH, CH_2O , and temperature profiles measured experimentally across a range of operating conditions and fuels. Importantly, the optimized EDC model also shows less sensitivity to boundary conditions, such as jet inlet turbulence intensity and jet temperature and robustness to the chemical composition of boundary conditions. The modification of the EDC parameters is physically justifiable due to the distributed reaction zone associated with MILD combustion, explaining these improvements in the accuracy of results. These results demonstrate the capabilities of simplified RANS-based models for the modeling of flames in hot and vitiated oxidant streams, including visually lifted flames in the transition to MILD combustion, which have not been reproduced previously using an EDC model.

ACKNOWLEDGMENTS

The authors wish to acknowledge the support of the Centre for Energy Technology (CET) and The University of Adelaide.

ORCID

M. J. Evans  <http://orcid.org/0000-0003-1004-5168>

P. R. Medwell  <http://orcid.org/0000-0002-2216-3033>

Z. F. Tian  <http://orcid.org/0000-0001-9847-6004>

FUNDING

The Australian Research Council (ARC) is acknowledged for funding support through the Discovery (DP and DECRA) grant schemes.

REFERENCES

- Afarin, Y., and Tabejamaat, S. 2013. The effect of fuel inlet turbulence intensity on H_2/CH_4 flame structure of MILD combustion using the LES method. *Combust. Theor. Model.*, **17**(3), 383–410.
- Aminian, J., Galletti, C., Shahhosseini, S., and Tognotti, L. 2011. Key modeling issues in prediction of minor species in diluted-preheated combustion conditions. *Appl. Therm. Eng.*, **31**(16), 3287–3300.
- Aminian, J., Galletti, C., Shahhosseini, S., and Tognotti, L. 2012. Numerical investigation of a MILD combustion burner: Analysis of mixing field, chemical kinetics and turbulence-chemistry interaction. *Flow Turbul. Combust.*, **88**(4), 597–623.

- Cabra, R., Chen, J.Y., Dibble, R., Karpetis, A., and Barlow, R. 2005. Lifted methane-air jet flames in a vitiated coflow. *Combust. Flame*, **143**(4), 491–506.
- Cabra, R., Myhrvold, T., Chen, J., Dibble, R., Karpetis, A., and Barlow, R. 2002. Simultaneous laser Raman-Rayleigh-Lif measurements and numerical modeling results of a lifted turbulent H₂/N₂ jet flame in a vitiated coflow. *Proc. Combust. Inst.*, **29**, 1881–1888.
- Cao, R.R., Pope, S.B., and Masri, A.R. 2005. Turbulent lifted flames in a vitiated coflow investigated using joint PDF calculations. *Combust. Flame*, **142**, 438–453.
- Cavaliere, A., and de Joannon, M. 2004. Mild combustion. *Prog. Energ. Combust. Sci.*, **30**(4), 329–366.
- Christo, F.C., and Dally, B.B. 2004. Application of transport PDF approach for modelling MILD combustion. In *Proceedings of the Fifteenth Australian Fluid Mechanics Conference*, M. Behnia, W. Lin, and G. D. McBain (eds.), University of Sydney, Sydney, Australia.
- Christo, F.C., and Dally, B.B. 2005. Modeling turbulent reacting jets issuing into a hot and diluted coflow. *Combust. Flame*, **142**(1–2), 117–129.
- Dally, B., Karpetis, A., and Barlow, R. 2002. Structure of turbulent non-premixed jet flames in a diluted hot coflow. *Proc. Combust. Inst.*, **29**, 1147–1154.
- Dally, B.B., Fletcher, D.F., and Masri, A.R. 1998. Flow and mixing fields of turbulent bluff-body jets and flames. *Combust. Theor. Model.*, **2**(2), 193–219.
- De, A., Oldenhof, E., Sathiah, P., and Roekaerts, D. 2011. Numerical simulation of Delft-jet-in-hot-coflow (DJHC) flames using the eddy dissipation concept model for turbulence-chemistry interaction. *Flow Turbul. Combust.*, **87**(4), 537–567.
- Elsamra, R.M.I., Vranckx, S., and Carl, S.A. 2005. CH(A²Δ) formation in hydrocarbon combustion: The temperature dependence of the rate constant of the reaction C₂H + O₂ → CH(A²Δ) + CO₂. *J. Phys. Chem.* **109**(45), 10287–10293.
- Frassoldati, A., Sharma, P., Cuoci, A., Faravelli, T., and Ranzi, E. 2010. Kinetic and fluid dynamics modeling of methane/hydrogen jet flames in diluted coflow. *Appl. Therm. Eng.*, **30**(4), 376–383.
- Galletti, C., Parente, A., and Tognotti, L. 2007. Numerical and experimental investigation of a mild combustion burner. *Combust. Flame*, **151**, 649–664.
- Gao, X., Duan, F., Lim, S.C., and Yip, M.S. 2013. NO_x formation in hydrogen-methane turbulent diffusion flame under the moderate or intense low-oxygen dilution conditions. *Energy*, **59**, 559–569.
- Gkagkas, K., and Lindstedt, R.P. 2007. Transported PDF modelling with detailed chemistry of pre- and auto-ignition in CH₄/air mixtures. *Proc. Combust. Inst.*, **31**, 1559–1566.
- Gordon, R.L., Masri, A.R., and Mastorakos, E. 2008. Simultaneous Rayleigh temperature, OH- and CH₂O-LIF imaging of methane jets in a vitiated coflow. *Combust. Flame*, **155**(1–2), 181–195.
- Gordon, R.L., Masri, A.R., Pope, S.B., and Goldin, G.M. 2007. A numerical study of auto-ignition in turbulent lifted flames issuing into a vitiated co-flow. *Combust. Theor. Model.*, **11**(3), 351–376.
- Hall, J.M., and Petersen, E.L. 2006. An optimized kinetics model for OH chemiluminescence at high temperatures and atmospheric pressures. *Int. J. Chem. Kinet.*, **38**(12), 714–724.
- Hidaka, Y., Takuma, H., and Suga, M. 1985. Shock-tube study of the rate constant for excited hydroxyl (OH*(²Σ⁺)) formation in the nitrous oxide-molecular hydrogen reaction. *J. Phys. Chem.*, **89**(23), 4903–4905.
- Ihme, M., and See, Y.C. 2011. LES flamelet modeling of a three-stream MILD combustor : Analysis of flame sensitivity to scalar inflow conditions. *Proc. Combust. Inst.*, **33**, 1309–1217.
- Ihme, M., Zhang, J., He, G., and Dally, B.B. 2012. Large-eddy simulation of a jet-in-hot-coflow burner operating in the oxygen-diluted combustion regime. *Flow Turbul. Combust.*, **89**, 449–464.
- Kerkemeier, S.G., Markides, C.N., Frouzakis, C.E., and Boulouchos, K. 2013. Direct numerical simulation of the autoignition of a hydrogen plume in a turbulent coflow of hot air. *J. Fluid Mech.*, **720**, 424–456.
- Kulkarni, R.M., and Polifke, W. 2013. LES of Delft-jet-in-hot-coflow (DJHC) with tabulated chemistry and stochastic fields combustion model. *Fuel Process. Technol.*, **107**, 138–146.
- Luo, Z., Yoo, C.S., Richardson, E.S., Chen, J.H., Law, C.K., and Lu, T. 2012. Chemical explosive mode analysis for a turbulent lifted ethylene jet flame in highly-heated coflow. *Combust. Flame*, **159**(1), 265–274.

- Magnussen, B.F. 1981. On the structure of turbulence and a generalized eddy dissipation concept for chemical reaction in turbulent flow. Presented at the 19th AIAA Aerospace Meeting, St. Louis, MO, January 12–15.
- Magnussen, B.F. 2005. The eddy dissipation concept a bridge between science and technology. Presented at the ECCOMAS Thematic Conference on Computational Combustion, Lisbon, Portugal, June 21–24.
- Mardani, A., Tabejamaat, S., and Ghamari, M. 2010. Numerical study of influence of molecular diffusion in the Mild combustion regime. *Combust. Theor. Model.*, **14**(5), 747–774.
- Mardani, A., Tabejamaat, S., and Hassanpour, S. 2013. Numerical study of CO and CO₂ formation in CH₄/H₂ blended flame under MILD condition. *Combust. Flame*, **160**(9), 1636–1649.
- Mardani, A., Tabejamaat, S., and Mohammadi, M.B. 2011. Numerical study of the effect of turbulence on rate of reactions in the MILD combustion regime. *Combust. Theor. Model.*, **15**(6), 753–772.
- Masri, A.R., Cao, R., Pope, S.B., and Goldin, G.M. 2003. PDF calculations of turbulent lifted flames of H₂/N₂ fuel issuing into a vitiated co-flow. *Combust. Theor. Model.*, **8**(1), 1–22.
- Medwell, P.R., Blunck, D.L., and Dally, B.B. 2014. The role of precursors on the stabilisation of jet flames issuing into a hot environment. *Combust. Flame*, **161**(2), 465–474.
- Medwell, P.R., and Dally, B.B. 2012. Effect of fuel composition on jet flames in a heated and diluted oxidant stream. *Combust. Flame*, **159**(10), 3138–3145.
- Medwell, P.R., Kalt, P.A.M., and Dally, B.B. 2007. Simultaneous imaging of OH, formaldehyde, and temperature of turbulent nonpremixed jet flames in a heated and diluted coflow. *Combust. Flame*, **148**(1–2), 48–61.
- Medwell, P.R., Kalt, P.A.M., and Dally, B.B. 2008. Imaging of diluted turbulent ethylene flames stabilized on a jet in hot coflow (JHC) burner. *Combust. Flame*, **152**, 100–113.
- Medwell, P.R., Kalt, P.A.M., and Dally, B.B. 2009. Reaction zone weakening effects under hot and diluted oxidant stream conditions. *Combust. Sci. Technol.*, **181**(7), 937–953.
- Najafizadeh, S.M.M., Sadeghi, M.T., Sotudeh-Gharebagh, R., and Roekaerts, D.J. 2013. Chemical structure of autoignition in a turbulent lifted H₂/N₂ jet flame issuing into a vitiated coflow. *Combust. Flame*, **160**(12), 2928–2940.
- Oldenhof, E., Tummers, M.J., van Veen, E.H., and Roekaerts, D.J.E.M. 2010. Ignition kernel formation and lift-off behaviour of jet-in-hot-coflow flames. *Combust. Flame*, **157**(6), 1167–1178.
- Oldenhof, E., Tummers, M.J., van Veen, E.H., and Roekaerts, D.J.E.M. 2011. Role of entrainment in the stabilisation of jet-in-hot-coflow flames. *Combust. Flame*, **158**(8), 1553–1563.
- Oldenhof, E., Tummers, M.J., van Veen, E.H., and Roekaerts, D.J.E.M. 2012. Transient response of the Delft jet-in-hot coflow flames. *Combust. Flame*, **159**(2), 697–706.
- Petersen, E.L., Kalitan, D.M., and Rickard, M.J. 2003. Calibration and chemical kinetics modeling of an OH chemiluminescence diagnostic. AIAA Paper, 2003–4493.
- Ren, Z., and Pope, S.B. 2009. Sensitivity calculations in PDF modelling of turbulent flames. *Proc. Combust. Inst.*, **32**, 1629–1637.
- Shabaniyan, S.R., Medwell, P.R., Rahimi, M., Frassoldati, A., and Cuoci, A. 2013. Kinetic and fluid dynamic modeling of ethylene jet flames in diluted and heated oxidant stream combustion conditions. *Appl. Therm. Eng.*, **52**, 538–554.
- Smith, G.P., Golden, D.M., Frenklach, M., Moriarty, N.W., Eiteneer, B., Goldenberg, M., Bowman, C.T., Hanson, R.K., Song, S., Gardiner, Jr., W.C., Lissianski, V.V., and Qin, Z. 2000. GRI-Mech 3.0. Available at: http://www.me.berkeley.edu/gri_mech/.
- Tamura, M., Berg, P.A., Harrington, J.E., Luque, J., Jeffries, J.B., Smith, G.P., and Crosley, D.R. 1998. Collisional quenching of CH(A), OH(A), and NO(A) in low pressure hydrocarbon flames. *Combust. Flame*, **114**(34), 502–514.
- Wang, F., Mi, J., and Li, P. 2013. Combustion regimes of a jet diffusion flame in hot co-flow. *Energy and Fuels*, **27**(6), 3488–3498.
- Yoo, C.S., Richardson, E.S., Sankaran, R., and Chen, J.H. 2011. A DNS study on the stabilization mechanism of a turbulent lifted ethylene jet flame in highly-heated coflow. *Proc. Combust. Inst.*, **33**, 1619–1627.

Chapter 8

Ignition Features of Methane and Ethylene Fuel-Blends in Hot and Diluted Coflows

Statement of Authorship

Title of Paper	Ignition Features of Methane and Ethylene Fuel-Blends in Hot and Diluted Coflows
Publication Status	<input type="checkbox"/> Published <input type="checkbox"/> Accepted for Publication <input checked="" type="checkbox"/> Submitted for Publication <input type="checkbox"/> Unpublished and Unsubmitted work written in manuscript style
Publication Details	Evans, MJ , Chinnici, A, Medwell, PR & Ye, J. "Ignition Features of Methane and Ethylene Fuel-Blends in Hot and Diluted Coflows". Submitted to: <i>Fuel</i> .

Principal Author

Name of Principal Author (Candidate)	Michael John Evans
Contribution to the Paper	Co-designed research concept, planned numerical approach, generation of computational fluid dynamics (CFD) data, and analysis of all data, interpreted data, wrote manuscript and acted as corresponding author.
Overall percentage (%)	75
Certification:	This paper reports on original research I conducted during the period of my Higher Degree by Research candidature and is not subject to any obligations or contractual agreements with a third party that would constrain its inclusion in this thesis. I am the primary author of this paper.
Signature	<div style="display: flex; justify-content: space-between; align-items: center;"> <div style="text-align: center;"> <small>Digitally signed by Michael Evans Date: 2016.10.18 20:00:28 +10'30'</small> </div> <div style="border-left: 1px solid black; padding-left: 10px;"> <small>Date</small> 18-Oct-2016 </div> </div>

Co-Author Contributions

By signing the Statement of Authorship, each author certifies that:

- i. the candidate's stated contribution to the publication is accurate (as detailed above);
- ii. permission is granted for the candidate to include the publication in the thesis; and
- iii. the sum of all co-author contributions is equal to 100% less the candidate's stated contribution.

Name of Co-Author	Alfonso Chinnici
Contribution to the Paper	Co-supervised development of work, generated "batch reactor" and "opposed flow" data, helped to evaluate and edit the manuscript.
Signature	<div style="display: flex; justify-content: space-between; align-items: center;"> <div style="text-align: center;">  <small>Alfonso Chinnici 2016.10.19 12:04:50 +10'30'</small> </div> <div style="border-left: 1px solid black; padding-left: 10px;"> <small>Date</small> 19/10/2016 </div> </div>

Name of Co-Author	Paul Ross Medwell
Contribution to the Paper	Supervised development of the work, co-designed and undertook experiments, helped to evaluate and edit the manuscript.
Signature	<div style="display: flex; justify-content: space-between; align-items: center;"> <div style="text-align: center;"> <small>Paul Medwell 2016.10.18 20:04:33 +10'30'</small> </div> <div style="border-left: 1px solid black; padding-left: 10px;"> <small>Date</small> 18-OCT-2016 </div> </div>

Name of Co-Author	Jingjing Ye
-------------------	-------------

Contribution to the Paper	Co-designed and undertook experiments, helped to evaluate and edit the manuscript.			
Signature	JINGJING YE	Digitally signed by JINGJING YE Date: 2016.10.19 14:41:18 +10'30'	Date	19-OCT-2016

Manuscript Number:

Title: Ignition Features of Methane and Ethylene Fuel-Blends in Hot and Diluted Coflows

Article Type: Research paper

Keywords: MILD Combustion; Non-Premixed Flames; Lifted Flames; Autoignition; Fuel Blends

Corresponding Author: Mr. Michael John Evans,

Corresponding Author's Institution: The University of Adelaide

First Author: Michael John Evans

Order of Authors: Michael John Evans; Alfonso Chinnici; Paul R Medwell; Jingjing Ye

Abstract: Turbulent flames in the moderate or intense low oxygen dilution (MILD) combustion regime have previously exhibited less susceptibility to lift-off than conventional autoignitive flames in a jet-in-hot-coflow (JHC) burner. This has been demonstrated through laser-based diagnostics and examination of CH* chemiluminescence. New experimental observations are presented of turbulent flames of natural gas, ethylene and blends of the two fuels, in coflows with temperatures from 1250-1385 K and oxygen concentrations from 3-11% (vol./vol.). Zero- and one-dimensional simulations, as well as turbulent flame modelling, are used to explain the trends seen experimentally with different coflows and fuels. Numerical simulations using simplified batch reactors and opposed-flow flames demonstrate that blending of methane and ethylene fuels is most significant near 1100 K. Near this temperature, pure ethylene exhibits a transition between high and low temperature ignition pathways. Further analyses show that a 1:1 methane/ethylene blend behaves more like ethylene near MILD combustion conditions, and more like methane in conventional autoignition conditions. Two-dimensional modelling results of the turbulent flames are then discussed and explained in the context of the simplified reactor results. The flames confined by the lean flammability-limit in the coflow and high strain-rates in jet shear layer, in agreement with previous work using a semi-empirical jet model. The two-dimensional modelling is additionally able to qualitatively replicate the trends in lift-off height, with normalised heat release rate profiles reproducing, and serving to explain, the effects seen in experimental campaigns.

Suggested Reviewers: Amir Mardani
Assistant Professor, Department of Aerospace Engineering, Sharif
University of Technology
amardani@sharif.edu
Expert in numerical modelling of MILD combustion

Chiara Galletti
Assistant Professor, Department of Civil and Industrial Engineering,
University of Pisa

chiara.galletti@unipi.it
Expert in MILD combustion

Venkateswaran Narayanaswamy
Assistant Professor, Department of Mechanical and Aerospace Engineering,
North Carolina State University
venkat.narayan@ncsu.edu
Expert in non-premixed, turbulent flames stabilised in hot coflows

Marco Derudi
Associate Professor, Dipartimento di Chimica, Materiali ed Ingegneria
Chimica "G. Natta", Politecnico di Milano
marco.derudi@polimi.it
Expert in MILD combustion and chemical engineering

Hao Liu
Professor, State Key Laboratory of Coal Combustion, Huazhong University
of Science and Technology
liuhao@mail.hust.edu.cn
Publishes on modelling MILD combustion.



Mr MICHAEL EVANS

Postgraduate Student

SCHOOL OF MECHANICAL ENGINEERING

The University of Adelaide

SA 5005 AUSTRALIA

TELEPHONE +61 8 8313 5460

FACSIMILE +61 8 8313 4367

m.evans@adelaide.edu.au

26 October 2016

Submission for Publication in *Fuel*

Ignition Features of Methane and Ethylene Fuel-Blends in Hot and Diluted Coflows

Please find enclosed a manuscript that we would like to publish in *Fuel*. This paper has not been submitted for publication elsewhere, but (in original manuscript form, and referenced as such) will form part of the Ph.D. thesis-by-publication of Mr. Michael John Evans. Please find below some suggested reviewers for this manuscript.

- Amir Mardani, Assistant Professor, Sharif University of Technology
amardani@sharif.edu
- Chiara Galletti, Assistant Professor, University of Pisa
chiara.galletti@unipi.it
- Venkateswaran Narayanaswamy, Assistant Professor, North Carolina State University
venkat.narayan@ncsu.edu
- Marco Derudi, Associate Professor, Politecnico di Milano
marco.derudi@polimi.it
- Hao Liu, Professor, Huazhong University of Science and Technology
liuhao@mail.hust.edu.cn

We look forward to hearing from you soon.

Yours sincerely,

Michael J. Evans

Alfonso Chinnici

Paul R. Medwell

Jingjing Ye

Ignition Features of Methane and Ethylene Fuel-Blends in Hot and Diluted Coflows

M.J. Evans*, A. Chinnici, P.R. Medwell, J. Ye

School of Mechanical Engineering, The University of Adelaide, South Australia, Australia

Abstract

Turbulent flames in the moderate or intense low oxygen dilution (MILD) combustion regime have previously exhibited less susceptibility to lift-off than conventional autoignitive flames in a jet-in-hot-coflow (JHC) burner. This has been demonstrated through laser-based diagnostics and examination of CH* chemiluminescence. New experimental observations are presented of turbulent flames of natural gas, ethylene and blends of the two fuels, in coflows with temperatures from 1250-1385 K and oxygen concentrations from 3-11% (vol./vol.). Zero- and one-dimensional simulations, as well as turbulent flame modelling, are used to explain the trends seen experimentally with different coflows and fuels. Numerical simulations using simplified batch reactors and opposed-flow flames demonstrate that blending of methane and ethylene fuels is most significant near 1100 K. Near this temperature, pure ethylene exhibits a transition between high and low temperature ignition pathways. Further analyses show that a 1:1 methane/ethylene blend behaves more like ethylene near MILD combustion conditions, and more like methane in conventional autoignition conditions. Two-dimensional modelling results of the turbulent flames are then discussed and explained in the context of the simplified reactor results. The flames confined by the lean flammability-limit in the coflow and high strain-rates in jet shear layer, in agreement with previous work using a semi-empirical jet model. The two-dimensional modelling is additionally able to qualitatively replicate the trends in lift-off height, with normalised heat release rate profiles reproducing, and serving to explain, the effects seen in experimental campaigns.

Keywords: MILD Combustion, Non-Premixed Flames, Lifted Flames, Autoignition, Fuel Blends

1. Introduction

Moderate or intense low oxygen dilution (MILD) combustion has been the subject of previous investigations due to its potential to reduce pollutant emissions and increase thermal efficiency in practical systems [1]. This combustion regime has already been successfully implemented in furnaces and burners with strong recirculation [2–4], and similar systems have been suggested for applications such as gas turbines [5], however further fundamental understanding is required for MILD combustion in these applications [6].

Previous experimental studies of non-premixed MILD combustion have been undertaken in jet-in-hot-co/cross-flow (JHC) burners [7–20]. These studies have investigated the combustion of gaseous, pre-vaporised

*Corresponding author. E-mail: m.evans@adelaide.edu.au, Tel.: +61 8 8313 5460, Fax: +61 8 8313 4367.

liquid and solid fuels under MILD combustion conditions, and in the transition between the MILD and conventional autoignitive combustion regimes. Among these, studies of natural gas (NG) and C_2H_4 have demonstrated non-monotonic trends in visual lift-off height with changing oxidant O_2 level [12, 19]. These trends are evident in laminar and turbulent flames in the transition between MILD and autoignitive combustion regimes, however, the underlying mechanisms behind these trends remain unresolved [12]. The flame structure and stabilisation mechanisms of non-premixed flames in the transition between MILD combustion and conventional, lifted, autoignitive flames are not very well understood [12, 19, 21], and exhibit significant instability and sensitivity to ambient conditions [2, 12, 13, 22].

The ignition of MILD flames has been widely investigated in premixed, homogeneous reactors [23–27]. These studies have used different measures of ignition to define ignition delay, such as the time required for a 10-K increase above the unreacted mixture temperature [23–25], or the onset of thermal runaway [26–28]. This initial temperature increase occurs almost simultaneously with thermal runaway in conventional autoignition, however these do not coincide during the more gradual ignition processes in MILD combustion [21]. Ignition processes in MILD combustion, have shown good agreement with a 10-K temperature increase threshold in predicting ignition delay and the onset of chemiluminescence [21, 23–25]. Although simplified reactors may be used to provide an estimate for the ignition delay of a homogeneous chemical mixture, neither well-stirred nor plug-flow reactors can provide insight on the effects of mixing, strain-rate or diffusion encountered in practical combustion systems.

Numerical modelling of non-premixed MILD combustion has been previously undertaken using opposed-flow simulations to build on the understanding of flame structure and stabilisation. Simplified opposed-flow flames have previously been used to predict species distributions within turbulent flames in mixture fraction (Z) space [7, 29], and to explain the distribution of species and heat release rate (HRR) within MILD flames [30, 31]. This modelling approach has additionally been used to assess the stability [10, 26] and ignition behaviour [10, 19, 21, 27] of MILD flames. These studies have suggested that MILD flames are stabilised through partial premixing of O_2 into the fuel stream [10], however transient analysis of opposed-flow flames determined that this simplified configuration is inappropriate for modelling ignition delay [21] without a reasonable estimate of the underlying physical flow-field [19].

The flow-field of a JHC burner may be modelled using CFD with a Reynolds-averaged Navier-Stokes (RANS) approach. The RANS approach has been used for the validation and verification of combustion models, with MILD combustion shown to require finite-rate chemistry modelling due to Damköhler numbers (Da) of order unity [32, 33]. Several modelling attempts have been made to compare combustion models against previously obtained experimental results using RANS and the eddy dissipation concept (EDC) combustion model [32–44] or higher-fidelity large-eddy simulations [45–47]. These studies have predominantly been for model validation or focussed on the structure of the flames downstream. Beyond the coflow-controlled region, however, the simulated oxidant composition is heavily dependent on the model boundary conditions and the flame is greatly affected by the entrainment of cold, ambient air [36]. Although RANS modelling studies with adjusted EDC constants have shown reasonable agreement with experimental data [35, 39, 40], there has been very little work using this approach to develop understanding of flame stabilisation in the

MILD combustion regime, or replicating the trends seen experimentally under these conditions [9, 12].

Many studies of MILD combustion have focussed on CH_4 – the primary constituent of NG [48], or C_2H_4 – an important intermediate in the combustion of larger hydrocarbons [48, 49]. Both of these fuels have previously been studied issuing into identical coflows, suggesting very similar ignition characteristics, however these were mixed with H_2 (1:1 by vol.), serving to stabilise the flames [11]. In the MILD combustion of CH_4 , CH_3 recombination serves to slow the overall reaction [25], and non-premixed combustion occurs without any regions of negative HRR [30]. At temperatures below approximately 1000 K, the ignition delay of CH_4 has displayed a negative temperature coefficient (NTC) region due to competition between the CH_3 pathway and a preference for ignition via the H_2 branching pathway at high temperature [24, 50]. The oxidation pathway of C_2H_4 in MILD combustion is through H abstraction to C_2H_3 and then to C_2H_2 [39, 48]. This process therefore also leads to significant production of H_2 at temperatures near 1000 K, similar to the operating conditions in previous investigations with a JHC burner [9]. The unique environment in MILD combustion suggests that the H_2 ignition pathway may be more pronounced under MILD conditions for both C_2H_4 and CH_4 combustion.

Both CH_4 and C_2H_4 are produced in significant quantities during combustion of larger hydrocarbons [49] and are key species in combustion systems using combinations of NG and other, larger hydrocarbon fuels. Blends of CH_4 and C_2H_4 have been previously studied numerically and experimentally to assess the chemical and physical effects on flame speed of mixtures of these fuels at room temperature and ignition delay of dilute mixtures [51, 52]. Analyses of CH_4 and C_2H_4 blends have shown that the flame speed of the mixture is more heavily dependent on kinetic influences than physical effects [52]. Kinetic analysis of different blends of CH_4 and C_2H_4 indicates that C_2 chemistry becomes significant for mixtures with more than 10% C_2H_4 [51]. The same study found that beyond this concentration, the reaction of $\text{C}_2\text{H}_4 + \text{OH} \rightarrow \text{C}_2\text{H}_3 + \text{H}_2\text{O}$ overwhelms $\text{CH}_4 + \text{OH} \rightarrow \text{CH}_3 + \text{H}_2\text{O}$ [51]. Further to this scavenging reaction, the reaction of atomic O with C_2H_4 , has been shown to favour CH_3 formation below temperatures near 1000 K [53]. However, it has not been determined how significant concentrations of C_2 -species, or the recombination of CH_3 in a blend of CH_4 and C_2H_4 fuels, change the flame behaviour during ignition and flame stabilisation in hot oxidants. The interaction between CH_4 and C_2H_4 under MILD conditions is unknown, although it is relevant for potential fuel blends of NG and larger hydrocarbon fuels.

Simplified reactors have been used to provide insight into the processes involved in ignition under MILD combustion conditions, however further work is required to explain the non-monotonic trends in lift-off height across the boundary of the MILD combustion regime. To meet these needs, this work will investigate trends from experimental observations and compare them against predictions from simplified reactors and RANS modelling. This will be used to assess whether trends in lift-off height may be described as the effects of ignition delay or flame extinction, or whether a more complete description of the flow-field is required. This study will not only investigate trends in the transition between the MILD and autoignitive combustion regimes, but will shed light on the ignition features of $\text{CH}_4/\text{C}_2\text{H}_4$ fuel blends in a hot and diluted conditions, to advance the current understanding of ignition processes under MILD combustion conditions.

Table 1: Experimental coflow compositions (% vol./vol.) and stoichiometric mixture fractions (Z_{st}) for different fuel compositions (ratios by vol.). Coflows are nominally 1250, 1315 or 1385 K.

Oxidiser composition (%)				Stoichiometric mixture fraction (Z_{st})				
O ₂	H ₂ O	CO ₂	N ₂	NG	2:1 NG/C ₂ H ₄	1:2 NG/C ₂ H ₄	C ₂ H ₄	
3.0	10.7	3.6	82.7	0.009	0.009	0.010	0.010	
6.0	10.7	3.6	79.7	0.017	0.019	0.020	0.020	
9.0	10.7	3.6	76.7	0.026	0.028	0.029	0.030	
11.0	10.7	3.6	74.7	0.031	0.033	0.035	0.036	

2. Methods

2.1. Experimental Observations of Turbulent Jet Flames

Photographs were taken of turbulent flames in a jet-in-hot-coflow (JHC) burner, which has been used widely in previous studies [7–12, 18, 19]. The JHC burner features a fuel jet issuing from a 4.6-mm-diameter pipe (with a length >100 times the pipe diameter) into a concentric coflow of hot combustion products from an 82-mm-diameter secondary burner. This results in a coflow-controlled environment extending approximately 100 mm downstream. The various compositions of the coflow are given in Table 1. The fuel issuing from the central jet of the JHC burner is natural gas (NG, $\geq 92\%$ CH₄), C₂H₄ or a blend in ratios of 1:2 or 2:1 (by vol.). In each case, the jet has a bulk Reynolds number (Re) of 10 000.

Photographs of turbulent flames in the JHC were taken using a Canon EOS 60D SLR camera, fitted with a 50 mm, $f_{\#}1.8$ lens. Photographs were taken with manual settings (including white balance), with the details presented later. Visual lift-off heights were determined by isolating the blue channel of these photographs, inverting them and identifying an “unequivocal” flame base or a weak-to-strong transition, similar to method of Medwell and Dally [12]. Additionally, the first instance of chemiluminescence was also identified from photographs of the same flame. In the absence of soot, the blue channel is taken to indicate CH* chemiluminescence at 430 nm [54].

2.2. Numerical Simulations of Simplified Reactors and Turbulent Jet Flames

Ignition delays of CH₄, C₂H₄ and CH₄/C₂H₄ fuels were evaluated using stoichiometric, constant pressure, batch reactors using the AURORA routine from the CHEMKIN software package. Ignition delay of these mixtures was taken to be the time required for a 10-K increase in temperature, based on previous analysis of premixed reactors [23–25]. The initial temperature is considered to be the oxidiser temperature. This temperature has been shown to be approximately equal to the temperature of the most-reactive mixture [55] in C₂H₄ flames with hot and diluted oxidants [21]. The oxidant stream is composed of 3–12% O₂ (vol./vol.), with other species described in Table 2 and with temperature in the range from 1100 to 1500 K. These compositions and temperatures are similar to those used experimentally in this, and previous [8–12, 18, 19], studies. Additional calculations were performed to include minor species in the coflow composition, as previous studies have highlighted the importance of intermediary species as additives and as part of the oxidant minor species pool [26, 27, 40, 42, 56–59]. In these cases, the oxidants were based on equilibrium calculations of the coflow stream, with the minor species pool including all species with mole fractions greater than 10⁻¹⁰ (0.1 ppb). The fuel stream is one of either CH₄, C₂H₄ or a blend of CH₄ and C₂H₄. This blend

Table 2: Simulated oxidant streams compositions (% vol./vol.) for simplified reactors and RANS models. Oxidants range from 1100-1500 K, and are 1100, 1300 or 1500 K for opposed-flow flames and RANS models.

Oxidiser composition (%)			
O ₂	H ₂ O	CO ₂	N ₂
3	10	3	84
6	10	3	81
9	10	3	78
12	10	3	75

is 1:1 in all analyses except that for Fig. 5, which features pure CH₄, a blend with 5% C₂H₄, and then blends from 10% C₂H₄ to pure C₂H₄ in 10% increments. All ratios and percentages are given by volume.

Non-premixed opposed-flow flames were simulated using the CHEMKIN OPPDIF routine, with fuel and oxidiser stream velocities chosen with equal momentum, resulting in a stagnation plane at $Z = 0.5$. Flames were initially simulated at low strain-rates which was gradually increased until flame extinction was identified. The different oxidiser compositions are given in Table 2 and had temperatures of 1100, 1300 or 1500 K.

Reynolds-averaged Navier-Stokes (RANS) modelling of CH₄, C₂H₄ and 1:1 CH₄/C₂H₄ flames was undertaken using ANSYS FLUENT 14.5. The current study used the same axisymmetric domain, and turbulence, radiation and combustion models, which have been described in a previous study to model visual lift-off in the same burner [40]. The flow-field is modelled using the standard k - ε turbulence model with $C_{1\varepsilon}$ modified to 1.6 from 1.44 [60]. Turbulence-chemistry interactions are modelled using the eddy-dissipation concept (EDC) combustion model with the constants C_ξ and C_τ modified from 2.1377 and 0.4082 to 1.0 and 3.0, respectively [40], consistent with previous studies of similar configurations [35, 37–40, 42]. In contrast to the previous study with the same domain [40], the number of elements in mesh was increased by a factor of four upstream of the jet exit plane and in the first 40 mm downstream of the jet exit plane, within a radius of 15 mm, to provide better resolution in Z -space. This refined mesh had a negligible impact on the solution in the refined region or further downstream. The RANS model was used to simulate the same combinations of fuel and oxidiser as the simplified reactors, with oxidiser compositions given in Table 2 with temperatures of 1100, 1300 or 1500 K. Fuels used were pure CH₄, C₂H₄ and a 1:1 (by vol.) blend of the two. Fuel temperature was 305 K with a jet bulk-velocity maintained at 17.7 m/s. Coflow bulk-velocities were set to 2.3 m/s, similar to previous experiments [8, 9].

The December 2014 version of the POLIMI C1-C3 high and low temperature kinetics scheme (for hydrocarbon fuels with up to three carbon atoms) with 107 species and 2642 reactions [61] was used to simulate CH₄, C₂H₄ and 1:1 CH₄/C₂H₄ combustion in the simplified reactors. A reduced version of this kinetics scheme was generated using the DoctorSMOKE++ kinetics reduction code, based on a species-targeted sensitivity analysis to ignition delay and flame speed [62]. This has previously been used for the reduction of larger hydrocarbon fuel mechanisms [63], and is a similar method [64] used by a previous study focussing on C₂H₄ fuel [21]. The resulting reduced scheme for this study has 49 chemical species and 365 reactions and was used for the RANS simulations.

3. Experimental Results

3.1. Observations of Turbulent Jet Flames in Hot and Diluted Flames

Photographs of a NG flame, a pure C₂H₄ flame and two blends of NG and C₂H₄ issuing into 1315-K coflows with 3 and 9% O₂ (vol./vol.), are shown in Fig. 1. Photographs of flames in 3% O₂ coflows were taken with exposure times of 4 s to demonstrate the relative chemiluminescent intensity of the flames and determine the “unequivocal maximum lift-off height” [12]. Photographs of flames in coflows with 9% O₂ (vol./vol.) at 1315 K (Fig. 1), were taken with exposure times of 0.5 s to minimise saturation near the flame bases. The decreasing lift-off height with increasing C₂H₄ concentration can be seen immediately from Fig. 1. This is a result of the increased reactivity of C₂H₄ relative to NG.

No flames stabilised in coflows with 3% O₂ feature well-defined flame bases, with chemiluminescence gradually intensifying with downstream distance (Fig. 1). Very faint NG flames stabilised in a 1315-K coflow with 3% O₂ are not clearly visible from photographs with 4 s exposure times, although long-exposure photographs reveal that they are attached to the jet exit plane. Downstream, the C₂H₄ flame demonstrates significant luminescence due to the presence of soot, which additionally illuminates the image background. The sooty region is, however, beyond the coflow-controlled region where flame is significantly affected by ambient air entrainment, and outside of the scope of this study. The absence of soot in the coflow-controlled region, conversely, has previously been used to indicate that such flames are within the MILD combustion regime [9, 12, 65].

Blends of NG and C₂H₄ fuels issuing into 1300-K coflows with 3% O₂ feature qualitatively similar flame base structures (see Fig. 1). The strong blue colour of the flames are, like both the NG and C₂H₄ flames, in the coflow-controlled region (hence, free of soot). Flame lift-off height decreases, and chemiluminescence intensity increases, monotonically with increasing proportions of C₂H₄ in the fuel jet. Downstream of this region, however, the 1:2 NG/C₂H₄ flame produces significant amounts soot, similar to the C₂H₄ flame.

The NG flame issuing into a 1315-K coflow with 9% O₂ appears to exhibit a “transition point” from gradual ignition to a distinct flame base [9, 12, 66]. This transition point can be described as a sudden change from faint chemiluminescence to a brighter, more intense flame, corresponding to a shift from “weak to strong OH levels” [9]. Flames with one-third or more C₂H₄, all appear lifted with distinct transition points, similar to previous observations of C₂H₄ flames [9, 12]. This suggests a different ignition mechanism between the NG flames and those with C₂H₄, which may be driven by turbulence-chemistry interactions, or chemistry alone.

3.2. Visual Lift-off of Turbulent Jet Flames in Hot and Diluted Flames

Figure 2 presents plots of the range of visual lift-off heights of NG/C₂H₄ flames against the percentage of C₂H₄ in the fuel for different coflow conditions given in Table 1. Each plot in Fig. 2 shows the trends for different O₂ levels at a single coflow temperature. The lift-off heights of pure C₂H₄ flames in coflows of different temperatures are shown separately, including coflows with 6% O₂, in Fig. 3.

Ranges of visual lift-off shown in each plot extends from the first visual indication of chemiluminescence to the “unequivocal maximum lift-off height” [12] from photographs taken with 4 s exposure times. This

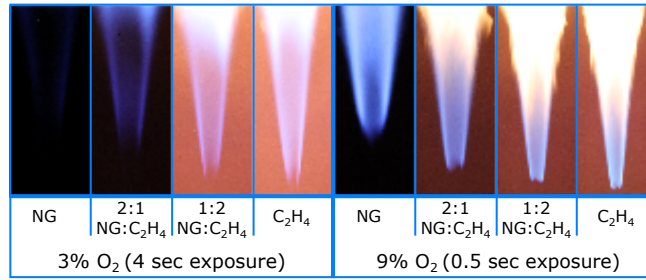


Fig. 1: Flames with different fuel compositions in 1315-K coflows with 3% (left) and 9% (right) O₂ (vol./vol.). The images are 65 mm × 150 mm, with ISO-1600, $f_{\#}$ 16, and 4 or 0.5 s exposure times. The jet exit plane is at the bottom edge of the photographs.

approach captures the low spatial-gradients of chemiluminescence in low luminosity flames, where a definite ‘flame base’ cannot be identified [12]. As previously mentioned, NG flames stabilised in 1315-K coflows with 3% O₂ exhibit very low luminosity (recall Fig. 1), however, long-exposure photographs reveal these are stabilised as very faint, attached flames. No NG flames could be stabilised in 1250-K coflows with 3% O₂, hence their absence from Fig. 2.

Flames stabilised in 1250 and 1315-K coflows with $\lesssim 6\%$ O₂ and $\gtrsim 9\%$ O₂ exhibit different lift-off behaviours (Fig. 2). Flames stabilised in coflows with $\lesssim 6\%$ O₂ demonstrate a trend of decreasing lift-off height with decreasing coflow O₂ level, whereas lift-off height decreases with increasing coflow O₂ level for $\gtrsim 9\%$ O₂. In each case, flames in coflows with 3% O₂ exhibit the lowest spatial-gradient in chemiluminescence (represented graphically by the larger bars in the plots), with this gradient being lowest for flames with large concentrations of NG as fuel. These observations are consistent with those from a previous study of NG and C₂H₄ fuels [12], with a subsequent study hypothesising that this may be a result of the shifting location of the most-reactive Z with respect to the shear layer [19]. This is seen for all flames in 1250- and 1315-K coflows, as well as for pure C₂H₄ (Fig. 3) and NG (not shown for brevity) flames at different temperatures, although the variation in lift-off heights lessens at higher temperatures. These results strengthen the need for further analysis to assess if this is a purely chemical phenomenon, or a result of interactions with the jet flow-field.

4. Ignition and Extinction in Simplified Reactors

4.1. Ignition Delays of Simple Hydrocarbons

The ignition delays of C₂H₄, CH₄ and a 1:1 blend of both pure fuels (by vol.), are presented as a function of $1000/T$ in Fig. 4. Oxidant compositions are given in Table 2. In each case, ignition delay is defined as the time taken for a 10-K increase in temperature in the batch reactor.

Figure 4 presents a plot showing the ignition delay of pure C₂H₄ as a function of temperature with three 3, 6 and 9% O₂. This figure indicates two separate trends in the ignition delays, below 1000 K and above 1200 K, which are more strongly dependent on temperature and oxidant O₂ level respectively. These trends are the result of previously reported competition between H₂ ignition below 1000 K, and the high temperature C₂ ignition pathway in C₂H₄ combustion [48]. The ignition delay times collapse to similar values for all three oxidant compositions in the transition between these ranges, near 1100 K.

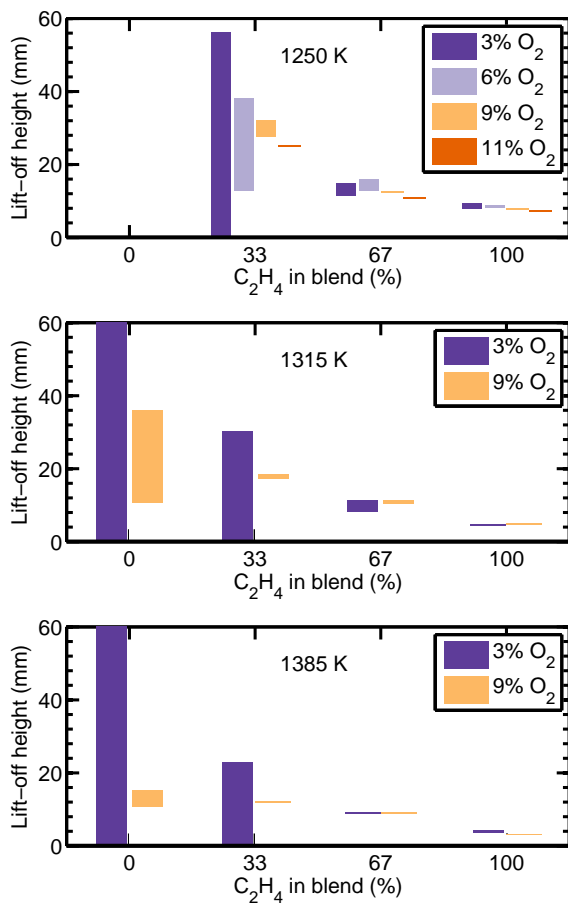


Fig. 2: Variation in lift-off heights of NG/C₂H₄ and C₂H₄ flames, in 1250, 1315, and 1385-K coflows. Lift-off height range is defined as initial observable chemiluminescence to that seen at ISO-1600, $f_{\#}$ 16 and a 4 s exposure time. Lift-off heights are plotted against %C₂H₄ in the fuel jet (by vol.), and coloured by coflow O₂ level.

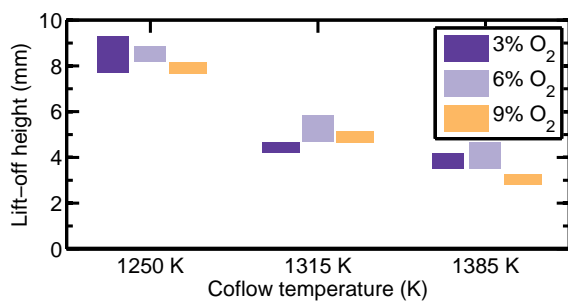


Fig. 3: Variation in lift-off heights of C₂H₄ flames in 1250, 1315, and 1385-K coflows, and coloured by coflow O₂ level.

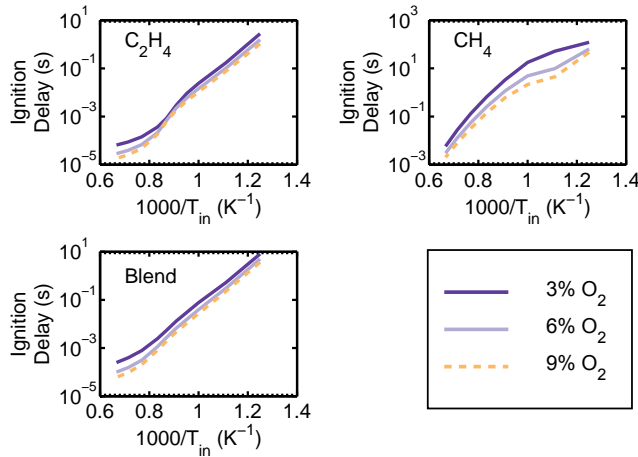


Fig. 4: Ignition delay times of CH_4 , C_2H_4 and 1:1 blend of $\text{CH}_4/\text{C}_2\text{H}_4$ with oxidants comprising of $\text{O}_2/\text{H}_2\text{O}/\text{CO}_2/\text{N}_2$ only.

At low temperatures, HO_2 is formed in preference to OH [48] and the oxidation of C_2H_4 by atomic O favours the production of CH_3 and HCO over the more reactive CH_2O and CH_2CHO [53]. This in turn, influences the oxidation and recombination pathways of CH_3 are, which are highly sensitive to temperature near 1000 K [24]. At high temperatures, the effects of oxidant O_2 level become more influential than variations in initial temperature. This is in line with the dominance of C_2 chemistry [48], and a reduction in both CH_3 formation [53] and recombination [24] – both favouring CH_2O production. These results appear to contradict the experimental trends of lift-off height presented in Fig. 2, which exhibit less change with O_2 in higher temperature coflows. The combination of these results suggests that ignition delay alone may not be sufficient to explain the onset of chemiluminescence seen experimentally, which is consistent with other studies of the MILD combustion regime [27].

The collapse in ignition delay near 1100 K may be compared with previous experimental observations of turbulent C_2H_4 flames stabilised in coflows of the same temperature with 3 and 9% O_2 [9]. This previous study reported the existence of a “weak $[\text{OH}]$ tail” below the visual flame base in the 9% O_2 case [9]. The flame in the 3% case was reported as being faint but, nonetheless, attached [9]. In both cases, thin OH structures appeared to extend towards the jet exit plane [9]. These structures have been hypothesised as laminar flames igniting in the lean side of the jet shear layer in conditions closely resembling the coflow velocity (2.3 m/s [9]) and temperature [19]. The ignition delays under these conditions (2-3 ms) suggest that the heat release from these flames would initiate within the first few millimetres downstream of the jet exit plane. This is consistent with the experimental findings of Medwell *et al.* [9], but cannot explain the associated “weak to strong” transition [9].

Ignition delays for pure CH_4 in oxidants with 3, 6 and 9% O_2 at stoichiometric conditions are presented in on the same set of axes in Fig. 4. The ignition delays for CH_4 do not exhibit any collapse similar to the C_2H_4 ignition profiles, and are, additionally, approximately 1-2 orders of magnitude longer than ignition of C_2H_4 . This trend is significantly different to the experimental results (see §3), where NG flames appeared attached, or with lift-off heights of the same order of magnitude as the C_2H_4 flames. This suggests that the NG flames observed experimentally may be stabilised through mechanisms other than autoignition, such as

propagation upstream, highlighting the need for more complex analyses of these flames.

The profiles of ignition delay of CH_4 and oxidants with 6 or 9% O_2 versus $1000/T$ both feature changes in slope with inlet temperatures near 900 K. This slope change has previously been described as negative thermal coefficient (NTC) behaviour in the context of CH_4 [24]. Negative thermal coefficient behaviour has previously been observed experimentally in a plug-flow reactor and investigated in depth using detailed kinetics [24]. The behaviour is due to the competition between high and low temperature pathways for CH_2O formation [24]. The onset of NTC can be seen using the oxidant with 3% O_2 , with the profile of ignition delays becoming less sensitive to temperature changes below 1000 K. This indicates that the NTC region is shifted towards significantly lower temperatures, and that the previously identified low temperature pathways of CH_4 from CH_3O_2 to CO , and H_2 [24] become less dominant, in very low O_2 mixtures. Thus the ignition behaviour of CH_4 in oxidants with 3% O_2 cannot simply be extrapolated from trends recognised at higher O_2 levels. A similar conclusion may be drawn from the experimental trends in Fig. 2, where NG flames exhibit different trends with changing O_2 level in coflows of different temperatures.

Figure 4 shows the profiles of ignition delay for a 1:1 blend of CH_4 and C_2H_4 . The profiles do not show the features seen in either of the pure C_2H_4 or CH_4 fuels, namely the collapse in ignition delay times or an NTC region, respectively. This suggests that the blending of the two pure fuels inhibits the competition between chemical pathways and resulting response of ignition delay to initial temperature is smoothed. The ignition delay profile of the fuel blend follows the general shape of the C_2H_4 curves, but with a less significant change of slope near 1100 K. Compared to pure C_2H_4 , the ignition of the blend is delayed by a factor of approximately 2-3 below 1000 K, and a factor of 3-5 above 1200 K. The blending of CH_4 and C_2H_4 in equal parts results in similar trends in ignition delay for all three oxidants. These similarities suggest that trends observed in the ignition of the blended fuel mixture in oxidants with 9% O_2 may be used to predict combustion in oxidants with as low as 3% O_2 . This ability to extrapolate is an advantage over pure CH_4 or C_2H_4 fuels (due to the different trends in oxidants with 3% O_2), and may be achieved without significant sacrifices in ignition delay relative to pure C_2H_4 .

Changes in ignition delay of a CH_4 and C_2H_4 fuel, blended in different ratios, are shown in Fig. 5. These plots show the smooth changes in ignition delay times from pure CH_4 , to pure C_2H_4 , fuels with initial temperatures of 800, 1100 and 1500 K. The largest rate of change coincides with the transition between pure CH_4 and the blend with 5% C_2H_4 . This is most prominent at 1100 K, with the largest changes occurring with an oxidant of 3% O_2 . Under these conditions, the inclusion of 5% C_2H_4 results in a four-fold reduction in ignition delay relative to the CH_4 case. This change is significantly greater than reductions by a factor of approximately two at either 800 or 1500 K.

The inclusion of 10% C_2H_4 in the fuel blend results in a four-fold decrease in ignition delay in the 800 K mixtures, and a three-fold decrease at 1500 K, compared with pure CH_4 . Conversely, the change at 1100 K is a full order of magnitude between pure CH_4 and with the addition of 10% C_2H_4 . This coincides with the collapse in ignition delay observed in Fig. 4, which is also evident in Fig. 5.

The ignition delays presented in Figs. 4 and 5 were calculated using oxidants composed of major species – O_2 , H_2O , CO_2 and N_2 – only. In order to gauge the effect of minor species on ignition delay, calculations

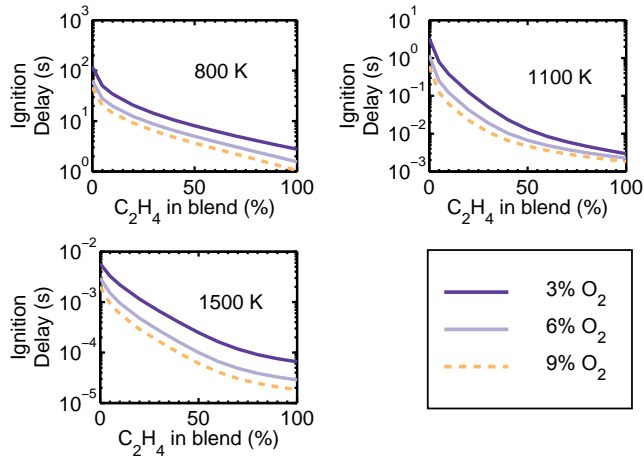


Fig. 5: Ignition delay times for stoichiometric blends of CH_4 and C_2H_4 , and oxidants with 3, 6 or 9% O_2 . Initial temperatures are 800, 1100 and 1500 K.

were performed using a detailed description of the oxidants at 1300 K. The inclusion of the minor species pool reduces the ignition delay of C_2H_4 by 20-40% for oxidants with 3-9% O_2 . The maximum change of 40% occurs in the oxidant with 3% O_2 . Ignition delay with the oxidant with 9% O_2 , conversely, only changes by 20%. The relative changes in ignition delays for CH_4 flames due to the inclusion of the minor species pool are negligible, however result in a 15-25% reduction in all ignition delays for the 1:1 $\text{CH}_4/\text{C}_2\text{H}_4$ fuel blend (with the greatest change in the 3% O_2 case). This observation that the inclusion of minor species in zero-dimensional reactors more significantly impacts C_2H_4 ignition than CH_4 is in agreement with conclusions drawn in a previous study [27]. These findings demonstrate both the importance of minor species in perfectly-stirred reactor models and the effect of CH_4 in mitigating the changes in ignition delay due to initial concentrations of minor species.

4.2. Extinction Strain Rates of Simple Hydrocarbon Flames

Figure 6 shows plots of extinction strain-rate versus oxidant temperature for oxidants with 3, 6 and 9% O_2 . Each plot shows extinction strain-rates for pure C_2H_4 , pure CH_4 and a 1:1 blend of $\text{CH}_4/\text{C}_2\text{H}_4$. The composition of each oxidant is the same as those used for the ignition delay calculations, with 10% H_2O , 3% CO_2 (vol./vol.), balanced with N_2 . The inclusion of the minor species pool in the oxidant description was found to have a negligible impact on the steady-state opposed-flow flames.

The profiles of extinction strain-rate for the oxidant with 3% O_2 are shown as a plot in Fig. 6. In this plot, the extinction strain-rate of C_2H_4 flames increases linearly above 1100 K, with the $\text{CH}_4/\text{C}_2\text{H}_4$ blend following a similar trend. The first signs of ignition in the fuel blend are delayed by ≈ 200 K relative to pure C_2H_4 . Pure CH_4 flames, however, are not sustained with oxidants containing 3% O_2 at any temperature in this range. The addition of CH_4 to C_2H_4 , however, does not have a significant effect on extinction strain-rates above 1100 K, compared with pure C_2H_4 . The effect of CH_4 at the lower temperatures may be, in part, due to the slow conversion rate of $\text{CH}_3 \rightarrow \text{CH}_2\text{O}$ below 1200 K [48].

The absence of any opposed-flow CH_4 flames in oxidants with 3% O_2 is in contrast to the experimental results, with NG flames stabilising in 1315-K (and hotter) coflows with 3% O_2 (see Fig. 2). This discrepancy

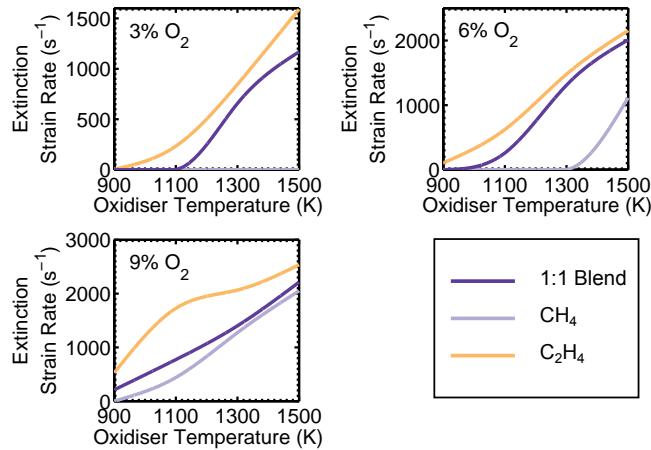


Fig. 6: Extinction strain-rates of flames with different fuel combinations and oxidants at different temperatures with different O_2 concentrations.

between the simulations and experimental results may indicate that NG flames in this JHC configuration do not ignite as opposed-flow flames.

Both pure C_2H_4 and the 1:1 CH_4/C_2H_4 blend flames feature similar extinction strain-rates above 1300 K with oxidants including 6% O_2 (see Fig. 6). The difference between these extinction rate profiles is more significant at lower temperatures and are within 15% at 1300 K and within 5% at 1500 K. This may be associated with a decrease in CH_3 recombination, which is known to retard the ignition process [24].

Figure 6 shows that oxidant streams with 9% O_2 result in flames for all fuels, with the extinction strain-rate of the fuel blend closer to that of pure CH_4 than pure C_2H_4 for every oxidant temperature. This is most pronounced above 1300 K, where extinction strain-rates of the blend are within 10% of those for pure CH_4 . These results are in contrast to cases with 3 or 6% O_2 in the oxidant stream, where extinction strain-rates closely follow profiles of C_2H_4 flames. This demonstrates that C_2H_4 is increasingly dominant over CH_4 in fuel blends with decreasing oxidant O_2 . A similar trend was also seen with ignition delay, recalling Fig. 5. These results show that the characteristics of CH_4/C_2H_4 fuel blends do not consistently follow the trends of either pure fuel in combustion with hot and diluted oxidants, but appears to have a preferred tendency towards one fuel or the other under different conditions. This may be a combination of the competition between $C_2H_4 + OH$ and $CH_4 + OH$ [51], and the preference of $C_2H_4 + O$ to form CH_3 below 1100 K [53], which is dominant in CH_4 ignition and preferentially recombines under MILD conditions [25]. The shifting preference towards one fuel or the other was not seen in previous studies of flame speed [51, 52] or extinction [51], although these studies focussed on initially cold mixtures of fuel and air [51, 52] or the effects of changes in ambient pressure [51].

5. Turbulent Simulations of Simple Hydrocarbon Flames

Two-dimensional modelling of jet flames using CFD may be used to provide insight into the interactions between combustion chemistry and the turbulent flow-field. In the simulations presented, reactions were present, with varying levels of net, positive heat release, at the jet exit plane in all cases.

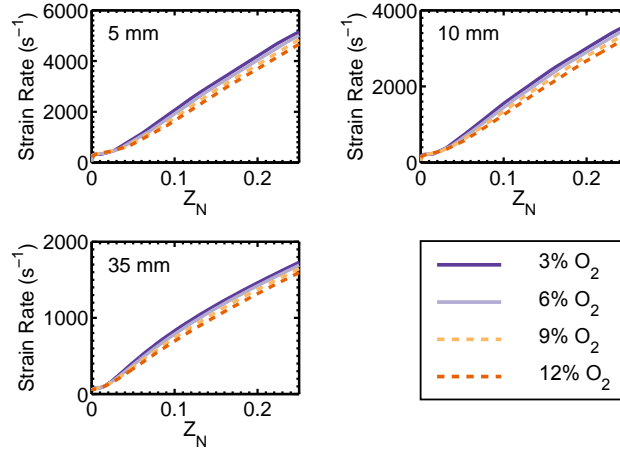


Fig. 7: Profiles of strain rates versus Z_N at different downstream locations from RANS modelling of C_2H_4 flames in 1300-K coflows with different compositions. Clockwise from top left-hand plot: 5 mm, 10 mm and 35 mm downstream.

Figure 7 shows profiles of strain-rate against normalised mixture fraction (Z_N) [9, 67] for C_2H_4 issuing into 1100-K, 1300-K and 1500-K coflows with 3, 6 or 9% O_2 . This normalisation ensures values of $Z_N = 1$ and 0 at the fuel and hot coflow inlets, respectively [9]. The three plots show the profiles of strain-rate at distances of 5, 10 and 35 mm downstream of the jet exit plane. These profiles are all within the coflow-controlled regions of the flame (refer to §2.1). These profiles all collapse in Z_N -space at each oxidant temperature, demonstrating that the relationship between Z_N and the flow-field does not change with changing coflow O_2 concentrations. The relationship is consistent with the assumptions made in a previously implemented, simplified model for jet mixing used to approximate the flow-field of a JHC burner [19]. The agreement between the modelled strain-rate fields is particularly good for low values of Z_N (below 0.025), near and below the stoichiometric mixtures of these flames (refer to Table 1). This is the range of Z_N where ignition is anticipated, initially occurring at the most reactive mixture fraction ($Z_{mr} < Z_{st}$, where $Z_{st} \sim 0.025$) [21, 55]. This region of low Z_N additionally corresponds to minima in axial velocities and the local turbulent Reynolds number, due to the boundary layers along the burner walls separating the jet and coflow streams (refer to §S1 in the Supplementary Data). Strain-rates increased by approximately 10% (for $Z_N > 0.025$) in more dense, 1100-K coflows, whereas strain-rates were decreased by approximately 15% (for $Z_N > 0.025$) in 1500-K coflows.

The plots in Figs. 8-9 show profiles of net heat release rate (HRR) and OH number density (n_{OH}) as a function of Z_N from two-dimensional RANS modelling. The cases presented show profiles from C_2H_4 flames issuing into 1100-K (Fig. 8) and 1300-K (Fig. 9) coflows with 3, 6 or 9% O_2 (vol./vol.) at three different downstream locations. Coflow compositions including the equilibrium minor species pool were assessed at 1300 K, but these did not have any significant impact on the results. This is consistent with previous studies of the effects of low concentrations (~ 10 ppm) of minor species in RANS models of turbulent flames [40].

Profiles of HRR in Z_N -space from C_2H_4 flames issuing into 1300-K coflows with coflows with 3, 6 or 9% O_2 are presented in Fig. 9. These profiles show the relative intensity of HRR between the three different flames, at three downstream locations. At a distance of 5 mm from the jet exit plane the peak HRR shifts

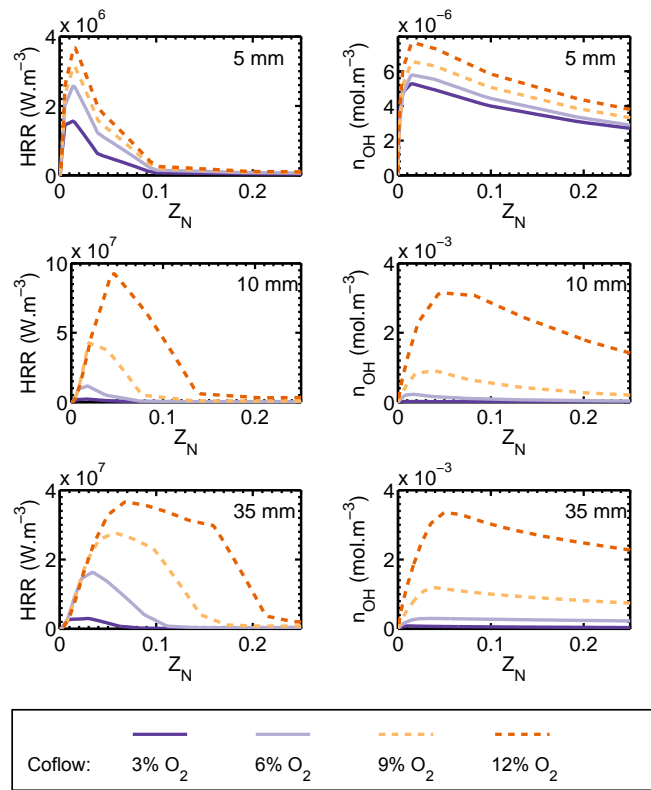


Fig. 8: Net heat release rate (HRR, left) and OH number density (n_{OH} , right) at three different downstream locations in RANS models of C_2H_4 flames in 1100-K coflows with different compositions. Data taken from 5 mm, 10 mm and 35 mm downstream.

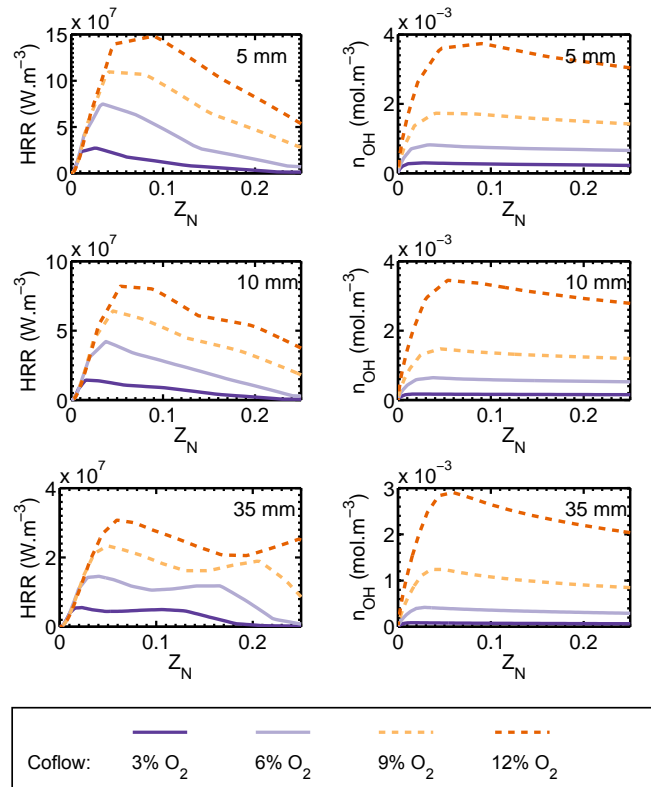


Fig. 9: Net heat release rate (HRR, left) and OH number density (n_{OH} , right) at three different downstream locations in RANS models of C_2H_4 flames in 1300-K coflows with different compositions. Data taken from 5 mm, 10 mm and 35 mm downstream.

towards regions of higher Z_N with increasing coflow O_2 level. This is consistent with both increased Z_{st} and increased resistance to extinction with increasing levels of O_2 in the coflow. A second peak, in significantly richer mixtures, is evident further downstream for all flames as the strain-rate field decays with downstream distance.

Comparisons of the HRR profiles in 1100 and 1300 K coflows show progressively more compressed HRR profiles with decreasing coflow temperature with lower peak HRR. This is also consistent with increasing the coflow temperature to 1500 K (omitted for brevity). These results show that, in lower temperature coflows, the combination of less reactive mixtures (due to lower oxidant temperatures) and increased flow-field strain-rates (due to higher coflow density), restricts the reaction zones of flames in hot and diluted coflows. This flow-field-imposed compression effect explains the ‘OH-tail’ structures of C_2H_4 flames issuing into 1100-K coflows with 3 and 9% O_2 [9], and why they were not observed in a jet-in-hot-crossflow configuration [16]. This will be discussed in further depth in §6.2.

Figure 9 shows the profiles of n_{OH} in Z_N -space for 1300-K coflows with 3, 6 or 9% O_2 , 5 mm from the jet exit plane. These profiles indicate a much flatter distribution of OH for flames in coflows with lower concentrations of O_2 . This figure additionally shows OH in the rich side ($Z_N > Z_{st}$) of the reaction zone, with the shapes of the n_{OH} profiles remaining similar with increased downstream distances. The description of the downstream evolution of these profiles is also consistent with flames issuing into 1500-K coflows (omitted for brevity), with similar n_{OH} distributions and peak quantities relative to the 1300-K case.

The distributions of n_{OH} in flames issuing into coflows of 1100 K are shown in Fig. 8. At a distance of 5 mm from jet exit plane, the profiles of n_{OH} are very similar for all three coflow compositions. This indicates similar structures and ignition behaviour, with small peak concentrations of OH, immediately after the jet exit. Further downstream, significant formation of OH occurs first in the coflow with 9% O_2 , then – and to a lesser extent – in the coflow with 6% O_2 (see Fig. 8). Noticeably, peaks of n_{OH} are located on the lean ($Z_N < Z_{st}$) side of the reaction zone, however there are significant concentrations of OH in the fuel rich region. Similar rapid increases in n_{OH} with downstream distance are not observed in the coflow with 3% O_2 . These results indicate the build-up of OH on the lean side of the reaction zone, near the jet exit plane in 1100-K coflows followed by more rapid ignition in coflows with higher O_2 levels, reminiscent of the ‘weak to strong’ OH transition seen in a coflow with 9% O_2 , by Medwell et al. [9].

The profiles of HRR and n_{OH} for 1:1 CH_4/C_2H_4 flames in 1300-K coflows are presented in Fig. 10. Strain-rates for the fuel blend in the same coflows as Fig. 7, are of similar magnitude, and exhibit the same trends that were seen in the C_2H_4 flames. This demonstrates that the choice of fuel composition does not significantly alter the strain field, and the differences observed between flames are significantly dependent on the chemistry. The profiles in Fig. 10 offer an interesting comparison with C_2H_4 flames in identical coflows. The profiles of HRR for the fuel blend are confined to a much smaller range of Z_N than the pure C_2H_4 flames at all downstream locations, with peak HRR for the blend being approximately 60% of that of the pure C_2H_4 flame. The profiles of n_{OH} , however, are almost identical for both the fuel blend and the pure C_2H_4 flames. This suggests that, although HRR is limited by blending with CH_4 , the species production and transport are dominated by characteristics of the C_2H_4 fuel.

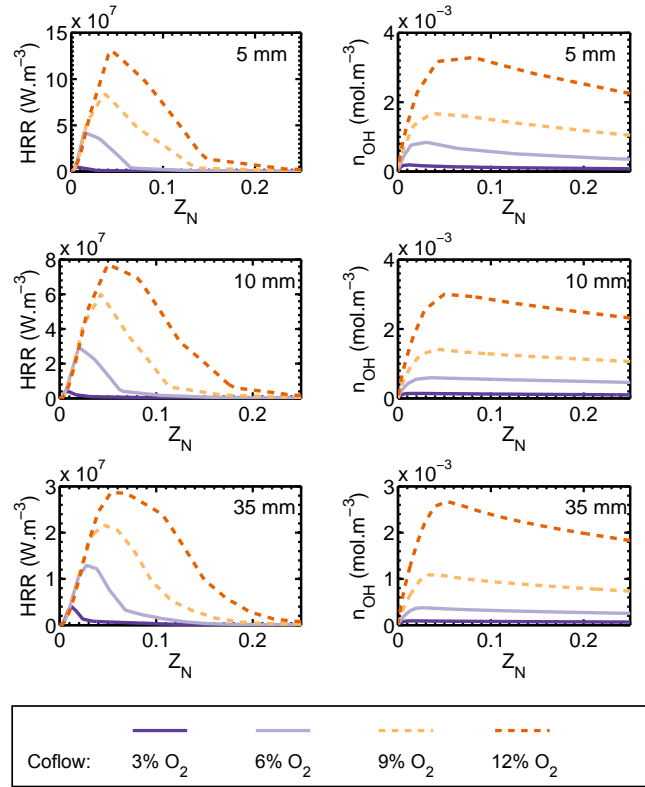


Fig. 10: Net heat release rate (HRR, left) and OH number density (n_{OH} , right) at three different downstream locations in RANS models of 1:1 $\text{CH}_4/\text{C}_2\text{H}_4$ flames in 1300-K coflows with different compositions. Data taken from 5 mm, 10 mm and 35 mm downstream.

The 1:1 blend of $\text{CH}_4/\text{C}_2\text{H}_4$ flames issuing 1100-K coflows behave quite differently to pure C_2H_4 flames in the same coflows (included in §S2 of the Supplementary Data). In an 1100-K coflow, all the flames with the blended fuel not only exhibit a significantly reduced HRR for all Z_N , but produce three orders of magnitude less OH than pure C_2H_4 flames. This indicates that CH_4 inhibits combustion in an 1100-K environment, in contrast to the effects in a 1300-K coflow.

6. Discussion

6.1. Comparison of Experimental Observations to Stoichiometric Ignition Delay Times

The calculated ignition delays of stoichiometric $\text{CH}_4/\text{oxidant}$ mixtures are 2-3 orders of magnitude longer than those of C_2H_4 (see Fig. 4). This relative difference is most significant near 1200 K for all oxidant O_2 levels, and decreases to two orders of magnitude near 1400 K. Experimentally, turbulent NG flames in 1315-K coflows appear attached or feature similar lift-off heights to C_2H_4 flames (see Fig. 2). As these flames have similar jet Re and momentum, the bulk velocity of the NG jet is approximately double that of the C_2H_4 jet. The differences in velocity may contribute to the increased lift-off height of the NG flame compared to the C_2H_4 flame [21], which are of the same order of magnitude. This, however, is in direct contrast to orders of magnitude discrepancy in ignition delay. Thus, under these conditions, the ignition delay in stoichiometric batch reactors, using the criterion of a 10-K temperature increase, does not correlate with changes in the initial onset of chemiluminescence seen in experimental observations.

6.2. Comparison of Modelled Flow-Field to Extinction Strain-Rates

The results of Reynolds-averaged Navier-Stokes (RANS) modelling suggest that the regions of significant HRR within the flames are confined within regions of low strain-rate, with higher strain-rates resulting in extinction. The RANS simulations do not exhibit sudden extinction at the extinction strain-rate calculated using one-dimensional OPPDIF simulations, however the peak of the Reynolds-averaged HRR profile occurs at a strain-rate below this extinction value. This is not unexpected, as RANS results are intrinsically time-averaged. Correspondingly, the inflection points on the rich side of the RANS HRR profiles appear to be consistent with extinction strain-rates predicted by OPPDIF for all but the CH₄ flames in oxidants with 3% O₂, which do not ignite in the OPPDIF simulations. These results imply that the flames are stabilised at very low Z_N , occurring within the laminar coflow, and hence at velocities similar to the coflow velocity. Subsequently, the reaction zones are confined by the extinction strain-rate, and the lean flammability limit at very low Z .

The conclusion that flames in hot coflows are stabilised within the oxidiser stream is consistent with a previous finding derived from transient flamelets superimposed onto a simplified flow-field [19]. This hypothesis explains transitional flame structure seen previously in this burner [9, 12], where unbroken OH structures have been reported in contrast to isolated ignition kernels in the turbulent mixing layer (seen in similar configurations in coflows with higher O₂ [13, 14, 68–71]). This RANS modelling approach, however, cannot provide transient information about the laminar flame self-ignition or propagation processes.

The one-dimensional OPPDIF results suggest that 1:1 blends of CH₄ and C₂H₄ preferentially behave like CH₄ with oxidants with 9% O₂ or C₂H₄ with oxidants with $\leq 6\%$ O₂. Such trends are inconsistent with the experimental results, with experimental values of lift-off changing almost linearly with fuel composition for coflows with 6 or 9% O₂ (see Fig. 2). Results from the RANS simulations, however, support the experimental results with the fuel blend behaving similarly to C₂H₄ in coflows with 6 or 9% O₂, but demonstrating significantly different behaviour in 3% O₂. This highlights that the lift-off heights of flames in hot coflows are a result of the strong coupling between chemistry, and the mixing and turbulence fields, specifically the location of Z_{st} and Z_{mr} relative to regions of high strain rate in the shear layer.

The peak HRR and reaction zone width in 1:1 CH₄/C₂H₄ flame in a 1300-K coflow with 3% O₂ is significantly reduced in comparison to the C₂H₄ flame. For both fuels, however, the ratio of peak HRR between flames in 6 and 9% O₂ coflows are similar. For pure C₂H₄, the peak HRR in the coflow with 9% O₂ is approximately 5 times that of the 3% case, however this increases to a factor of 10 for the 1:1 fuel blend. The width of the reaction zone in the 3% O₂ case with the fuel blend is also reduced by a factor of 3 compared with the C₂H₄ flame. In contrast, the widths of the HRR profiles in the 6 and 9% O₂ cases with the fuel blends are similar to those in the C₂H₄ flames. This may indicate that the width of the HRR profile for the fuel-blend flame in a coflow with 3% O₂ is limited by factors other than strain-rate-based extinction, such as the inhibition of ignition, which is most prevalent in oxidants with 3% O₂ (recalling §4.1).

6.3. Comparison of Modelled Lift-Off Heights to Experimental Observations

Simulated peaks in OH* chemiluminescence have previously been shown to agree with HRR in opposed-flow flames [16, 18] and have been used to analyse the relative HRR in the JHC burner configuration [18, 19].

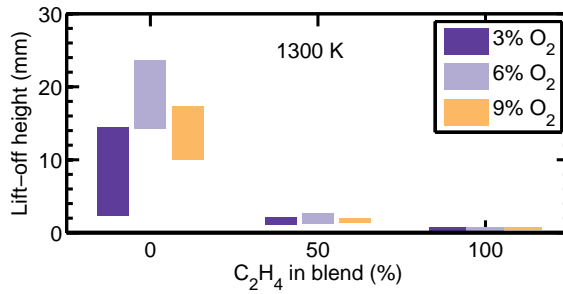


Fig. 11: Variation in lift-off heights of CH₄/C₂H₄ flames in 1300-K coflows, coloured by coflow O₂ level.

Specifically, rapid increases in OH* chemiluminescence have shown good agreement with approximately 20% of normalised HRR for $Z < Z_{st}$ in ethanol flames [18]. A HRR criterion has previously been applied to non-autoignitive, lifted, turbulent CH₄ jet flames issuing into quiescent air [72, 73]. Accordingly, isocontours of 20% normalised HRR were used to compare the lift-off heights from RANS modelling to the “unequivocal maximum” [12] estimated from experimental observations. Isocontours of 5% normalised HRR were used to compare the initial onset of chemiluminescence. This value was chosen as a surrogate for the initial stages of ignition, and hence initial temperature increases, which have been used successfully in studies of premixed reactors [23].

The lowest [axial] point in the 5 and 20% HRR isocontours were taken to be the range of lift-off heights. This approach is comparable to those taken in separate experimental [29] and direct numerical simulation [69, 74] studies, which used a fixed percentage of minor species increase to denote lift-off height in conventional autoignition. Such a species-based approach, however, has not shown similar success in simulations in more gradual, non-premixed MILD combustion [21].

The trends in lift-off height in the RANS simulated are shown in Fig. 11. The model shows good agreement with the predicted and observed lift-off heights of the NG flame in the 1315-K coflow with 9% O₂ and the trend reported by Medwell and Dally [12]. These results also capture the trend of decreasing lift-off height with increasing C₂H₄ concentrations. The 5% HRR threshold does not capture the attached NG flame in the 3% O₂ coflow however, regions of net positive heat release extended to the jet exit plane, as previously stated in §5.

The simulated predictions of C₂H₄ flames ‘lifted’ by <1 mm is consistent with the observations of flames detached from, yet stabilised very close to, the jet exit by ~5 mm (recall Fig. 2). These discrepancies may be due to assumptions of a constant temperature coflow in the model, in contrast to experimental heat transfer to the cooled jet, which results in a slightly lower coflow temperature near the jet exit plane. This effect is not accounted for in the simulations, however the primary role of this study is to analyse the consistency between the observed and simulated trends in lift-off height, as opposed to their absolute values.

Modelled trends in lift-off height qualitatively replicate those observed experimentally, with changing fuel composition, coflow temperature and coflow O₂ level. These trends, along with the profiles of strain-rate, HRR and n_{OH} in Z -space provide insights on the stabilisation and structure of flames in the transition between the MILD conventional autoignitive combustion regimes.

7. Conclusions

Experimental and numerical investigations of CH₄, C₂H₄ and blended-fuel flames in hot coflows have been studied separately, and their results compared, to better understand the structure of turbulent jet flames and the effects of blending gaseous fuels. This work has combined experimental observations in a JHC burner and numerical studies of batch reactors, one-dimensional opposed-flow flames and two-dimensional RANS simulations to draw the following conclusions:

- Fuel blends with greater than 50% C₂H₄, in 1300-K and hotter coflows, are more sensitive to changes in coflow temperature than changes in coflow O₂ level.
- Fuel blends which are predominantly CH₄, especially in coflows cooler than 1300 K, are very sensitive to the composition of the coflow oxidant stream.
- The NTC region of CH₄, under MILD combustion conditions, occurs at significantly lower temperatures than NTC in the conventional autoignition regime.
- Unlike CH₄ and fuel blends, C₂H₄ shows a unique collapse of ignition delays near 1100 K, due to the competition between the H/H₂ and C₂ ignition pathways.
- Blending CH₄ and C₂H₄ only has a minor effect on OH distribution in flames stabilised in hot coflows, however results in significant decrease in HRR compared to C₂H₄.
- Trends in the initial onset of chemiluminescence in a JHC burner cannot be directly estimated through batch reactors or simplified opposed-flow flames alone, but can be replicated with knowledge of the underlying flow-field.
- Two-dimensional RANS modelling supports the hypothesis that flames stabilise in regions of low strain-rate, on the lean side of the jet shear layer.
- Distributions of HRR from two-dimensional RANS modelling can qualitatively replicate the gradual ignition processes and non-monotonic trends in visual lift-off seen experimentally in the transition to the MILD combustion regime.

The results of these studies provide a better understanding of the structure of CH₄, C₂H₄ and blended CH₄/C₂H₄ flames in hot coflows, improving the understanding of the evolution and stabilisation of flames in hot and diluted coflows.

Acknowledgements

The authors thank Dr Alessandro Stagni from the Politecnico di Milano for providing the reduced chemical mechanism used in the turbulent modelling. The authors acknowledge support from The University of Adelaide. Financial support was provided by through the Endeavour Scholarships and Fellowship grant programme; the Australian Research Council (ARC) Discovery (DP and DECRA) grant scheme; and the United States Asian Office for Aerospace Research and Development (AOARD).

References

- [1] A. Cavaliere, M. de Joannon, *Mild Combustion*, *Prog. Energ. Combust.* 30 (4) (2004) 329–366.
- [2] J. A. Wünnig, J. G. Wünnig, *Flameless oxidation to reduce thermal no-formation*, *Prog. Energ. Combust.* 23 (1) (1997) 81–94.
- [3] B. Dally, E. Riesmeier, N. Peters, *Effect of fuel mixture on moderate and intense low oxygen dilution combustion*, *Combust. Flame* 137 (4) (2004) 418–431.
- [4] M. Saha, A. Chinnici, B. B. Dally, P. R. Medwell, *Numerical Study of Pulverized Coal MILD Combustion in a Self-Recuperative Furnace*, *Energy Fuels* 29 (11) (2015) 7650–7669.
- [5] K. Döbbling, J. Hellat, H. Koch, *25 Years of BBC/ABB/Alstom Lean Premix Combustion Technologies*, *J. Eng. Gas Turb. Power* 1 (2007) 2–12.
- [6] O. Lammel, H. Schütz, G. Schmitz, R. Lückerrath, M. Stöhr, B. Noll, M. Aigner, M. Hase, W. Krebs, *FLOX[®] combustion at high power density and high flame temperatures*, *J. Eng. Gas Turb. Power* 132 (12) (2010) 121503.
- [7] B. Dally, A. Karpetis, R. Barlow, *Structure of turbulent non-premixed jet flames in a diluted hot coflow*, *Proc. Combust. Inst.* 29 (2002) 1147–1154.
- [8] P. R. Medwell, P. A. M. Kalt, B. B. Dally, *Simultaneous imaging of OH, formaldehyde, and temperature of turbulent nonpremixed jet flames in a heated and diluted coflow*, *Combust. Flame* 148 (1-2) (2007) 48–61.
- [9] P. R. Medwell, P. A. M. Kalt, B. B. Dally, *Imaging of diluted turbulent ethylene flames stabilized on a Jet in Hot Coflow (JHC) burner*, *Combust. Flame* 152 (2008) 100–113.
- [10] P. R. Medwell, P. A. M. Kalt, B. B. Dally, *Reaction Zone Weakening Effects under Hot and Diluted Oxidant Stream Conditions*, *Combust. Sci. Technol.* 181 (7) (2009) 937–953.
- [11] P. R. Medwell, B. B. Dally, *Effect of fuel composition on jet flames in a heated and diluted oxidant stream*, *Combust. Flame* 159 (10) (2012) 3138–3145.
- [12] P. R. Medwell, B. B. Dally, *Experimental Observation of Lifted Flames in a Heated and Diluted Coflow*, *Energy Fuels* 26 (9) (2012) 5519–5527.
- [13] E. Oldenhof, M. J. Tummers, E. H. van Veen, D. J. E. M. Roekaerts, *Ignition kernel formation and lift-off behaviour of jet-in-hot-coflow flames*, *Combust. Flame* 157 (6) (2010) 1167–1178.
- [14] E. Oldenhof, M. J. Tummers, E. H. van Veen, D. J. E. M. Roekaerts, *Role of entrainment in the stabilisation of jet-in-hot-coflow flames*, *Combust. Flame* 158 (8) (2011) 1553–1563.
- [15] C. Duwig, B. Li, Z. Li, M. Aldén, *High resolution imaging of flameless and distributed turbulent combustion*, *Combust. Flame* 159 (1) (2012) 306–316.
- [16] J. Sidey, E. Mastorakos, *Visualization of MILD combustion from jets in cross-flow*, *Proc. Combust. Inst.* 35 (3) (2015) 3537–3545.
- [17] M. Saha, B. B. Dally, P. R. Medwell, A. Chinnici, *Effect of particle size on the MILD combustion characteristics of pulverised brown coal*, *Fuel Process. Technol.* DOI: 10.1016/j.fuproc.2016.04.003.
- [18] J. Ye, P. R. Medwell, B. B. Dally, M. J. Evans, *The transition of ethanol flames from conventional to MILD combustion*, *Combust. Flame* 171 (2016) 173–184.
- [19] M. J. Evans, P. R. Medwell, H. Wu, A. Stagni, M. Ihme, *Classification and Lift-Off Height Prediction of Non-Premixed MILD and Autoignitive Flames*, *Proc. Combust. Inst.* DOI: 10.1016/j.proci.2016.06.013.
- [20] M. Saha, B. B. Dally, P. R. Medwell, A. Chinnici, *Burning characteristics of Victorian brown coal under MILD combustion conditions*, *Combust. Flame* 172 (2016) 252–270.
- [21] M. J. Evans, P. R. Medwell, Z. F. Tian, A. Frassoldati, A. Cuoci, A. Stagni, *Ignition Characteristics in Spatially Zero-, One- and Two-Dimensional Laminar Ethylene Flames*, *AIAA J.* 54 (10) (2016) 3255–3264.
- [22] A. Effuggi, D. Gelosa, M. Derudi, R. Rota, *Mild Combustion of Methane-Derived Fuel Mixtures: Natural Gas and Biogas*, *Combustion Science and Technology* 180 (3) (2008) 481–493.
- [23] M. de Joannon, A. Cavaliere, R. Donnarumma, R. Ragucci, *Dependence of autoignition delay on oxygen concentration in mild combustion of high molecular weight paraffin*, *Proc. Combust. Inst.* 29 (1) (2002) 1139–1146.
- [24] P. Sabia, M. de Joannon, A. Picarelli, A. Chinnici, R. Ragucci, *Modeling Negative Temperature Coefficient region in methane oxidation*, *Fuel* 91 (1) (2012) 238–245.
- [25] P. Sabia, M. de Joannon, A. Picarelli, R. Ragucci, *Methane auto-ignition delay times and oxidation regimes in MILD combustion at atmospheric pressure*, *Combust. Flame* 160 (1) (2013) 47–55.
- [26] P. R. Medwell, D. L. Blunck, B. B. Dally, *The role of precursors on the stabilisation of jet flames issuing into a hot environment*, *Combust. Flame* 161 (2) (2014) 465–474.
- [27] P. R. Medwell, M. J. Evans, Q. N. Chan, V. R. Katta, *Laminar flame calculations for analysing trends in autoignitive jet flames in a hot and vitiated coflow*, *Energy Fuels* DOI: 10.1021/acs.energyfuels.6b01264.
- [28] T. Echehki, J. H. Chen, *Direct numerical simulation of autoignition in non-homogeneous hydrogen-air mixtures*, *Combust. Flame* 134 (3) (2003) 169–191.
- [29] R. Cabra, T. Myhrvold, J. Chen, R. Dibble, A. Karpetis, R. Barlow, *Simultaneous laser raman-rayleigh-lif measurements and numerical modeling results of a lifted turbulent H₂/N₂ jet flame in a vitiated coflow*, *Proc. Combust. Inst.* 29 (2002) 1881–1888.
- [30] M. de Joannon, P. Sabia, G. Cozzolino, G. Sorrentino, A. Cavaliere, *Pyrolytic and Oxidative Structures in Hot Oxidant Diluted Oxidant (HODO) MILD Combustion*, *Combust. Sci. Technol.* 184 (7-8) (2012) 1207–1218.
- [31] J. A. Sidey, E. Mastorakos, *Simulations of laminar non-premixed flames of methane with hot combustion products as oxidiser*, *Combust. Flame* 163 (2016) 1–11.
- [32] F. C. Christo, B. B. Dally, *Modeling turbulent reacting jets issuing into a hot and diluted coflow*, *Combust. Flame* 142 (1-2) (2005) 117–129.
- [33] A. Parente, M. R. Malik, F. Contino, A. Cuoci, B. B. Dally, *Extension of the Eddy Dissipation Concept for turbulence/chemistry interactions to MILD combustion*, *Fuel* 163 (2016) 98–111.
- [34] J. Aminian, C. Galletti, S. Shahhosseini, L. Tognotti, *Key modeling issues in prediction of minor species in diluted-preheated combustion conditions*, *Appl. Therm. Eng.* 31 (16) (2011) 3287–3300.
- [35] A. De, E. Oldenhof, P. Sathiah, D. Roekaerts, *Numerical Simulation of Delft-Jet-in-Hot-Coflow (DJHC) Flames Using the Eddy Dissipation Concept Model for Turbulence-Chemistry Interaction*, *Flow Turbul. Combust.* 87 (4) (2011) 537–567.

- [36] A. Frassoldati, P. Sharma, A. Cuoci, T. Faravelli, E. Ranzi, Kinetic and fluid dynamics modeling of methane/hydrogen jet flames in diluted coflow, *Appl. Therm. Eng.* 30 (4) (2010) 376–383.
- [37] A. Mardani, S. Tabejamaat, M. B. Mohammadi, Numerical study of the effect of turbulence on rate of reactions in the MILD combustion regime, *Combust. Theor. Model.* 15 (6) (2011) 753–772.
- [38] J. Aminian, C. Galletti, S. Shahhosseini, L. Tognotti, Numerical Investigation of a MILD Combustion Burner: Analysis of Mixing Field, Chemical Kinetics and Turbulence-Chemistry Interaction, *Flow Turbul. Combust.* 88 (4) (2012) 597–623.
- [39] S. R. Shabaniyan, P. R. Medwell, M. Rahimi, A. Frassoldati, A. Cuoci, Kinetic and fluid dynamic modeling of ethylene jet flames in diluted and heated oxidant stream combustion conditions, *Appl. Therm. Eng.* 52 (2013) 538–554.
- [40] M. J. Evans, P. R. Medwell, Z. F. Tian, Modeling Lifted Jet Flames in a Heated Coflow using an Optimized Eddy Dissipation Concept Model, *Combust. Sci. Technol.* 187 (7) (2015) 1093–1109.
- [41] F. Wang, J. Mi, P. Li, Combustion Regimes of a Jet Diffusion Flame in Hot Co-flow, *Energy Fuels* 27 (6) (2013) 3488–3498.
- [42] F. Wang, P. Li, J. Mi, J. Wang, M. Xu, Chemical kinetic effect of hydrogen addition on ethylene jet flames in a hot and diluted coflow, *Int. J. Hydrogen Energy.* 40 (46) (2015) 16634–16648.
- [43] Y. Tu, K. Su, H. Liu, S. Chen, Z. Liu, C. Zheng, Physical and chemical effects of CO₂ addition on CH₄/H₂ flames on a Jet in Hot Coflow (JHC) burner, *Energy Fuels* 30 (2) (2016) 1390–1399.
- [44] J. Aminian, C. Galletti, L. Tognotti, Extended EDC local extinction model accounting finite-rate chemistry for MILD combustion, *Fuel* 165 (2016) 123–133.
- [45] M. Ihme, Y. C. See, LES flamelet modeling of a three-stream MILD combustor: Analysis of flame sensitivity to scalar inflow conditions, *Proc. Combust. Inst.* 33 (2011) 1309–1217.
- [46] M. Ihme, J. Zhang, G. He, B. B. Dally, Large-Eddy Simulation of a Jet-in-Hot-Coflow Burner Operating in the Oxygen-Diluted Combustion Regime, *Flow, Turbul. Combust.* 89 (2012) 449–464.
- [47] R. Bhaya, A. De, R. Yadav, Large Eddy Simulation of MILD combustion using PDF based turbulence-chemistry interaction models, *Combust. Sci. Technol.* 186 (9) (2014) 1138–1165.
- [48] C. K. Westbrook, F. L. Dryer, Chemical kinetic modeling of hydrocarbon combustion, *Prog. Energy Combust. Sci.* 10 (1) (1984) 1–57.
- [49] J. Prager, H. Najm, M. Valorani, D. Goussis, Structure of n-heptane/air triple flames in partially-premixed mixing layers, *Combust. Flame* 158 (11) (2011) 2128–2144.
- [50] P. Sabia, G. Sorrentino, A. Chinnici, A. Cavaliere, R. Ragucci, Dynamic Behaviors in Methane MILD and Oxy-Fuel Combustion. Chemical Effect of CO₂, *Energy Fuels* 29 (3) (2015) 1978–1986.
- [51] W. Liu, A. Kelley, C. Law, Flame propagation and counterflow nonpremixed ignition of mixtures of methane and ethylene, *Combust. Flame* 157 (5) (2010) 1027–1036.
- [52] S. Ravi, T. Sikes, A. Morones, C. Keesee, E. Petersen, Comparative study on the laminar flame speed enhancement of methane with ethane and ethylene addition, *Proc. Combust. Inst.* 35 (1) (2015) 679 – 686.
- [53] X. Li, A. W. Jasper, J. Zádor, J. A. Miller, S. J. Klippenstein, Theoretical kinetics of O + C₂H₄, *Proc. Combust. Inst.* DOI: 10.1016/j.proci.2016.06.053.
- [54] R. M. I. Elsamra, S. Vranckx, S. A. Carl, CH(A²Δ) Formation in Hydrocarbon Combustion: The Temperature Dependence of the Rate Constant of the Reaction C₂H + O₂ → CH(A²Δ) + CO₂, *J. Phys. Chem.* 109 (45) (2005) 10287–10293.
- [55] E. Mastorakos, Ignition of turbulent non-premixed flames, *Prog. Energy Combust. Sci.* 35 (1) (2009) 57–97.
- [56] T. Faravelli, A. Frassoldati, E. Ranzi, Kinetic modeling of the interactions between NO and hydrocarbons in the oxidation of hydrocarbons at low temperatures, *Combust. Flame* 132 (1-2) (2003) 188–207.
- [57] A. Frassoldati, T. Faravelli, E. Ranzi, Kinetic modeling of the interactions between NO and hydrocarbons at high temperature, *Combust. Flame* 135 (1-2) (2003) 97–112.
- [58] T. Wada, J. K. Lefkowitz, Y. Ju, Plasma Assisted MILD Combustion, 53rd AIAA Aerospace Sciences Meeting .
- [59] D. M. Manias, E. A. Tingas, C. E. Frouzakis, K. Boulouchos, D. A. Goussis, The mechanism by which CH₂O and H₂O₂ additives affect the autoignition of CH₄/air mixtures, *Combust. Flame* 164 (2016) 111–125.
- [60] B. B. Dally, D. F. Fletcher, A. R. Masri, Flow and mixing fields of turbulent bluff-body jets and flames, *Combust. Theor. Model.* 2 (2) (1998) 193–219.
- [61] E. Ranzi, A. Frassoldati, R. Grana, A. Cuoci, T. Faravelli, A. Kelley, C. Law, Hierarchical and comparative kinetic modeling of laminar flame speeds of hydrocarbon and oxygenated fuels, *Prog. Energy Combust. Sci.* 38 (4) (2012) 468–501, current version of mechanism available from <http://creckmodeling.chem.polimi.it/>.
- [62] A. Stagni, A. Frassoldati, A. Cuoci, T. Faravelli, E. Ranzi, Skeletal mechanism reduction through species-targeted sensitivity analysis, *Combust. Flame* 163 (2016) 382 – 393.
- [63] A. Stagni, L. Esclapez, P. Govindaraju, A. Cuoci, T. Faravelli, M. Ihme, The role of preferential evaporation on the ignition of multicomponent fuels in a homogeneous spray/air mixture, *Proc. Combust. Inst.* DOI: 10.1016/j.proci.2016.06.052.
- [64] A. Stagni, A. Cuoci, A. Frassoldati, T. Faravelli, E. Ranzi, Lumping and reduction of detailed kinetic schemes: an effective coupling, *Ind. Eng. Chem. Res.* 53 (22) (2013) 9004–9016.
- [65] B. Choi, S. Chung, Autoignited laminar lifted flames of methane, ethylene, ethane, and n-butane jets in coflow air with elevated temperature, *Combust. Flame* 157 (12) (2010) 2348–2356.
- [66] C. Duwig, M. J. Dunn, Large Eddy Simulation of a premixed jet flame stabilized by a vitiated co-flow: Evaluation of auto-ignition tabulated chemistry, *Combust. Flame* 160 (12) (2013) 2879–2895.
- [67] R. Bilger, S. Stårner, R. Kee, On reduced mechanisms for methane · air combustion in nonpremixed flames, *Combust. Flame* 80 (2) (1990) 135–149.
- [68] E. Oldenhof, M. J. Tummers, E. H. van Veen, D. J. E. M. Roekaerts, Transient response of the Delft jet-in-hot coflow flames, *Combust. Flame* 159 (2) (2012) 697–706.
- [69] C. S. Yoo, E. S. Richardson, R. Sankaran, J. H. Chen, A DNS study on the stabilization mechanism of a turbulent lifted ethylene jet flame in highly-heated coflow, *Proc. Combust. Inst.* 33 (2011) 1619–1627.
- [70] C. Arndt, J. Gounder, W. Meier, M. Aigner, Auto-ignition and flame stabilization of pulsed methane jets in a hot vitiated coflow studied with high-speed laser and imaging techniques, *Appl. Phys. B* 108 (2) (2012) 407–417.
- [71] A. Ramachandran, D. A. Tyler, P. K. Patel, V. Narayanaswamy, K. M. Lyons, Global Features of Flame Stabilization in Turbulent Non-premixed Jet Flames in Vitiated Coflow, 45th AIAA Fluid Dynamics Conference .
- [72] D. Bradley, P. Gaskell, X. Gu, The mathematical modeling of liftoff and blowoff of turbulent non-premixed methane jet

- flames at high strain rates, *Proc. Combust. Inst.* 27 (1) (1998) 1199–1206.
- [73] T. Mahmud, S. Sangha, M. Costa, A. Santos, Experimental and computational study of a lifted, non-premixed turbulent free jet flame, *Fuel* 86 (5–6) (2007) 793–806.
- [74] C. S. Yoo, R. Sankaran, J. H. Chen, Three-dimensional direct numerical simulation of a turbulent lifted hydrogen jet flame in heated coflow: flame stabilization and structure, *J. Fluid Mech* 640 (2009) 453–481.

Chapter 9

Summary and Conclusions

Moderate or intense low oxygen dilution (MILD) combustion offers a range of potential benefits over conventional combustion systems. A comprehensive literature review, however, demonstrated that a better understanding of MILD combustion was required to improve the understanding of the defining features and stabilisation mechanisms of MILD reaction zones. In this thesis:

1. Distinctions have been established between the ignition mechanisms and reaction zone structure of both MILD and autoignitive lifted jet flames in heated coflows, providing methods of demarcating the two regimes.
2. The effects of oxidiser and jet conditions on the structure of flames in the MILD and autoignitive combustion regimes has been explored.
3. The validity of simplified zero-, one- and two-dimensional models in predicting the ignition delay and structure of experimental jet flames has been assessed in MILD, transitional and autoignitive conditions.

The gaps in the current literature have been addressed across five publications in leading, international peer-reviewed journals. The following subsections describe how the body of knowledge in this thesis provides a significantly improved understanding of the stabilisation mechanisms in the MILD combustion regime, and in the transition between MILD combustion and conventional autoignition.

9.1 Identifying and Understanding MILD Combustion

The MILD combustion regime has been previously been ‘defined’ in premixed reactors as either: self-igniting combustion where the increase in temperature is less than the mixture self-ignition temperature [4]; or a gradual transition from mixing to

burning, described by a degenerate S-shaped curve [21]. Chapter 4 compares these two descriptions of premixed MILD combustion in premixed and non-premixed reactors and, critically, presents the derivation of a simple, analytical criterion for non-premixed MILD combustion. This criterion alleviates the necessity for any pre-determined quenching or self-ignition temperatures, which may depend on pre-selected numerical time scales. Instead, this criterion incorporates an effective activation energy, an intrinsic property of the fuel-and-oxidant mixture. The newly derived criterion for non-premixed MILD combustion is presented in Chapter 4 as regime maps for comparison with detailed kinetics, and for arbitrary fuels – facilitating direct comparison between previous studies. Observations of flames from new, and previously studied [2, 3, 7, 20, 22], experimental cases conformed with the new analytical criterion for MILD combustion or conventional, autoignitive ignition.

The structure of experimental and simulated laminar, non-premixed flames are investigated in Chapters 5 and 6. These configurations, in contrast to the opposed-flow configuration in Chapter 4, allow for both ignition and flame propagation and, hence, qualitative comparison between experimental observations and simulations. Initially, the validity of using the blue channel from photographs of laminar flames as a means to compare changes in flame structure with changing conditions, was confirmed in Chapter 5. Observations from these images were then used to distinguish [spatially] gradual, MILD ignition, from conventional spontaneous ignition (Chapter 5) and, in Chapter 8, to describe trends in visual lift-off height – consistent with those reported previously [18]. Numerical investigation of a range of $\text{CH}_4/\text{C}_2\text{H}_4$ flames in Chapter 8 demonstrated that trends observed in new experiments could be qualitatively replicated, following the optimisation of the eddy dissipation concept (EDC) turbulence-chemistry model (Chapter 7). The combined results from Chapters 4, 7 and 8 have shown that flames in hot and diluted coflows stabilise in low velocity, low strain-rate regions of the coflow. The most upstream ignition points of the flames shift towards regions of higher strain rate with increasing oxidant O_2 concentration or decreasing oxidant temperature.

Two-dimensional, laminar simulations were examined against the classification of MILD reaction zones as edge flame structures without a triple point. In this description, MILD combustion is defined when only a single peak in net heat release is evident in mixture-fraction (Chapter 5), in conjunction with more gradual ignition processes (Chapter 6). Increasing the oxygen level or temperature of the oxidant stream resulted in a shift to a tribrachial flame structure, where regions of heat release corresponded to multiple peaks in precursor species distributions (Chapter 5). It was shown that these species are produced in highest quantities upstream

of the flame and diffuse to either side of the downstream reaction zone (Chapter 5). Although CH_2O has previously been accepted as an appropriate indicator of tri-brachial structures in CH_4/NG flames [13], the work presented in Chapter 5 shows that the hydroperoxyl radical (HO_2) is a more appropriate indicator of tribrachial flame structures in flames where the H/H_2 ignition path is significant.

Although the numerical studies contained within this thesis adopt different chemical kinetics mechanisms (specifically Gri-Mech 3.0 [31], the C1-C3 sub-mechanism from POLIMI [24] and the USC-II C1-C4 mechanism [33]), they have been verified previously [29], and within this thesis (see Chapter 5), as providing qualitatively similar ignition pathways for the fuels under considered. In addition to these comments throughout the thesis, it must be noted that both the C1-C3 sub-mechanism from POLIMI [24] and the USC-II C1-C4 mechanism [33] produce similar opposed-flow flamelet structures, with the USC-II mechanism used in Chapter 4 as it is less computationally demanding.

A simple criterion for the existence of a degenerate S-shaped curve has been derived to represent the boundary of the MILD combustion regime. This criterion is a function of the initial conditions of the mixture only, and is independent of the underlying flow-field. Additionally, two-dimensional laminar simulations have been analysed to discern the mechanisms of species production and transport in MILD reaction zones, with comparisons made against conventional spontaneous ignition processes. The transition between these reaction zone structures is flow-field dependent, as was shown by comparing simulations to experimental observations, and in accordance with the findings of Ye *et al.* [34]. These conclusions are evidence of the role that mixture fraction and residence time have on the structure of non-premixed reaction zones. The qualitative features of these descriptions have been used separately to describe MILD combustion, however the current analyses suggest that both conditions may need to be met to encompass all the features of the MILD combustion regime. Whilst MILD combustion can be described as meeting both the S-shaped curve [14, 21, 23] and the heat-release rate [1, 5, 6, 9–11] criteria, it remains unclear if these descriptions can be unified to provide a single, simplified definition of the MILD combustion regime.

9.2 Factors Influencing Ignition with Hot and Diluted Oxidants

Oxidant temperature and O_2 concentration play a key role on the structure of non-premixed MILD reaction zones [9–11, 30]. Few studies, however, have simultaneously investigated the existence of coupling of these parameters with the underlying flow-field on reaction structure, or have only done so for limited conditions [30]

or fuels [34]. The results within this thesis show that decreased temperature and increased initial temperatures, result in reduced temperature increases and, hence, a shift towards gradual ignition described by a degenerate S-shaped curve (Chapter 4). Conversely, increased temperatures (as well as increased oxygen concentrations) result in faster reaction rates and a shift away from temporally and spatially gradual ignition (Chapters 5 and 8). This latter shift with hotter oxidants with higher levels of O_2 also coincides with a trend towards flames with tribrachial flame structures (Chapter 4). These trends describe the changes in reaction structure in the scalar-dissipation-rate, time and mixture-fraction domains, and highlight the importance of their interactions. Interactions between chemistry and mixing fields describe the phenomena seen experimentally, as highlighted in §9.1, revealing the importance of the flow-field in contributing to flame structures in the MILD combustion regime, and in the transition to conventional autoignition.

Ignition in the MILD combustion regime, and in the transition to conventional autoignition, has previously demonstrated significant sensitivity to small concentrations of combustion radical and precursor species [17]. These were assessed in the current work using zero-dimensional reactors, demonstrating that minor species have a negligible impact on the initial stages of heat release (Chapter 8). In non-premixed laminar flames, the inclusion of ~ 10 ppm of OH in the oxidant significantly accelerated ignition in a MILD reaction zone, but had a negligible effect on conventional spontaneously igniting flames (Chapter 5). This demonstrates that radicals and flame precursors must be accounted for in the modelling, and analysis, of MILD combustion. Further increases in OH concentration (up to 1000 ppm) resulted in attachment of the MILD flame (Chapter 5). Although the addition of OH resulted in a significantly intensified MILD reaction zone, it did not result in a shift to a conventional spontaneously igniting, tribrachial flame structure. In contrast, minor species were shown to have little effect on laminar opposed-flow flames in either regime at steady-state (Chapters 5 and 8). Simulations of turbulent jet flames in Chapters 7 and 8 similarly showed that equilibrium levels of minor species (with concentrations of up to ~ 10 ppm) have little effect on flame structure, however a large concentration (10 000 ppm) of hydroxyl (OH) resulted in flame attachment (Chapter 7).

The results in Chapters 4, 5, 7 and 8 indicate that fuel properties, oxidant temperature and O_2 concentration, and the underlying flow-field, govern the transition between MILD combustion and conventional autoignition. Conversely, however, even relatively large concentrations of minor species do not play an important role in the shift between MILD combustion and conventional spontaneous ignition, de-

spite accelerating ignition under MILD combustion conditions.

9.3 Prediction of Non-Premixed Ignition Delay

Ignition delay may be 'defined' by several means in zero- and one-dimensional reactors. This work has assessed the validity of different approaches to predicting ignition delay in non-premixed flames using such spatially-simplified simulations.

Zero-dimensional reactor simulations have been used to calculate the ignition delay by means of absolute increases in temperature, or the gradients of temperature or radical species. These were assessed in Chapters 6 and 8 in which it was shown that thermal runaway in a zero-dimensional reactor correlates well with both autoignition events in isolated fluid kernels, and the weak-to-strong transition point in non-premixed ethylene flames (Chapter 6). This was concluded for both planar, laminar flames, and the visual lift-off height of previously observed simulated [35] and experimental flames [18], normalised by their bulk jet exit velocity. In contrast, ignition delay defined as the first, small temperature increase [8, 25] did not correlate with any experimental observations (Chapter 8). These results suggest that the weak chemiluminescence observed near the jet exit plane of flames in a JHC burner configuration may not be a direct result of localised self-ignition.

Transient and steady-state analyses of one-dimensional, laminar opposed-flow flames have been compared to experimental and modelled flames in Chapters 4-6 and 8. Although steady-state opposed flow-flow flames cannot capture transient effects of ignition (Chapter 5), they may be used to estimate the extinction limits of non-premixed flames, and hence explain the interplay between turbulence and chemistry in turbulent flames (Chapter 8). Two studies of transient opposed-flow flames, however, demonstrated that visual lift-off heights may be predicted by small increases in temperature only when the underlying flow-field is taken into account (Chapters 4 and 6). Similarly, modelling of turbulent flames was shown to be able to directly predict the weak-to-strong transition in OH concentration at the visual flame base (Chapter 7). The same modelling approach was subsequently used to reproduce the trends in weak-to-strong transition heights seen experimentally, using contours of normalised peak heat-release rates (Chapter 8).

Flame ignition may be described in terms of zero- or one-dimensional reactors. These approaches may be used to estimate the weak-to-strong transition height of non-premixed flames with hot oxidants, or the transient ignition processes respectively. The use of these reactors is not trivial, however, and the prediction of features reported in experimental flames requires estimation or modelling of the underlying flow-field.

9.4 Future Work

The current body of work has provided significant insight into fluidic and chemical structure of MILD combustion, and the behaviour of non-premixed flames in the transition between the MILD and autoignitive combustion regimes. The current work, however, may be complemented in future with further work with the following foci:

- *Investigation of the relationship between autoignition events and the features of laminar, opposed-flow flames with hot and diluted oxidants.*

The body of work in this thesis has focussed on two key features of non-premixed MILD combustion. These features are: a monotonic relationship between temperature and scalar dissipation rate (that is, a degenerate S-shaped curve), and an edge flame structure stabilised without a triple point. The former suggests MILD combustion should be readily achievable with very high temperature oxidants, whereas the latter showed the opposite trend in numerical simulations. Future work could investigate a potential unification of these descriptions, through studying a possible correlation of these two criteria along with analyses of ignition/flame-propagation behaviour, may result in a more general description of MILD combustion, or add further constraints to the current description of the MILD combustion regime.

- *Investigation of the effects of pressure on the transition between the MILD and autoignitive combustion regimes.*

Oxygen concentration and temperature are the dominant parameters governing the transition between the MILD and autoignitive combustion regimes at atmospheric pressure. Although these have been established in this work, the effects of pressure on this transition have not previously been assessed, and provide scope for future numerical and experimental studies.

- *The effects of diluent on non-premixed, gaseous combustion near the transition between MILD and autoignitive combustion regimes.*

The non-premixed studies in this work have dealt almost exclusively with 'pure' fuels, with only N_2 as a diluent for C_2H_4 in one case from a previous experimental study [20]. Both N_2 and C_2H_4 have nearly identical molecular weights (≈ 28 g/mol). Varying the ratio of C_2H_4 to N_2 would therefore shift the stoichiometric mixture fraction, but not greatly affect the mixing field of the jet flame. This could be used to separate the effects of turbulence and chemistry in non-premixed jet flames. Such studies could be further extended to

diluents with significantly different molecular weights, such as He (2.0 g/mol) or Kr (83.8 g/mol). Alternatively, fuel could be diluted with reasonably stable (albeit not inert [12, 26–28, 32]) admixtures such as CO₂ (44 g/mol) or H₂O vapour (18 g/mol). These would simultaneously shift the stoichiometric mixture fraction, and alter the flow-field of the non-premixed flame and could be employed to study both of these coupled effects.

- *Laser imaging of flames near the transition between MILD and autoignitive combustion regimes.*

A transition between MILD and autoignitive combustion regimes has been identified in non-premixed flames, through photographs and OH* chemiluminescence imaging supported by numerical analyses. Further work could extend these diagnostics of the flow-field, temperature-field and flame intermediary species such as OH, CH₂O, CH₃ and/or HO₂. Temperature and the former two species have both previously been measured in a jet-in-hot-coflow configuration [19, 20], however only for several specific cases. Planar imaging techniques of CH₃ [16] and/or HO₂ [15] have not, however, been applied to MILD combustion burners, despite the importance of these species in flame stabilisation. These diagnostics, combined with the improved understanding of MILD combustion from this body of work, could add further insight into the study of non-premixed combustion in hot and diluted oxidants.

- *Extension of the eddy dissipation concept (EDC) combustion model to adaptively span conventional and MILD combustion regimes.*

The use of the EDC combustion model in this work was shown to require adjusted coefficients to compensate for the reaction zone structures in MILD combustion in the jet-in-hot-coflow configuration. These coefficients were empirically determined for highly turbulent flow-fields following the derivation of the EDC equations from first-principles. Substituting these coefficients with *a priori* or *posteriori* functional forms could expand the functionality of the EDC model and avoid the need for *ad hoc* model tuning.

9.5 Conclusions

Moderate or intense low oxygen dilution (MILD) combustion offers benefits of increased efficiency and reduced pollutants over conventional combustion systems. The behaviour and structure of reaction zones in this, and in the transition between this and the similar conventional autoignitive, combustion regime, however, has not previously been described comprehensively or systematically.

Previously proposed criteria for MILD combustion have been assessed in this thesis, comparing analytical and numerical models to experimental observations of jet flames in hot coflows. These have resulted in a new, generalised regime diagram for gradual ignition, and facilitated the distinction between MILD reaction zones and conventional autoignitive flames, but highlight the importance of the flow-field in the analysis of non-premixed ignition. Following verification, these criteria have been used to describe the phenomenological changes between MILD combustion and conventional autoignition, along with the chemical structure of the reaction zone and the upstream pool of precursor species. An important finding of these results was the suitability of the HO_2 radical in describing the reaction zone structure of non-premixed ethylene combustion with hot and diluted oxidants. These results highlighted the importance of the O_2 concentration in the oxidant stream, as well as oxidant temperature, as the dominant factors in determining the regime transition between MILD and conventional autoignitive combustion.

Transient ignition processes in the MILD combustion regime have been shown to be significantly more sensitive to the inclusion of small concentrations of the OH radical, than conventional autoignitive flames. The OH radical plays an important role in flame stabilisation, and must be accounted for in modelling or describing the spatial and temporal evolution of MILD reaction zones. Conversely, the inclusion of minor species in the numerical description of a hot oxidant have very little effect on the formative stages of heat release or the steady-state reaction zone structure in either MILD or conventional autoignitive combustion.

The numerical analysis of MILD combustion using simplified reactors and Reynolds-averaged modelling is non-trivial. The onset of thermal runaway in zero-dimensional batch reactors have been seen to correspond to the weak-to-strong transition in non-premixed ethylene flames, in hot and diluted oxidants. This relationship is consistent with conventional autoignition. Although the transient evolution of non-premixed MILD, and conventional autoignitive, reaction zones cannot be described without prior estimation of a flow-field, the ignition and extinction characteristics of MILD reaction zones (or lack thereof) show good agreement with experimental observations and numerical modelling. An appropriate relationship between mixing and scalar dissipation, however, may be used to provide a representative description of the ignition processes in these flames. Such a relationship may be approximated semi-empirically, or through Reynolds-averaged computational fluid dynamics.

The use of Reynolds-averaged computational fluid dynamics has been employed with a modified eddy-dissipation concept turbulence-chemistry interaction

model. Adjustments made to this model during optimisation may be physically interpreted as increasing chemical residence times, whilst simultaneously reducing the size of fine structures in the combustion model. This is consistent with the description that the viscous mixing-field in a jet-in-hot-coflow burner restricts mixing between the fuel and oxidant streams, resulting in smaller fine reaction structures, with longer residence times, than in conventional non-premixed flames. The optimised modelling approach used in this body of work has demonstrated improved physical accuracy over previous modelling attempts and the ability to replicate trends in visual lift-off heights seen experimentally, but not previously predicted numerically.

The ignition and stabilisation of non-premixed flames in the MILD combustion regime and in the transition between MILD and conventional autoignitive combustion have been investigated and described. The results of this body of work provide insight to the mechanisms and important features of MILD reaction zones, the boundaries of the MILD combustion regime, and the nuances of MILD combustion relevant to numerical modelling. The improved understanding of non-premixed combustion derived from this thesis, bolsters the knowledge-base which underpins future development and implementation of more efficient combustion technologies.

References

- [1] Al-Noman, S. M., Choi, S. K., & Chung, S. H. (2016). Numerical study of laminar nonpremixed methane flames in coflow jets: Autoignited lifted flames with tribrachial edges and MILD combustion at elevated temperatures. *Combust. Flame*, *171*, 119–132.
- [2] Arndt, C. M., Schießl, R., Gounder, J. D., Meier, W., & Aigner, M. (2013). Flame stabilization and auto-ignition of pulsed methane jets in a hot coflow: Influence of temperature. *Proc. Combust. Inst.*, *34*, 1483–1490.
- [3] Cabra, R., Myhrvold, T., Chen, J., Dibble, R., Karpetis, A., & Barlow, R. (2002). Simultaneous laser raman-rayleigh-lif measurements and numerical modeling results of a lifted turbulent H₂/N₂ jet flame in a vitiated coflow. *Proc. Combust. Inst.*, *29*, 1881–1888.
- [4] Cavaliere, A., & de Joannon, M. (2004). Mild Combustion. *Prog. Energ. Combust.*, *30*(4), 329–366.
- [5] Choi, B., & Chung, S. (2010). Autoignited laminar lifted flames of methane,

- ethylene, ethane, and n-butane jets in coflow air with elevated temperature. *Combust. Flame*, 157(12), 2348–2356.
- [6] Choi, B. C., & Chung, S. H. (2012). Autoignited laminar lifted flames of methane/hydrogen mixtures in heated coflow air. *Combust. Flame*, 159(4), 1481–1488.
- [7] Dally, B., Karpetis, A., & Barlow, R. (2002). Structure of turbulent non-premixed jet flames in a diluted hot coflow. *Proc. Combust. Inst.*, 29, 1147–1154.
- [8] de Joannon, M., Cavaliere, A., Donnarumma, R., & Ragucci, R. (2002). Dependence of autoignition delay on oxygen concentration in mild combustion of high molecular weight paraffin. *Proc. Combust. Inst.*, 29(1), 1139–1146.
- [9] de Joannon, M., Matarazzo, A., Sabia, P., & Cavaliere, A. (2007). Mild Combustion in Homogeneous Charge Diffusion Ignition (HCDI) regime. *Proc. Combust. Inst.*, 31(2), 3409–3416.
- [10] de Joannon, M., Sabia, P., Cozzolino, G., Sorrentino, G., & Cavaliere, A. (2012). Pyrolytic and Oxidative Structures in Hot Oxidant Diluted Oxidant (HODO) MILD Combustion. *Combust. Sci. Technol.*, 184(7-8), 1207–1218.
- [11] de Joannon, M., Sorrentino, G., & Cavaliere, A. (2012). MILD combustion in diffusion-controlled regimes of Hot Diluted Fuel. *Combust. Flame*, 159, 1832–1839.
- [12] Glarborg, P., & Bentzen, L. L. B. (2008). Chemical Effects of a High CO₂ Concentration in Oxy-Fuel Combustion of Methane. *Energy Fuels*, 22(1), 291–296.
- [13] Gordon, R. L., Masri, A. R., & Mastorakos, E. (2008). Simultaneous Rayleigh temperature, OH- and CH₂O-LIF imaging of methane jets in a vitiated coflow. *Combust. Flame*, 155(1-2), 181–195.
- [14] Ihme, M., Zhang, J., He, G., & Dally, B. B. (2012). Large-Eddy Simulation of a Jet-in-Hot-Coflow Burner Operating in the Oxygen-Diluted Combustion Regime. *Flow, Turbul. Combust.*, 89, 449–464.
- [15] Johansson, O., Bood, J., Li, B., Ehn, A., Li, Z., Sun, Z., Jonsson, M., Konnov, A., & Aldén, M. (2011). Photofragmentation laser-induced fluorescence imaging in premixed flames. *Combust. Flame*, 158(10), 1908–1919.

-
- [16] Li, B., Zhang, D., Yao, M., & Li, Z. (2016). Strategy for single-shot CH₃ imaging in premixed methane/air flames using photofragmentation laser-induced fluorescence. *Proc. Combust. Inst.*. DOI: 10.1016/j.proci.2016.07.082.
- [17] Medwell, P. R., Blunck, D. L., & Dally, B. B. (2014). The role of precursors on the stabilisation of jet flames issuing into a hot environment. *Combust. Flame*, 161(2), 465–474.
- [18] Medwell, P. R., & Dally, B. B. (2012). Experimental Observation of Lifted Flames in a Heated and Diluted Coflow. *Energy Fuels*, 26(9), 5519–5527.
- [19] Medwell, P. R., Kalt, P. A. M., & Dally, B. B. (2007). Simultaneous imaging of OH, formaldehyde, and temperature of turbulent nonpremixed jet flames in a heated and diluted coflow. *Combust. Flame*, 148(1-2), 48–61.
- [20] Medwell, P. R., Kalt, P. A. M., & Dally, B. B. (2008). Imaging of diluted turbulent ethylene flames stabilized on a Jet in Hot Coflow (JHC) burner. *Combust. Flame*, 152, 100–113.
- [21] Oberlack, M., Arlitt, R., & Peters, N. (2000). On stochastic Damköhler number variations in a homogeneous flow reactor. *Combust. Theor. Model.*, 4(4), 495–510.
- [22] Oldenhof, E., Tummers, M. J., van Veen, E. H., & Roekaerts, D. J. E. M. (2010). Ignition kernel formation and lift-off behaviour of jet-in-hot-coflow flames. *Combust. Flame*, 157(6), 1167–1178.
- [23] Plessing, T., Peters, N., & Wüning, J. G. (1998). Laseroptical investigation of highly preheated combustion with strong exhaust gas recirculation. *Proc. Combust. Inst.*, 27(2), 3197–3204.
- [24] Ranzi, E., Frassoldati, A., Grana, R., Cuoci, A., Faravelli, T., Kelley, A., & Law, C. (2012). Hierarchical and comparative kinetic modeling of laminar flame speeds of hydrocarbon and oxygenated fuels. *Prog. Energy Combust. Sci.*, 38(4), 468–501. Current version of mechanism available from <http://creckmodeling.chem.polimi.it/>.
- [25] Sabia, P., de Joannon, M., Picarelli, A., & Ragucci, R. (2013). Methane auto-ignition delay times and oxidation regimes in MILD combustion at atmospheric pressure. *Combust. Flame*, 160(1), 47–55.

- [26] Sabia, P., de Joannon, M., Sorrentino, G., Giudicianni, P., & Ragucci, R. (2015). Effects of mixture composition, dilution level and pressure on auto-ignition delay times of propane mixtures. *Chem. Eng. J.*, 277, 324–333.
- [27] Sabia, P., Lavadera, M. L., Giudicianni, P., Sorrentino, G., Ragucci, R., & de Joannon, M. (2015). CO₂ and H₂O effect on propane auto-ignition delay times under mild combustion operative conditions. *Combust. Flame*, 162(3), 533–543.
- [28] Sabia, P., Lubrano Lavadera, M., Sorrentino, G., Giudicianni, P., Ragucci, R., & de Joannon, M. (2016). H₂O and CO₂ Dilution in MILD Combustion of Simple Hydrocarbons. *Flow, Turbul. Combust.*, 96(2), 433–448.
- [29] Shabanian, S. R., Medwell, P. R., Rahimi, M., Frassoldati, A., & Cuoci, A. (2013). Kinetic and fluid dynamic modeling of ethylene jet flames in diluted and heated oxidant stream combustion conditions. *Appl. Therm. Eng.*, 52, 538–554.
- [30] Sidey, J. A., & Mastorakos, E. (2016). Simulations of laminar non-premixed flames of methane with hot combustion products as oxidiser. *Combust. Flame*, 163, 1–11.
- [31] Smith, G. P., Golden, D. M., Frenklach, M., Moriarty, N. W., Eiteneer, B., Goldenberg, M., Bowman, C. T., Hanson, R. K., Song, S., William C. Gardiner, J., Lissianski, V. V., & Qin, Z. (2000). GRI-Mech 3.0. Mechanism available from http://www.me.berkeley.edu/gri_mech/.
- [32] Tu, Y., Su, K., Liu, H., Chen, S., Liu, Z., & Zheng, C. (2016). Physical and chemical effects of CO₂ addition on CH₄/H₂ flames on a Jet in Hot Coflow (JHC) burner. *Energy Fuels*, 30(2), 1390–1399.
- [33] Wang, H., You, X., Joshi, A. V., Davis, S. G., Laskin, A., Egolfopoulos, F., & Law, C. K. (2007). USC Mech Version II. High-Temperature Combustion Reaction Model of H₂/CO/C₁-C₄ Compounds. Mechanism available from http://ignis.usc.edu/USC_Mech_II.htm.
- [34] Ye, J., Medwell, P. R., Dally, B. B., & Evans, M. J. (2016). The transition of ethanol flames from conventional to MILD combustion. *Combust. Flame*, 171, 173–184.
- [35] Yoo, C. S., Richardson, E. S., Sankaran, R., & Chen, J. H. (2011). A DNS study on the stabilization mechanism of a turbulent lifted ethylene jet flame in highly-heated coflow. *Proc. Combust. Inst.*, 33, 1619–1627.

Appendix A

Supplementary Data for Chapter 5

The following pages contain the supplementary data for the paper entitled: *Effects of Oxidant Stream Composition on Non-Premixed Laminar Flames with Heated and Diluted Coflows*.

Effects of Oxidant Stream Composition on Non-Premixed Laminar Flames with Heated and Diluted Coflows

Supplementary Data

M.J. Evans^{a*}, P.R. Medwell^a, Z.F. Tian^a, J. Ye^a, A. Frassoldati^b, A. Cuoci^b

^aSchool of Mechanical Engineering, The University of Adelaide, South Australia, 5005, AUSTRALIA

^bDipartimento di Chimica, Materiali ed Ingegneria Chimica “G. Natta”, Politecnico di Milano, 20133, Milan, ITALY

*Corresponding author. Tel.: +61 8 8313 5460, Fax: +61 8 8313 4367. m.evans@adelaide.edu.au

S1. Profiles of heat release rates from key reactions, and their reaction rates

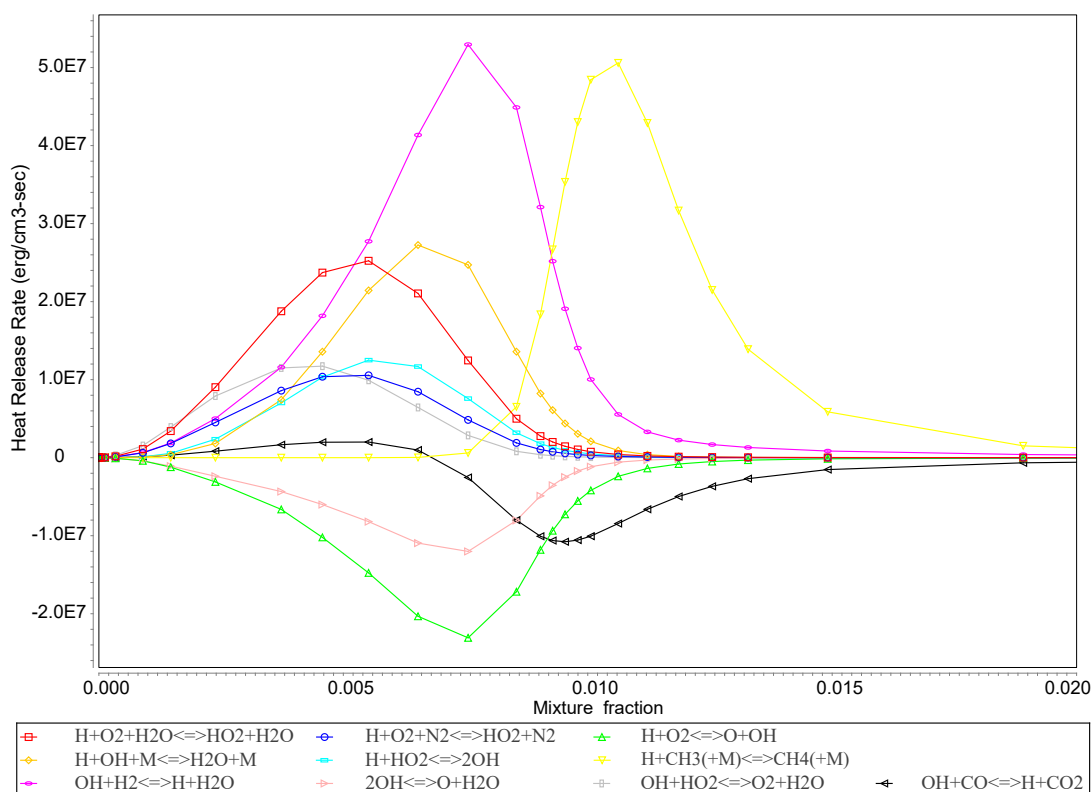


Figure S1. Heat release rate profiles for a steady-state, laminar, opposed-flow flame with HM1-like streams.

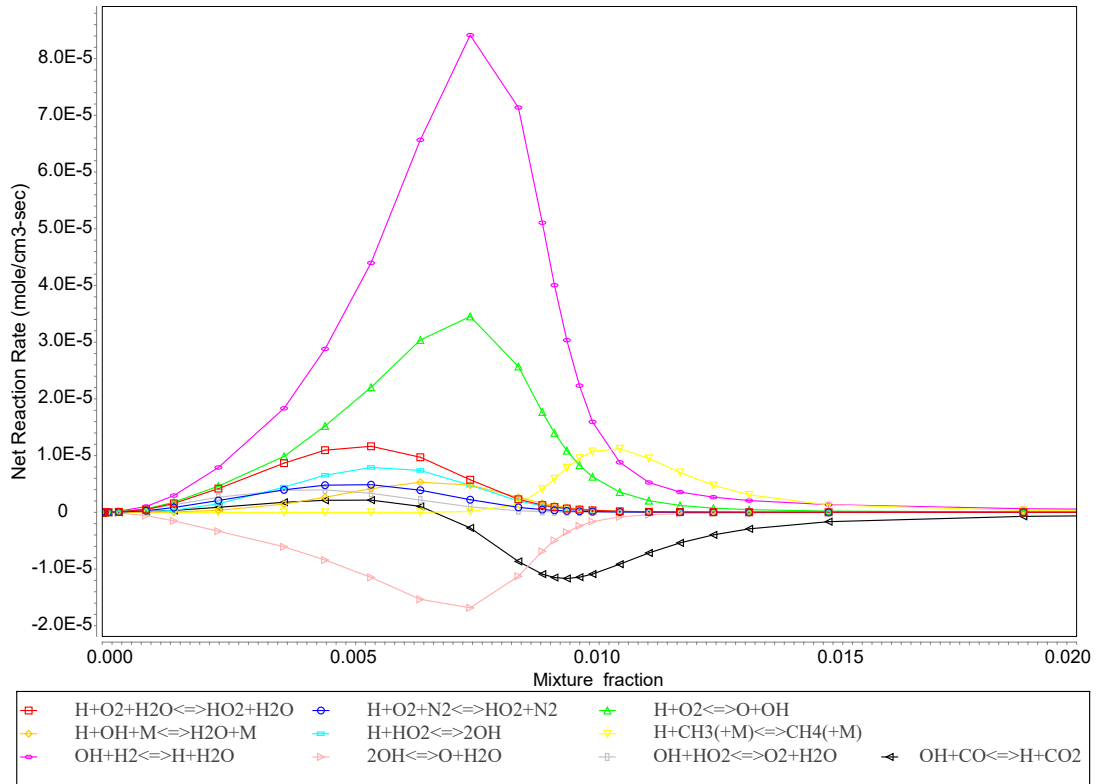


Figure S2. Net reaction-rates of dominant reactions for a steady-state, laminar, opposed-flow flame with HM1-like streams.

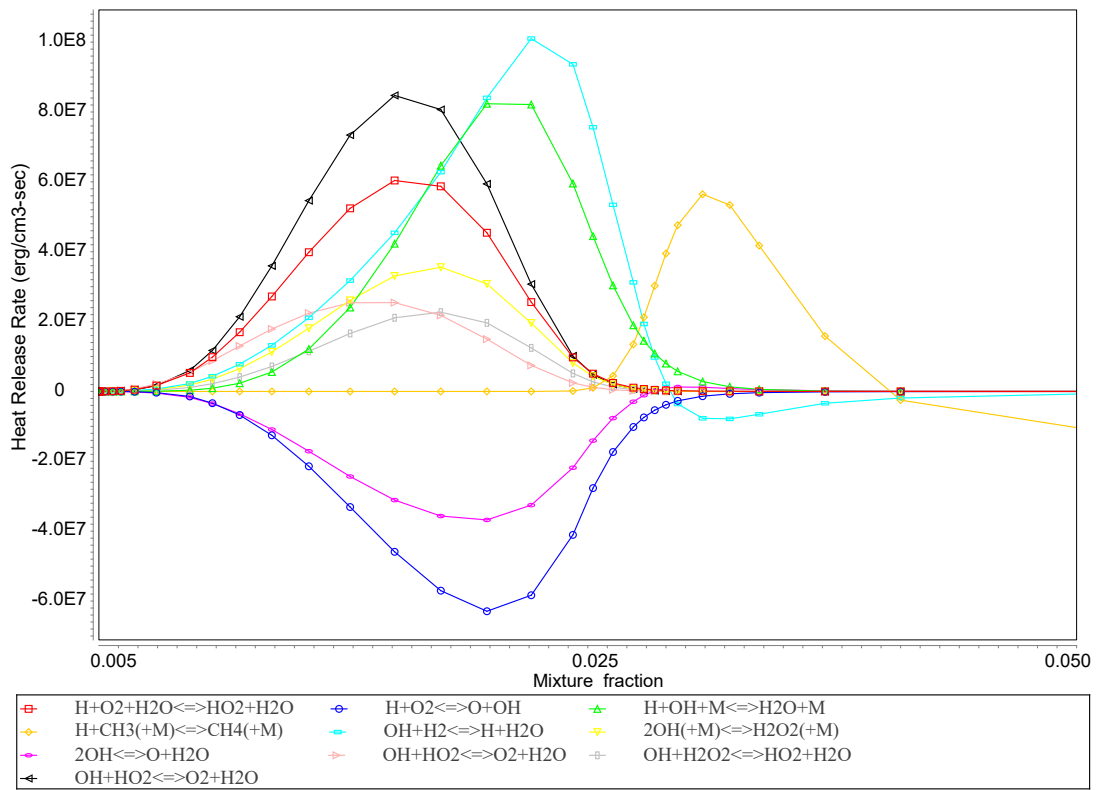


Figure S3. Heat release rate profiles for a steady-state, laminar, opposed-flow flame with HM3-like streams.

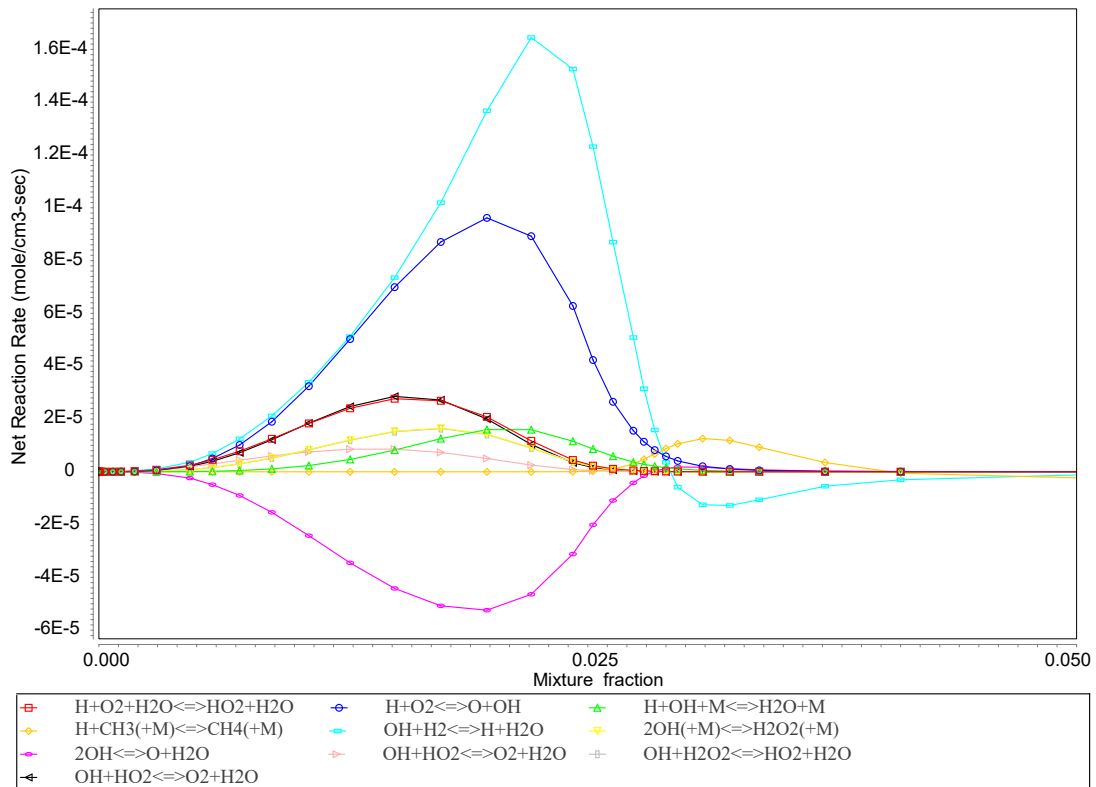


Figure S4. Net reaction-rates of dominant reactions for a steady-state, laminar, opposed-flow flame with HM3-like streams.

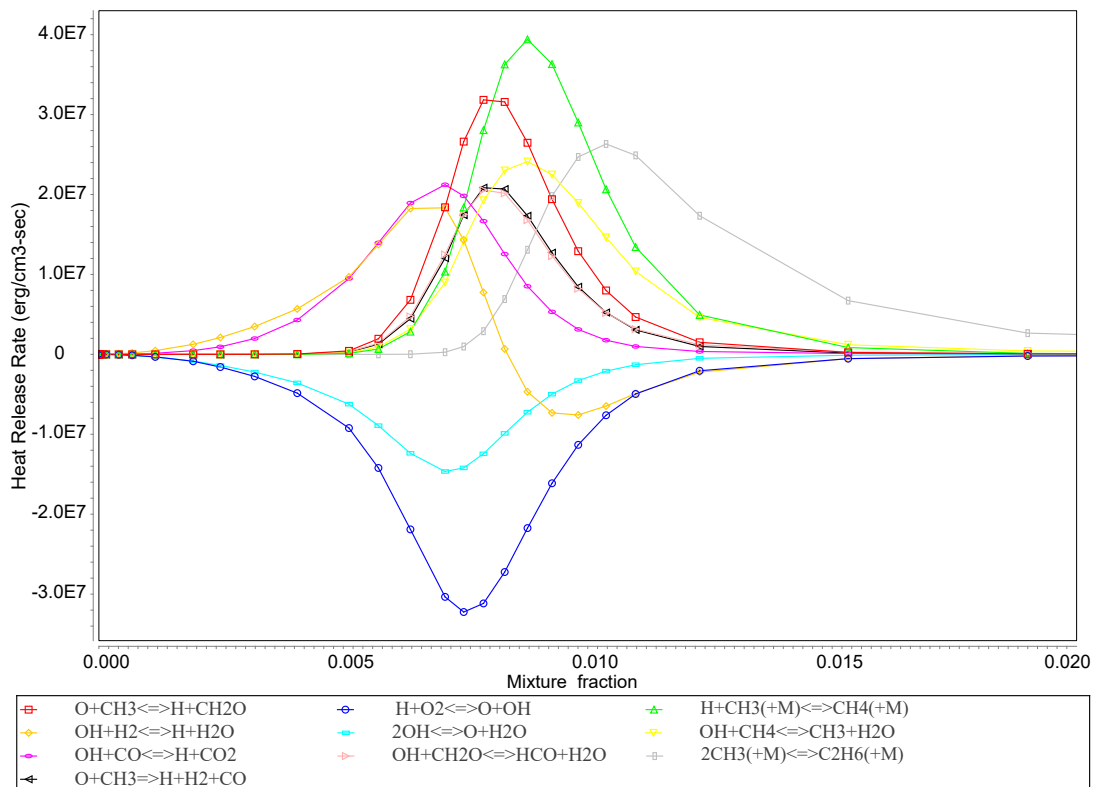


Figure S5. Heat release rate profiles for a steady-state, laminar, opposed-flow CH₄ flame with 1300-K oxidant with 3% O₂ (O₂, N₂, H₂O, CO₂ only).

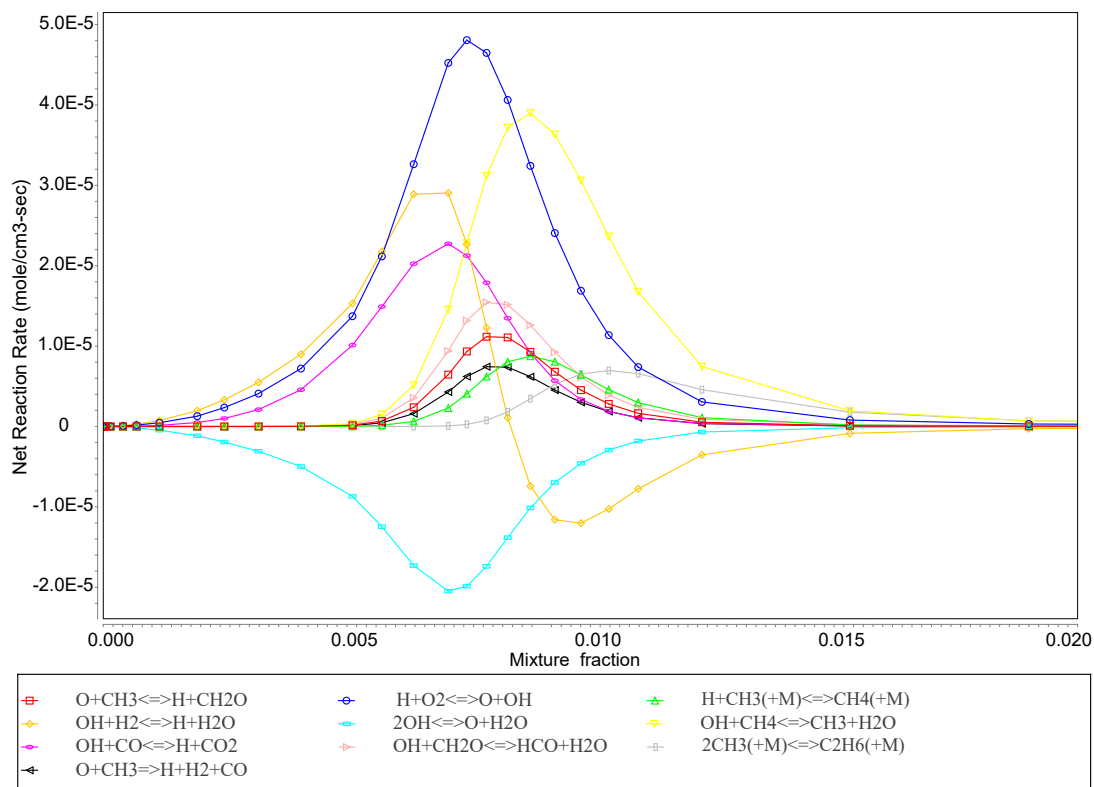


Figure S6. Net reaction-rates of dominant reactions for a steady-state, laminar, opposed-flow CH₄ flame with 1300-K oxidant with 3% O₂ (O₂, N₂, H₂O, CO₂ only).

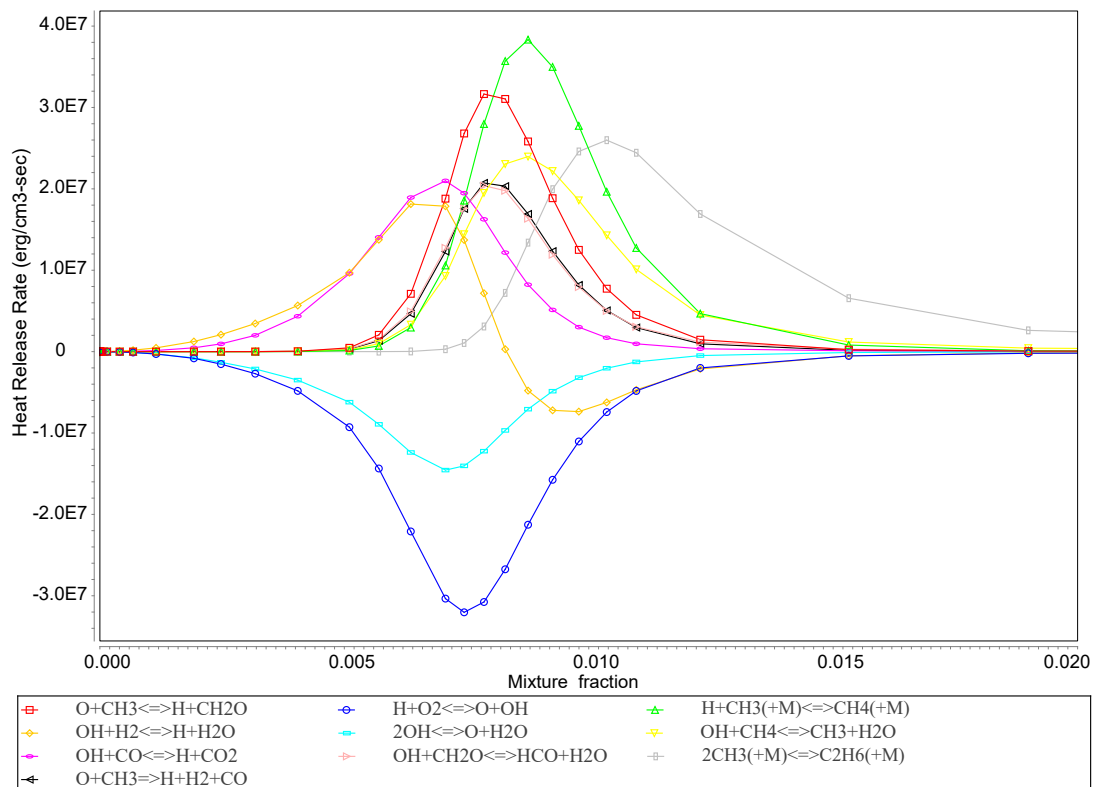


Figure S7. Heat release rate profiles for a steady-state, laminar, opposed-flow CH₄ flame with 1300-K oxidant with 3% O₂ (including equilibrium concentrations of OH).

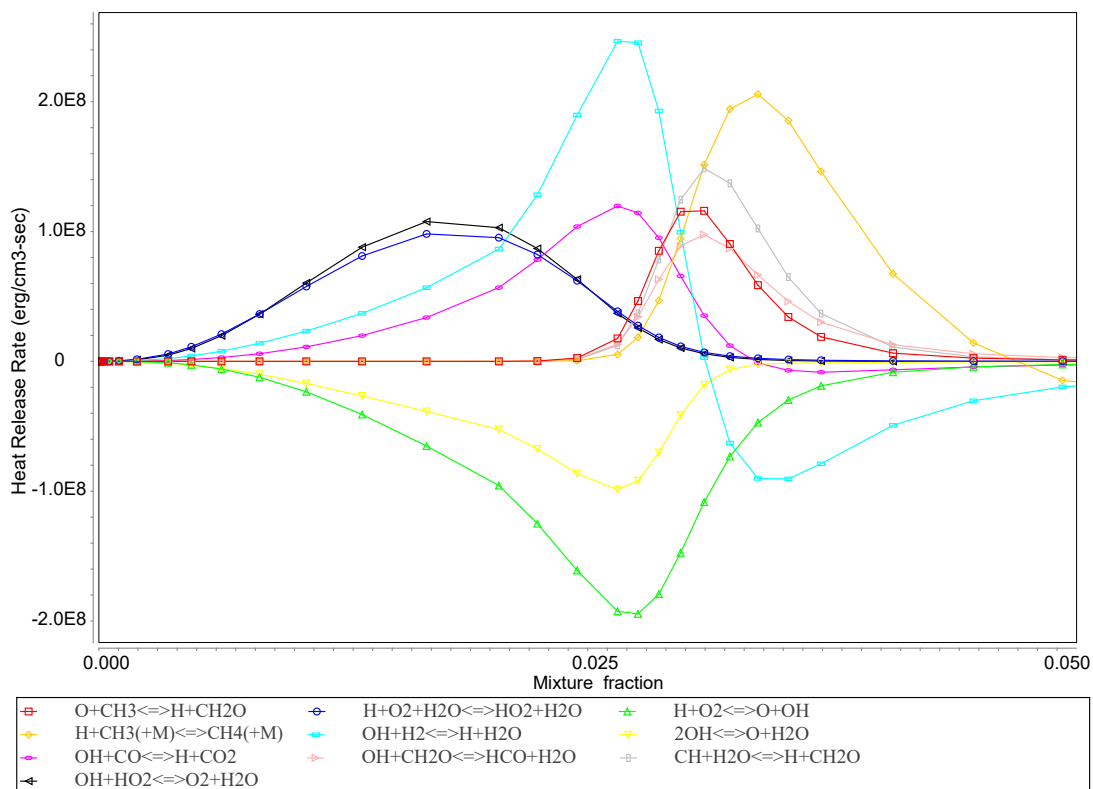


Figure S8. Heat release rate profiles for a steady-state, laminar, opposed-flow CH₄ flame with 1300-K oxidant with 9% O₂.

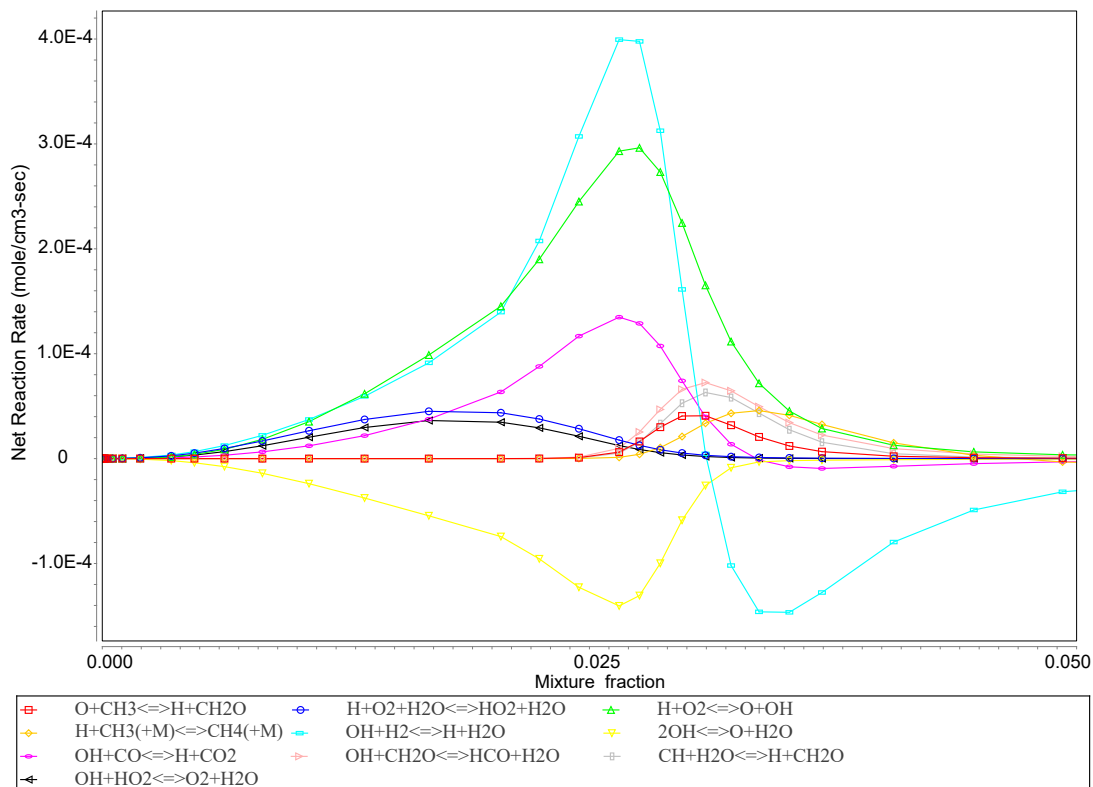


Figure S9. Net reaction-rates of dominant reactions for a steady-state, laminar, opposed-flow CH₄ flame with 1300-K oxidant with 9% O₂.

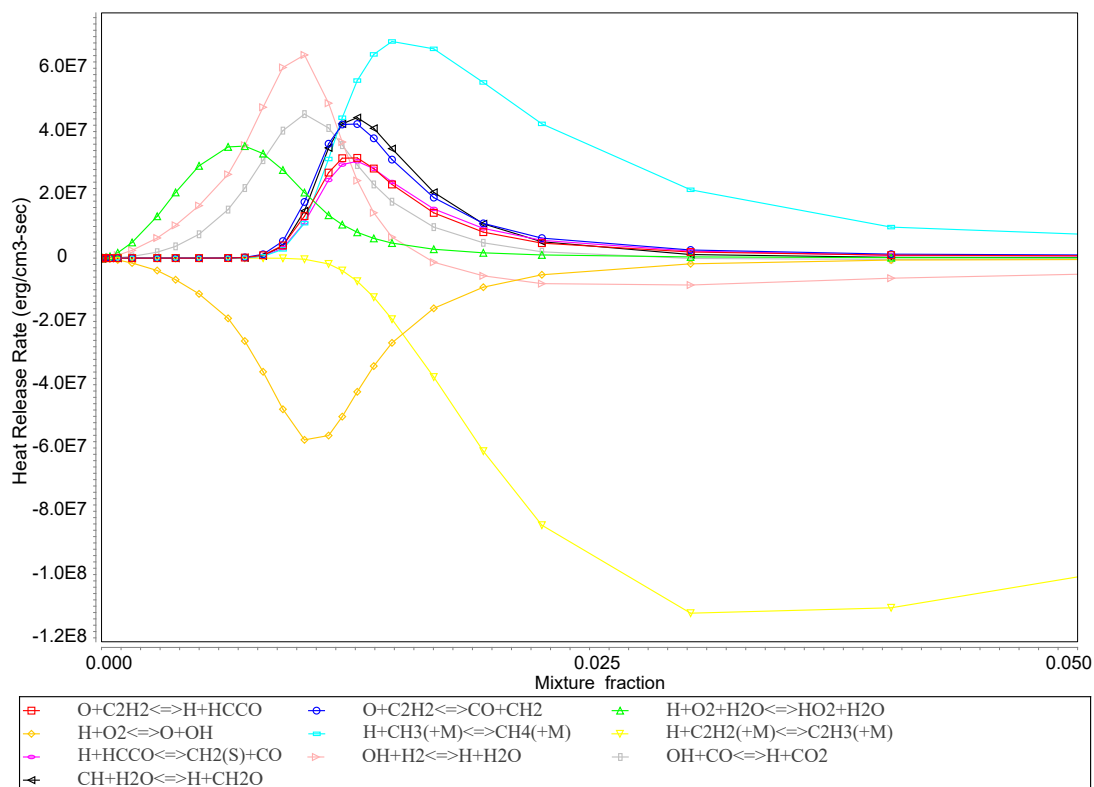


Figure S10. Heat release rate profiles for a steady-state, laminar, opposed-flow C₂H₄ flame with 1300-K oxidant with 3% O₂.

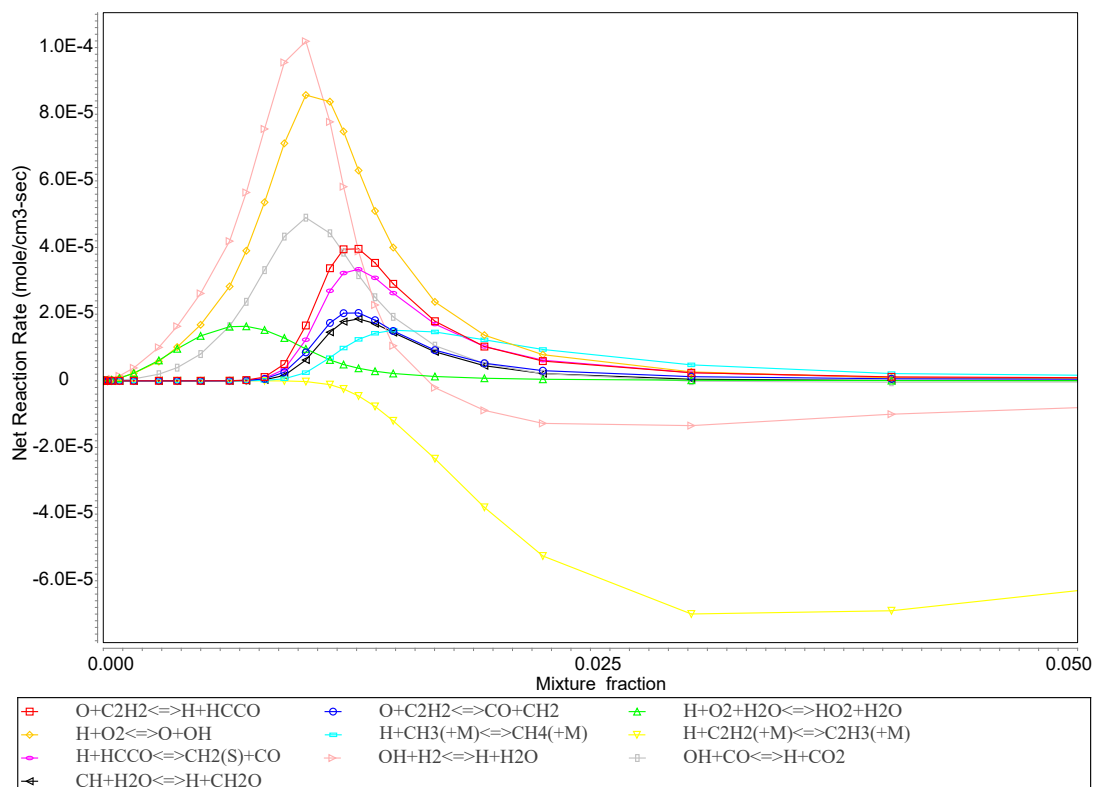


Figure S11. Net reaction-rates of dominant reactions for a steady-state, laminar, opposed-flow C₂H₄ flame with 1300-K oxidant with 3% O₂.

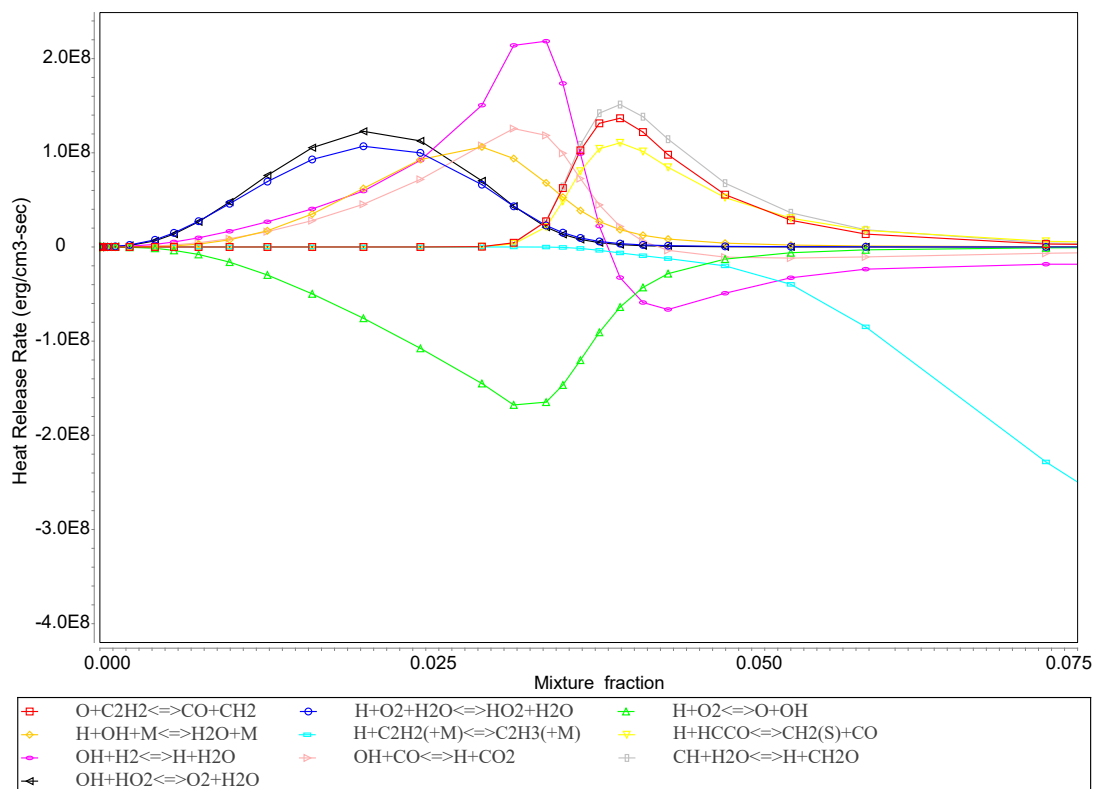


Figure S12. Heat release rate profiles for a steady-state, laminar, opposed-flow C_2H_4 flame with 1300-K oxidant with 9% O_2 .

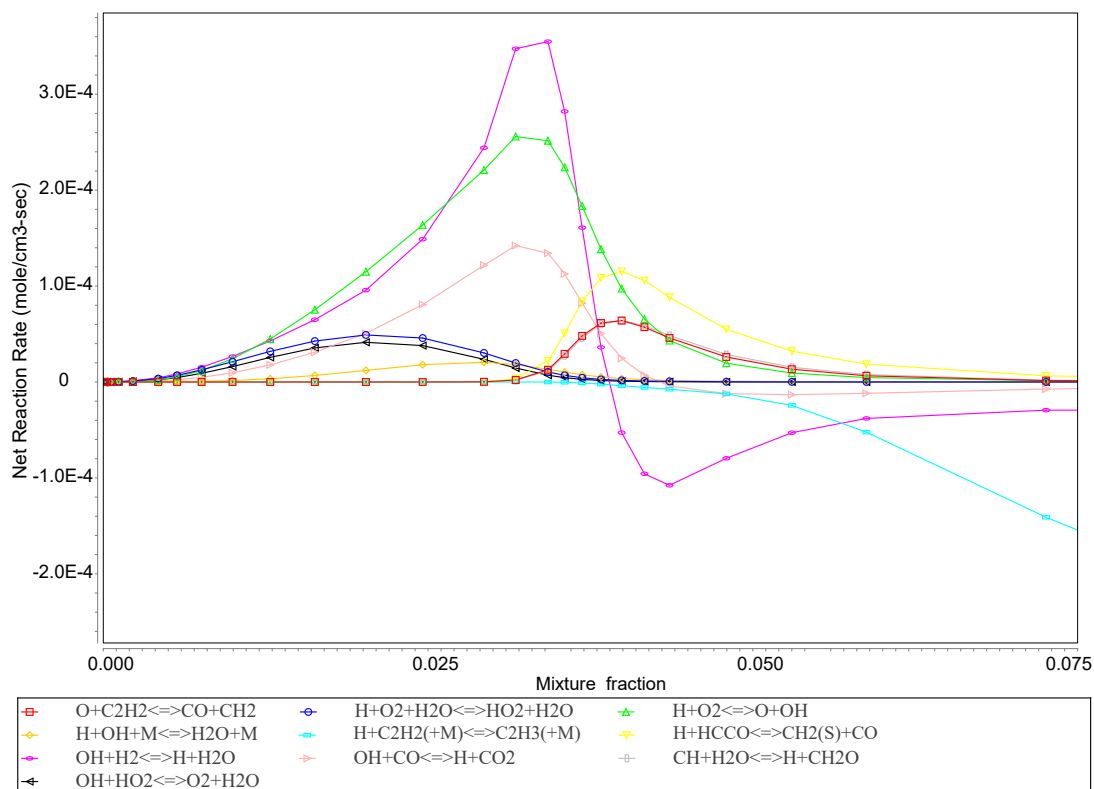


Figure S13. Net reaction-rates of dominant reactions for a steady-state, laminar, opposed-flow C_2H_4 flame with 1300-K oxidant with 9% O_2 .

S2. Formaldehyde reaction rates and transport in non-premixed CH₄ combustion with a hot-and-diluted-oxidant

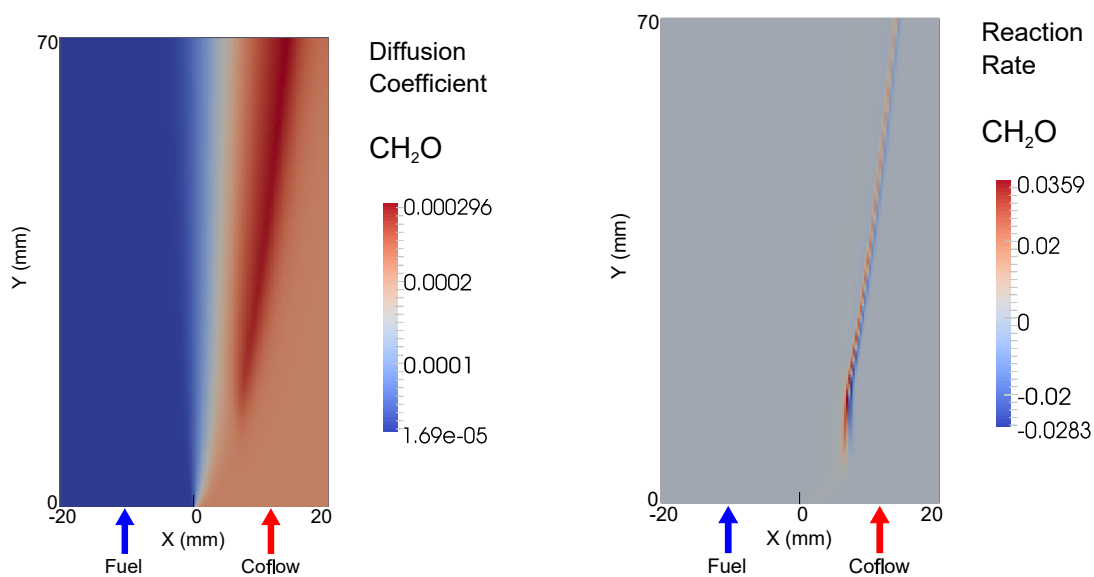


Figure S14. Diffusion coefficients ($\text{m}^2\cdot\text{s}^{-1}$) and reaction rates ($\text{kg}\cdot\text{m}^{-3}\cdot\text{s}^{-1}$) of CH₂O, for non-premixed CH₄ and a 1300-K oxidant with 3% O₂. Domain is 40 mm × 70 mm.

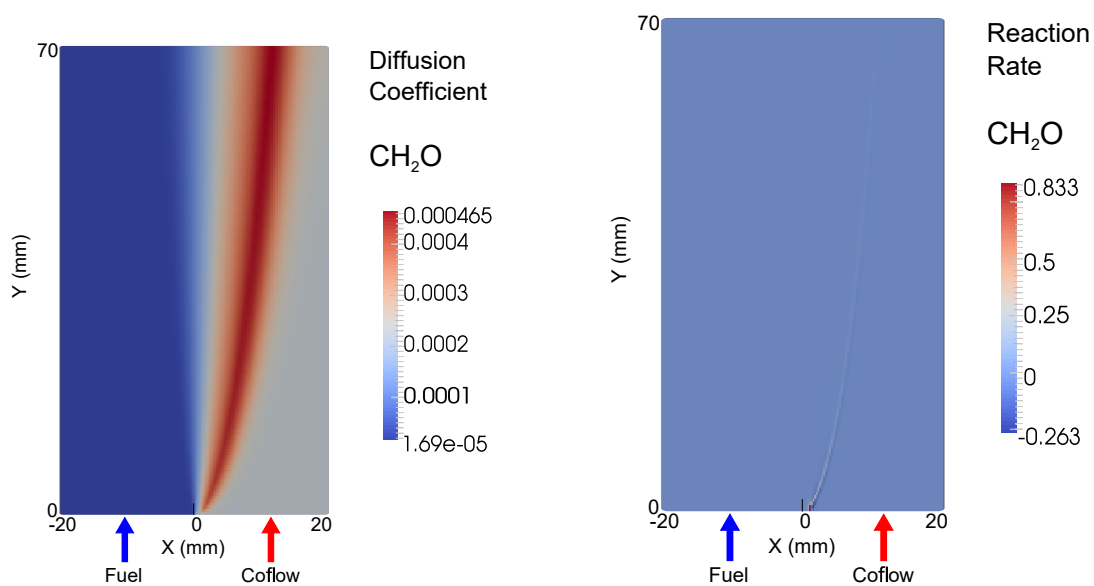
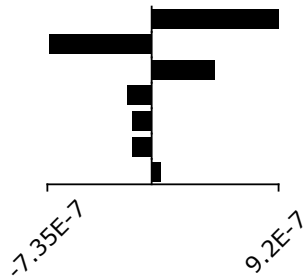
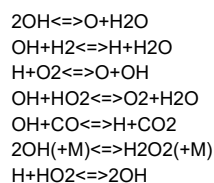


Figure S15. Diffusion coefficients ($\text{m}^2\cdot\text{s}^{-1}$) and reaction rates ($\text{kg}\cdot\text{m}^{-3}\cdot\text{s}^{-1}$) of CH₂O, for non-premixed CH₄ and a 1300-K oxidant with 9% O₂. Domain is 40 mm × 70 mm.

S3. Absolute rate of production and sensitivities of key combustion species in a steady-state, laminar opposed flow CH₄ flame and a 1300-K oxidant with 3% O₂

Absolute Rate of Production OH



Normalized Sensitivity OH

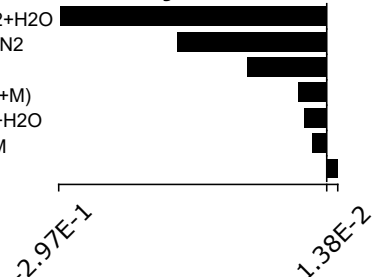
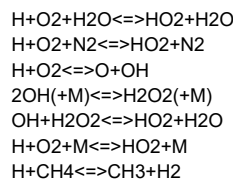
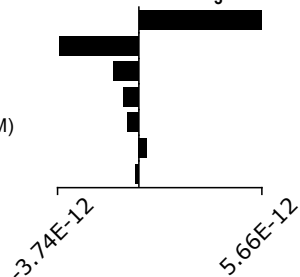
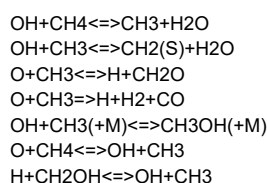


Figure S16. Key reactions for OH production and consumption in lean side of the reaction zone.

Absolute Rate of Production CH₃



Normalized Sensitivity CH₃

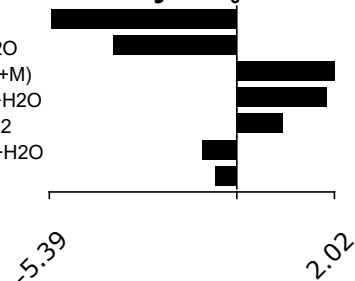
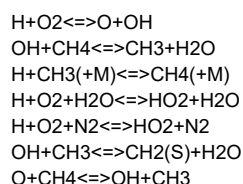
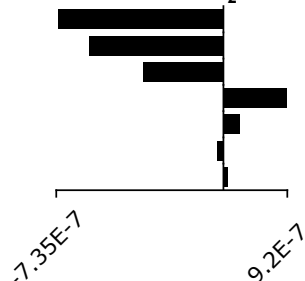
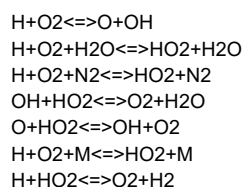


Figure S17. Key reactions for CH₃ production and consumption in lean side of the reaction zone.

Absolute Rate of Production O₂



Normalized Sensitivity O₂

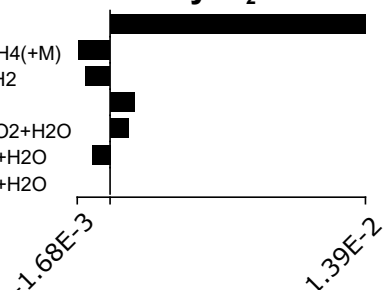
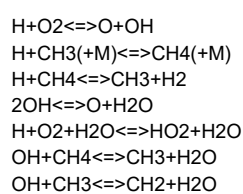
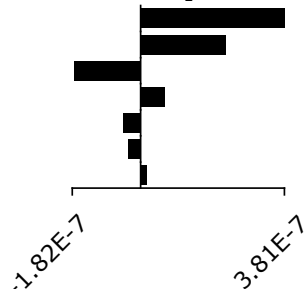
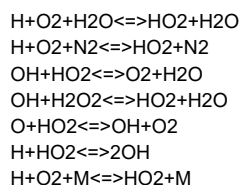


Figure S18. Key reactions for O₂ production and consumption in lean side of the reaction zone.

Absolute Rate of Production HO₂



Normalized Sensitivity HO₂

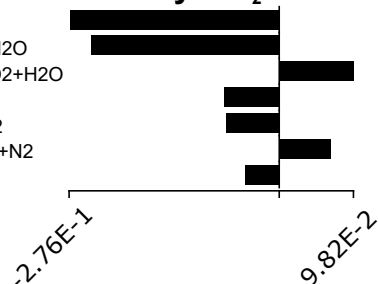
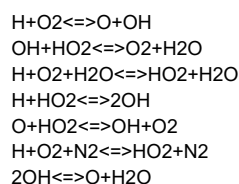


Figure S19. Key reactions for HO₂ production and consumption in lean side of the reaction zone.

S4. Temperature and species profiles for CH₄ flames with inverted C/H levels in the oxidant stream

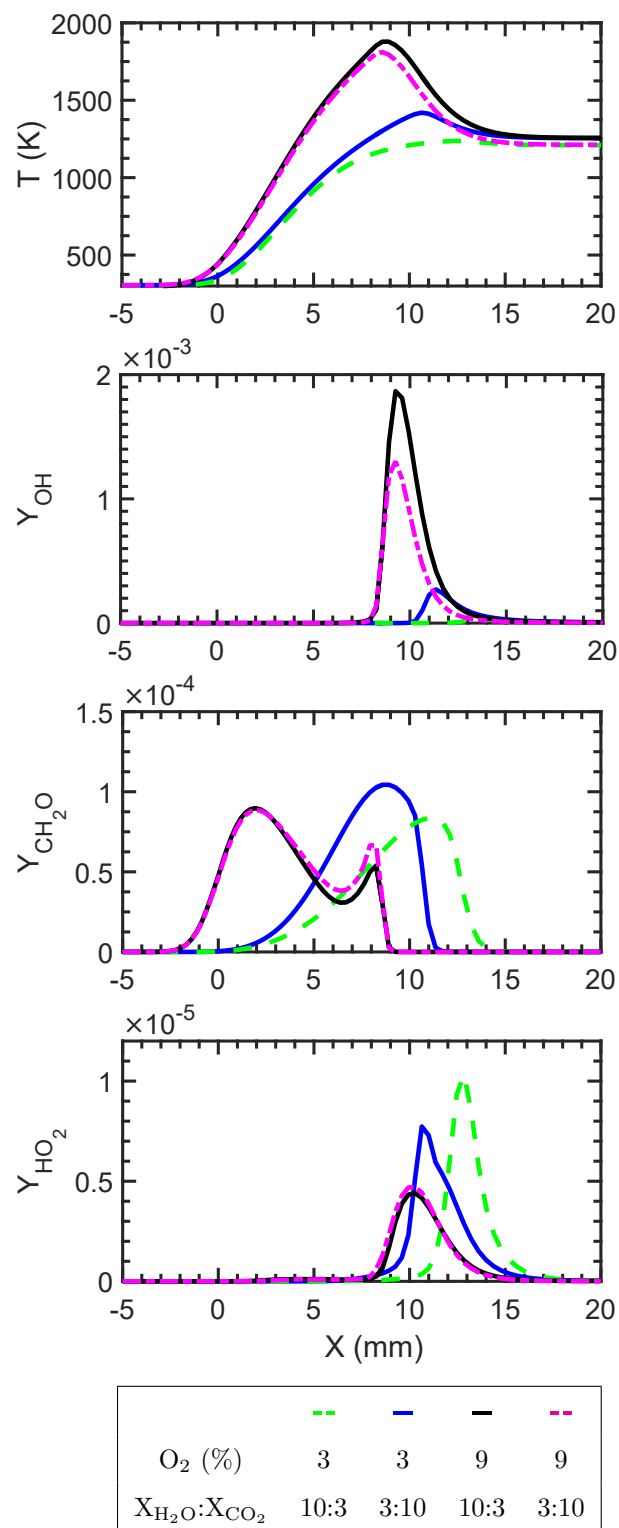


Figure S20. The effects of changing H₂O and CO₂ concentrations in the coflow from 10 and 3% to 3 and 10% (vol./vol.), respectively. Plots show profiles from CH₄ flames of temperature (also presented in the main paper), OH, CH₂O and HO₂ mass fractions against X, 30 mm downstream of the inlet plane, for 1300-K oxidants with 3 and 9% O₂ (vol./vol.).

Appendix B

Supplementary Data for Chapter 8

The following pages contain the supplementary data for the paper entitled: *Ignition Features of Methane and Ethylene Fuel-Blends in Hot and Diluted Coflows*.

Ignition features of methane and ethylene fuel-blends in hot and diluted coflows

Supplementary Data

M.J. Evans*, A. Chinnici, P.R. Medwell, J. Ye

School of Mechanical Engineering, The University of Adelaide, South Australia, Australia

*Corresponding author. E-mail: m.evans@adelaide.edu.au, Tel.: +61 8 8313 5460, Fax: +61 8 8313 4367.

S1. Axial Velocity and Turbulent Reynolds Number for C_2H_4 Flames in 1300-K Coflows

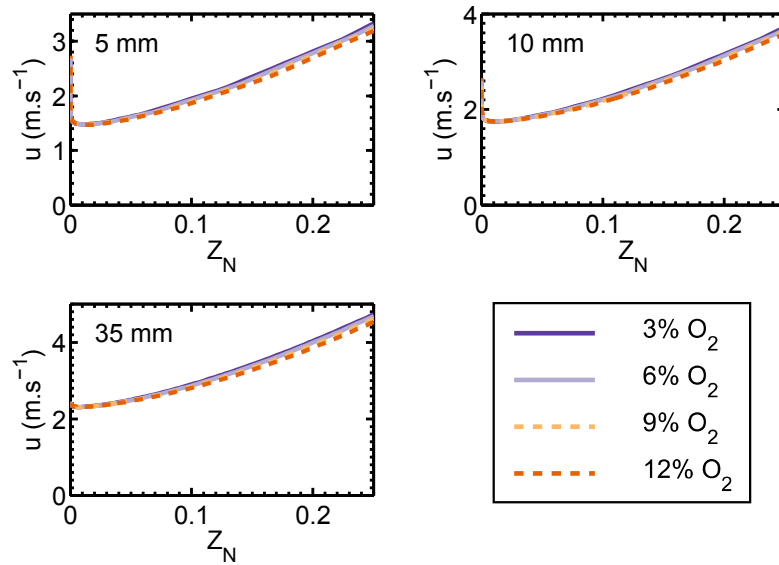


Fig. S1: Profiles of axial velocity (u) versus Z_N at different downstream locations from RANS modelling of C_2H_4 flames in 1300-K coflows with different compositions. Clockwise from top left-hand plot: 5 mm, 10 mm and 35 mm downstream.

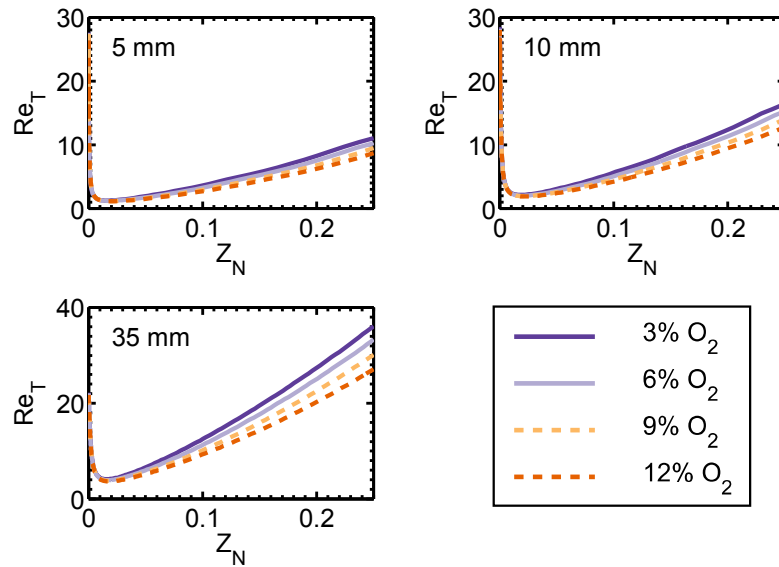


Fig. S2: Profiles of turbulent Reynolds number (Re_T) versus Z_N at different downstream locations from RANS modelling of C_2H_4 flames in 1300-K coflows with different compositions. Clockwise from top left-hand plot: 5 mm, 10 mm and 35 mm downstream.

S2. Heat Release Rate and OH Profiles of CH₄/C₂H₄ Flames in 1100-K Coflows

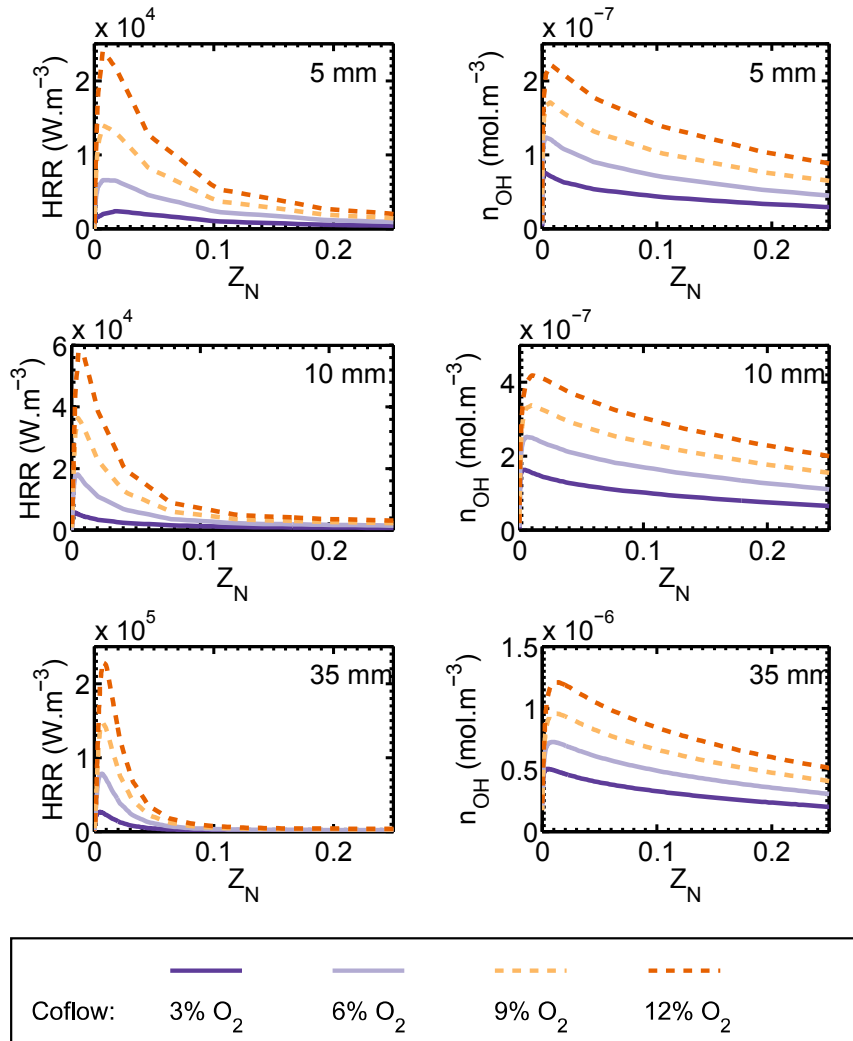


Fig. S3: Net heat release rate (HRR, left) and OH number density (n_{OH} , right) at three different downstream locations in RANS models of 1:1 CH₄/C₂H₄ flames in 1100-K coflows with different compositions. Data is taken from 5 mm, 10 mm and 35 mm downstream.